Ryspek Usubamatov

Theory of Gyroscopic Effects for Rotating Objects

Gyroscopic Effects and Applications

Springer

Theory of Gyroscopic Effects for Rotating Objects

Ryspek Usubamatov

Theory of Gyroscopic Effects for Rotating Objects

Gyroscopic Effects and Applications

Springer

Ryspek Usubamatov
Kyrgyz State Technical University
Bishkek, Kyrgyzstan

ISBN 978-981-15-6474-1 ISBN 978-981-15-6475-8 (eBook)
https://doi.org/10.1007/978-981-15-6475-8

© The Editor(s) (if applicable) and The Author(s), under exclusive license to Springer Nature Singapore Pte Ltd. 2020
This work is subject to copyright. All rights are solely and exclusively licensed by the Publisher, whether the whole or part of the material is concerned, specifically the rights of translation, reprinting, reuse of illustrations, recitation, broadcasting, reproduction on microfilms or in any other physical way, and transmission or information storage and retrieval, electronic adaptation, computer software, or by similar or dissimilar methodology now known or hereafter developed.
The use of general descriptive names, registered names, trademarks, service marks, etc. in this publication does not imply, even in the absence of a specific statement, that such names are exempt from the relevant protective laws and regulations and therefore free for general use.
The publisher, the authors and the editors are safe to assume that the advice and information in this book are believed to be true and accurate at the date of publication. Neither the publisher nor the authors or the editors give a warranty, expressed or implied, with respect to the material contained herein or for any errors or omissions that may have been made. The publisher remains neutral with regard to jurisdictional claims in published maps and institutional affiliations.

This Springer imprint is published by the registered company Springer Nature Singapore Pte Ltd.
The registered company address is: 152 Beach Road, #21-01/04 Gateway East, Singapore 189721, Singapore

Dedicated in memory of my dear mother Saikal, to my daughters Dinara and Anara, sister Aigul and brother Damir

Preface

The topic of gyroscopic effects is not new, but more than two centuries still attracts numerous researchers. The term gyroscopic effects is related to the spinning objects and expresses the action of the inertial forces generated by their rotating mass and motions of objects in the space. In engineering, the primary and remarkable effect of a spinning object is maintaining its axis that uses mostly in gyroscopic devices of aerospace and ship industries. The gyroscopic effects are subject to the dynamics of rotating objects that is a crucial part of the knowledge in engineering. The action of the one inertial torque has been analytically formulated by the famous mathematician L. Euler on the principle of kinetic energy conservation and the change in the angular momentum. However, practice demonstrates that this analytic approach is not full and cannot describe the physics of gyroscopic effects related to the numerous rotating objects. The movable, spinning components of different mechanisms manifest gyroscopic effects. The spinning disc and other rotating objects are the parts of numerous mechanisms and machines that call gyroscopic devices in different industries. Such rotating movable objects created many problems in computing acting inertial forces and motions. These parts can be the aircraft's, helicopter's and ship's propellers, gas turbines, projectiles, wheels, cones, rotors, spheres, paraboloids, etc. The action of gyroscopic effects results in motions of rotating objects in space. These motions should be analytically described and explained by the physics of acting forces.

Beginning from the time of the Industrial Revolution published probably tons of manuscripts, several dozen theories and today every year are published around hundreds of papers dedicated to gyroscopic problems. Today, this phenomenon has an explanation. The gyroscopic effects are the result of the action of the system of interrelated inertial torques linked with the kinetic energy conservation law. Scientists of the eighteen century could not solve gyroscope problems in principle because the physical terms of the kinetic and potential energies were developed in the middle of the nineteenth century. Researchers could not describe mathematically the physics of gyroscopic effects for the simple spinning disc. This is an unusual reality in the science of classical mechanics in which methods can solve more complex problems. Unsolved gyroscopic effects forced researchers to spawn artificial terms and anti-scientific statements that gyroscopic devices possess non-inertial and

non-gravitational properties, etc. Practically, for solutions of the gyroscope problems in engineering is used numerical modelling of gyroscopic effects and properties that have specific mathematics and software. However, numerical modelling does not discover the physics of the acting forces and motions of the rotating objects.

Contemporary machines and mechanisms are characterized by the intensification of the work and functioning that lead to increasing the magnitudes of the acting inertial forces. This trend will be kept in the future of engineering. The inertial forces of the rotating object can destroy it at the condition of the high angular velocity. For solving these problems, engineering needs exact solutions for gyroscopic effects. Recent investigations and detailed analysis of the inertial forces acting on the rotating objects discovered the action of the system of interrelated inertial torques. These torques are generated by centrifugal, common inertial and Coriolis forces of the rotating mass elements, as well as the change in the angular momentum, which are well known in classical mechanics. The Euler's principle of the change in the angular momentum constitutes only the sixth part of all torques acting on the rotating objects that were out from consideration in the known gyroscope theories. This fact is the reason that all known gyroscope theories did not match practical tests. The new system of interrelated inertial torques of the spinning objects mentioned above constitutes the true fundamental principles of the gyroscope theory. The new principles are based on causative dependencies of the acting interrelated internal torques and kinetic energy conservation law that are used for formulating the mathematical models of the gyroscope motions. The principles of the gyroscopic effects have been formulated for the simple spinning disc, but they are universal and can be applied to any designs of rotating objects. The mathematical models for the inertial torques will be different that depend on their geometry rotating objects.

Obtained results show that the physics of the gyroscopic effects is more complicated in mathematics than presented in known publications with simplified analytical models and correction coefficients. The reason for a delusion of all researchers, scientists and scholars is mathematical modelling of acting forces and motions based on the centre mass of rotating objects. They did not pay attention to the action of the distributed masses of the objects in which geometries can have different designs. For example, the distributed masses of the spinning disc are located on the 2/3 of its external radius. The rotating objects with lengthened designs have distributed masses located on their radii and lengths that manifest their gyroscopic effects. The solved problems of gyroscopic effects in classical mechanics cover the gap in the knowledge of the dynamics of rotating objects.

The theory of gyroscopic effects considers the dynamics of the rotating objects in which mathematical models for the inertial forces and motions are presented in the Euler's form. The analytical approaches were treated by the methods of mathematical analysis. This type of presentation enables easy understanding and helps to avoid the cumbersome mathematical models that are expressed by 3D Lagrange's and Euler's angles method. The analytic approaches are based on the vector and differential analysis methods and assumed that the reader knows these mathematical methods. The exact and straightforward treatment for motions of gyroscopic devices is considered in the standard system of coordinate axes throughout the book. Formulation

of the theory of gyroscopic effects and solutions does not contain analytic approximations and simplifications for mathematical models to fit with practical results.

The manifestation of the several inertial torques expresses the action of the external loads on the gyroscopic devices. These torques include the operation of frictional forces on the supports of gyroscopic mechanisms. The analysis demonstrates the work of minor frictional forces can dramatically reduce the kinetic energy of the inertial torques generated by masses of the rotating objects. The external torques acting around different gyroscope's axes are considered in several examples that result in the change in the kinetic energy of the rotating objects that lead to the gyroscope's lift up and oscillation and nutation. The design features of rotating objects are considered in several working examples and assisting in clarifying the mathematical method for solving gyroscopic effects for the spinning disc. The mathematical models tested on the most unsolvable cases of the gyroscope with spinning disc are suspended from the flexible cord and with one side pivoted support. The result of the practical tests perfectly matches the mathematical models of the gyroscope motions. This fact is the best validation of their correctness.

The gyroscope theory for rotating objects has formulated by complicated analytical means. The reason for such a statement is interrelations of the nine inertial torques acting around three axes based on kinetic energy conservation law. The mathematical modelling of the complex problem is a regular routine process with omissions and corrections in science and engineering solutions. Nevertheless, all gyroscopic effects that ascribed to rotating objects are finally solved analytically. However, any and all mistakes are, of course, solely the author's responsibility. I would greatly appreciate any comments, suggestions or problems related to any matters that will be used to improve the content of this work.

The object of this work is to give fundamental principles of the theory of gyroscopic effects. It presents mathematical methods and models for inertial forces and motions, which can be used for solving the vast engineering problems generated by the rotating objects. The new analytical approach has been enabled for writing the complete theory of gyroscopic effects that is accurate, systematic and clear in physical processes. The gyroscope theory for rotating objects opens a new direction in classical mechanics for computing inertial forces and motions of the objects. Science and engineering receive a new powerful analytical tool that enables to improve the education process at universities and the quality of work of objects with gyroscopic effects in engineering. The mathematical models for gyroscopic forces and motions are concerned with fundamental principles of physics. Accurate treatment for gyroscopic effects, solutions in working examples and practical tests are used in the SI system. Derived theory of gyroscopic effects included important components from publications of previous research and collected information that assisted in writing this book. Each chapter contains references to the essential publications dedicated to gyroscope problems. The new fundamental principles of the gyroscope theory can be applied to numerous mechanical gyroscopic devices in engineering and present challenges for practitioners, researchers, engineers, lecturers and students of universities.

Bishkek, Kyrgyzstan Ryspek Usubamatov

Contents

About the Author

Ryspek Usubamatov graduated from the Moscow State Technical University after N. Bauman with a Professional Engineer in Mechanical and Manufacturing Engineering. He obtained his Ph.D. in Industrial Engineering from the same university and Dr. Sc. in Academy of Sciences of Kyrgyzstan. His industrial experience includes work as a registered Professional Engineer in machine tools design at the Bishkek Engineering Plant of Kyrgyzstan. His professional experience has involved teaching the University Putra Malaysia, University Malaysia Perlis and currently, he is a full Professor at Kyrgyz State Technical University after I. Razzakov. His major areas are mechanical, manufacturing and industrial engineering where published 8 books around 400 manuscripts, and 61 patents of inventions. He is the Academician of the Moscow International Academy of Higher Education, Member of the American Association for the Advancement of Science, Universal Association of Mechanical and Aeronautical Engineers, American Physical Society and International Institute of Engineers. He is the editorial board member for the Journals: *Robotics and Automation Engineering Journal*, *International Robotics and Automation Journal*, *International Journal of Advanced Intelligent Manufacturing Technology*, *Scholar Journal of Applied Sciences and Research*. His honours and awards: State medal: "Valorous Labour", Kyrgyzstan; Silver and bronze medals "New washing process and washing machine" 2009, 20214 ITEX, Exhibitions of Inventions, Malaysia; Order of Merit, World Inventor Award Festival, WIAF 2012, Korea.

Nomenclature

A	Work of inertial torques of a gyroscope
E	Energy
F_{cr}	Coriolis force
F_{ct}	Centrifugal force
F_{cti}	Component of the centrifugal force about axis i
f_{ct}	Centrifugal force of the mass element
f_{cr}	Coriolis force of the mass element
f_{cri}	Component of Coriolis force of the mass element about axis i
f_n	Normal component of the force
F_i	Axial component of the forces about axis i
f_{ini}	Component of the inertial forces about axis i
H	Angular momentum of the spinning rotor
ΔH	Change of the angular momentum of the spinning rotor
J_i	Mass moment of inertia for the rotor's disc about axis i
K	Kinetic energy of a gyroscope
l_i	Distance of the location of gyroscope's component i
M	Mass of a rotating object
m	Mass element of a rotating object
P	Potential energy of a gyroscope
R	External radius of a rotor
R_c	Conventional radius of a rotor
r	Radius rotation of the point
r_m	Radius location of the mass element
T	Torque applied
T_{am}	Torque generated by the rate change in the angular momentum
$T_{ct.i}$, $T_{cr.i}$, $T_{in.i}$	Torque generated by the centrifugal, Coriolis and inertial forces, respectively, about axis i
t	Time interval
V	Linear velocity
x_c, y_c	Centroid about axis ox and oy, respectively

V_{in}	Initial linear velocity
V_e	Extra linear velocity
U	Potential energy
W	Weight of a gyroscope
ω	Angular velocity
ω_e	Extra angular velocity
ω_p	Angular velocity of precession
ω_i	Angular velocity of precession about axis i
ω_{in}	Initial angular velocity
ω_u	Ultimate angular velocity
α	Acceleration, an angle of rotation
a_{cr}	Coriolis acceleration
α_i	Component of acceleration around axis i
α_t	Tangential acceleration
α_r	Radial acceleration
ε	Angular acceleration of a rotating point
$\Delta\alpha$	Small angle of rotation
Δf_i	Change in the axial component of the force about the axis i
ΔV	Change of magnitude of a velocity
γ	Angle of rotation, inclination, tilting, position
$\Delta\gamma$	Small angle of rotation, inclination, tilting

Chapter 1
Gyroscopic Effects in Engineering

1.1 A Short History of Gyroscopic Effects and Applications in Engineering

Numerous fundamental publications present extensive information regarding a mechanical gyroscope, which is a simple mechanism with a rotating disc. Definitions of a gyroscope describe it as a device for measuring or maintaining orientation, based on the principles of the rotating disc angular momentum. In the initial stages of the history of mechanics, specific properties of rotating objects were studied by the famous mathematician L. Euler (1707–1783), who formulated equations of the rotational motion of a rigid body around a fixed pivot point. His theory of the motion of rigid bodies (1765) became a seminal contribution to the contemporary theory of gyroscopes. The phenomenon of preserving a position in inertial space of a self-balancing fast-spinning body around its symmetry axis attracted the attention of many outstanding scientists, paving the way for the formulation of the known gyroscope theory.

The gyroscope theory is based on a branch of mechanics dealing with the rotational motion of a rigid body around a fixed point. The development of the theory of spinning bodies ensued from the works of I. Newton (1642–1726), J. L. R. D'Alembert (1717–1783), Lagrange (1736–1813), L. Poinsot (1777–1859), L. Foucault (1819–1868), S. D. Poisson (1781–1840), Lord Kelvin (1824–1907) and other famous scientists and researchers. The French mathematician P.S. Laplace (1749–1827) was the first that proposes some type of gyro-compass that insensitive to a magnetic field. Other brilliant scientists investigated, developed and added new interpretations of the gyroscopic effects, as displayed in the rotor's persistent maintenance of its plane of rotation [1].

The applied theory of gyroscope emerged mainly in the twentieth century; however, the first attempts at a practical application of gyroscopes had been made much earlier. In the nineteenth century, L. Foucault decided to prove the existence of the Earth's rotation in 1852 experimentally. To this end, he put a fast-spinning, axially symmetric body in a Cardan joint and called the device a gyroscope. However,

© The Editor(s) (if applicable) and The Author(s), under exclusive license to Springer Nature Singapore Pte Ltd. 2020

R. Usubamatov, *Theory of Gyroscopic Effects for Rotating Objects*,
https://doi.org/10.1007/978-981-15-6475-8_1

not all the results were convincing due to technical and theoretical difficulties. The main challenges concerned the considerable friction in the bearings of the Cardan suspension rings, and the imperfection of a mathematical model did not give the ability to describe the gyroscopic effects. L. Foucault demonstrated the possibility of using a gyroscope to determine the meridian line at any given latitude. However, scientific and engineering problems delayed practical applications of gyro-compass, which appeared in the early twentieth century. Since L. Foucault's experiments, the history of the development of gyroscopes developed along the way to increase the load torques and an increase in the angular velocity of gyroscopes.

Nevertheless, modern gyroscope theories have not been clearly distinguished from theoretical principles formulated in past centuries. L. Euler's principle of the change in the angular momentum of the spinning rotor based on the conservation of kinetic energy is still considered fundamental. G. Greenhill, in the book Gyroscope theory (1914), presents a simplified treatment of gyroscope properties [2]. Other gyroscopic theories do not match practice, i.e. there has not been a complete gyroscope theory for centuries. This fact is an unusual phenomenon in the science of classical mechanics that solving more complex problems rather than defining mathematical models for torques acting on a simple rotating disc [3, 4]. Researchers have developed the numerical modelling of the gyroscopic effects (Klein and Sommerfield 1913) for solutions in engineering, which later used for the software [5].

The objectives of the gyroscope theory are the presentation of mathematical models of forces and motions for rotating objects with qualitative verification. The theory of gyroscopes is a very important aspect of the dynamics of rotating objects. Gyroscopic effects are relayed in many engineering calculations of rotating parts, and to derive a complete gyroscope theory is a crucial challenge. The contemporary gyroscope theory in classical mechanics is one of the most complex and intricate in terms of analytic solutions. The known numerical modelling of gyroscopic motions in Lagrange's equations, 3-D presentation, is mainly based on severe mathematics and software. These statistical and mathematical models of gyroscope motions are used for digital solutions of engineering problems linked with gyroscopic effects.

Researchers of the gyroscopic effects intuitively pointed out that inertial forces act in gyroscopic effects. However, this statement did not formulate in mathematical models. Most textbooks describe the unexplained gyroscopic effects using severe 3-D mathematics, which is not very helpful for developing physical intuition and engineering calculations. Artificial terms present the action of unexplainable inertial forces on rotating objects. These expressions are gyroscopic couples, resistance, precessions and attributed by fantastic properties as a non-inertial and non-gravitational system, etc. Such delusions originated from the absence of knowledge and mathematical models relating to the internal inertial forces acting on a rotating object. This is the reason that for centuries, researchers are still trying to resolve the gyroscopic problems via intricate theories. Since the Industrial Revolution, probably tons of publications and dozens of approaches have been dedicated to the gyroscopic effects. Even today, every year, around a hundred manuscripts with solutions to the gyroscopic problems are published in journals. This fact demonstrates that gyroscopic effects remain unsolved until recent times.

What is the main reason for such phenomena of gyroscopic effects? The answer is simple; researchers did not pay attention to the action of distributed masses of the rotating objects. They considered only the operation of their centre mass. Recent research demonstrated the correctness of this statement and mathematical models for the inertial forces generated by rotating distributed masses validated that. This book presents the theory of dynamics of rotating objects that removed all artificial terms that formed "gyroscope mystery" from the glossary of engineering mechanics. This theory of dynamics of rotating objects is based only on the known fundamental principles of classical mechanics.

The history of gyroscopic devices is fascinating and exciting to trace evolution. The tops, rotating discs and their varied applications (Fig. 1.1) present the most straightforward gyroscopic tools. Tops were invented in different civilizations thousands of years ago and still attract attention by their unusual behaviour and amazing unique gyroscopic properties. The top is one of the most remarkable and widely recognized toys in the world. Scientists have realized the importance of studying and understanding their spin and from there to develop a vast number of practical applications in engineering. Until the contemporary time, numerous devices, including the flight instruments, gyro-compass, autopilot, gyroscopic devices of stabilization and navigation for ships, airplanes, space stations and satellites, are widely used the inertial gyroscopes.

A mechanical gyroscope presents a system containing a heavy metal disc or rotor, universally mounted with three degrees of freedom: spinning freedom at about an axis perpendicular to its centre; tilting freedom at about a horizontal axis at right angles to the spin axis and veering freedom around a vertical axis perpendicular to both other axes. The three degrees of freedom are obtained by mounting the rotor

Fig. 1.1 Tops and gyroscope applications

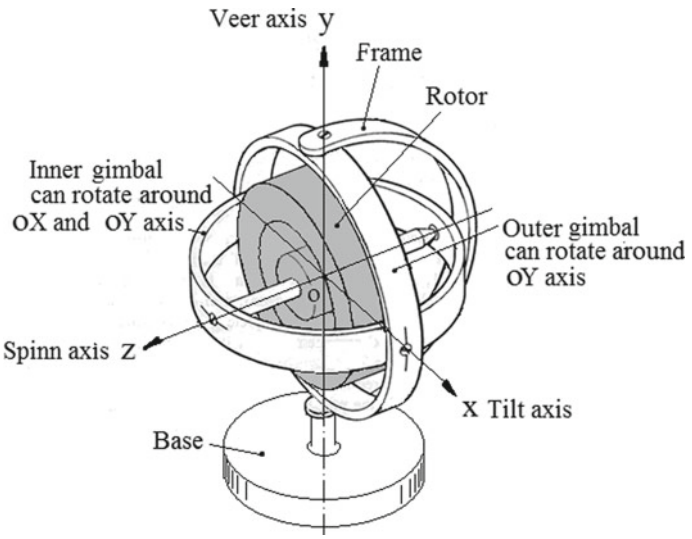

Fig. 1.2 Mechanical gyroscope and its components

in two concentrically pivoted rings called inner and outer rings or gimbals. The laboratory gyroscope presents this construction in Fig. 1.2.

The whole assembly is known as the gimbal system of a free or space gyroscope. The gimbal system is mounted in a frame with supports and base so that it is in its normal operating position. All axes of a gyroscope are at right angles to one another and intersect at the centre of the rotor's gravity. Such a gyroscope is called static or balanced, whereas, on the contrary case, it is called heavy. The rotor's centre of gravity can be in a fixed position or may be offset from an axis of oscillation. For the latter one, the rotor's centre of gravity and its centre of suspension do not coincide. A spinning rotor is journaled to spin around one axis, in which the axle defines the spin axis.

The journals of the rotor are mounted on an inner gimbal; the inner gimbal is journaled for oscillation in an outer gimbal for two gimbals. The outer gimbal is mounted on pivot about an axis. Its design has the supports on the frame located on a base or platform. This outer gimbal possesses one degree of rotational freedom, while its axis possesses none. The next inner gimbal is mounted in the gyroscope outer gimbal to pivot about an axis in its plane, which is always perpendicular to the pivotal axis of the gyroscope outer gimbal. This inner gimbal has two degrees of rotational freedom. The spinning rotor responds to a force applied at about the input axis by reaction forces about the output axis. The spinning rotor that is mounted on a set of gimbals can simultaneously rotate around the other two axes and is free to turn in any direction about the fixed point. Hence, if the gimbals are tilted in any direction, the spinning rotor remains in the original plane. This peculiarity of the gyroscope design is used to measure the pitch, roll and yaw attitude angles in an aircraft, ships and others.

The gyroscope manifests several interesting properties, which can be observed in rotating celestial bodies, artillery shells or projectiles, tops, turbine rotors on aircraft, ships and other mechanisms and machines. The gyroscope forced motion generates resistance and precession torques. The latter one expresses the movement that is called precession. The action of the system of inertial torques represents the rotational motions around axes is called the gyroscopic effects. The system will not exhibit any gyroscopic effects unless the rotor is spinning. If the rotor is made to rotate at high-speed and displaced at about its axis, then the rotor torques manifest valid gyroscope properties that possess essential fundamental functions. The gyroscopic device orientation remains nearly fixed, regardless of the mounting platform motion.

The permanent orientation of a gyroscope in space is made manifest when the following conditions are met (Fig. 1.2): external torque is applied to the gyroscope's spinning rotor, and gyroscope's axis of rotation must be capable of changing its orientation in space.

If the gyroscope is subjected to an external torque tending to rotate around some axis, the external torque generates several inertial torques of the spinning rotor. These conditions demonstrate the following properties:

- The rotor's axis *oz* of the gyroscope starts to rotate (precession) in a right angle direction to the external torque.
- Simultaneously, the gyroscope, as well as its gimbals, starts to turn around axes *ox* and *oy* but with different angular velocities and minor accelerations.
- The gyroscope spinning rotor will be resisted to change its axis location. If the action of the external torque ceases, then precession ceases simultaneously.
- The axis of the gyroscope may manifest nutation, which consists of small, but fast oscillations of the axis at about its mean position. The gyroscope's slow oscillations with large amplitudes are called galloping.

Gyroscopic properties form the basis of various devices and instruments that are widely applied in modern engineering technology for the following: determination of the horizon or geographic meridian; measurement of translational motions and angular velocities of moving objects and for many other purposes. The gyroscopic property was used for gyro-compasses that passed in design from simple constructions to complex and perfect ones. The gyro-compasses were designed in different industrial countries by the following researchers: J. Serson (1743), G. J. Bohnenberger (1817), W. R. Johnson (1832), M. G. van den Bos (1885), Obri (1898), H. Anschütz-Kaempfe (1908), and E. Sperry (1911) [6–11].

Following continual improvements to these types of gyro-compass came modern devices that replace magnetic compasses in ships, aircraft, spacecraft and vehicles in general. A gyro-compass is the oldest aeronautic gyroscopic instrument pointing in a northern geographic direction. The rotation of an airplane about the gyroscope is transmitted on a 360-degree scale. Presently, gyroscopes are widely applied in control systems of flying objects and gyroscopic stabilizers. As aviation continues to develop, vertical gyroscopes and course gyroscopes were commonly used as pilotage instruments necessary for flights without any external visual reference on the ground. The mechanical gyroscope is the one most known in engineering and still has wide

Fig. 1.3 Autopilot gyroscope and gyro-compass

application as a flight instrument and navigation system. Typical assembled gyro-compass devices are presented in Fig. 1.3.

Nevertheless, new gyroscopes in which physical principles are different replace mechanical gyroscopes because they possess better technical characteristics. Contemporarily, gyroscopes are represented by different designs—from mechanical to laser, optic, quartz and integrating systems with various technical features and physical principles of work [12–16]. All groups of gyroscopes are different by the operating laws, improvements in designs in terms of performance and the cost. The various indicators of gyroscopes determine their scope in industries. Figure 1.4 demonstrates the gyroscope characteristics, their factor stability as a function of the bias stability, which the primary problem is related to the error in measuring the angular velocity [14].

The extremely sensitive gyroscopes are based on operating principles such as electronic, micro-electro-mechanical systems with a vibrating ring, fibre optic, laser, piezoelectric, fork and integrating systems. These types of gyroscopic devices are

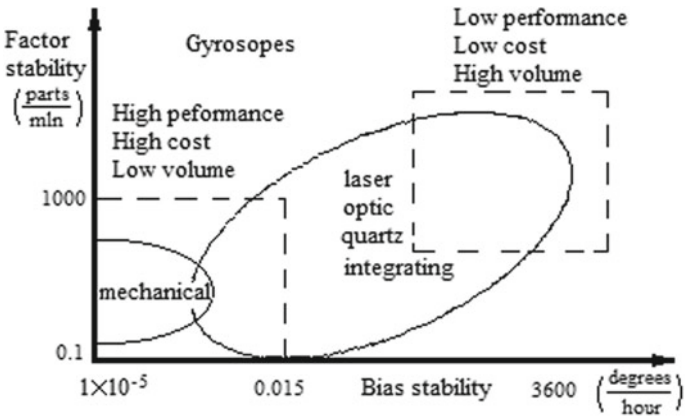

Fig. 1.4 Factor stability as a function of the bias stability of gyroscopes

not considered in the book because the principles of their work are different that should have different methods for mathematical modelling of their properties.

Observation of the different designs and properties of the gyroscope makes it possible to summarize the applications of gyroscopes in engineering. The gyroscope's acting forces and motions are calculated for devices of directional control, as reactions in the bearings of any moving vehicles with rotating components such as jet engines, electric motors, spinning discs, etc. The change in the direction of gyroscopic devices in space generates the inertial torques of the spinning rotor that acting on other components of the design. The action of the inertial torques results in the motions of gyroscopic devices that should be computed. These calculations allow for the use of mathematical models of motions and torques generated by the inertial forces of the spinning rotor.

1.2 Basic Principles of Engineering Mechanics for the Theory of Gyroscopic Effects

The gyroscope theory is based on mathematical models, which describe the forces and motions acting on the gyroscope by fundamental principles of classical mechanics. Classical mechanics consider the interrelations of the principle concepts, which are force, mass and movement. Newton's laws of motion and the first relating kinematic and dynamic quantities represent the interdependence of these physical concepts. Newtonian mechanics are based on the following concepts: the laws of motion are only valid for an inertial reference frame, the balance of momentum and the reaction principle. Newton's laws are derived from the three laws that are the conservation of energy, momentum and angular momentum that are central concepts of gyroscope theory [17–22].

The fundamental principles of classical mechanics enable for the formulating problems of gyroscope theory by accurate mechanical and mathematical models. The laws of classical mechanics are based on governing equations that are represented in gyroscope theory by the vector analysis of gyroscope forces, velocities and accelerations, the balance equations for mass, conservation of angular momentum and energy. Hence, the gyroscope, which primary component is spinning rotor, has mass, produces forces and the same laws, principles and definitions that are represented above describe motions.

Physical quantities are used for the qualitative and quantitative description of gyroscopic effects [22]. They represent measurable properties of physical items. Every specific value of a quantity can be written as the product of a number and a unit. Base quantities are defined independently in a way that all quantities are derived by multiplication or division. The physical quantities are presented in the International System of Units (SI) documented by ISO 1000. The SI base units form a set of mutually independent dimensions as required by dimensional analysis commonly

Table 1.1 Fundamental physical quantities of SI units applied to gyroscope theory

Base quantity		Symbol	SI base unit	Dimension
Length		l	Metre (m)	L
Plane angle		θ	Radian, degree (rad)	1
Mass		m	Kilogram (kg)	M
Time		t	Second (s)	T
Velocity	Linear	$\vec{v}$	m/s	$L\,T^{-1}$
	Angular	ω	rad/s	T^{-1}
Acceleration	Linear	$\vec{a}$	m/s^2	$L\,T^{-2}$
	Angular	ω_a	rad/s^2	T^{-2}
Force		$\vec{F}$	Newton ($N = kg\ m\ s^{-2}$)	$M\,L\,T^{-2}$
Torque		T	Newton-metre (N m)	$M\,L^2\,T^{-2}$
Energy			Joule (J)	$M\,L^2\,T^{-2}$
Work		W	Joule (J)	$M\,L^2\,T^{-2}$
Power		P	Watt (W)	$M\,L^2\,T^{-3}$
Moment of inertia		I	$kg\ m^2$	$M\,L^2$
Angular momentum		L	$kg\ m^2/s$	$M\,L^2\,T^{-1}$
Area		A	A	L^2
Volume		V	V	L^3
Weight		w	W	$M\,L\,T^{-2}$

employed in science and technology. The fundamental physical quantities applied to the gyroscope theory are represented in Table 1.1.

The complexity of acting forces and motions on gyroscopic devices is represented by the gyroscope theory that is formulated on the following fundamental laws and principles of engineering mechanics. Mathematical equations express formulated principles and rules that applied for gyroscope theory.

The concept of velocity and acceleration. Velocity and acceleration are essential concepts in kinematics, the branch of classical mechanics that describes the motion of an object. The velocity of an object is the rate of change of its position to a frame of reference and is a function of time. Velocity is a physical vector quantity; both magnitude and direction are needed to define it. Speed is expressed for two types of motions that are linear and angular.

The linear velocity is represented by the following:

$$v = s/t,\ (\text{m/s}),\ [\text{LT}^{-1}] \tag{1.1}$$

where s is the distance, t is the time.

The angular velocity of an object is the time rate of change of its angular displacement relative to the origin. Angular velocity is represented by the following:

$$\omega = \gamma/t, \text{(rad/s)}, [\mathrm{T}^{-1}] \tag{1.2}$$

where γ is the angle, t is the time.

The acceleration is the rate of change of velocity of an object concerning time. Acceleration is a physical vector quantity; both magnitude and direction are needed to define it. Acceleration is expressed for two types of motions that are linear and angular. *The acceleration* is represented by the following:

$$a = v/t, \left(\mathrm{m/s}^2\right), [\mathrm{LT}^{-2}] \tag{1.3}$$

The angular acceleration is represented by the following:

$$\varepsilon = \omega/t, \left(\mathrm{rad/s}^2\right), [\mathrm{T}^{-2}] \tag{1.4}$$

where ω is the angular velocity, t is the time.

The radial, tangential and angular acceleration of circular motion. Uniform circular motion is an example of a body experiencing acceleration resulting in the velocity of constant magnitude but the change of direction. In this case, because the course of the object's motion is continually changing, being tangential to the circle, the object's linear velocity vector also varies, but its speed does not. This acceleration is a radial acceleration which is directed towards the centre of the circle and takes the magnitude. *The radial acceleration* is represented by the following:

$$a = v^2/r, \left(\mathrm{m/s}^2\right), \left[\mathrm{LT}^{-2}\right] \tag{1.5}$$

where v is the object's linear speed along the circular path of radius r. Equivalently, the radial acceleration vector a may be calculated from the object's angular velocity:

$$a = -r\omega^2, \left(\mathrm{m\ rad/s}^2\right), \left[\mathrm{LT}^{-2}\right] \tag{1.6}$$

where r is a vector directed from the centre of the circle and equal in magnitude to the radius. The negative shows that the acceleration vector is directed towards the centre of the circle (opposite to the radius).

With a non-uniform circular motion, a tangential acceleration is produced equal to the rate of change of the angular speed around the circle times the radius of the circle.

The tangential acceleration is represented by the following

$$a_t = r\varepsilon, \left(\mathrm{m\ rad/s}^2\right), \left[\mathrm{LT}^{-2}\right] \tag{1.7}$$

The tangential acceleration is directed at right angles to the radius vector and takes the sign of the angular acceleration a_t. [22].

Newton's Second Law. Every object in a state of uniform motion tends to remain in that state of motion unless an external force is applied to it; the relationship between

an object's mass m (kg), its acceleration a (m/s^2), and the applied or inertial force F (N) is product of a mass and an acceleration that is

$$F = ma, \left(N = \text{kg m/s}^2\right), [\text{M L T}^{-2}] \tag{1.8}$$

Acceleration and force are vectors, which direction is the same; for every action, there is an equal and opposite reaction. Newton's Second Law applies to a wide range of physical phenomena, where the force is the net external force.

The concept of moment of rotational inertia. The moment of the rotational inertia of a rigid body determines the torque needed for a desired angular acceleration about a rotational axis. It depends on the body's mass distribution, and the axis is chosen. The moment of rotational inertia of the object, J, is defined as the ratio of an applied torque T to the angular acceleration ε along a principal axis of the object, $T = J\varepsilon$. The moment of inertia of the object J is the product of the mass m and radius r squared of location mass,

$$J = mr^2, (\text{kg m}^2), [\text{M L}^2] \tag{1.9}$$

where r is the radius of gyration.

The concept of parallel axis theorem of mass moment of inertia. The equation of the parallel axis theorem defines the mass moment of inertia of the object relative to an alternate parallel axis. The following equation presents a parallel axis transfers equation of mass moment of inertia from i-axis to a parallel x-axis:

$$J_x = J_i + ml^2, (\text{kg m}^2), [\text{M L}^2] \tag{1.10}$$

where l is the perpendicular distance between the two parallel axes, other parameters are as specified above.

The concept of conservation of angular momentum. Conservation of angular momentum is a physical property of a spinning system such that its spin remains constant unless it is acted upon by an external torque. The angular momentum vector of a point particle is parallel and directly proportional to the angular velocity vector ω of the particle, where the constant of proportionality depends on both the mass of the particle and its distance from the origin. The total angular momentum of any rigid object contains two main components: the angular momentum of the centre of mass about the origin, plus the spin angular momentum of the object about the centre of mass. Torque can be defined as the rate of change of angular momentum. Angular momentum is a vector and measure of the amount of rotation an object has, taking into account its mass, shape and speed. For a rigid body rotating around an axis of symmetry, the angular momentum H is expressed as the product of the body's moment of inertia J and its angular velocity ω. The angular momentum represents the product of a moment of inertia, and angular speed about a particular axis is as follows:

$$H = J\omega, \left(\text{kg m}^2 \text{ rad/s}\right), \text{M L}^2 \text{ T}^{-1} \tag{1.11}$$

where J is the moment of inertia of the object.

The Concept of centrifugal force. The centrifugal force is an inertial force directed away from the axis of rotation that appears to act on all objects when viewed in a rotating frame of reference. The equation of the centrifugal force for the objective of the circular motion is as follows.

$$F = ma = m\omega^2 r = mv^2/r, (N = \text{kg m s}^{-2}), \left[\text{M L T}^{-2}\right] \tag{1.12}$$

The Concept of Coriolis acceleration and force. The Coriolis force is an inertial force that acts on objects that are in motion relative to a rotating reference frame. Newton's laws of motion describe the motion of an object in an inertial (non-accelerating) frame of reference. When Newton's laws are transformed into a rotating frame of reference, the Coriolis force and centrifugal force appear. Both forces are proportional to the mass of the object. The Coriolis force is equivalent to the rotation rate, and the centrifugal force is proportional to the square of the rotation rate. The Coriolis force acts in a direction perpendicular to the rotation axis and the velocity of the body in the rotating frame. It is proportional to the object's speed in the rotating frame. The centrifugal force acts outwards in the radial direction and is equivalent to the distance of the body from the axis of the rotating frame. These additional forces are termed inertial forces.

In non-vector terms: the magnitude of Coriolis acceleration of the object is proportional to the velocity of object and to sine of the angle between the motion of object and axis of rotation.

The vector formula for the magnitude and direction of the Coriolis acceleration is derived through vector analysis and is presented by two expressions.

$$a_c = -2v\omega \quad \text{and} \quad a_c = -v\omega, (\text{m/s}^2), \left[\text{L T}^{-2}\right] \tag{1.13}$$

where a is the acceleration of the particle in the rotating system, v is the velocity of the particle concerning to the rotating system, and ω is the angular velocity vector having a magnitude equal to the rotation rate ω, with a direction along the axis of rotation of the rotating reference frame. This book uses the second expression that described and validated in Chap. 2.

The equation may be multiplied by the mass of the relevant object to produce the Coriolis force:

$$F_c = -ma_c = -mv\omega, (\text{kg m/s}^2), \left[\text{M L T}^{-2}\right] \tag{1.14}$$

The Coriolis effect is the behaviour added by the Coriolis acceleration. The formula implies that the Coriolis acceleration is perpendicular both to the direction of the velocity of the moving mass and to the frame's rotation axis [23–25].

The principle of conservation of mechanical energy. In the physical sciences, mechanical energy is the sum of potential energy and kinetic energy. It is the energy associated with the motion and position of an object. The principle of conservation of mechanical energy states that in an isolated system that is only subject to conservative forces, the mechanical energy is constant. If an object is moved in the opposite direction of a conservative net force, the potential energy will increase, and if the speed of the object is changed, the kinetic energy of the object is changed as well. In all real systems, frictional forces and other non-conservative forces are present. The difference between a conservative and a non-conservative force is that when a conservative force moves an object from one point to another, the work done by the conservative force is independent of the path. On the contrary, when a non-conservative force acts upon an object, the work done by the non-conservative force is dependent on the path.

Conservation laws in classical mechanics include conservation of mechanical energy, conservation of linear momentum and conservation of angular momentum. A conservation law is expressed mathematically as a continuity equation, a partial differential equation which gives a relation between the amount of the quantity, and the "transport" of that quantity. Energy is a scalar quantity, and the mechanical energy of a system is the sum of the potential and kinetic energy. The potential energy is measured by the position of the parts of the system. The kinetic energy is the energy of motion.

$$E_{\mathrm{m}} = U + K, \left(J = ml^2/t^2\right), [\mathrm{M\,L^2T^{-2}}] \tag{1.15}$$

The potential energy, U, depends on the position of an object subjected to a conservative force. It is defined as the object's ability to do work and is increased as the object is moved in the opposite direction of the force. Common types of potential energy include the gravitational potential energy of an object that depends on its mass and its distance from the centre of mass of another object and the elastic potential energy of extended spring.

Gravitational potential energy is https://en.wikipedia.org/wiki/Mechanical_energy-cite_note-tamuk-5

$$U = mgh, \left(\mathrm{kg}\ \left(\mathrm{m/s^2}\right)\ \mathrm{m}\right) \quad \text{or } (\mathrm{N\ m}), \left[\mathrm{M\,L^2\ T^{-2}}\right] \tag{1.16}$$

where m is the mass of the object, g is the gravity acceleration, and h is the position in height of the object. The dimension of the energy is N m = Joule.

The potential energy of a linear spring exerts a force $F = (-kx, 0, 0)$ that is proportional to its deflection in the x direction. The function of the potential energy of a linear spring is

$$U_x = -(1/2)kx^2, (\mathrm{N\ m}), \left[\mathrm{M\,L^2\ T^{-2}}\right] \tag{1.17}$$

Elastic potential energy arises as a consequence of a force that tries to restore the object to its original shape. If the stretch is released, the energy is transformed into kinetic energy.

The kinetic energy, K, of an object is the energy that it possesses due to its motion. It is defined as the work needed to accelerate an object of a given mass from rest to its stated velocity. The object maintains this kinetic energy unless its speed changes. The same amount of work is done by the object when decelerating from its current speed to a state of rest. The kinetic energy of a non-rotating rigid object depends on its mass as well as its speed. It is defined as one half the product of the object's mass with the square of its speed.

$$K = (1/2)mv^2, \text{(N m)}, \left[\text{M L}^2\ \text{T}^{-2}\right] \tag{1.18}$$

where m is the mass and v is the speed of the object.

If a rigid body is rotating about any line through the centre of mass, then it has *rotational kinetic energy* which is simply the sum of the kinetic energies of its moving parts and is thus given by:

$$K = (1/2)J\omega^2, \text{(N m)}, \left[\text{M L}^2\ \text{T}^{-2}\right] \tag{1.19}$$

where ω is the body's angular velocity; r is the distance of any mass from that line; J is the body's moment of inertia.

In this equation, the moment of inertia must be taken about an axis through the centre of mass, and the rotation measured by ω must be around that axis; more general equations exist for systems where the object is subject to wobble due to its eccentric shape. Objects at rest have no kinetic energy.

The concept of the work. The work is the energy associated with the action of a force. The work is a displacement of the object of application in the direction of the force. Work is calculated as the product of the force and the distance through which the body moves. The formulae for computing work are as follows:

$$W = Fs, \text{(N m)}, \left[\text{M L}^2\ \text{T}^{-2}\right] \tag{1.20}$$

where F is the force; s is the distance.

The concept of power. Power is the rate of doing work or the rate of using energy, which is numerically the same. The work (joule) in one second is power (watts). The formulae for computing power are

$$P = \text{W/t}, \left(ml^2t^{-3}\right) = \text{(J/s)}, [\text{M L}^2\ \text{T}^{-3}] \tag{1.21}$$

where t is time.

The axioms of engineering mechanics are formulated as balance laws or conservation laws for mechanical quantities like mass, momentum, energy, etc., and established as equations of integrals over a material object or as local equations. These

fundamental equations are formulated in Euler's form, which means that all quantities are expressed as functions of the coordinates of a material point in the actual configuration. The kinetic energy and external work applied to a gyroscope, the postulate of the balance of mechanical energy, can be formulated as follows: the real-time rate of the total energy of an object is equal to the sum of the rate of work done by external forces acting on a gyroscope. The balance of mechanical energy presents the problem that formulated the system where all forces are balanced.

The principle of virtual work for a rigid body in space is presented by the constraint of rigidity that expressed all acting forces should be zero. The energy balance equations of forces acting in gyroscope represent extreme principles for energy type quantities, like work, kinetic energy, etc. In engineering, a constitutive equation is a relation between two physical quantities that are specific to an object and approximates the response of that object on applied forces. They are combined with other equations governing physical laws to solve physical problems as the connection between applied forces to motions.

All presented above laws; equations are universal and valid for the gyroscope. For gyroscope effects and properties, it is necessary to find the general mathematical models of acting gyroscope forces and motions. For solution should be used certain basic principles of material theory and formulate criteria to classify the gyroscope effects to obtain concrete models for certain motions of the gyroscope. Practical experiments and tests should validate formulated analytic models of the gyroscope effects.

Gyroscopic effects are based on the specific and deterministic relation between acting forces and motions. Several variable components represent the mathematical model of this relation in a functional form. A common practice in mechanics is accepted as the following: the acting forces are independent variables, and motions are dependent ones. The completely external and internal acting forces that are invariants determine the movements of a gyroscope, at a specific instant of time. This principle is substantial restrictions on the gyroscopic effects that enable for generating of motions of defined magnitude to the inertial system.

References

1. Newton, I.: The Principia: Mathematical Principles of Natural Philosophy. [S.l.]. Snowball Publcations (2010)
2. Greenhill, G.: Report on Gyroscopic Theory. Relink Books, Fallbrook (2015)
3. Deimel, R.F.: Mechanics of the Gyroscope. Dover Publications Inc., New York (2003)
4. Awrejcewicz, J., Koruba, Z.: Theory of gyroscopes. In: Classical Mechanics, pp. 125–147. Springer Science + Business Media, Nature, New York
5. Klein, F., Sommerfeld, A.: The Theory of the Top. I–IV, pp. 2008–2014. Springer, Birkhäuser, New York (2008)
6. Range, Sh.K., Mullins, J.: Brief History of Gyroscopes (2015)
7. King, A.D.: Inertial navigation—forty years of evolution. GEC Rev. **13**, 140–149 (1998)
8. NASA. Available online: https://solarsystem.nasa.gov/news/2005/03/14/brief-history-of-gyroscopes. Accessed on 24 June 2017

9. Iurato, G.: On the historical evolution of gyroscopic instrumentation: a very brief account (2015). HAL Id: hal-01136829. https://hal.archives-ouvertes.fr/hal-01136829
10. Turner, G.: Gyroscopes, 1st ed. Brightfusion Ltd., London (2007)
11. Elliott-Laboratories: The Anschutz Gyro-Compass and Gyroscope Engineering, pp. 7–24. Wexford College Press, Kiel, Germany (2003). ISBN 978-1-929148-12-7
12. Xie, H., Fedder, G.K.: Integrated microelectromechanical gyroscopes. J. Aerosp. Eng. **16**, 65–75 (2003)
13. Zhanshe, G., Fucheng, C., Boyu, L., Le, C., Chao, L., Ke, S.: Research development of silicon MEMS gyroscopes: a review. Microsyst. Technol. **21**, 2053–2066 (2015)
14. Passaro, V.M.N., Cuccovillo, A., Vaiani, L., et al.: Gyroscope technology and applications: a review in the industrial perspective. Sensors **17**, 2284 (2017). https://doi.org/10.3390/s17102284
15. Lefevre, H.: The Fiber Optic Gyroscope, 3rd ed. Artech House, London (1993). ISBN 9781608076963
16. Aronowitz, F.: The laser gyro. In: Ross, M. (ed.) Laser Applications, vol. 1. Academic Press, New York (1971). ISBN 0124319017
17. Germain, P., Piau, M., Caillerie, D.: Theoretical and Applied Mechanics. Elsevier, Amsterdam (2012)
18. Crew, H.: The Principles of Mechanics. BiblioBazaar, LLC, Charleston (2008)
19. Millard, B. F.: Principles of Engineering Mechanics: Dynamics—The Analysis of Motion. Springer, Berlin (2006)
20. Thornton, M.: Classical Dynamics of Particles and Systems, 5th ed. Brooks/Cole (2004)
21. Taylor, J.R.: Classical Mechanics. University Science Books, Sausalito (2004)
22. Resnick, R.; Walker, J.: Fundamentals of Physics, 7 Sub edition. Wiley, New York (2004)
23. Hibbeler, R.C.: Equations of Motion: Normal and Tangential Coordinates. Engineering Mechanics: Dynamics, 12th ed. Prentice Hall, Upper Saddle River (2009)
24. Dronkers, J.: Coriolis acceleration. Available from http://www.coastalwiki.org/wiki/Coriolis_acceleration (2017)
25. Usubamatov, R., Ismail, K.A., Sah, J.M.: Analysis of coriolis acceleration. J. Adv. Sci. Eng. Res. **4**(1), 1–8 (2014)

Chapter 2
Acceleration Analysis of Rotating Objects

2.1 Acceleration Analysis of a Rotating Object Around a Fixed Point

The gyroscope effects are generated by its primary component that is the spinning rotor, which mass moves with tangential, radial and axial velocities. The external torque applied to a gyroscope generates several internal inertial forces that are products of masses and accelerations. The latter should be computed with high accuracy. The most textbooks in classical mechanics represent the analysis of acceleration of the rotating mass in a form that calls into question due to uncertainty in solution and needs in-depth analysis [1–4]. The studies of these accelerations are conducted with assumptions that should have solid mathematical validations for the components of equations. Mathematical models of accelerations of spinning mass should be considered in detail without simplifications. The incorrectness in a formulation of accelerations for rotating mass is resulting in wrong equations and magnitudes of inertial forces and velocities of moving objects.

The variable velocity of a moving point in a general path is the vector quantity, which has both magnitude and direction and can be tangential and radial components. The value and the course of the velocity vector can change over time because acceleration is the time rate of velocity changes. Acceleration analysis is essential because inertial forces are proportional to their rectilinear and angular accelerations accordingly. For motion about a fixed point, angular acceleration should be defined for a change in the value and direction of angular velocity. Hence, angular acceleration is not directed along the instantaneous axis of rotation. The loads must be determined in advance to ensure that a machine is adequately designed to handle these dynamic loads. For planar motion, the vector direction of acceleration is commonly separated into the tangential and radial components of a point on a rotating object.

The most textbooks in physics, kinematics and dynamics of machinery consider the magnitude of a radial acceleration at the condition when an object rotates with a constant angular velocity [5–8]. The value of the tangential acceleration is considered based on acceleration for a rotating object. Such a condition of presentation of

© The Editor(s) (if applicable) and The Author(s), under exclusive license to Springer Nature Singapore Pte Ltd. 2020

R. Usubamatov, *Theory of Gyroscopic Effects for Rotating Objects*,
https://doi.org/10.1007/978-981-15-6475-8_2

magnitudes for two components of acceleration presents the unfounded mathematical approach and vagueness of solution for acceleration analysis for the rotating. The new analytic expressions for the radial and absolute accelerations of a rotating point cover the gap in the theoretical study of acceleration analysis.

The known publications demonstrate that curvilinear motion of an object with variable speed is going on with a linear acceleration, which is commonly separated into two elements: tangential and centripetal or radial components of acceleration. The tangential component is changed in the magnitude of the linear velocity vector, and its direction is perpendicular to the line that connects the point with the centre of rotation. The radial component is changed proportionally to change of the linear velocity vector, and its direction is always towards the centre of the rotating point. These two components are mutually perpendicular. An expression of an absolute acceleration α of an object is the vector sum of the tangential αt and radial αr components as shown by fundamental equation [9, 10]:

$$\bar{\alpha} = \bar{\alpha}_{\mathrm{t}} + \bar{\alpha}_{\mathrm{r}} \quad \text{or} \quad a = \sqrt{a_t^2 + a_r^2} \tag{2.1}$$

where α is an absolute acceleration; $\alpha_{\mathrm{t}} = r\varepsilon$ is a tangential acceleration and $\alpha_{\mathrm{r}} = r\omega^2$ is a radial acceleration; ε is an angular acceleration; r is a radius of rotation; ω is an instantaneous angular velocity of rotation of an object.

Substituting defined components into Eq. (2.1) and transformation yields the expression of absolute acceleration of a rotating an object that has the following equation:

$$\alpha = r\sqrt{\varepsilon^2 + \omega^4} \tag{2.2}$$

where all components are as specified above.

Radical expressions of absolute and radial accelerations Eqs. (2.1) and (2.2) presented in textbooks and handbooks [11, 12]. Nevertheless, these accepted equations of the accelerations contain simplification, and assumptions do not give accurate results in computing. This statement is presented and confirmed by the following analysis. In classical mechanics, an angular velocity of a rotating object with acceleration is variable at the time. Expression of tangential acceleration (Eq. (2.1)) is formulated at the condition of an object rotation with angular acceleration, ε. The radial acceleration (Eq. (2.1) is formulated at the condition of constant angular velocity, ω of a rotating object, i.e. no angular acceleration. This analytical formulation of the absolute acceleration combines tangential and radial accelerations that contradict each other. The angular velocity of a rotating object is variable due to its angular acceleration. At the condition when an angular velocity is constant, the rotating object does not have a tangential acceleration.

Equation (2.2) contains logical and mathematical vagueness that results in the incorrect magnitude of centrifugal and inertial forces and the magnitude of the absolute acceleration of a rotating object. Some textbooks present a variable angular velocity of a rotating object by adding the component with acceleration for the

instant angular velocity ω. Such expression does not give more clarity because it does not have a strong validation of accepted assumptions. The calculation of an instant angular velocity ω for the rotating object is conducted by the following fundamental equation [13].

$$\omega = \omega_{\text{in}} + \varepsilon t \tag{2.3}$$

where ω is terminal angular velocity, ω_{in} is initial angular velocity, t is a time interval considered, other parameters specified above.

According to these assumptions, substituting Eq. (2.3) into Eq. (2.2) yields the equation of absolute acceleration of a rotating object that presented by the following expression:

$$\alpha = r\sqrt{\varepsilon^2 + (\omega_{\text{in}} + \varepsilon t)^4} \tag{2.4}$$

where all parameters are as specified above.

However, Eqs. (2.3) and (2.4) contain the vagueness. Equation (2.3) cannot be substituted into Eq. (2.2), due to the unfounded mathematical approach and incorrectness of initial conditions of acceleration analysis for the rotating object. An instant angular velocity ω has the component of an angular acceleration ε that represented by Eq. (2.3). This expression ω with the component of the acceleration is substituted into Eq. (2.2), which ω accepted for the condition of constant angular velocity, i.e., absent of the angular acceleration of rotating object, $\varepsilon = 0$. Such substituting of components is intolerable by mathematical logic. This condition is logical and mathematical vagueness in tangential and radial accelerations of rotating objects presented in the textbooks [9–13]. Nevertheless, there is an explicit dependency between these two components of accelerations of rotating objects about a fixed axis.

It is known that rotation of an object around a fixed axis with an angular acceleration gives steadily increasing angular velocity of its rotation. The magnitude of a centrifugal force and other inertial forces will increase with increasing angular velocity. Wrong calculation of acting inertial forces leads to an increase in the weight of a machine and reflects on the quality of its work. In such a case, experts cannot prove the disparity of mechanisms and devices due to the incorrect formula of the accelerations in textbooks, handbooks and standard methods for calculating forces acting on rotating components of machines. Fortunately, in reality, the magnitude of the radial and total acceleration is less than estimated by Eqs. (2.2) and (2.4). Users of these equations calculate the acceleration that gives high magnitude and mechanisms designed for high loads and stresses than have fewer values. This circumstance is the reason that devices do not have failures. However, the sufficient magnitude of the acceleration of machine elements leads to an increase in the sizes, weight and cost of machines that decrease their quality. The factors mentioned above impose a need to derive correct equations of the radial and absolute accelerations of a rotating object about a fixed axis.

An angular acceleration deals with a motion of a rigid object, and it is the time rate of change of its angular velocity. Figure 2.1 shows the link *op* with the radius *r* in a pure rotation, pivoted at point *o* on the *xoy* plane. A solution to the acceleration problem of a rotating object graphically requests only three equations: $V = \omega r$ is a linear velocity, αt is a tangential acceleration, and αr is a radial acceleration of a rotating object.

The corrected analytic approach considers acceleration analysis of the rotating object, which is subjected to a variable angular velocity. Figure 2.1 demonstrates two positions of the point *p* that are separated by an angle α. The velocity vector of the point *p* will change along the curvature of motion and due to a rotation with a variable speed. The magnitudes of linear velocities of initial V_{in} and final V_{fn} of the point *p* are different. Hence, the velocity polygon of the rotating point *p* is vectorially solved for these changes in the velocity, V_{c}.

$$V_{\text{c}} = V_{\text{in}} + V_{\text{fn}} \tag{2.5}$$

The vector, V_{c}, is the change in the linear velocity that can be presented by two vectors that are radial velocity V_{r} and tangential one V_{t}. The tangential velocity of any point on an object rotating about a fixed point is determined as the product of angular velocity and a radius of rotation, $V_{\text{t}} = r\omega$.

$$V_{\text{c}} = V_{\text{r}} + V_{\text{t}} \tag{2.6}$$

The radial velocity vector V_{r} to this curvature is directed towards the centre *o* of rotation and crosses the vector velocity V_{fn} at the point *f*.

The expression of the variable linear velocity of a point is given by the following equation:

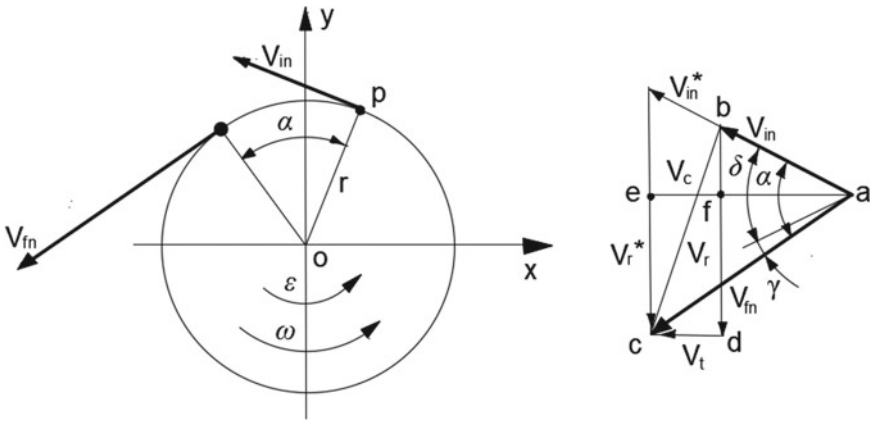

Fig. 2.1 Velocity vectors polygon of the rotating point

$$V_{\text{fn}} = r\omega_{\text{in}} + \varepsilon rt \tag{2.7}$$

where $V_{\text{in}} = r\omega_{\text{in}}$, ω_{in}—an initial angular velocity of a rotating point, and εrt is an extra velocity of a moving point due to an acceleration one, other parameters of equation are as specified above.

For the following analysis, the radial velocity vector V_{r} is represented as the sum of two vectors $V_{\text{r·bf}}$ and $V_{\text{r·fd}}$, of segments bf and fd, respectively (Fig. 2.1).

$$V_{\text{r}} = V_{\text{r·bf}} + V_{\text{r·fd}} \tag{2.8}$$

The small angle α is presented by the following expression $\alpha = \omega_{\text{in}}t + \frac{\varepsilon t^2}{2}$ that is the sector with the accelerated angular velocity of the rotating point p (Fig. 2.1). This sector is represented by the following components: $\alpha = \delta + \gamma$, where $\delta = \omega_{\text{in}}t$ is the sector with initial angular velocity and $\gamma = \alpha - \delta = \frac{\varepsilon t^2}{2}$ is the sector with accelerated angular velocity. The two components of Eq. (2.8) are expressed by the following equations:

$$V_{\text{r·bf}} = V_{\text{in}} \sin \delta/2 \tag{2.9}$$

$$V_{\text{r·fd}} = V_{\text{fn}} \sin(\delta/2 + \gamma) \tag{2.10}$$

where the vector $V_{\text{r·fd}}$ is presented by the segment fd= ec.

Substituting Eqs. (2.9) and (2.10) into Eq. (2.8) yields the following equation of the radial velocity for the rotating point p.

$$V_{\text{r}} = V_{\text{in}} \sin \delta/2 + V_{\text{fn}} \sin(\delta/2 + \gamma) \tag{2.11}$$

For the small angle, $\sin \varphi = \Delta\varphi$. Then, the change of the radial velocity (Eq. 2.11) is presented by the following equation:

$$\Delta V_{\text{r}} = V_{\text{in}}(\Delta\delta/2) + V_{\text{fn}}(\Delta\delta/2 + \Delta\gamma) \tag{2.12}$$

where defined above expressions of $V_{\text{in}} = \omega_{\text{in}}r$, $V_{\text{fn}} = \omega_{\text{in}}r + \varepsilon rt$, $\Delta\delta = \omega_{\text{in}}\Delta t$, and $\Delta\gamma = \varepsilon\Delta t^2/2$, which the change in the angle depends on the change in the time. Substituting defined parameters into Eq. (2.12), transformation and simplification yield the following equation:

$$\begin{aligned}\Delta V_{\text{r}} &= \omega_{\text{in}} r \frac{\omega_{\text{in}}\Delta t}{2} + (\omega_{\text{in}}r + \varepsilon tr)\left(\frac{\omega_{\text{in}}\Delta t}{2} + \frac{\varepsilon\Delta t^2}{2}\right) \\ &= \omega_{\text{in}}^2 r\Delta t + \frac{\omega_{\text{in}} r\varepsilon\Delta t^2}{2} + \frac{\varepsilon tr\omega_{\text{in}}\Delta t}{2} + \frac{\varepsilon^2 tr\Delta t^2}{2}\end{aligned} \tag{2.13}$$

In this case, the radial acceleration of the rotating point is expressed by the first derivative of Eq. (2.13) concerning to time

$$\frac{\mathrm{d}V_r}{\mathrm{d}t} = \omega_{\mathrm{in}}^2 r\frac{\mathrm{d}t}{\mathrm{d}t} + \frac{\omega_{\mathrm{in}} r\varepsilon}{2}\frac{\mathrm{d}t^2}{\mathrm{d}t} + \frac{\varepsilon t r\omega_{\mathrm{in}}}{2}\frac{\mathrm{d}t}{\mathrm{d}t} + \frac{\varepsilon^2 t r}{2}\frac{\mathrm{d}t^2}{\mathrm{d}t}$$
$$= \omega_{\mathrm{in}}^2 r\frac{\mathrm{d}t}{\mathrm{d}t} + \frac{\omega_{\mathrm{in}} r\varepsilon t}{4}\frac{\mathrm{d}t}{\mathrm{d}t} + \frac{\omega_{\mathrm{in}} r\varepsilon t}{2}\frac{\mathrm{d}t}{\mathrm{d}t} + \frac{\varepsilon^2 t^2 r}{4}\frac{\mathrm{d}t}{\mathrm{d}t} \tag{2.14}$$

where $\mathrm{d}V_{\mathrm{r}}/\mathrm{d}t = a_{\mathrm{r}}$ is the expression of the radial acceleration of a rotating point at the condition of a variable angular velocity.

Solving Eq. (2.14) and transformation yields the expression of the radial acceleration of the rotating point

$$a_{\mathrm{r}} = r\left[\omega_{\mathrm{in}}^2 + \frac{3}{4}\varepsilon t\omega_{\mathrm{in}} + \left(\frac{\varepsilon t}{2}\right)^2\right] \tag{2.15}$$

where all parameters are as specified above.

The equation of the absolute acceleration of a rotating point, with the variable angular velocity, obtained by substituting the tangential acceleration (a component of Eq. 2.2) and Eq. (2.15) of the radial one into Eq. (2.2). Converting and transformation of a defined equation give the following expression:

$$a = \sqrt{(\varepsilon r)^2 + \left\{r\left[\omega_{\mathrm{in}}^2 + \frac{3}{4}\varepsilon t\omega_{\mathrm{in}} + \left(\frac{\varepsilon t}{2}\right)^2\right]\right\}^2} = r\sqrt{\varepsilon^2 + \left[\omega_{\mathrm{in}}^2 + \frac{3}{4}\varepsilon t\omega_{\mathrm{in}} + \left(\frac{\varepsilon t}{2}\right)^2\right]^2} \tag{2.16}$$

The new equation of an absolute acceleration of a rotating object is significantly different from the fundamental equation that represented in textbooks, (Eq. (2.4) [13]. Analysis of Eq. (2.16) demonstrates the values of the radial and absolute accelerations are several times less than computed by Eq. (2.4). The new mathematical model for acceleration analysis of the rotating object is common and contains the correct presentation of its absolute and radial acceleration [14]. These new equations of accelerations enable for computing dynamic parameters of rotating objects about a fixed axis in engineering that gives accurate results than computed by a known method. In engineering, a machine works with a variable velocity of rotating components that are the real condition of the functioning of any mechanism. It is very important to calculate an exact result of acting forces for machine rotating components with acceleration. Calculation of the dynamic forces that are results of acceleration is important for the reliable work of a machine. Comparative analysis of Eq. (2.4) and Eq. (2.16) shows the following logical results:

1. The object rotates with a constant angular velocity, ω, and no an angular acceleration, $\varepsilon = 0$. Equations (2.4) and (2.15) convert to the expression $a = r\omega^2$ that is the known formula in classical mechanics.
2. The object starts to rotate when initial angular velocity $\omega_{\mathrm{in}} = 0$, and angular acceleration of a rotating object is ε. Equations (2.4) and (2.16) convert to the

expressions $a = r\sqrt{\varepsilon^2 + (\varepsilon t)^4}$ and $a = r\sqrt{\varepsilon^2 + [(\varepsilon t/2)^2]^2}$, respectively, that have different results.

3. The object rotates with an initial angular velocity ωin, and an angular acceleration of a rotating object is ε. Equations (2.5) and (2.16) have different expressions. The main incorrectness of Eq. (2.4) is the presentation of the radial acceleration αr at the condition of absent the angular acceleration $\varepsilon = 0$. Textbooks derive the expression of the radial acceleration when the tangential velocity of the rotating object is constant. Substituting the instant angular velocity by Eq. (2.2) that has the component of the angular acceleration $\varepsilon \neq 0$ is not a rightful solution.
4. Equation (2.4) of the absolute accelerations of the rotating object cannot give the correct result for transient conditions of the rotation with acceleration.
5. New Eq. (2.16) of an acceleration of the rotating object is common and can give correct results in the calculation of the acceleration at any conditions, i.e. start the rotation with acceleration, transient (rotation with acceleration) and stable rotation without acceleration.

The new acceleration analysis of a rotating object should be used in the educational process of kinematics and dynamics of machinery. In addition, engineers and researchers for analysis of a machine work at transient conditions can use the new equations of accelerations of a rotating object about the fixed axis. Computing the inertial forces generated by the rotating mass elements of spinning objects that manifest gyroscopic effects should be conducted by the derived equations of the acceleration presented above.

2.1.1 Case Study

The rotating object shown in Fig. 2.1 has the initial angular velocity of 10 rad/s, accelerates at the rate of 5 rad/s^2 and has the radius of rotation of 0.1 m. It is necessary to determine the magnitudes of the tangential component and the radial component of accelerations and absolute one of the point p after 5 s of rotation.

The radial acceleration is defined by Eq. (2.15) and the component of Eq. (2.4), which the results are shown as

- Solution by Eq. (2.15)

$$\begin{aligned} a_{\mathrm{r}} &= r\left[\omega_{\mathrm{in}}^2 + \frac{3}{4}\varepsilon t\omega_{\mathrm{in}} + \left(\frac{\varepsilon t}{2}\right)^2\right] \\ &= 0.1 \times \left[10^2 + (3/4) \times 5 \times 5 \times 10 + (5 \times 5/2)^2\right] \\ &= 44.375 \text{ m/s}^2 \end{aligned}$$

- Solution by the component of Eq. (2.4)

$$\alpha_r = r(\omega_{in} + \varepsilon t)^2 = 0.1 \times (10 + 5 \times 5)^2 = 122.5 \text{ m/s}^2$$

The absolute acceleration of the rotating point defined by Eqs. (2.16) and (2.4), which the results are shown as:

- Solution by Eq. (2.15)

$$\begin{aligned} a &= r\sqrt{\varepsilon^2 + \left[\omega_{in}^2 + \frac{3}{4}\varepsilon t \omega_{in} + \frac{(\varepsilon t)^2}{4}\right]^2} \\ &= 0.1\sqrt{5^2 + \left[10^2 + (3/4) \times 5 \times 5 \times 10 + \frac{(5 \times 5)^2}{4}\right]^2} \\ &= 44.377 \text{ m/s}^2 \end{aligned}$$

- Solution by the component of Eq. (2.4)

$$a = r\sqrt{\varepsilon^2 + (\omega_{in} + \varepsilon t)^4} = 0.1\sqrt{5^2 + [10 + 5 \times 5]^4} = 122.6 \text{ m/s}^2$$

The results of calculations obtained for the radial and absolute accelerations of a rotating object by new Eqs. (2.15) and (2.16) and by Eqs. (2.3) and (2.4) of textbooks are significantly different. New equations of radial and absolute accelerations give results that almost three times less than presented in the fundamental equations of textbooks. Practitioners and researchers should take such a big difference in results into account because it leads to a decrease in the dimensions and weights of the machine parts and increases their quality of work.

2.2 Analysis of Coriolis Acceleration of a Rotating Object

The external torque applied to a gyroscope generates several internal inertial forces, which action is manifested by gyroscopic effects. Among the inertial forces acting on a gyroscope, the Coriolis force should be considered in detail due to its specificity. The rotating mass elements of the spinning object and its rotation around an axis that perpendicular to the axis of its spin generate variable Coriolis accelerations and forces that should be computed in detail. The most textbooks in classical mechanics represent an analysis of the Coriolis acceleration in the form of the linear motion of the object on the rotating disc with uniform velocities. The known method for computing the Coriolis acceleration is based on relative motion analysis using a rotating axis. This acceleration is conducted with a mathematical approach that is not accepted for computing inertial forces generated by rotating mass elements of the spinning rotor which acting on a gyroscope. For the gyroscopic effect, a new mathematical model of the Coriolis acceleration should be derived, based on the variable tangential velocity of mass elements.

The textbooks present the Coriolis acceleration as the product of the linear velocity of the moving object that moves on a rotating disc with defined angular velocity [1–3, 15]. The uniform velocities of a moving object are considered for the common condition. Practically, the magnitudes of the Coriolis acceleration can vary according to the accepted condition of motion of an object. The new mathematical models of the Coriolis acceleration for the rotating object are considered at conditions of its uniform, accelerated and combined motions and thereby fill a gap in the study of acceleration analysis.

In classical mechanics, there are several analytical approaches to derive equations for different types of accelerations for the moving objects. In engineering, there are many mechanisms with relative and combined motions of their components that generate the Coriolis acceleration and force. Most textbooks derive the Coriolis acceleration, and it is a force for the common case on a basis of the uniform linear and angular velocities of moving objects. Textbooks in classical mechanics present the Coriolis acceleration and the Coriolis force by the following equations:

$$a_{\mathrm{cr}} = 2V\omega \tag{2.17}$$

$$F_{\mathrm{cr}} = 2mV\omega \tag{2.18}$$

where a_{cr} is the Coriolis acceleration, ω is the angular velocity of the disc, and V is the linear velocity of the object travelling on the table, m is the mass of the object, and F_{cr} is the Coriolis force.

Equations (2.17) and (2.18) are classical formulas. The components of the angular velocity ω and the linear velocity V are applied for uniform motions of machine elements. However, this approach cannot be accepted for accelerated and combined motions because any differences in motions of elements of mechanisms are resulting in the equations that describe these processes. The magnitude of Coriolis accelerations for the variable linear and angular velocities of the machine components are different.

Nevertheless, Wikipedia and other encyclopaedias contain the second equation of Coriolis acceleration that presented by the following expressions: $a_{cr} = V\omega$, where all components are as specified above. This expression is not presented in textbooks but has a right for computing of Coriolis acceleration and use in engineering. Following analysis of Coriolis acceleration for different regimes of linear and angular motions of the object on a disc derived by the different methods and validated the correctness of the second expression of Coriolis acceleration.

It is considered an object of the mass m that travels from the centre O towards B on the edge of a rotating disc (Fig. 2.2). The linear velocity V of the object m and angular velocity ω of the disc is uniform. The travelling from point O to B takes time Δt, so the distance $OB = V \times \Delta t$. The distance OB is calculated by the physics equations of the uniform motion, $OB = V \times \Delta t$. The rotation of the table in the counter-clockwise direction on the angle γ for the time Δt results in point B from its original position to a new position A. The angle is $\gamma = \omega\Delta t$, where ω presents

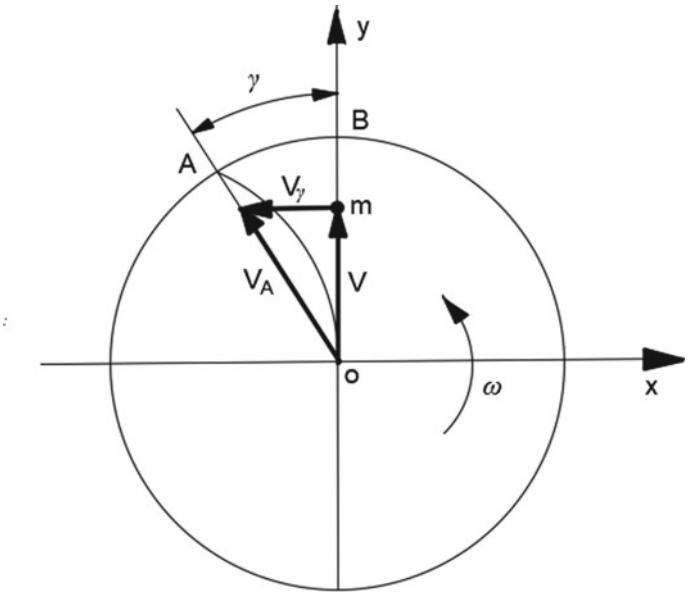

Fig. 2.2 Sketch for calculation of the Coriolis acceleration

the constant angular velocity. However, the distance AB is calculated by the physics equations of the accelerated motion, $AB = \alpha t^2/2$. Finally, the Coriolis acceleration for this type of approach is depicted in Eq. (2.18).

However, the following analysis of the accepted motions of the object m on a rotating disc shows the following circumstances (Fig. 2.2):

(a) The motion of the object m and the rotation of the disc are independent, and no forces are acting between the object m and the disc.
(b) The linear motion of the object m and the rotary motion of the disc are uniformed; hence, the relative trajectory of a motion OA of the object m on the rotating disc is the Archimedes curve. The principle of the Archimedes curve states that any point of the curve gives uniform velocities of components and without acceleration.
(c) The distance AB is a result of uniform motions and calculated by the equation $AB = \omega \times (OB) \times \Delta t = V_{\mathrm{tB}} \times \Delta t$, where V_{tB} is the constant tangential velocity of point B.
(d) The circular distance AB is the length between the point B of the disc and the point A of the Archimedes curve as calculated by Eq. (2.17), which expresses the rotation of the disc with acceleration that contradicts to the accepted initial conditions.
(e) These circumstances show that Eq. (2.17), which describes the motion with acceleration, cannot be used for analysis and the following derivation of the Coriolis acceleration.

Analysis of the physics of two motions and the Coriolis acceleration for represented example gives the following. Free linear motion with a uniform velocity of the object m on the rotating disc of the uniform angular velocity does not generate acceleration and therefore force. The Coriolis acceleration and its force act when the object m travels on the guideway of the rotating disc. The linear velocity of the object and angular velocity of the rotating disc can be uniform and/or accelerated.

The object, which moves on the rotating disc, can have different values of the Coriolis acceleration and a force. This study examines four types of motions:

(a) a uniform motion of the object and the disc
(b) a uniform motion of the object and the accelerated rotation of the disc
(c) an accelerated motion of the object and the uniform rotation of the disc
(d) an accelerated motion of the object and the disc

2.2.1 *Coriolis Acceleration for Uniform Motions of an Object and a Rotating Disc*

The object m travels on the rotating disc and its trajectory presented by the line OA (Fig. 2.2). Rotation of the disc on the angle γ changes the vector velocity direction V of the object m on the vector velocity direction V_A. The vector V_γ expresses this change in the direction of the vector velocity and represents by the following equation:

$$V_\gamma = -V \sin\gamma \quad V_\gamma = -V \sin\gamma \tag{2.19}$$

where γ is an angle of rotation of a disc, other components are as specified above.

The magnitude of the vector velocity V_γ depends on the change in the object radius location on the disc. The change in the magnitude of the velocity V_γ is presented by the following equation [10]:

$$\Delta V_\gamma = -\left[V \sin(\gamma + \Delta\gamma) - V \sin\gamma\right] = -V\left[\sin(\gamma + \Delta\gamma) - \sin\gamma\right] \tag{2.20}$$

Trigonometric expression in square brackets is represented by the identity $\sin\alpha - \sin\beta = 2\cos\frac{\alpha+\beta}{2}\sin\frac{\alpha-\beta}{2}$, [27]. Substituting this identity into Eq. (2.21) and multiplying on $\left(\frac{\Delta\gamma/2}{\Delta\gamma/2}\right)$, then the change in the tangential velocity V_γ is expressed the following equation:

$$\Delta V_\gamma = -V \times 2\cos\left(\frac{\gamma + \Delta\gamma + \gamma}{2}\right)\sin\left(\frac{\gamma + \Delta\gamma - \gamma}{2}\right)\left(\frac{\Delta\gamma/2}{\Delta\gamma/2}\right) \tag{2.21}$$

which transformation yields the following

$$\Delta V_\gamma = -V \times 2\cos\left(\gamma + \frac{\Delta\gamma}{2}\right)\sin\left(\frac{\Delta\gamma}{2}\right)\left(\frac{\Delta\gamma/2}{\Delta\gamma/2}\right) \tag{2.22}$$

Analysis of Eq. (2.22) shows when $\Delta\gamma \to 0$, then $\lim_{\Delta\gamma\to 0}\cos\left(\gamma + \frac{\Delta\gamma}{2}\right) = \cos\gamma$, and $\lim_{\Delta\gamma\to 0}\frac{\sin(\Delta\gamma/2)}{\Delta\gamma/2} = 1.0$. Substituting defined expressions into Eq. (2.22) and transformation yields the following

$$\Delta V_\gamma = -V \times 2\cos\gamma \times (\Delta\gamma/2) = -V\cos\gamma \times \Delta\gamma \tag{2.23}$$

It is assumed the angle $\Delta\gamma$ is a small value, and hence, it is accepted $\cos\gamma = 1$. Equation (2.22) presented in the differential form, and then, the change in the velocity will have the following equation:

$$\mathrm{d}V_\gamma = -V\,\mathrm{d}\gamma \tag{2.24}$$

The rate change in the velocity per time represents an acceleration of the object, which expression has the following equation:

$$\frac{\mathrm{d}V_\gamma}{\mathrm{d}t} = -V\frac{\mathrm{d}\gamma}{\mathrm{d}t} \tag{2.25}$$

where $\mathrm{d}V_\gamma/\mathrm{d}t = a_\mathrm{c}$ is the Coriolis acceleration of the object, $\mathrm{d}\gamma/\mathrm{d}t = \omega$ is the angular velocity of the rotating disc.

Substituting defined components into Eq. (2.25) and transformation, the acceleration of the object results in the following expression:

$$a_\mathrm{c} = -V\omega \tag{2.26}$$

Equation (2.26) is the expression of the Coriolis acceleration for uniform motions of the object and the rotating disc. Hence, the Coriolis force will have the next equation

$$F_\mathrm{c} = mV\omega \tag{2.27}$$

where all parameters are as specified above.

The direction of the Coriolis force vector is opposite to the direction of the vector of acceleration. Equation (2.26) can be derived from another mathematical approach. The distances AB and OB can be calculated by the equations of $AB = V_\gamma t$ and $OB = Vt$ (Fig. 2.2). The angle γ of triangle AOB is small, then $AB = OB\sin\gamma$ and accepted $\sin\gamma = \gamma$. After substituting defined magnitudes of the triangle sides, the new equation has the following expression: $V_\gamma t = Vt\gamma$ which simplification yields $V_\gamma = V\gamma$. Then, the rate change of the velocity per time represents an acceleration

of the object, which expression is the same as Eqs. (2.25) and (2.26). Coriolis acceleration expressed by Eq. (2.27). These Coriolis equations are the same as presented in encyclopaedias.

2.3 Coriolis Accelerations for Combinations of the Uniform and Accelerated Motions of the Object and the Disc

The method for computing of Coriolis accelerations for the combinations of the uniform and accelerated motions of the object and the disc is the same as presented in Sect. 2.2. A detailed solution for the Coriolis acceleration is described in the last paragraph of Sect. 2.2.1 after Eq. (2.24). The expressions of the equations for the motions are derived on a base of the vectorial diagram of velocities and geometrical parameters represented in Fig. 2.2. The solutions for Coriolis accelerations for each combination of motions of the object and the disc are represented in Table 2.1.

Relevant equations developed for Coriolis accelerations of a moving object on a rotating disc that represented for different conditions of motions of a system. New equations consider combinations for uniform and accelerated linear and the angular velocities of a system. These equations are different from the fundamental equation of the Coriolis acceleration depicted in textbooks of physics, kinematics and machine dynamics. In engineering, all machines work with accelerations of components that are a real condition of the functioning of any mechanism. It is very important to calculate the exact value of forces acting on machine components. The new equations of Coriolis accelerations should be used for computing of inertial torques generated by the rotating masses of the objects for gyroscopic devices.

Table 2.1 Coriolis accelerations for uniform and accelerated motions of the object and the rotating disc

Motion	Tangential velocity V_γ	Radial velocity V	Angle γ	Coriolis acceleration
Uniform for disc and accelerated for object	$at^2/2_c$	$at^2/2$	ωt	$a_c = (at^2/2)\omega$
Accelerated for disc and uniform for object	$at^2/2$	V	$\varepsilon t^2/2$	$a_c = V\varepsilon$
Accelerated for disc and object	$at^2/2$	$at^2/2$	$\varepsilon t^2/2$	$a_c = a\varepsilon t^2/2$
V, a	Linear velocity and acceleration respectively			
ω, ε	Angular velocity and acceleration respectively			
t	Time			

Table 2.2 Results of the Coriolis acceleration

Motion	Uniform		Accelerated	Uniform	Uniform	Accelerated	Accelerated	
	Object	Disc	Object	Disc	Object	Disc	Object	Disc
Coriolis acceleration: m/s^2	$a_c = V\omega = 0.5 \times 2 = 1.0$		$a_c = (at^2/2)\omega = (1.0 \times 3.0^2/2) \times 2 = 9$		$a_c = V\varepsilon = 0.5 \times 3 = 1.5$		$a_c = a\varepsilon t^2/2 = 1.0 \times 3 \times 3^2/2 = 13.5$	

2.4 Working Example

The disc has an angular velocity of 2.0 rad/s and accelerates at the rate of 3.0 rad/s^2 (Fig. 2.2.) The object of 0.1 kg mass moves with a linear velocity of 0.5 m/s and accelerates at the rate of 1.0 m/s^2. Determine the values of Coriolis accelerations for four types of motions (Table 2.1) after 3.0 s of motions.

The results of calculations of the Coriolis acceleration by the equations of Table 2.1 and by Eq. (2.18) of textbooks are represented in Table 2.2. The differences in results of uniform motions of the object and the disc are explained by the different analytical approaches for analysis of the Coriolis acceleration.

A fundamental analytic solution for Coriolis acceleration that is presented in textbooks of classical mechanics and encyclopaedias gives the expression of Coriolis acceleration which a result is twice bigger than represented in this chapter and known publications. Following mathematical models for the Coriolis forces, inertial torques acting on the gyroscope and equations of the gyroscope motions represented in the book take into account the expression of Coriolis acceleration that gives twice less result. Application of the expression of Coriolis acceleration presented in the textbooks of classical mechanics does not give correct results in mathematical models of the gyroscope motions. This fact additionally confirms the correctness of the formula for Coriolis acceleration which represented in this chapter and as an alternative solution in known publications.

The main contribution of the original analysis of accelerations for the rotating object is represented by two components. The first is the derivation of a new equation for the resulting and radial acceleration of the rotating object about a fixed axis. The second contribution is the validation of the Coriolis acceleration for uniform linear and angular motions of an object. Additionally, the equations for Coriolis accelerations for combinations of variable linear and angular motions of an object and a rotating disc are derived.

References

1. Taylor, J.R.: Classical Mechanics. University Science Books, Sausalito CA (2004)
2. Gregory, D.R.: Classical Mechanics. Cambridge University Press, New York (2006)
3. Thornton, M.: Classical Dynamics of Particles and Systems, 5th ed. Brooks/Cole (2004)
4. Nolting, W.: Theoretical Physics 1: Classical Mechanics. Springer, Cham (2016)

5. Aardema, M.D.: Analytical Dynamics. Theory and Application. Academic/Plenum Publishers, New York (2005)
6. Hibbeler, R.C.: Engineering Mechanics—Statics and Dynamics, 12th edn. Prentice Hall, Pearson (2010)
7. Dreizler, R.: Theoretical Mechanics: Theoretical Physics 1. Springer, Boca Raton (2010)
8. Jewett, J., Serway, R.A.: Physics for Scientists and Engineers, 10th ed. Cengage Learning, Boston (2018)
9. Smith, P.F., Longley, W.R.: Theoretical Mechanics. Franklin Classics, Boston (2018)
10. Baumann, G.: Mathematica for Theoretical Physics. Springer, New York (2003)
11. Germain, P., Piau, M., Caillerie, D.: Theoretical and Applied Mechanics. Elsevier, Amsterdam (2012)
12. Millard, B.F.: Principles of Engineering Mechanics: Dynamics—The Analysis of Motion. Springer, Berlin (2006)
13. Russell, K., Shen, Q., Sodhi, R.S.: Kinematics and Dynamics of Mechanical Systems, 2nd ed. Implementation in MATLAB and SimMechanics. Taylor & Francis, Boca Raton (2019)
14. Usubamatov, R., Abdykerimova, D., Dotalieva, Z.: A Mathematical Model for an Acceleration of a Rotating Object about a Fixed Axis. J. Appl. Comput. Math. **7**(2), 2–4 (2018). https://doi.org/10.4172/2168-9679.1000394
15. Dronkers, J.: Coriolis acceleration. Available from http://www.coastalwiki.org/wiki/Coriolis_acceleration (2017)

Chapter 3
Inertial Forces and Torques Acting on Simple Spinning Objects

3.1 Inertial Forces and Torques Acting on Simple Spinning Objects

Rotating objects in engineering constitute a vast group of machine components of a different form that manifest the gyroscopic effects. The known publications contain the mathematical models for motions of the spinning disc that do not coincide practice. The rotating masses of the spinning objects produce the system of interrelated inertial torques in which action manifests gyroscopic effects. The centrifugal, Coriolis and common inertial forces and the change in the angular momentum are generated by the rotating masses constitute the part of fundamental principles of gyroscope theory. This chapter considers the method for deriving mathematical models for inertial torques produced by rotating masses of a spinning disc, cylinder and ring that are one group of design. This method can be applied to rotating objects of different forms and describes the physics of gyroscopic effects.

3.1.1 Centrifugal Forces and Torques Acting on a Spinning Disc

The primary component of a gyroscopic device is a rotating disc mounted on the axle [1–3]. The known publications contain the mathematical models for motions of the spinning disc that do not coincide practice [4–10]. Analysis of motions of the spinning thin disc demonstrates the centre mass and mass element of the rotating disc, whose locations and actions are different, generate several inertial forces. The analysis of the action of the inertial torques generated by the rotating masses is considered on the example of the thin spinning disc. The action of centrifugal forces on a disc rotating around axis oz with an angular velocity of ω in a counterclockwise direction is considered in Fig. 3.1. The disc's mass elements m are disposed on the circle of radius $(2/3)R$ and rotate around axis oz with a constant tangential velocity.

© The Editor(s) (if applicable) and The Author(s), under exclusive license to Springer Nature Singapore Pte Ltd. 2020

R. Usubamatov, *Theory of Gyroscopic Effects for Rotating Objects*,
https://doi.org/10.1007/978-981-15-6475-8_3

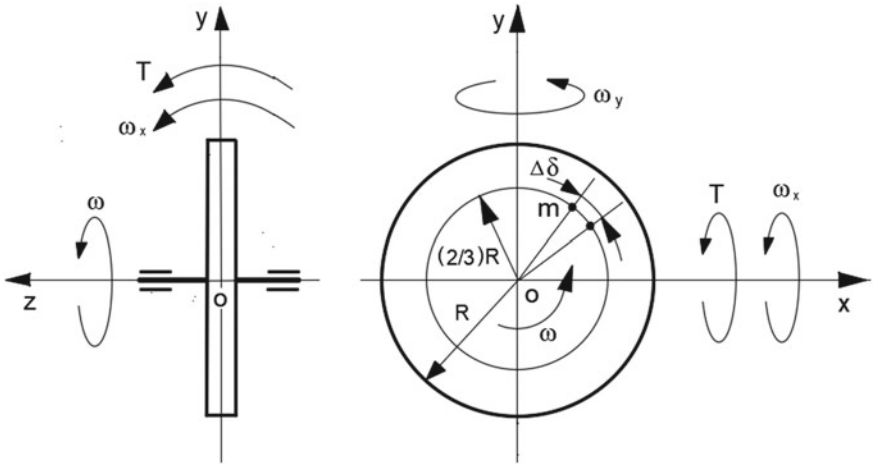

Fig. 3.1 Schematic of the spinning disc

The direction of the vector of tangential velocity changes continuously, i.e. the mass elements move with acceleration. The rotation of mass elements with acceleration generates the plane of centrifugal forces, which disposes of perpendicular to the axis of the spinning disc [6–9]. If an external torque is applied to the spinning disc, the plane of the rotating centrifugal forces inclines and resists to the action of the external torque (Fig. 3.2).

The turning of the plane of the rotating centrifugal forces around axis *ox* that passes along the diameter line leads to the change in the directions and locations of centrifugal force vectors f_{ct} generated by the mass elements. Vectors f_{ct}, whose directions coincide with the line of axis *ox* (i.e. located on 0° and 180° from the line of axis *ox*), remain on the plane *xoy*. Other centrifugal force vectors f_{ct} are located on the inclined plane *xoy** and exhibit a non-identical change in their directions. The maximal declination of vectors f^*_{ct} from the line of axis *oy* shows vectors that are located at 90° and 270° from the line of axis *ox* (Fig. 3.2). These variable directions of centrifugal force vectors generate a change in vector components $f_{ct\cdot z}$ that are parallel to rotating disc axle *oz*. The integrated product of the components' vector changes in centrifugal forces $f_{ct\cdot z}$, and their variable radius of location relative to axis *ox* generates the torque T_{ct} that acts opposite to the action of the external torque T.

The following analytical approach formulates the resistance torque produced by the change in the location of centrifugal forces generated by the rotating mass elements of the disc due to the action of the external torque being applied to the rotating disc. At this stage, for the mathematical modelling, the weight of the rotor axle and the action of frictional forces are disregarded. The rotating centrifugal forces of the disc are in balance, and their directions are at right angles to axis *oz*. The action of external torque turns the plane *xoy* of rotating centrifugal forces to angle $\Delta\gamma$ around axis *ox* with a new disposition of the plane *xoy**. The change in the plane of the centrifugal forces generates the integrated resistance torque produced

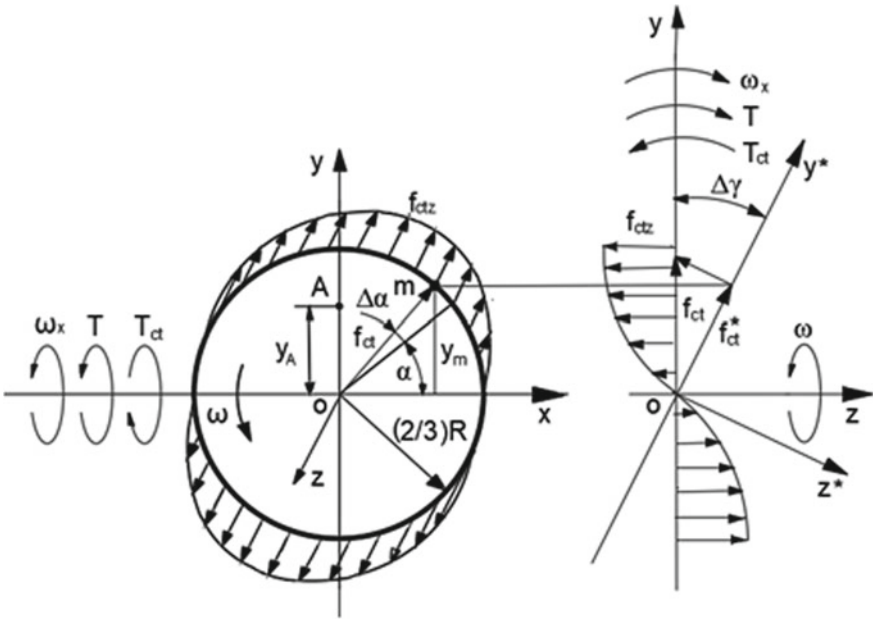

Fig. 3.2 Schematic of acting centrifugal forces, torques and motions of the spinning disc

by the centrifugal force of the mass element (Fig. 3.2) and is expressed as follows:

$$\Delta T_{\mathrm{ct}} = -f_{\mathrm{ct}\cdot z} y_{\mathrm{m}} = -m a_z y_{\mathrm{m}} \tag{3.1}$$

where ΔT_{ct} is the torque generated by the centrifugal force of the mass element, $f_{\mathrm{ct}\cdot z}$ is the change in the centrifugal force and y_{m} is the distance of the disposal of the mass element along axis *oy*.

The sign (−) of the resistance torque T_{ct} means the action in the clockwise direction. The change in centrifugal force of the mass element is expressed by the following equation:

$$\begin{aligned} f_{\mathrm{ct}\cdot z} &= f_{\mathrm{ct}} \sin\alpha \sin\Delta\gamma = mr\omega^2 \sin\alpha \sin\Delta\gamma \\ &= \left[\frac{M(2/3)R\omega^2}{2\pi}\Delta\delta\right] \sin\alpha \sin\Delta\gamma = \frac{MR\omega^2}{3\pi}\Delta\delta\Delta\gamma \sin\alpha \end{aligned} \tag{3.2}$$

where $f_{\mathrm{ct}} = mr\omega^2 = \left[\frac{M(2/3)R\omega^2}{2\pi}\Delta\delta\right] = \frac{MR\omega^2}{3\pi}\Delta\delta$ is the centrifugal force of the mass element m; $m = \frac{M}{2\pi[(2/3)R]}\Delta\delta\frac{2}{3}R = \frac{M}{2\pi}\Delta\delta$ in which M is the mass of the disc; $r = (2/3)R$ is the radius of the mass elements location; R is the external radius of the disc; $\Delta\delta$ is the sector's angle of the mass element's location; ω is the constant angular velocity of the disc; α is the angle of the mass element's location; $\Delta\gamma$ is the angle of turn for the disc's plane ($\sin\Delta\gamma = \Delta\gamma$ for the small values of the angle).

Substituting the defined parameters into Eq. (3.1) yields the equation of the resistance torque produced by the centrifugal forces of the mass element.

$$\Delta T_{\mathrm{ct}} = -\frac{MR\omega^2}{3\pi} \times \Delta\delta \times \Delta\gamma \times \sin\alpha \times y_{\mathrm{m}} \tag{3.3}$$

where $y_{\mathrm{m}} = (2/3)R\sin\alpha$ is the distance of the mass element's location on the disc's plane relative to axis ox (Fig. 3.2) and the other components are as specified above.

Equation (3.3) allows for the definition of the integrated torque produced by a change in the centrifugal forces generated by the disc's mass elements, wherein all components should be presented in a form appropriate for integration. Moreover, Eq. (3.3) contains variable parameters whose incremental components are independent and represented by different symbols. The change in centrifugal forces represents the distributed load applied along the length of the circle and angle α where the disc's mass elements are located. Figure 3.2 depicts the locations of the change in centrifugal forces $f_{\mathrm{ct}\cdot z}$ of the disc. A distributed load can be equated with a concentrated load applied at a specific point along axis oy, which is the centroid at the semicircle. The location of the resultant force is the centroid (point A, Fig. 3.2) of the area under the curve, which is calculated by the known integrated equation.

$$y_A = \frac{\int_{\alpha=0}^{\pi} f_{\mathrm{ct}\cdot z} y_{\mathrm{m}} \mathrm{d}\alpha}{\int_{\alpha=0}^{\pi} f_{\mathrm{ct}\cdot z} \mathrm{d}\alpha} \tag{3.4}$$

where $f_{\mathrm{ct}} = \frac{MR\omega^2}{3\pi}\Delta\delta\Delta\gamma\sin\alpha$.

Substituting Eq. (3.2) and other components into Eq. (3.4) and transformation yields the following expression.

$$\begin{aligned} y_A &= \frac{\int_{\alpha=0}^{\pi} f_{\mathrm{ct}\cdot z} y_{\mathrm{m}} \mathrm{d}\alpha}{\int_{\alpha=0}^{\pi} f_{\mathrm{ct}\cdot z} \mathrm{d}\alpha} = \frac{\int_{\alpha=0}^{\pi} \frac{MR\omega^2}{3\pi}\Delta\delta \times \Delta\gamma \times \frac{2}{3}R\sin\alpha\sin\alpha \mathrm{d}\alpha}{\int_{\alpha=0}^{\pi} \frac{MR\omega^2}{3\pi}\Delta\delta \times \Delta\gamma \sin\alpha \mathrm{d}\alpha} \\ &= \frac{\frac{MR\omega^2}{3\pi}\Delta\delta\Delta\gamma \int_{\alpha=0}^{\pi} \frac{2}{3}R\sin^2\alpha \mathrm{d}\alpha}{\frac{MR\omega^2}{3\pi}\Delta\delta\Delta\gamma \int_{\alpha=0}^{\pi} \sin\alpha \mathrm{d}\alpha} \\ &= \frac{\frac{R}{3}\int_0^{\pi}(1-\cos 2\alpha)\mathrm{d}\alpha}{\int_0^{\pi}\sin\alpha \mathrm{d}\alpha} \end{aligned} \tag{3.5}$$

where the expression $\frac{MR\omega^2}{3\pi}\Delta\delta\Delta\gamma$ is accepted as constant for the Eq. (3.5); the expression $\sin^2\alpha = (1-\cos 2\alpha)/2$ is a trigonometric identity that replaced in the equation, and other parameters are as specified above.

A differential form presents Eq. (3.3). Substituting Eq. (3.5) into Eq. (3.3), replacing $\sin\alpha = \int_0^{\pi}\cos\alpha \mathrm{d}\alpha$ by the integral expression with defined limits and presenting other components by the integral forms, the following equation emerges:

$$\int_0^{T_{\mathrm{ct}}} \mathrm{d}T_{\mathrm{ct}} = -\frac{MR\omega^2}{3\pi} \times \int_0^{\pi} \mathrm{d}\delta \times \int_0^{\gamma} \mathrm{d}\gamma \times \int_0^{\pi} \cos\alpha \mathrm{d}\alpha \times \frac{R\int_0^{\pi}(1-\cos 2\alpha)\mathrm{d}\alpha}{3\int_0^{\pi}\sin\alpha \mathrm{d}\alpha} \tag{3.6}$$

Solving integral Eq. (3.6) yields the following result

$$T_{\mathrm{ct}}\Big|_0^{T_{\mathrm{ct}}} = -\frac{MR\omega^2}{3\pi} \times \left(\delta\Big|_0^{\pi}\right) \times \left(\gamma\Big|_0^{\gamma}\right) \times 2\left(\sin\alpha\Big|_0^{\pi/2}\right) \times \frac{R\left(\alpha - \frac{1}{2}\sin 2\alpha\right)\Big|_0^{\pi/2}}{-3\cos\alpha\Big|_0^{\pi}}$$

where the change of the limits of $\sin\alpha$ from 0 to $\pi/2$ due to symmetrical location of the centrifugal force diagram relatively axis oy should be compensated for the following integration by multiplication on two; the change of the limits for $\sin 2\alpha$ does not play a role because the location of the centroid is symmetrical and the same for the quarters of a circle.

Thus, giving rise to the following:

$$T_{ct} = -\frac{MR\omega^2}{3\pi} \times (\pi - 0) \times (\gamma - 0) \times 2(1-0) \times \frac{R\left(\frac{\pi}{2} - 0\right)}{-3(-1-1)} = -\frac{MR^2\omega^2\pi}{18} \times \gamma \tag{3.7}$$

where all parameters are as specified above.

The rate of change in torque T_{ct} per time is expressed by the differential equation

$$\frac{\mathrm{d}T_{ct}}{\mathrm{d}t} = -\frac{MR^2\omega^2\pi}{18}\frac{\mathrm{d}\gamma}{\mathrm{d}t} \tag{3.8}$$

where $t = \alpha/\omega$ is the time taken relative to the angular velocity of the disc and the other parameters are as defined above.

The differential of time is:$\mathrm{d}t = \frac{\mathrm{d}\alpha}{\omega}$; the expression $\frac{\mathrm{d}\gamma}{\mathrm{d}t} = \omega_x$ is the angular velocity of the spinning disc's precession around axis ox. Substituting the defined components into Eq. (3.8) and transformation yields a new differential equation with the following expression:

$$\frac{\omega \mathrm{d}T_{\mathrm{ct}}}{\mathrm{d}\alpha} = -\frac{MR^2\omega^2\omega_x\pi}{18} \tag{3.9}$$

Separation of the variables of Eq. (3.9) and transformation yields the following equation.

$$\mathrm{d}T_{\mathrm{ct}} = -\frac{MR^2\omega\omega_x\pi}{18}\mathrm{d}\alpha \tag{3.10}$$

Equation (3.10) is represented by the integral form with defined limits and yields the integral equation:

$$\int_0^{T_{ct}} \mathrm{d}T_{\mathrm{ct}} = -\int_0^{\pi} \frac{MR^2\omega\omega_x\pi}{18}\mathrm{d}\alpha \tag{3.11}$$

Solving Eq. (3.11) yields

$$T_{\mathrm{ct}}\Big|_0^{T_{\mathrm{ct}}} = -\frac{MR^2\omega\omega_x\pi}{18}\alpha\Big|_0^{\pi} \tag{3.12}$$

If the change in centrifugal forces acts on the upper and lower sides of the disc's plane, then the total resistance torque T_{ct} is obtained when the result of Eq. (3.12) is increased twice.

$$T_{\mathrm{ct}} = -\frac{2\pi^2 MR^2\omega\omega_x}{18} = -\frac{2}{9}\pi^2 J\omega\omega_x \tag{3.13}$$

where $J = MR^2/2$ is the disc's mass moment of inertia. The other parameters are as specified above.

Analysis of Eq. (3.13) demonstrates that the resistance torque generated by the change in the centrifugal forces of the spinning rotor depends proportionally on the rotor's mass moment of inertia and angular velocity and the angular velocity of the precession. The resistance torque generated by the change in centrifugal forces acts only on the action of the external load torque. The direction of the resistance torque's action is in the clockwise direction which expressed by the sign (−) and opposite to the action of the external torque and the direction of the angular velocity around axis *ox*. This resistance torque is restraining torque and acting only in case of gyroscope motion around axis *ox* under the action of the external torque. The value of the resistance torque is always less than the value of the external torque.

3.1.2 Common Inertial Forces and Torques Acting on the Spinning Disc

External torque applied to a gyroscope causes the plane of the spinning rotor to turn around axis ox, as shown in Fig. 3.2. This turn leads to a change in the direction of the mass elements' tangential velocity. The change in tangential velocity is expressed in the acceleration of rotating mass elements and their inertial forces. This change varies along the circumference where mass elements are disposed of. The directions of the variable change in tangential velocity vectors V_z are parallel to the spinning rotor's axle oz (Fig. 3.3). The maximal changes in direction have the velocity vectors V^* of the mass element located on the line of axis *ox*. The two vectors V located 90° and 270° from the line of axis *ox* and whose directions are parallel to the line of axis *ox* do not exhibit any changes. A change in the velocity vectors refers to the accelerated motions a_z of the rotor's mass elements m that generate inertial forces

f_{in}. The integrated product of the components of the inertial forces f_{in} of the mass elements and their variable radius of disposition relative to axis oy represent inertial torque T_{in} acting on axis oy. This torque is the result of the external torque's action and represents the precession torque that is directed to turn the rotor's plane around axis oy. Precession torque T_{in} generated by the common inertial forces of the rotating mass elements is represented by the following equation:

$$\Delta T_{\text{in}} = f_{\text{in}} x_{\text{m}} = m a_{\text{z}} x_{\text{m}} \tag{3.14}$$

where ΔT_{in} is the torque generated by the inertial force of the spinning disc's mass element f_{in}, a_z is the acceleration of the mass element m along axis oz and $x_{\text{m}} = (2/3)R \cos a$ is the distance to the mass element's location along axis ox. The equation for mass element m is represented by the explanation of Eq. (3.2) in Sec. 3.1.1.

The expression for distance x_{m} for the mass element's location along axis ox is represented by Eq. (3.3) but with a change in the indices of the axes and forces. The equation for acceleration a_z of the mass element is defined by the first derivative of the change in the tangential velocity, whose value depends on the angle of its location on the spinning disc that varies with time. The expression for a_z is presented by the following equation.

$$\alpha_z = \frac{\mathrm{d}(-V_z)}{\mathrm{d}t} = \frac{\mathrm{d}[-V \cos\alpha \sin\Delta\gamma]}{\mathrm{d}t} = V\Delta\gamma \sin\alpha \frac{\mathrm{d}\alpha}{\mathrm{d}t} = \frac{2}{3} R\omega^2 \Delta\gamma \sin\alpha \tag{3.15}$$

where $a_z = \mathrm{d}(-V_z)/\mathrm{d}t$ is the acceleration of the mass element along axis oz, $V_z = -V\cos\alpha \sin\Delta\gamma$ is the change in tangential velocity V, $\Delta\gamma$ is the angle of the turn of the disc's plane around axis oy ($\sin\Delta\gamma = \Delta\gamma$ for small values of the angle), $V = (2/3)R\omega$, $\omega = \mathrm{d}\alpha/\mathrm{d}t$ is the angular velocity of the disc, α is the angular disposition of the mass element, t is time, and the other components are as specified above.

Substituting the defined parameters and Eq. (3.2) into Eq. (3.14) yields

$$\Delta T_{\text{in}} = \frac{M}{2\pi} \times \Delta\delta \times \Delta\gamma \times \frac{2}{3} R\omega^2 \sin\alpha \times x_{\text{m}} = \frac{MR\omega^2}{3\pi} \times \Delta\delta \times \Delta\gamma \times \sin\alpha \times x_{\text{m}} \tag{3.16}$$

where all parameters are as specified above.

Equation (3.17) allows for the definition of the integrated torque produced by a change in the inertial forces generated by the disc's mass elements, wherein all components should be presented in a form appropriate for integration. Expression of Eq. (3.16) is the same as Eq. (3.3), and the following solution is the same that yields the equation for precession torque. The change in inertial forces represents the distributed load applied along the length of the circle and angle α where the disc's mass elements are located. Figure 3.3 depicts the locations of the change in inertial forces $f_{\text{in}\cdot z}$ of the disc. A distributed load can be equated with a concentrated load applied at a specific point along axis ox, which is the centroid at the semicircle. The

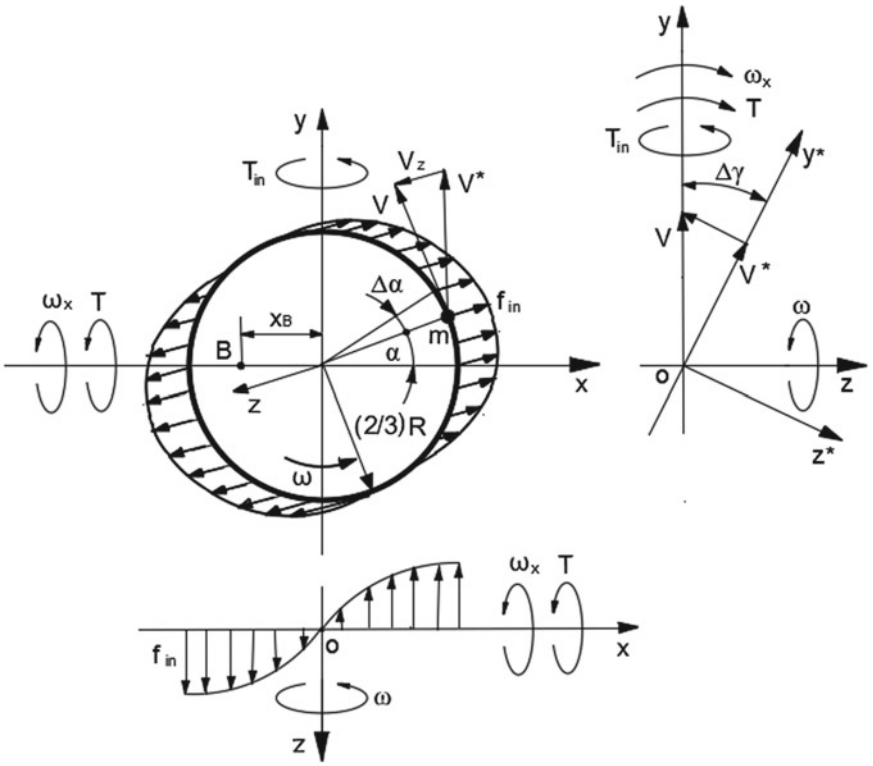

Fig. 3.3 Schematic of acting forces, torques and motions of the spinning disc

location of the resultant force is the centroid (point *B*, Fig. 3.3) of the area under the curve, which is calculated by the known integrated equation.

$$y_B = \frac{\int_{\alpha=0}^{\pi} f_{\text{in}\cdot z} x_{\text{m}} \mathrm{d}\alpha}{\int_{\alpha=0}^{\pi} f_{\text{in}\cdot z} \mathrm{d}\alpha} \tag{3.17}$$

where $f_{\text{in}} = \frac{MR\omega^2}{3\pi} \Delta\delta\Delta\gamma \sin\alpha$

Substituting Eq. (3.2) and other components into Eq. (3.17) and transformation yields the following expression.

$$\begin{aligned} y_B &= \frac{\int_{\alpha=0}^{\pi} f_{\text{in}\cdot z} x_{\text{m}} \mathrm{d}\alpha}{\int_{\alpha=0}^{\pi} f_{\text{in}\cdot z} \mathrm{d}\alpha} = \frac{\int_{\alpha=0}^{\pi} \frac{MR\omega^2}{3\pi} \Delta\delta \times \Delta\gamma \times \frac{2}{3} R \cos\alpha \sin\alpha \mathrm{d}\alpha}{\int_{\alpha=0}^{\pi} \frac{MR\omega^2}{3\pi} \Delta\delta \times \Delta\gamma \sin\alpha \mathrm{d}\alpha} \\ &= \frac{\frac{MR\omega^2}{3\pi} \Delta\delta\Delta\gamma \int_{\alpha=0}^{\pi} \frac{2}{3} R \cos\alpha \sin\alpha \mathrm{d}\alpha}{\frac{MR\omega^2}{3\pi} \Delta\delta\Delta\gamma \int_{\alpha=0}^{\pi} \sin\alpha \mathrm{d}\alpha} = \frac{\frac{2R}{3\times 2} \int_0^{\pi} \sin\alpha \mathrm{d} \sin\alpha}{\int_0^{\pi} \sin\alpha \mathrm{d}\alpha} \end{aligned} \tag{3.18}$$

where the expression $\frac{MR\omega^2}{3\pi}\Delta\delta\Delta\gamma$ is accepted as constant for the Eq. (3.18); the expression $\cos\alpha\sin\alpha\mathrm{d}\alpha = (\sin\alpha\mathrm{d}\sin\alpha)/2$ that replaced in the equation, and other parameters are as specified above.

Substituting Eq. (3.18) into Eq. (3.16), replacing $\sin\alpha = \int_0^{\pi/2}\cos\alpha\mathrm{d}\alpha$ by the integral expression with defined limits, and presenting other components by the integral forms, the following equation emerges:

$$\int_0^{T_{\text{int}}}\mathrm{d}T_{in} = -\frac{MR\omega^2}{3\pi}\times\int_0^{\pi}\mathrm{d}\delta\times\int_0^{\gamma}\mathrm{d}\gamma\times\int_0^{\pi}\cos\alpha\mathrm{d}\alpha\times\frac{\frac{R}{3}\int_0^{\pi}\sin\alpha\mathrm{d}\sin\alpha}{\int_0^{\pi}\sin\alpha\mathrm{d}\alpha} \tag{3.19}$$

Solving integral Eq. (3.19) yields the following result

$$T_{\text{in}}\Big|_0^{T_{\text{int}}} = -\frac{MR\omega^2}{3\pi}\times\left(\delta\Big|_0^{\pi}\right)\times\left(\gamma\Big|_0^{\gamma}\right)\times 2\left(\sin\alpha\Big|_0^{\pi/2}\right)\times\frac{\frac{R}{3\times 2}\sin^2\alpha\Big|_0^{\pi/2}}{-\cos\alpha\Big|_0^{\pi}}$$

where the change of the limit of sinα leads to the increase twice its value, for sinα of Eq. (3.19) remains the same due to the symmetrical location of the centroid.

Thus, giving rise to the following:

$$\begin{aligned} T_{\text{in}} &= -\frac{MR\omega^2}{3\pi}\times(\pi-0)\times(\gamma-0)\times 2(1-0)\times\frac{R(1-0)}{-6(-1-1)} \\ &= -\frac{MR^2\omega^2\pi}{18}\times\gamma \end{aligned} \tag{3.20}$$

where all parameters are as specified above.

Expression of Eq. (3.20) is the same as Eq. (3.7), and the following solution is the same that yields the equation for precession torque, which is expressed as follows:

$$T_{\text{in}} = \frac{2}{9}\pi^2 J\omega\omega_x \tag{3.21}$$

Equation (3.21) represents the precession torque generated by the change in the common inertial forces produced by the rotating mass elements of the disc. The external torque acting on the rotating disc around axis *ox* generates the precession torque that turns the disc's plane around axis *oy* in the counterclockwise direction. The precession and resistance torques generated by the common inertial and centrifugal forces, respectively, are expressed by a single equation but with different signs (+) and (−), albeit acting around different axes. The separate actions of each torque on a spinning disc are impossible. This is an unusual mathematical model and at first sight, contradicts to rules of mathematical analysis and classical mechanics, but analytical development and physics of action of these torques are correct. The two inertial

torques of different physics acting simultaneously around two perpendicular axes are expressed by one equation and represented a peculiarity of gyroscopic torques.

3.1.3 *Coriolis Forces and Torques Acting on the Spinning Disc*

In classical mechanics, Coriolis acceleration and force are products of the linear motion of a mass on a rotating disc and its angular velocity. The action of the Coriolis acceleration and force generated by mass elements is revealed in the spinning rotor when its plane turns around the axis perpendicular to the disc's axle. The resulting action of Coriolis force produced by the rotating mass elements of the disc is expressed as the integrated resistance torque counteracting the external torque [10]. Figure 3.4 depicts the mass element m that ravels in a circle on the disc, which turns on the plane yoz in precession angle $\Delta\gamma$ around axis ox. This turn leads to a change in the direction of the tangential velocity of mass elements and produces the acceleration and Coriolis forces of the rotating mass elements. The turn of the disc's plane around axis ox leads to a non-identical change in the directions of the tangential velocity vectors. The maximal changes in direction result in the velocity vectors V^* of the mass element being located on the line of axis ox (Fig. 3.4). The two vectors do not have any changes in tangential velocity V, whose directions are parallel, to the line of axis ox, that is, located on 90° and 270° from axis ox. These variable changes in tangential velocity vectors are represented by the vector's components V_z whose

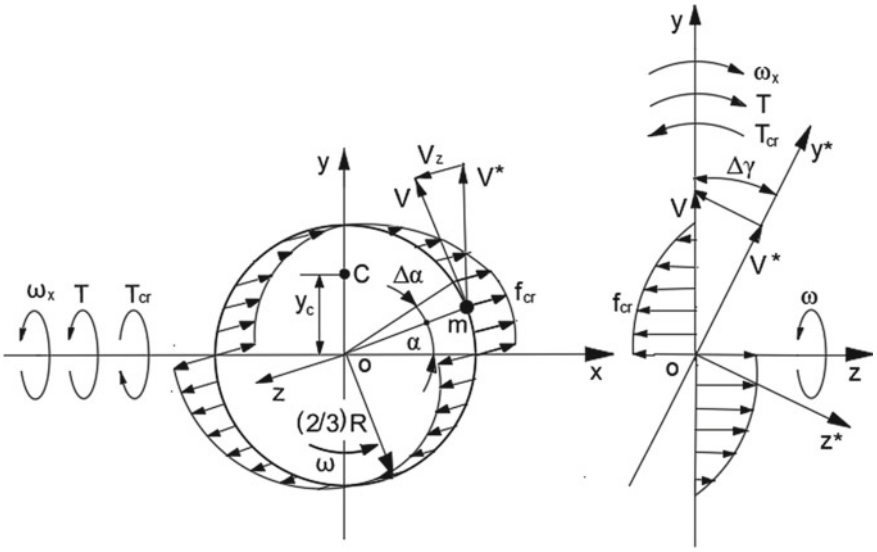

Fig. 3.4 Schematic of the acting forces, torques and motions of the spinning disc

directions are parallel to the rotor's axle *oz*. Changes in velocity are represented by an acceleration of the mass elements and are hence inertial forces.

The resistance torque generated by the Coriolis force of the rotating mass element is expressed by

$$\Delta T_{\mathrm{cr}} = -f_{\mathrm{cr}} y_{\mathrm{m}} = -m a_{\mathrm{z}} y_{\mathrm{m}} \tag{3.22}$$

where ΔT_{cr} is the torque generated by Coriolis force f_{cr} of the disc's mass element m; a_z is the Coriolis acceleration of the mass element along axis *oz;* $y_m = (2/3)R \sin \alpha$ is the distance to the mass element's location along axis *oy*; the sigh (−) means the action in the clockwise direction around axis *ox*; and the other components are represented in Eq. (3.2).

The equation for Coriolis acceleration a_z is defined by the first derivative of the change in tangential velocity, whose value depends on the angle of its location on plane *yoz*, which

varies with time (Sect. 2.2; [10]). The expression for a_z is represented by the following equation.

$$\alpha_z = \frac{\mathrm{d}V_z}{\mathrm{d}t} = \frac{\mathrm{d}(V \cos\alpha \sin\Delta\gamma)}{\mathrm{d}t} = V \cos\alpha \frac{\mathrm{d}\gamma}{\mathrm{d}t} = \frac{2}{3} R\omega\omega_x \cos\alpha \tag{3.23}$$

where $a_z = \mathrm{d}V_z/\mathrm{d}t$ is the Coriolis acceleration along axis *oz*, $V_z = V\cos\alpha\sin\Delta\gamma$ is the change in the tangential velocity, $\Delta\gamma$ is the small angle of the rotor's plane turning around axis *ox* ($\sin\Delta\gamma = \gamma$ for small value of the angle), $V = (2/3)R\omega$, α is the angular location of the mass element, $\omega_x = \mathrm{d}\gamma/\mathrm{d}t$ is the angular velocity of precession around axis *ox,* and other components are as specified above.

Substituting the defined parameters into Eq. (3.22) and transformation yields the following equation.

$$\Delta T_{\mathrm{cr}} = -\frac{M\Delta\delta}{2\pi} \times \frac{2}{3} R\omega\omega_x \cos\alpha \times y_{\mathrm{C}} = -\frac{MR\omega\omega_x\Delta\delta}{3\pi} \cos\alpha \times y_{\mathrm{C}} \tag{3.24}$$

The Coriolis forces represent the distributed load along the circumference where the disc's mass elements are disposed. Figure 2.4 depicts the locations of Coriolis forces generated by the motion of rotating mass elements m around axes *oz* and *ox*. A distributed load can be equated with a concentrated load applied at a specific point along the semicircle. The location of the resultant force is the centroid (point *C*, Fig. 3.4) of the area under the Coriolis force's curve calculated by Eq. (3.4) but with its symbols. Substituting the defined parameters into Eq. (3.4) and transformation yields the following equation.

$$y_C = \frac{\int_{\alpha=0}^{\pi} f_{\text{ct}\cdot z}\, y_{\text{m}} \mathrm{d}\alpha}{\int_{\alpha=0}^{\pi} f_{\text{ct}\cdot z}\, \mathrm{d}\alpha} = \frac{\int_0^{\pi/2} \frac{MR\omega\omega_x\Delta\delta}{3\pi} \cos\alpha \times \frac{2}{3} R \sin\alpha \mathrm{d}\alpha}{\int_0^{\pi/2} \frac{MR\omega\omega_x\Delta\delta}{3\pi} \cos\alpha \mathrm{d}\alpha}$$
$$= \frac{\int_0^{\pi/2} \frac{MR\omega\omega_x\Delta\delta}{3\pi} \cos\alpha \times \frac{2}{3} R \sin\alpha \mathrm{d}\alpha}{\int_0^{\pi/2} \frac{MR\omega\omega_x\Delta\delta}{3\pi} \cos\alpha \mathrm{d}\alpha}$$
$$= \frac{\frac{MR^2\omega\omega_x\Delta\delta}{3\pi} \int_0^{\pi/2} \frac{2}{3} \cos\alpha \sin\alpha \mathrm{d}\alpha}{\frac{MR^2\omega\omega_x\Delta\delta}{3\pi} \int_0^{\pi/2} \cos\alpha \mathrm{d}\alpha} = \frac{\int_0^{\pi/2} \frac{1}{3} \sin 2\alpha \mathrm{d}\alpha}{\int_0^{\pi/2} \cos\alpha \mathrm{d}\alpha} \tag{3.25}$$

where the expression $\frac{MR\omega\omega_x\Delta\delta}{3\pi} \cos\alpha$ is accepted as constant for Eq. (3.25), the expression $2 \sin\alpha \cos\alpha = \sin 2\alpha$ is a trigonometric identity that is replaced in the equation, and the other parameters are as specified above.

When substituting Eq. (3.25), a differential form presents Eq. (3.24). Replacing $\cos\alpha = \int_0^{\pi} -\sin\alpha \mathrm{d}\alpha$ with the integral expression with defined limits and presenting other components by the integral forms yield the following:

$$\int_0^{T_{cr}} \mathrm{d}T_{\text{cr}} = \frac{MR^2\omega\omega_x}{3\pi} \times \int_0^{\pi} \mathrm{d}\delta \times \int_0^{\pi} -\sin\alpha \mathrm{d}\alpha \times \frac{\frac{1}{3}\int_0^{\pi/2} \sin 2\alpha \mathrm{d}\alpha}{\int_0^{\pi/2} \cos\alpha \mathrm{d}\alpha} \tag{3.26}$$

Solving integral Eq. (3.26) yields the following result.

$$T_{\text{cr}}\Big|_0^{T_{\text{cr}}} = \frac{MR^2\omega\omega_x}{3\pi} \times \left(\delta\Big|_0^{\pi}\right) \times \left(\cos\alpha\Big|_0^{\pi}\right) \times \frac{-\frac{1}{3\times 2} \cos 2\alpha\Big|_0^{\pi/2}}{\sin\alpha\Big|_0^{\pi/2}} \tag{3.27}$$

where the limits of integration for the centroid are taken for the quarter of the circle because its location in other quarters is the same.

If Coriolis forces act on the upper and lower sides of the disc's plane, then the total resistance torque T_{cr} is obtained when the result of Eq. (3.23) is increased twice.

$$T_{\text{cr}} = -2 \times \frac{MR^2\omega\omega_x}{3\pi} \times (\pi - 0) \times (-1 - 1) \times \frac{[-(-1 - 1)]}{6(1 - 0)} = -\frac{4MR^2\omega\omega_x}{9}$$
$$= -\frac{8}{9} J\omega\omega_x \tag{3.28}$$

where $J = MR^2/2$ is the rotor's mass moment of inertia; the sign (−) means the action in the clockwise direction; and the other parameters are as specified above.

Analysis of Eq. (3.28) demonstrates that the resistance torque generated by Coriolis forces of the disc's mass elements depends proportionally on the same components as represented in Eqs. (3.13) and (3.21).

3.1.4 The Change in the Angular Momentum of the Spinning Disc

Euler's fundamental principle of gyroscope theory is well described. The action of the change in the angular momentum about the centre of mass for the rotating disc and precession is demonstrated by placing a spinning disc with its axis horizontal (Fig. 3.5). The external torque T is turning the spinning disc around axis ox and the torque of the change in the angular momentum turning it around axis oy in the counterclockwise directions, the latter one is called precession. This precession effect is explained by the action of the external torque that generated the inertial precession torque. The two turns of the gyroscope are presented by interdependent motions around axis ox and around axis oy that are perpendicular to each other. The vector of the angular momentum H of the centre of mass of a rotating disc is located along axis oz, and the vector of the external torque T is located along axis ox, both perpendicular to each other as shown (Fig. 3.5). The external torque T acts on the rotating disc and changes the location of the angular momentum vector on the small angle $\Delta\gamma$ that is represented by the vector H^*. The change in the location of the angular momentum vector is represented by the vector ΔH which direction is up along the axis oy. Hence, the precession torque generated by the change in the angular momentum ΔH is acting around axis oy in the counterclockwise direction and represented by the following equation:

$$\Delta H = H \sin \Delta\gamma \tag{3.29}$$

where $H = J\omega$ is the angular momentum about the centre of mass for the rotating disc, $\sin\Delta\gamma = \Delta\gamma$ is the small angle of the change the location of the angular momentum vector, and other parameters are as specified above.

Substituting defined parameters into Eq. (3.29) and expressing the time rate change in angular momentum yield the following equation:

$$T_{\text{am}\cdot x} = \frac{\Delta H}{\Delta t} = J\omega\frac{\Delta\gamma}{\Delta t} = J\omega\omega_x = J\varepsilon_y = \frac{MR^2}{2}\varepsilon_y \tag{3.30}$$

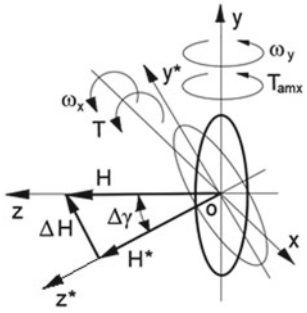

Fig. 3.5 Schematic the change in the angular momentum about the centre of mass for the spinning disc

where $T_{am} = \Delta H/\Delta t$ is the time rate change in the angular momentum that represents the precession torque acting around axis *oy* in the counterclockwise direction; $J = MR^2/2$ is the mass moment of disc's inertia; $\omega_x = \Delta\gamma/\Delta t$ is the angular velocity of precession around axis *ox,* which direction in the counterclockwise direction; $\varepsilon_y = \omega\omega_x$ is the angular acceleration of the rotating disc around axis *oy*; and other parameters are as specified above.

The analysis of Eq. (3.30) and Fig. 3.5 demonstrates that the precession torque depends on the mass moment of rotor's inertia, angular velocity and the angular velocity of the rotating disc around axis *ox*. The precession torque generated by the change in the angular momentum about the centre of mass for the rotating disc is the load torque acting around axis *oy*.

3.1.5 Attributes of Inertial Torques Acting on a Spinning Disc

The external torque applied to the spinning disc has generated the system of inertial torques acting on the rotating disc. These torques are resulting in resistance and precession torques, as well as the motions of the spinning disc around axes. The inertial torques are generated by the centrifugal, common inertial, Coriolis forces and the rate change in the angular momentum of the rotating disc. The resistance and precession torques are produced by one load torque, but act around two different axes *ox* and *oy*. All expressions of inertial torques contain the angular velocity of precession around axis *ox* and the angular velocity of the spinning rotor.

The resistance torques generated by the centrifugal and Coriolis forces act around axis *ox* in the one direction. The total initial resistance torque is represented their sum, whose equation is as follows:

$$T_r = T_{ct} + T_{cr} = \left(\frac{2\pi^2 + 8}{9}\right) J\omega\omega_x \tag{3.31}$$

where T_r is the total initial resistance torque acting around axis *ox*.

The torques generated by the common inertial forces (Eq. 3.21) and by the change in angular momentum (Eq. 3.26) act around axis *oy.* The total initial precession torque is represented their sum, whose equation is as follows:

$$T_p = T_{in} + T_{am} = \frac{2\pi^2 + 9}{9} J\omega\omega_x \tag{3.32}$$

where T_p is the total initial precession torque acting around axis *oy*.

At the starting condition, the external torque produces the initial resistance and precession torques generated by four inertial forces of rotating masses which are acting around axes *ox* and *oy*, respectively. The precession torques acting around axis oy are the result of the action of the load torque T around axis *ox*. These precession torques are the load torque which generates the resistance inertial torques acting

around the axis *oy*. The precession and resistance torques acting around axis *oy*, in turn, generate the precession torques acting around axis *ox* that are added to resistance and external torques acting around axis *ox*. Then, resulting torque acting around axis *ox* generates the precession torques acting around axis *oy*. This peculiarity of the interdependent action of the external and inertial torques of the gyroscopic devices is considered in the following chapters.

Analysis of the acting inertial forces on the rotating disc enables for stating that actual gyroscopic effects have more complex physics than represented in known publications. The external torque acting on the rotating disc produces the system of interrelated inertial torques generated by its rotating masses. The inertial torques are generated by the known inertial forces of classical mechanics that are the centrifugal, common inertial and Coriolis forces, as well as the change in the angular momentum. The combined action of the eight inertial torques around two axes manifests all gyroscopic effects of any rotating objects. These four types of inertial torques generated by the rotating masses are the part of the fundamental principles of gyroscope theory L. Euler's principle constitutes only the sixth part of all inertial torques generated by the spinning rotor.

Table 3.1 represents four different torques generated by the inertial pseudo forces of the spinning disc by the action of the external torque applied on the gyroscopic devices.

All these inertial torques constitute one system that is originated by the action of mass elements of the rotating disc. Any inertial torque cannot be separated from the action of the system of inertial torque that manifests all gyroscopic effects of rotating objects. This is the physical principle of the gyroscope theory [11–15]. The new equations for inertial torques enable for formulating any mathematical models for the motions of the gyroscopic devices. This analytical approach allows the physics of gyroscopic effects to be described clearly by known laws of classical mechanics.

Table 3.1 Equations of the inertial torques acting on the spinning disc generated by the external load torque

Type of the torque generated by	Equation	Percentage of action (%)
Centrifugal forces	$T_{\text{ct}} = T_{\text{in}} = \frac{2}{9}\pi^2 J\omega\omega_x$	34.95
Inertial forces		34.95
Coriolis forces	$T_{\text{cr}} = (8/9)J\omega\omega_x$	14.16
Change in angular momentum	$T_{\text{am}} = J\omega\omega_x$	15.94
Total		100
Resistance torque $T_r = T_{ct} + T_{cr}$	$T_{\text{r}} = \left(\frac{2\pi^2+8}{9}\right)J\omega\omega_x$	49.11
Precession torque $T_{\text{p}} = T_{\text{in}} + T_{\text{am}}$	$T_{\text{p}} = \left(\frac{2\pi^2+9}{9}\right)J\omega\omega_x$	50.89
Total		100

3.1.6 Working Example

The disc has a mass of 1.0 kg and a radius of 0.1 m and rotates at 3000 pm. An external torque acts on the disc, which precesses with an angular velocity of 0.05 rpm. Determine the values of the torques generated by the centrifugal, common inertial, Coriolis force and the change in the angular momentum. Compute the value of initial resistance and precession torques generated by the external torque. The problems are solved by equations represented in Table 3.2. Substituting the given data into defined equations and transformation yields the following results.

1. The torque generated by the centrifugal T_{ct} and common inertial T_{in} forces

$$T_{\mathrm{ct}} = T_{\mathrm{in}} = \frac{2}{9}\pi^2 J\omega\omega_x = \frac{2}{9}\pi^2 \times \frac{1.0 \times 0.1^2}{2} \times \frac{3000 \times 2\pi}{60} \times \frac{0.05 \times 2\pi}{60} = 0.018038720 \text{ Nm}$$

2. The torque generated by Coriolis T_{cr} forces

$$T_{\mathrm{cr}} = (8/9)J\omega\omega_x = \frac{8}{9} \times \frac{1.0 \times 0.1^2}{2} \times \frac{3000 \times 2\pi}{60} \times \frac{0.05 \times 2\pi}{60} = 0.007310818 \text{ Nm}$$

3. The initial resistance torque T_{r}

$$T_{\mathrm{r}} = \left(\frac{2\pi^2 + 8}{9}\right) J\omega\omega_x = \left(\frac{2\pi^2 + 8}{9}\right) \times \frac{1.0 \times 0.1^2}{2} \times \frac{3000 \times 2\pi}{60} \times \frac{0.05 \times 2\pi}{60} = 0.025349538 \text{ Nm}$$

4. The initial precession torque T_{p}

$$T_{\mathrm{p}} = \left(\frac{2\pi^2 + 9}{9}\right) J\omega\omega_x = \left(\frac{2\pi^2 + 9}{9}\right) \times \frac{1.0 \times 0.1^2}{2} \times \frac{3000 \times 2\pi}{60} \times \frac{0.05 \times 2\pi}{60} = 0.026263390 \text{ Nm}$$

where $J = MR^2/2$ is the moment of inertia of the disc [6].

3.2 Inertial Forces and Torques Acting on a Spinning Cylinder

3.2.1 Centrifugal Forces and torques Acting on a Spinning Cylinder

The spinning cylinder is the typical component of the gyroscopic device. The action of the inertial forces generated by the mass elements of the spinning cylinder definitely should be considered. The cylinder is spinning with a constant angular velocity ω around its horizontal axis oz in a counterclockwise direction when viewed from the tip of axis oz (Fig. 3.6). The system of coordinates $\Sigma oxyz$ locates at the centre of the cylinder's symmetry. The cylinder's mass elements m are located on the radius is $(2/3)R$ and along the length L, creating the rotating cylinder around axes oz. An external torque is applied to the spinning cylinder and generated the centrifugal forces of the cylinder's mass elements that are resisted on the action of external torque.

The analytical approach for the modelling of the action of the centrifugal forces f_{ct} generated by the mass elements of the spinning cylinder is the similar as represented for the spinning disc in Sect. 3.1.1. It is considered the rotating mass elements located on the cylindrical surface of a 2/3 radius for the left side of the spinning cylinder (Fig. 3.6). These mass elements generate the change in the vector's components $f_{ct\cdot z} = f_{ct} \sin \Delta\gamma$, whose directions are parallel to the axis oz. Other components of the centrifugal forces that located at upper and low sides and left and right sides of the

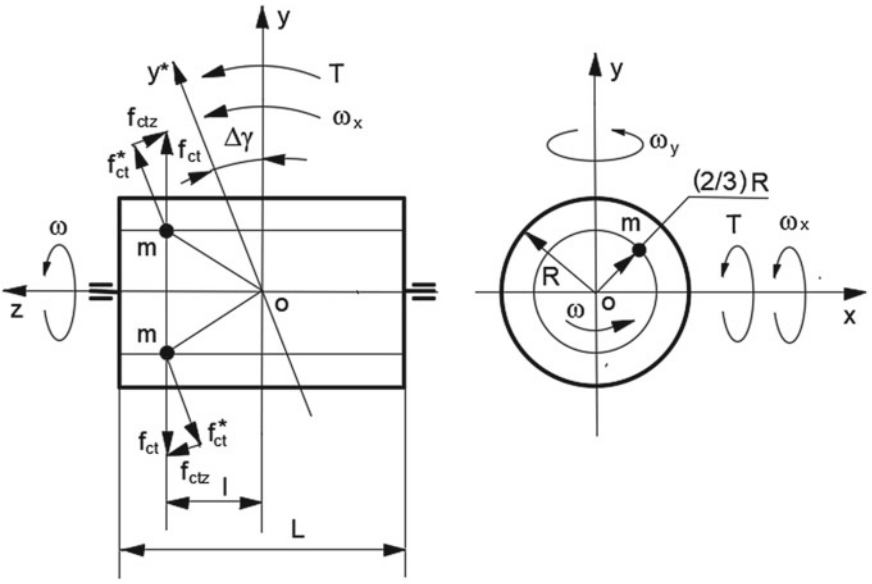

Fig. 3.6 Schematic of the spinning cylinder

spinning cylinder are similar. The integrated product of components for the vectors changes in centrifugal forces $f_{ct\cdot x}$, and their radius of location relative to axis ox generates the resistance torque $T_{ct\cdot x}$ acting opposite to the external torque.

Similar resistance torques are generated by the mass elements located on the planes of the cylinder that parallel to the plane xoy (Fig. 3.6). The analysis of the inertial torque generated by the centrifugal forces of the rotating cylinder is similar as described the inertial resistance torque produced by the centrifugal forces of the spinning disc as the reaction on the action of the external torque. The action of the external torque leads to the turning of the cylinder's plane xoy onto the small angle $\Delta\gamma$ around axis ox and to changing its location represented by the plane y^*ox (Fig. 3.2). The resistance torque produced by the centrifugal force of the mass element is expressed by the following equation:

$$\Delta T_{ct} = f_{ct\cdot z} y_m \tag{3.33}$$

where ΔT_{ct} is the torque generated by the centrifugal force of the spinning cylinder's mass element; $f_{ct\cdot z}$ is the axial component of the centrifugal force.

The following expression represents the equation for the component of the mass element's centrifugal force for the arbitrarily chosen plane that is perpendicular to axis of the cylinder (Fig. 3.2):

$$f_{ct\cdot z} = f_{ct} \sin \Delta\gamma = m\omega^2 \frac{2R}{3} \sin\alpha \sin \Delta\gamma \tag{3.34}$$

where $f_{ct} = m\omega^2(2/3)R\sin\alpha$ is the centrifugal force of the mass element m (Fig. 3.2); $m = [(M/2)/2\pi l]\Delta\delta\Delta l$; $M/2$ is the mass of the half cylinder; $l = L/2$ is the line that forms the left side of the cylinder surface of the mass element's location; R is the external radius of the cylinder; α is the angle of the mass element's location; $\Delta\delta$ is the sector's angle of the mass element's location on the plane that parallel to plane xoy; Δl is the element of the cylinder's length; ω is the constant angular velocity of the cylinder; $\Delta\gamma$ is the angle of turn of the cylinder's plane around axis ox ($\sin\Delta\gamma = \Delta\gamma$ for the small values of the angle).

Substituting the defined parameters into Eq. (3.34) yields the following equation:

$$f_{ct\cdot z} = \frac{M\omega^2 2R\sin\alpha}{2\times 2\pi(L/2)\times 3}\Delta l\Delta\delta\Delta\gamma = \frac{M\omega^2 R}{3\pi L}\Delta\delta\Delta\gamma\Delta l\sin\alpha \tag{3.35}$$

where all components are as specified above.

Substituting Eq. (3.35) into Eq. (3.33) brings the equation of the resistance torque produced by the centrifugal forces of the mass element.

$$\Delta T_{\text{ct}} = \frac{MR\omega^2}{3\pi L} \times \Delta\delta \times \Delta\gamma \times \Delta l \times \sin\alpha \times y_{\text{m}} \tag{3.36}$$

where $y_{\text{m}} = (2/3)R \sin\alpha$ is the distance of the mass element's location on the disc's plane relative to axis ox (Fig. 3.2) and other components are as specified above.

Equation (3.36) contains variable parameters whose incremental components are independent and represented by different symbols. Additionally, Eq. (3.36) allows for defining the integrated torque generated by the action of the centrifugal forces' axial components of the spinning cylinder's mass elements, wherein all components should be presented in a form appropriate for integration. The action of the centrifugal forces' axial components represents the distributed load applied across the length of the line forming the cylinder. Figure 3.2 depicts locations of the axial components of centrifugal forces $f_{\text{ct}\cdot z}$ generated by the mass elements m of the arbitrary plane of the spinning cylinder. The distributed loads are equated with a concentrated load applied at a specific point along axis oy, which is the centroid at the semicircle of the cylinder. The location of the resultant force is the centroid (point A, Fig. 3.2) of the area under the curve of each plane of the mass element along axis oz. The distance of the location of point A is defined by the expression y_m that is represented by the following equation:

$$\begin{aligned} y_A &= \frac{\int_{\alpha=0}^{\pi}\int_{l=0}^{L/2} f_{\text{ct}\cdot z}\, y_{\text{m}}\, \text{d}\alpha\text{d}l}{\int_{\alpha=0}^{\pi}\int_{l=0}^{L/2} f_{\text{ct}\cdot z}\, \text{d}\alpha\text{d}l} = \frac{\int_{\alpha=0}^{\pi} \frac{M\omega^2 R}{3\pi L}\Delta\gamma\Delta\delta \times \frac{2}{3}R\sin\alpha\sin\alpha\text{d}\alpha \int_0^{L/2}\text{d}l}{\int_{\alpha=0}^{\pi} \frac{M\omega^2 R}{3\pi L}\Delta\gamma\Delta\delta\sin\alpha d\alpha \int_{l=0}^{L/2}\text{d}l} \\ &= \frac{\frac{M\omega^2 R}{3\pi L}\Delta\gamma\Delta\delta\frac{2}{3}R\int_{\alpha=0}^{\pi}\sin^2\alpha\text{d}\alpha\int_0^{L/2}\text{d}l}{\frac{M\omega^2 R}{3\pi L}\Delta\gamma\Delta\delta\int_{\alpha=0}^{\pi}\sin\alpha\text{d}\alpha\int_0^{L/2}\text{d}l} = \frac{R\int_0^{\pi}(1-\cos 2\alpha)\text{d}\alpha}{3\int_0^{\pi}\sin\alpha\text{d}\alpha} \end{aligned} \tag{3.37}$$

where the expression $\frac{M\omega^2 R}{3\pi L}\Delta\delta\Delta\gamma$ is accepted at this stage of computing as constant for the Eq. (3.37); the expression $\sin^2\alpha = (1-\cos 2\alpha)/2$ is a trigonometric identity that is replaced in the equation, and other parameters are as specified above.

The total torque is the product of integrated resistance torques of the centrifugal forces and the centroid distance. Combining Eq. (3.37) and Eq. (3.36), and replacing $\sin\alpha = \int_0^{\pi/2}\cos\alpha\text{d}\alpha$ by the integral expression with defined limits, and representing other components by the integral forms, and transformation, the following equation emerges:

$$\int_0^{T_{ct}} \text{d}T_{\text{ct}} = \frac{M\omega^2 R}{3\pi L} \times \int_0^{\pi}\text{d}\delta \times \int_0^{\pi}\cos\alpha\text{d}\alpha \times \int_0^{\gamma}\text{d}\gamma \times \int_0^{L/2}\text{d}l \times \frac{R\int_0^{\pi}(1-\cos 2\alpha)\text{d}\alpha}{3\int_0^{\pi}\sin\alpha\text{d}\alpha} \tag{3.38}$$

where the limits of integration for the trigonometric expression of sinus are taken for the quarter of the circle and result is increased twice.

Solving of integral Eq. (3.38) yields the following result:

$$T_{\mathrm{ct}}\Big|_0^{T_{\mathrm{ct}}} = \frac{M\omega^2 R}{3\pi L} \times \delta\Big|_0^{\pi} \times \left(2\sin\alpha\Big|_0^{\pi/2}\right) \times (\gamma) \times \left(l\Big|_0^{L/2}\right) \times \frac{R\left(\alpha - \frac{1}{2}\sin 2\alpha\right)\Big|_0^{\pi/2}}{-3\cos\alpha\Big|_0^{\pi}}$$

Thus, giving rise to the following:

$$\begin{aligned} T_{\mathrm{ct}} &= \frac{M\omega^2 R}{3\pi L} \times \pi \times 2(1-0) \times (\gamma - 0) \times \left(\frac{L}{2} - 0\right) \times \frac{R(\pi/2 - 0)}{-3(-1-1)} \\ &= \frac{MR^2\pi\omega^2}{36} \times \gamma \end{aligned} \tag{3.39}$$

where all parameters are as specified above.

The rate of change in the torque T_{ct} per time is expressed by the differential equation

$$\frac{\mathrm{d}T_{\mathrm{ct}}}{\mathrm{d}t} = \frac{MR^2\pi\omega^2}{36}\frac{\mathrm{d}\gamma}{\mathrm{d}t} \tag{3.40}$$

where $t = \alpha/\omega$ is the time taken relative to the angular velocity of the rotor and other parameters are as specified above.

The differential of time and the angle is:$\mathrm{d}t = \frac{\mathrm{d}\alpha}{\omega}$; the expression $\frac{\mathrm{d}\gamma}{\mathrm{d}t} = \omega_x$ is the angular velocity of the spinning rotor's precession around axis ox. Substituting the defined components into Eq. (3.40) and transformation yields a new differential equation with the following expression:

$$\frac{\omega \mathrm{d}T_{\mathrm{ct}}}{\mathrm{d}\alpha} = \frac{MR^2\pi\omega^2\omega_x}{36} \tag{3.41}$$

Separation of the variables of Eq. (3.41) and transformation brings the following equation.

$$\mathrm{d}T_{\mathrm{ct}} = \frac{MR^2\pi\omega\omega_x}{36}\mathrm{d}\alpha \tag{3.42}$$

Equation (3.42) is represented by the integral form with defined limits that is expressed by the following integral equation:

$$\int_0^{T_{\mathrm{ct}}} \mathrm{d}T_{ct} = \int_0^{\pi} \frac{MR^2\pi\omega\omega_x}{36}\mathrm{d}\alpha \tag{3.43}$$

Solving of Eq. (3.43) yields

$$T_{\text{ct}}\Big|_0^{T_{\text{ct}}} = \frac{MR^2\pi\omega\omega_x}{36}\alpha\Big|_0^{\pi}$$

Thus, giving rise to the following:

$$T_{\text{ct}} = \frac{MR^2\pi^2\omega\omega_x}{36} \tag{3.44}$$

The change in centrifugal forces acts on the upper, lower, left and right sides of the cylinder; then, the total resistance torque T_{ct} is obtained when the result of Eq. (3.40) is increased four times. Then Eq. (3.44) is represented by the following expression:

$$T_{\text{ct}} = \frac{4MR^2\pi^2\omega\omega_x}{36} = \frac{2}{9}\pi^2 J\omega\omega_x \tag{3.45}$$

For the half cylinder with the length L and full mass M, the resistance torque is presented by the following equation:

$$T_{\text{ct}} = \frac{2MR^2\pi^2\omega\omega_x}{18} = \frac{2}{9}\pi^2 J\omega\omega_x \tag{3.46}$$

where $J = MR^2/2$ is the cylinder's mass moment of inertia and other parameters are as specified above.

Analysis of Eqs. (3.46) shows that the resistance torque generated by the centrifugal forces of the spinning cylinder that locates symmetrically and unsymmetrically relatively of supports is the same as for the disc (Eq. 3.13).

3.2.2 Common Inertial Forces and Torques Acting on a Spinning Cylinder

The analytical approach for the modelling of the action of common inertial forces generated by the mass elements of the spinning cylinder is the same as represented in Sect. 3.1.2. The expression (Eq. (3.46)) for the resistance torque generated by the centrifugal forces for the spinning cylinder and spinning disc (Eq. 3.13) is the same. It means that the expression for the precession torque generated by the common inertial forces for the spinning cylinder will be the same and represented by the following equation:

$$T_{\text{in}} = \frac{2}{9}\pi^2 J\omega\omega_x \tag{3.47}$$

The change in the angular momentum represents a precession torque generated by the centre mass of the spinning cylinder and expressed by the well-known equation $T_{\text{am}} = J\omega\omega_{x.}$ The total precession torque acting on the cylinder around axis *oy* has represented a sum of the precession torques generated by the inertial forces of the mass elements and the change in the angular momentum *whose equation is as follows*:

$$T_{\text{p}x} = T_{\text{in}x} + T_{\text{am}x} = \left(\frac{2\pi^2 + 9}{9}\right) J\omega\omega_x \tag{3.48}$$

where $T_{\text{p}x}$ is the total precession torque acting around axis *oy* and other components are as specified above.

3.2.3 *Coriolis Forces and Torques Acting on a Spinning Cylinder*

The torques generated by the centrifugal and common inertial forces of the spinning cylinder and the spinning disc have the same expression (Sect. 3.1.2). This result enables for the making a conclusion that the expression of the torques generated by the Coriolis forces of the spinning cylinder will be the same as for the spinning disc and presented by the following equation:

$$T_{\text{cr}\cdot i} = \frac{8}{9} J\omega\omega_i \tag{3.49}$$

The total resistance torque acting on the cylinder around axis *ox* has represented a sum of the resistance torques generated by the centrifugal and Coriolis forces of the mass elements whose equation is as follows:

$$T_{\text{r}x} = T_{\text{ct}x} + T_{\text{cr}x} = \left(\frac{2\pi^2 + 8}{9}\right) J\omega\omega_x \tag{3.50}$$

where $T_{\text{r}x}$ is the total resistance torque acting around axis *oy* and other components are as specified above.

Analysis of the expressions of inertial torques acting on the spinning cylinder demonstrates that all of them are the same as for the spinning disc and can be used for the modelling of motions for the spinning objects that have the same surfaces.

3.3 Inertial Forces and Torques Acting on a Spinning Thin Ring

3.3.1 Centrifugal Forces and Torques Acting on a Spinning Ring

The analysis of the inertial torques acting on the spinning thin ring with a constant angular velocity ω is considered the location of its mass elements m on the middle radius R. The action of centrifugal forces on a ring spinning around axis oz with an angular velocity of ω in a counterclockwise direction is considered in Fig. 3.7. The rotation of mass elements generates the plane of centrifugal forces, which disposes of perpendicular to the axis of the spinning ring. The action of an external torque on the spinning ring inclines the plane of the rotating centrifugal forces that resist the action of the external torque.

The following analysis of acting forces and motion of the spinning ring is similar as for rotation disc represented in Sect. 3.1, this chapter. There is a minor difference in the presentation of location of the mass elements of the ring R. The variable directions of centrifugal force vectors generate a change in vector components $f_{\text{ct}\cdot z}$ that are parallel to rotating ring axis oz (Fig. 3.2, this chapter). The change in the plane of the centrifugal force generates the resistance torque ΔT_{ct} of the mass element and is expressed as follows:

$$\Delta T_{\text{ct}} = -f_{\text{ct}\cdot z} y_{\text{m}} = -m a_z y_{\text{m}} \tag{3.51}$$

where $f_{\text{ct}\cdot z}$ is the change in the centrifugal force and y_{m} is the distance of the disposal of the mass element along axis oy.

The change in the centrifugal force of the mass element is expressed by the following equation:

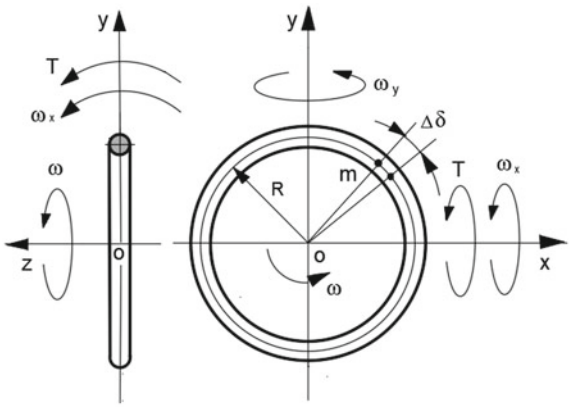

Fig. 3.7 Schematic of the spinning thin ring

$$f_{\text{ct}\cdot z} = f_{\text{ct}} \sin\alpha \sin\Delta\gamma = \left(\frac{MR\omega^2}{2\pi}\right)\Delta\delta \sin\alpha \sin\Delta\gamma = \frac{MR\omega^2}{2\pi}\Delta\delta\Delta\gamma \sin\alpha \tag{3.52}$$

where $f_{\text{ct}} = \frac{MR\omega^2}{2\pi}\Delta\delta$ is the centrifugal force of the mass element m; $m = \frac{M}{2\pi R}\Delta\delta R = \frac{M}{2\pi}\Delta\delta$ in which M is the mass of the ring; R is the radius of the mass elements location; $\Delta\delta$ is the sector's angle of the mass element's location; ω is the constant angular velocity of the ring; α is the angle of the mass element's location; $\Delta\gamma$ is the angle of turn for the ring's plane ($\sin\Delta\gamma = \Delta\gamma$ for the small values of the angle) around axis ox.

Substituting the defined parameters into Eq. (3.51) yields the equation of the resistance torque produced by the centrifugal forces of the mass element.

$$\Delta T_{\text{ct}} = -\frac{MR\omega^2}{2\pi} \times \Delta\delta \times \Delta\gamma \times \sin\alpha \times y_{\text{m}} \tag{3.53}$$

where $y_{\text{m}} = R \sin\alpha$ is the distance of the mass element's location on the ring's relative to axis ox and the other components are as specified above.

The location of the resultant force is the centroid (point A, Fig. 3.2, this chapter), which is calculated by the known integrated equation.

$$y_A = \frac{\int_{\alpha=0}^{\pi} f_{\text{ct}\cdot z}\, y_{\text{m}}\, \text{d}\alpha}{\int_{\alpha=0}^{\pi} f_{\text{ct}\cdot z}\, \text{d}\alpha} \tag{3.54}$$

Substituting Eq. (3.52) and other components into Eq. (3.54) and transformation yields the following expression.

$$\begin{aligned} y_A &= \frac{\int_{\alpha=0}^{\pi} f_{\text{ct}\cdot z}\, y_{\text{m}}\, \text{d}\alpha}{\int_{\alpha=0}^{\pi} f_{\text{ct}\cdot z}\, \text{d}\alpha} = \frac{\int_{\alpha=0}^{\pi} \frac{MR\omega^2}{2\pi}\Delta\delta \times \Delta\gamma \times R \sin\alpha \sin\alpha \text{d}\alpha}{\int_{\alpha=0}^{\pi} \frac{MR\omega^2}{2\pi}\Delta\delta \times \Delta\gamma \sin\alpha \text{d}\alpha} \\ &= \frac{\frac{MR\omega^2}{2\pi}\Delta\delta\Delta\gamma \int_{\alpha=0}^{\pi} R \sin^2\alpha \text{d}\alpha}{\frac{MR\omega^2}{2\pi}\Delta\delta\Delta\gamma \int_{\alpha=0}^{\pi} \sin\alpha \text{d}\alpha} = \frac{\frac{R}{2}\int_0^{\pi}(1-\cos 2\alpha)\text{d}\alpha}{\int_0^{\pi}\sin\alpha \text{d}\alpha} \end{aligned} \tag{3.55}$$

The following solutions are the same as presented in Sect. 3.1, and all comments are omitted.

$$\int_0^{T_{\text{ct}}} \text{d}T_{\text{ct}} = -\frac{MR\omega^2}{2\pi} \times \int_0^{\pi} \text{d}\delta \times \int_0^{\gamma} \text{d}\gamma \times \int_0^{\pi} \cos\alpha \text{d}\alpha \times \frac{R\int_0^{\pi}(1-\cos 2\alpha)\text{d}\alpha}{2\int_0^{\pi}\sin\alpha \text{d}\alpha} \tag{3.56}$$

where the first integral of the cosines is increased twice due to accepted limits of integration; the second integral of the cosines remains the same due to the symmetrical location of the centroid.

$$T_{\mathrm{ct}}\Big|_0^{T_{\mathrm{ct}}} = -\frac{MR\omega^2}{2\pi} \times \left(\delta\Big|_0^{\pi}\right) \times \left(\gamma\Big|_0^{\gamma}\right) \times 2\left(\sin\alpha\Big|_0^{\pi/2}\right) \times \frac{R\left(\alpha - \frac{1}{2}\sin 2\alpha\right)\Big|_0^{\pi/2}}{-2\cos\alpha\Big|_0^{\pi}}$$

$$T_{\mathrm{ct}} = -\frac{MR\omega^2}{2\pi} \times (\pi - 0) \times (\gamma - 0) \times 2(1 - 0) \times \frac{R\left(\frac{\pi}{2} - 0\right)}{-2(-1 - 1)} = -\frac{MR^2\omega^2\pi}{8} \times \gamma \tag{3.57}$$

$$\frac{\mathrm{d}T_{\mathrm{ct}}}{\mathrm{d}t} = -\frac{MR^2\omega^2\pi}{8}\frac{\mathrm{d}\gamma}{\mathrm{d}t} \tag{3.58}$$

$t = \frac{\alpha}{\omega}$, $\mathrm{d}t = \frac{\mathrm{d}\alpha}{\omega}$, $\frac{\mathrm{d}\gamma}{\mathrm{d}t} = \omega_x$.

$$\frac{\omega \mathrm{d}T_{\mathrm{ct}}}{\mathrm{d}\alpha} = -\frac{MR^2\omega^2\omega_x\pi}{8} \tag{3.59}$$

$$\int_0^{T_{\mathrm{ct}}} \mathrm{d}T_{\mathrm{ct}} = -\int_0^{\pi} \frac{MR^2\omega\omega_x\pi}{8}\mathrm{d}\alpha \tag{3.60}$$

$$T_{\mathrm{ct}}\Big|_0^{T_{\mathrm{ct}}} = -\frac{MR^2\omega\omega_x\pi}{8}\alpha\Big|_0^{\pi}$$

The total resistance torque T_{ct} is obtained when the result of Eq. (3.60) is increased twice because centrifugal forces act on the upper and lower sides of the ring.

$$T_{\mathrm{ct}} = -\frac{2\pi^2 MR^2\omega\omega_x}{8} = -\frac{1}{4}\pi^2 J\omega\omega_x \tag{3.61}$$

where $J = MR^2$ is the thin ring's mass moment of inertia. The other parameters are as specified above.

3.3.2 *Common Inertial Forces and Torques Acting on a Spinning Thin Ring*

The modelling of the acting common inertial forces generated by the mass elements of the spinning ring is the same as represented in Sect. 3.3.1. The equation of the precession torque generated by the common inertial forces of the ring is the same as for the resistance torque generated by the centrifugal forces and presented the Eq. (3.61):

$$T_{\mathrm{in}} = \frac{5}{72}\pi^3 J\omega\omega_x \tag{3.62}$$

where all components are represented in Sect. 3.3.1.

3.3.3 Coriolis Forces and Torques Acting on a Spinning Thin Ring

The resistance torque ΔT_{cr} generated by the Coriolis force of the rotating mass element is expressed by

$$\Delta T_{\mathrm{cr}} = -f_{\mathrm{cr}} y_{\mathrm{m}} = -m a_z y_{\mathrm{m}} \tag{3.63}$$

where all components are as specified above.

The following solution is the same as presented in this chapter, Sect. 3.3, in which comments are omitted

$$\alpha_z = \frac{\mathrm{d}V_z}{\mathrm{d}t} = \frac{\mathrm{d}(-V\cos\alpha\sin\Delta\gamma)}{\mathrm{d}t} = V\cos\alpha\frac{\mathrm{d}\gamma}{\mathrm{d}t} = R\omega\omega_x\cos\alpha \tag{3.64}$$

$$\Delta T_{\mathrm{cr}} = -\frac{M\Delta\delta}{2\pi} \times R\omega\omega_x\cos\alpha \times y_{\mathrm{C}} = -\frac{MR\omega\omega_x\Delta\delta}{2\pi}\cos\alpha \times y_{\mathrm{C}} \tag{3.65}$$

The centroid (point C, Fig. 3.3, this chapter) is expressed by the following equation.

$$\begin{aligned} y_{\mathrm{C}} &= \frac{\int_{\alpha=0}^{\pi} f_{\mathrm{ct}\cdot z} y_{\mathrm{m}}\mathrm{d}\alpha}{\int_{\alpha=0}^{\pi} f_{\mathrm{ct}\cdot z}\mathrm{d}\alpha} = \frac{\int_0^{\pi/2} \frac{MR\omega\omega_x\Delta\delta}{2\pi}\cos\alpha \times R\sin\alpha\mathrm{d}\alpha}{\int_0^{\pi/2} \frac{MR\omega\omega_x\Delta\delta}{2\pi}\cos\alpha\mathrm{d}\alpha} \\ &= \frac{\int_0^{\pi/2} \frac{MR\omega\omega_x\Delta\delta}{2\pi}\cos\alpha \times R\sin\alpha\mathrm{d}\alpha}{\int_0^{\pi/2} \frac{MR\omega\omega_x\Delta\delta}{2\pi}\cos\alpha\mathrm{d}\alpha} \\ &= \frac{\frac{MR^2\omega\omega_x\Delta\delta}{2\pi}\int_0^{\pi/2}\cos\alpha\sin\alpha\mathrm{d}\alpha}{\frac{MR^2\omega\omega_x\Delta\delta}{2\pi}\int_0^{\pi/2}\cos\alpha\mathrm{d}\alpha} = \frac{\int_0^{\pi/2}\frac{1}{2}\sin 2\alpha\mathrm{d}\alpha}{\int_0^{\pi/2}\cos\alpha\mathrm{d}\alpha} \end{aligned} \tag{3.66}$$

$$\int_0^{T_{\mathrm{cr}}} \mathrm{d}T_{\mathrm{cr}} = \frac{MR^2\omega\omega_x}{2\pi} \times \int_0^{\pi}\mathrm{d}\delta \times \int_0^{\pi} -\sin\alpha\mathrm{d}\alpha \times \frac{\frac{1}{2}\int_0^{\pi}\sin 2\alpha\mathrm{d}\alpha}{\int_0^{\pi}\cos\alpha\mathrm{d}\alpha} \tag{3.67}$$

$$T_{\mathrm{cr}}\Big|_0^{T_{\mathrm{cr}}} = \frac{MR^2\omega\omega_x}{2\pi} \times \left(\delta\Big|_0^{\pi}\right) \times \left(\cos\alpha\Big|_0^{\pi}\right) \times \frac{-\frac{1}{2\times 2}\cos 2\alpha\Big|_0^{\pi/2}}{\sin\alpha\Big|_0^{\pi/2}} \tag{3.68}$$

where the limits of integration for the centroid are taken for the quarter of the circle because its location is symmetrical at other quarters and the value is the same.

The total resistance torque T_{cr} is obtained when the result of Eq. (3.68) is increased twice.

$$T_{\mathrm{cr}} = -2 \times \frac{MR^2\omega\omega_x}{2\pi} \times (\pi - 0) \times (-1 - 1) \times \frac{[-(-1-1)]}{4(1-0)}$$

$$= -MR^2\omega\omega_x = -J\omega\omega_x \tag{3.69}$$

The inertial torque generated by the change in the angular momentum of the ring is presented by the following equation:

$$T_{\text{cr}} = MR^2\omega\omega_x = J\omega\omega_x \tag{3.70}$$

where all components are as specified above.

Mathematical models for the inertial torques acting on a spinning thin cylinder will be the same. This statement is substantiated by the obtained results of analytical approaches for inertial torques of the spinning disc and cylinder represented in Sects. 3.1 and 3.2.

3.3.4 *Attributes of Inertial Torques Acting on a Spinning Thin Ring*

The total initial resistance torque T_r acting around axis ox generated by the external torque is represented as the sum of the torques generated by the centrifugal and Coriolis forces whose equation is as follows

$$T_{\text{r}} = T_{\text{ct}} + T_{\text{cr}} = \left(\frac{\pi^2 + 4}{4}\right) J\omega\omega_x \tag{3.71}$$

The torques generated by the common inertial forces (Eq. 3.62) and by the change in angular momentum (Eq. 3.61) are acted around one axis oy. A total initial precession torque T_{p} is generated by the external torque and represented as their sum, whose equation is as follows

$$T_{\text{p}} = T_{\text{in}} + T_{\text{am}} = \left(\frac{\pi^2 + 4}{4}\right) J\omega\omega_x \tag{3.72}$$

Table 3.2 represents the four different torques generated by the inertial forces of the spinning thin ring and cylinder.

Analysis of the inertial torques acting on the spinning thin ring (Table 3.2) demonstrates differences in the results compared with a spinning disc and cylinder (Table 3.1) [16].

Table 3.2 Equations of the inertial torques acting on the spinning thin ring

Type of the torque generated by	Equation
Centrifugal forces, T_{ct}	$T_{ct} = T_{in} = \frac{1}{4}\pi^2 J\omega\omega_x$
Inertial forces, T_{in}	
Coriolis forces, T_{cr}	$T_{cr} = T_{am} = J\omega\omega_x$
Change in angular momentum, T_{am}	
Resistance torque $T_r = T_{ct} + T_{cr}$	$T_r = T_p = \left(\frac{\pi^2+4}{4}\right) J\omega\omega_x$
Precession torque $T_p = T_{in} + T_{am}$	

3.3.5 *Working Example*

The ring has a mass of 1.0 kg, a radius of 0.1 m on the spin axis and spinning at 3000 rpm. An external torque acts on the disc, which precesses with an angular velocity of 0.05 rpm. It determined the value of the torques generated by the centrifugal common inertial, Coriolis force and the change in the angular momentum and initial resistance and precession torques generated by the external torque. This problem is solved by equations of Table 3.2. Substituting the given data into equations of Table 3.2 and transformation yields the following result.

1. The torque generated by the centrifugal T_{ct} and common inertial T_{in} forces

$$\begin{aligned} T_{ct} = T_{in} &= \frac{1}{4}\pi^2 J\omega\omega_x \\ &= \frac{1}{4}\pi^2 \times 1.0 \times 0.1^2 \times \frac{3000 \times 2\pi}{60} \times \frac{0.05 \times 2\pi}{60} \\ &= 0.04058712 \text{ Nm} \end{aligned}$$

2. The torque generated by Coriolis T_{cr} forces and the change in the angular momentum T_{am}

$$\begin{aligned} T_{cr} = T_{am} = J\omega\omega_x &= 1.0 \times 0.1^2 \times \frac{3000 \times 2\pi}{60} \\ &\times \frac{0.05 \times 2\pi}{60} = 0.016449340 \text{ Nm} \end{aligned}$$

3. The initial resistance T_r and precession T_p torques

$$\begin{aligned} T_r = T_p = \left(\frac{\pi^2+4}{4}\right) J\omega\omega_x &= \left(\frac{\pi^2+4}{4}\right) \times 1.0 \times 0.1^2 \\ &\times \frac{3000 \times 2\pi}{60} \times \frac{0.05 \times 2\pi}{60} = 0.057036461 \text{ Nm} \end{aligned}$$

where $J = MR^2$ is the moment of inertia of the ring [6, 9].

References

1. Cordeiro, F.J.B.: The Gyroscope. Createspace, Scotts Valley (2015)
2. Greenhill, G.: Report on Gyroscopic Theory. Relink Books, Fallbrook (2015)
3. Scarborough, J.B.: The Gyroscope Theory and Applications. Nabu Press, London (2014)
4. Neil, B.: Gyroscope. The Charles Stark Draper Laboratory, Inc., Cambridge (2014). http://dx.doi.org/10.1036/1097-8542.304100
5. Weinberg, H.: Gyro Mechanical Performance: the most important parameter, Technical Article MS-2158, pp. 1–5. Analog Devices, Norwood (2011)
6. Hibbeler, R.C., Yap, K.B.: Mechanics for Engineers—Statics and Dynamics, 13th edn. Prentice Hall, Pearson (2013)
7. Gregory, D.R.: Classical Mechanics. Cambridge University Press, New York (2006)
8. Taylor, J.R.: Classical Mechanics. University Science Books, California (2005)
9. Aardema, M.D.: Analytical Dynamics. Theory and Application. Academic/Plenum Publishers, New York (2005)
10. Usubamatov, R., Ismail, K.A., Sah, J.M.: Analysis of coriolis acceleration. J. Adv. Sci. Eng. Res. **4**(1), 1–8 (2014)
11. Usubamatov, R.: Inertial forces acting on gyroscope. J. Mech. Sci. Technol. **32**(1), 101–108 (2018)
12. Usubamatov, R.: New analytical approach for finding the gyroscope forces and its properties. Asian J. Sci. Res. **10**, 380–386 (2017)
13. Usubamatov, R.: Mathematical models for gyroscope properties. Math. Eng. Sci. Aerospace **8**(3), 359–371 (2017)
14. Usubamatov, R.: Mathematical models for principles of gyroscope theory. Am. Inst. Phys. **1798**, 020133 (2017). https://doi.org/10.1063/1.497272
15. Usubamatov, R.: Mathematical model for gyroscope effects. AIP Conf. Proc. **1660**, 050018 (2015). https://doi.org/10.1063/1.4915651
16. Usubamatov, R.: Mathematical models for inertial torques acting on a spinning ring. Int. Robot. Autom. J. **5**(4), 147–151 (2019)

Chapter 4
Properties and Specifies of Gyroscopic Torques

4.1 Interrelations of Gyroscopic Torques

Classical mechanics considers the inertial forces as the pseudo which action demonstrates the property of the real external force [1–6]. Nevertheless, new investigations demonstrate the phenomena of deactivation of the gyroscopic inertial forces, i.e., the nature of the pseudo forces is more complex than presented in publications [7–11]. The interrelated action of the system of external and the inertial torques generated by the rotating masses of the spinning objects expresses their causal dependencies in 3D axes coordinate systems [12–16]. The knowledge of the reasonable dependencies in the action of the inertial torques enables for computing physical parameters of a wide spectrum of the rotating objects that manifest gyroscopic effects [17–20]. Mathematical models for the inertial torques generated by the external load acting on the rotating disc represented in Table 3.1 (Sect. 3.1). The combined action of the external and inertial torques has resulted in the rotations of the gyroscopic devices around axes at the accepted system of Cartesian coordinates. The classical schema of the mathematical model for the motion of any object contains the external load force applied to the object and demonstrates its motion in the defined direction. The action of the external torque around one axis on the spinning disc manifests its motions around two axes. Such dual motions of a spinning disc under the action of one external torque are the result of the action of interrelated inertial torques. The combined action of the torques manifests unusual reactions and motions of rotating objects in space that are called gyroscopic effects. This term is accepted in known publications that express the interrelated action of the torques and multiaxis motions of rotating objects. The physics of the gyroscopic effects of the spinning disc should be considered in detail and thoroughly described. The reason for such a statement is motivated by the long-time absence of the true mathematical models for the theory of gyroscopic effects in the known publications. Analysis of the action of the external torques on the spinning disc demonstrates the sequence chain of a generation of inertial torques and their actions around axes. The action external and inertial torque on a spinning disc around two axes is strictly perpendicular to each other. This fact

© The Editor(s) (if applicable) and The Author(s), under exclusive license to Springer Nature Singapore Pte Ltd. 2020

R. Usubamatov, *Theory of Gyroscopic Effects for Rotating Objects*,
https://doi.org/10.1007/978-981-15-6475-8_4

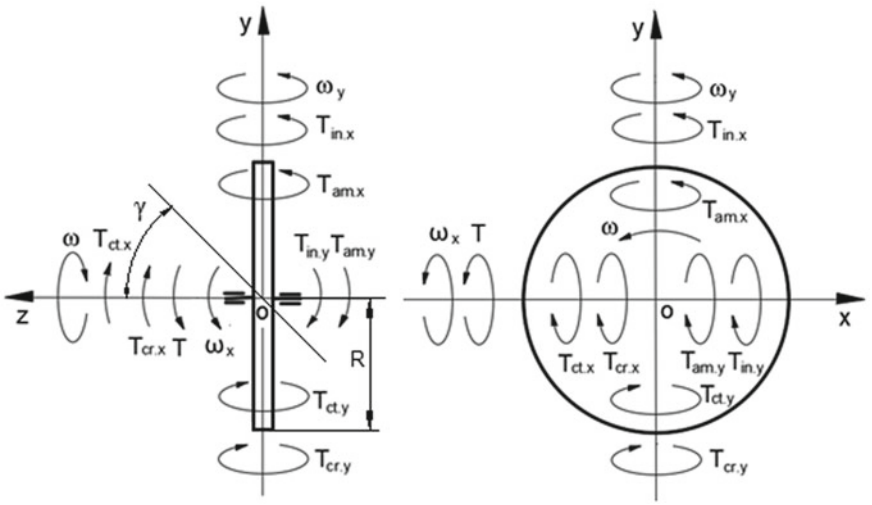

Fig. 4.1 External and inertial torques acting around axes on the spinning disc

is explained by the geometry of the rotating disc which axis and the plane of the disc are strictly perpendicular to each other. The action of the interrelated torques is manifested by the big difference in the angular velocities around axes of the spinning disc. The ratio of their angular velocities around axes is maintained and can be changed by the action of complex interdependency of the external and inertial torques on the spinning disc. The interrelated action of all torques on the spinning disc is described by the studies presented below. The action of the external and inertial torques around axes on the rotating disc is demonstrated in Fig. 4.1 where the disc locates symmetrically relatively of its supports at the system of coordinate $\Sigma oxyz$. The interrelated action of the inertial torques is considered for the common case when the axis of the spinning disc turns in counterclockwise direction around axis ox. For the starting condition is considered, the horizontal location of the spinning disc axis $\gamma = 0$.

The following steps consider the action of the external torque T on the spinning disc that generates the sequential simultaneous activation of the inertial torques around two axes. The gyroscope motions around axes are implemented due to interrelations of the inertial torques generated by the spinning disc.

1. The spinning disc rotates ω in the counterclockwise direction (it is considered from the tip of axis oz) and turns down in the counterclockwise direction around axis ox under the action of the external load torque T:

   - At the starting condition, the external torque T produces the resistance torques ($T_{ct.x}$ and $T_{cr.x}$) that generated by the centrifugal and Coriolis forces, which are restraint torques acting around axis ox and contradict to the action of the external torque.

- The resistance torques ($T_{ct.x}$ and $T_{cr.x}$) act in the clockwise direction, i.e. opposite to the action of the external torque T but the turn of the spinning disc is in the direction of the action of the external torque.

2. At the starting condition, the external torque T generates the precession torques ($T_{\text{in}\cdot x}$ and $T_{\text{am}\cdot x}$) that produced by the common inertial forces and the change in the angular momentum. These precession torques are load torques for the spinning disc are originated along axis *ox* but acting around axis *oy* in the counterclockwise direction. The resistance ($T_{\text{ct}\cdot x}$ and $T_{\text{cr}\cdot x}$) and precession ($T_{\text{in}\cdot x}$ and $T_{\text{am}\cdot x}$) torques are acting around axes *ox* and *oy,* respectively, and simultaneously. The equations of their inertial torques contain one angular velocity ω_x around axis *ox*.
3. The spinning disc turns in the counterclockwise direction around axis *oy* under the action of the precession torques ($T_{\text{in}\cdot x}$ and $T_{\text{am}\cdot x}$):

   - The precession torques ($T_{\text{in}\cdot x}$ and $T_{\text{am}\cdot x}$) acting around axis *oy* generate the resistance torques ($T_{\text{ct}\cdot y}$ and $T_{\text{cr}\cdot y}$) of centrifugal and Coriolis forces acting around axis *oy,* which act in a clockwise direction and represent the restraint torques.
   - The resulting torque, which is the combination of the precession ($T_{\text{in}\cdot x}$ and $T_{\text{am}\cdot x}$) and resistance ($T_{\text{ct}\cdot y}$ and $T_{\text{cr}\cdot y}$) torques, acts around axis *oy.* This resulting torque $T_{r.y} = T_{\text{in}\cdot x} + T_{\text{am}\cdot x} - T_{\text{ct}\cdot y} - T_{\text{cr}\cdot y}$ generates the precession torques ($T_{\text{in}\cdot y}$ and $T_{\text{am}\cdot y}$) of common inertial forces and the change in the angular momentum acting around axis *ox*. The precession torques ($T_{\text{in}\cdot y}$ and $T_{\text{am}\cdot y}$) act opposite to the direction of the external torque *T.* The resistance torques ($T_{\text{ct}\cdot x}$ and $T_{\text{cr}\cdot x}$) and the precession torques ($T_{\text{in}\cdot y}$ and $T_{\text{am}\cdot y}$) in a sum constitute the resulting resistance torque ($\Sigma T_{\text{r}\cdot x} = T_{\text{ct}\cdot x} + T_{\text{cr}\cdot x} + T_{\text{in}\cdot y} + T_{\text{am}\cdot y}$) acting opposite to the direction of the external torque *T.*

4. The equation of the total resulting torque acting around axis *ox* is represented by the following equation $T_{\text{t}\cdot x} = T - \Sigma T_{\text{r}\cdot x} = T - (T_{\text{ct}\cdot x} + T_{\text{cr}\cdot x} + T_{\text{in}\cdot y} + T_{\text{am}\cdot y})$. The total resulting torque acting around axis *ox* $T_{\text{t}\cdot x}$ represents the combination of the external and inertial torques that generates the precession torques acting around axis *oy* ($T^*_{\text{in}\cdot x}$ and $T^*_{\text{am}\cdot x}$) that is not the same as at starting condition (paragraph 1). The precession torques *(*$T^*_{\text{in}\cdot x}$ and $T^*_{\text{am}\cdot x}$) in turn generate the resistance torque ($T^*_{\text{ct}\cdot y}$ and $T^*_{\text{cr}\cdot y}$). The equation of the total resulting torque acting around axis *oy* is presented by the following equation $T_{\text{t}\cdot y} = T^*_{\text{in}\cdot x} + T^*_{\text{am}\cdot x} - (T^*_{\text{ct}\cdot y} + T^*_{\text{cr}\cdot y})$.

The chain of the sequencing and simultaneous action of the inertial torques generated by the one external torque results in the motions of the spinning disc around two axes. The action of the external and internal inertial torques on the spinning disc is the demonstration of their interrelations that implemented at one time. The system of inertial torques cannot be separated on the action of an individual or a group of torques. Any inertial torque cannot be omitted from the system of inertial torques because all of them are generated by one rotating mass of the spinning disc. This picture of interrelations of acting external and inertial torques shows their reasonable dependencies. A described peculiarity of the action of gyroscopic torques on

the spinning disc expresses clearly the physics of their origination that is manifested by gyroscopic motions around axes. The dual action of the external torque and the interrelation with the inertial torques around two axes can be formulated by two mathematical equations [12–16].

Practically, gyroscopic devices can operate at different conditions of the action of the external torques and the angular velocities of the gyroscope around axes. The action of the several external torques will generate own system and values of the inertial torques of spinning objects. Due to interrelations of the external and inertial torques acting on spinning objects, any change in values of inertial torques originated along one axis will lead to a change in values of inertial torques acting around another axis and vice versa. This statement follows up from the interrelations of the gyroscopic torques described above.

Analysis of the acting external and inertial torques around two axes demonstrates the following:

- The inertial torques acting around axis *oy* contain the resistance and precession inertial torques generated by the centrifugal, Coriolis and common inertial forces as well as the change in the angular momentum ($T_{\text{ct}\cdot y}$, $T_{\text{cr}\cdot y}$, $T_{\text{in}\cdot x}$ and $T_{\text{am}\cdot x}$).
- The inertial torques acting around axis *ox* contain the resistance and precession inertial torques generated by the same inertial forces pointed above ($T_{\text{ct}\cdot x}$, $T_{\text{cr}\cdot x}$, $T_{\text{in}\cdot y}$ and $T_{\text{am}\cdot y}$).
- The inertial torques acting around each axis contain one combination of the resistance and precession inertial torques. These inertial torques indirectly express kinetic energies generated by the potential energy of the external torque and kinetic energy of the spinning disc. The kinetic energies of the inertial torques acting around axes originated and distributed equally along axes *ox* and *oy* due to their interrelations.
- The value of the inertial torques, angular velocities and their interrelations around axes of the spinning disc is maintained by the principle of the mechanical energy conservation law.
- The external load torque generates the resistance and precession inertial torques acting around two axes. The precession torques represent the internal load that can be expressed by the external torque.

4.1.1 The Ratio of the Angular Velocities of Gyroscope Around Two Axes

The statement of equality of kinetic energies along axes for the spinning disc (Fig. 4.1) is proofed by the following confinement. The inertial torques originated along each axis indirectly express the potential and kinetic energies of the spinning disc. The sum of these inertial torques of one axis in the absolute value should be equal to the sum of the inertial torques in the absolute value of another axis. This statement presents the principle of the conservation of mechanical energy. The inertial torques

that originated along axis *ox* have presented the torques generated by the action of centrifugal, Coriolis and common inertial forces and the change in the angular momentum. The same internal torques originated along axis *oy*. The inertial torques acting around two axes are interrelated and expressed their energies originated along axes *ox* and *oy*. The equality of the potential and kinetic energies of the inertial torques is expressed by the equality of the absolute values of inertial torques acting around own axis and presented by the following equation:

$$|T_{\text{ct}\cdot x}| + |T_{\text{cr}\cdot x}| + \left|T_{\text{in}\cdot y}\right| + \left|T_{\text{am}\cdot y}\right| = |T_{\text{in}\cdot x}| + |T_{\text{am}\cdot x}| + \left|T_{\text{ct}\cdot y}\right| + \left|T_{\text{cr}\cdot y}\right| \tag{4.1}$$

Substituting expressions of the torques (Table 3.1, Chap. 3) into Eq. (4.1) and transformation yields the following equation:

$$\frac{2\pi^2}{9} J\omega\omega_x + \frac{8}{9} J\omega\omega_x + \frac{2\pi^2}{9} J\omega\omega_y + J\omega\omega_y = \frac{2\pi^2}{9} J\omega\omega_x + J\omega\omega_x + \frac{2\pi^2}{9} J\omega\omega_y + \frac{8}{9} J\omega\omega_y \tag{4.2}$$

where all parameters are as specified above.

Simplification of Eq. (4.2) yields the equality of the angular velocities of the spinning disc around axes *ox* and *oy*:

$$\omega_x = \omega_y \tag{4.3}$$

Equation (4.3) demonstrates the equality of the angular velocities around two axes, i.e. the equality of potential and kinetic energies of the inertial torques along two axes. This result is the validation of the statement of the equality of the potential and kinetic energies of the rotating disc along axes *ox* and *oy*.

The action of the external torque on the spinning disc demonstrates the different angular velocities of the disc around two axes. It means the value of the inertial torques acting around one axis does not coincide with the value of inertial torques around another axis. If the value of the inertial torque is big, then the value of the angular velocity should be small for one axis and vice versa. This is the principle of the conservation of mechanical energy for the rotating objects. The equality of the kinetic energies of the spinning disc motions around two axes *ox* and *oy* enables for expressing the equation of the equality of the inertial torques acting around the same axes. This analytical expression is represented by the following equation (Fig. 4.1):

$$-T_{\text{ct}\cdot x} - T_{\text{cr}\cdot x} - T_{\text{in}\cdot y} - T_{\text{am}\cdot y} = T_{\text{in}\cdot x} + T_{\text{am}\cdot x} - T_{\text{ct}\cdot y} - T_{\text{cr}\cdot y} \tag{4.4}$$

Substituting expressions of the torques (Table 3.1, Chap. 3) into Eq. (4.4) and transformation yields the following equation:

$$-\frac{2\pi^2}{9}J\omega\omega_x - \frac{8}{9}J\omega\omega_x - \frac{2\pi^2}{9}J\omega\omega_y - J\omega\omega_y = \frac{2\pi^2}{9}J\omega\omega_x + J\omega\omega_x - \frac{2\pi^2}{9}J\omega\omega_y - \frac{8}{9}J\omega\omega_y \quad (4.5)$$

where the sign (−) and (+) means the clockwise and counterclockwise directions of the action of the inertial torques around two axes, respectively.

Simplification of Eq. (4.5) yields the following result:

$$\omega_y = -(4\pi^2 + 17)\omega_x \quad (4.6)$$

where the sign (−) means the direction of the action of the inertial torque that can be omitted from the following analytical considerations.

Equation (4.6) demonstrates the actual ratio of the angular velocities of the spinning disc around two axes for the given example of consideration (Fig. 4.1). Analysis of Eqs. (4.5) and (4.6) shows the following peculiarity. The expression of the resistance torque $T_{\text{ct}\cdot y} = \frac{2\pi^2}{9}J\omega\omega_y$ generated by the centrifugal forces acting around axis *oy* is the same as the expression of the precession torque $T_{\text{in}\cdot y}$ generated by the inertial forces acting around axis *ox* $T_{\text{in}\cdot y} = \frac{2\pi^2}{9}J\omega\omega_y$. These expressions have the same sign, value, condition of origination and can be compensated in Eq. (4.5) by the algebraic rule: $-\frac{2}{9}\pi^2 J\omega\omega_y = -\frac{2}{9}\pi^2 J\omega\omega_y$. In the equations of the spinning disc motions around two axes, the initial resistance torque of one axis is compensated by the initial precession torque of another axis, which actions are around different axes do not coincide. This fact contradicts the principle of physics but accepted by abstract mathematical rules. This peculiarity of the mathematical models for the inertial torques is saved and used for other equations for motions of rotating objects around axes.

The combinations of the action of external and inertial torques can change the values of the angular velocities of the spinning disc around axes. The mechanical kinetic energy of each axis in absolute value remains constant at the time according to the principle of conservation of mechanical energy. This statement enables the combination of the mechanical energies of the rotating disc around two axes to be described. The change in the value of external torque leads to a change in the value of the kinetic energy of the spinning disc that expresses in the inertial torques acting around two axes. The values of inertial torques are always less than the value of the external torque that generates the kinetic energies of inertial torques acting around axes of a gyroscope.

For the spinning disc with inclined axis on the angle γ of the common location and with the load torque acting around axes *ox* and *oy* (Fig. 4.1), the equality of the kinetic energies of the spinning disc is represented by the modified Eq. (4.4):

$$-T_{\text{ct}\cdot x} - T_{\text{cr}\cdot x} - T_{\text{in}\cdot y} - T_{\text{am}\cdot y} = T_{\text{in}\cdot x}\cos\gamma + T_{\text{am}\cdot x}\cos\gamma - T_{\text{ct}\cdot y}\cos\gamma - T_{\text{cr}\cdot y}\cos\gamma \quad (4.7)$$

Substituting expressions of the torques (Table 3.1, Chap. 3) into Eq. (4.7) and transformation yields the following equation:

$$-\frac{2\pi^2}{9}J\omega\omega_x - \frac{8}{9}J\omega\omega_x - \frac{2\pi^2}{9}J\omega\omega_y - J\omega\omega\gamma = \frac{2\pi^2}{9}J\omega\omega_x\cos\gamma + J\omega\omega_x\cos\gamma - \frac{2\pi^2}{9}J\omega\omega_y\cos\gamma - \frac{8}{9}J\omega\omega_y\cos\gamma \quad (4.8)$$

Simplification of Eq. (4.8) yields the following result:

$$\omega_y = -\left[\frac{2\pi^2 + 8 + (2\pi^2 + 9)\cos\gamma}{2\pi^2 + 9 - (2\pi^2 + 8)\cos\gamma}\right]\omega_x \quad (4.9)$$

where the sign (−) means the direction of the action of the inertial torque that can be omitted from the following analytical considerations.

Equation (4.9) represents the variable ratio of the angular velocities for the precession of the spinning disc of the common location around two axes. For the horizontal location of the spinning disc axis ($\gamma = 0$), Eq. (4.9) is transformed into Eq. (4.6) where components of the common inertial and centrifugal inertial torques ($T_{\text{in}\bullet y}$, $T_{\text{ct}\bullet y}$) generated around axis *oy* are compensated and removed from Eq. (4.5). Equation (4.9) expresses the changes in the angular velocities of the spinning disc around two axes. The equations of the gyroscope motions describe its motion around separate axes at the accepted system of coordinates with the changes in the angular velocities (Eq. 4.9). The components of the inertial torques ($T_{\text{in}\bullet y}$, $T_{\text{ct}\bullet y}$) are remaining in the physics of motions but compensated due to internal relations as described above (Eq. 4.6). These components are removed from equations of gyroscope motions despite different expressions. The interrelation of equations is represented by the expression of the change in the angular velocities of the gyroscope around axes.

The dependency (Eq. 4.9) of the angular velocities of the gyroscope around axes is common and can be used for any orientations of the gyroscope relatively accepted axes of the coordinate system. The change in the axis of the action of the external torque and hence of the axes of inertial torques will reflect on the change in symbols of the angular velocities around axes (Eqs. 4.8 and 4.9). The ratio ω_y/ω_x of the angular velocities of the gyroscope around axis *oy* and *ox* is variable and depends on the angle of the axis of the spinning disc location (Fig. 4.2).

The diagram of Fig. 4.2 demonstrates the following. The turn of the spinning disc axis on the angle γ leads to the change of the ratio ω_y/ω_x of the angular velocities of the gyroscope around axis *oy* and *ox*. This ratio is changed from maximal value to zero with the change of the angular location of the spinning disc.

For the angle $\gamma = 0$, the ratio ω_y/ω_x is maximal as is follows:

$$\frac{\omega_y}{\omega_x} = \left[\frac{2\pi^2 + 8 + (2\pi^2 + 9)\cos 0}{2\pi^2 + 9 - (2\pi^2 + 8)\cos 0}\right] = 4\pi^2 + 17 = 56.478417604 \quad (4.10)$$

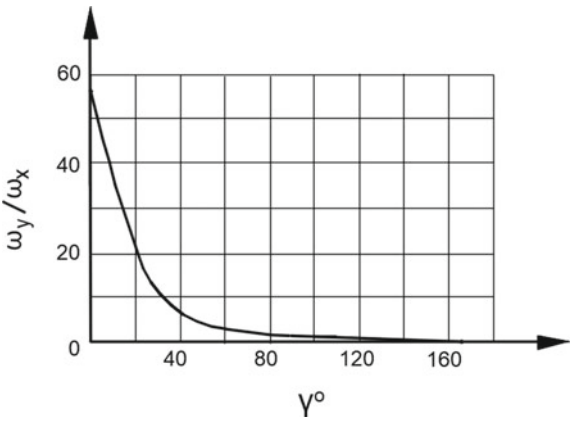

Fig. 4.2 Change of the ratio ω_y/ω_x of the angular velocities of the gyroscope around axis oy and ox versus the angle γ of the outer gimbal turn

For the motion of the gyroscope on the angle $\phi_{\max} = 164.841101855°$, when the axis of the spinning disc locates vertically, the ratio ω_y/ω_x is null as is follows

$$\frac{\omega_y}{\omega_x} = \left[\frac{2\pi^2 + 8 + (2\pi^2 + 9)\cos 164.841101855°}{2\pi^2 + 9 - (2\pi^2 + 8)\cos 164.841101855°}\right] = 0, \tag{4.11}$$

It means the ratio is active until the turn of the gyroscope around axis ox on the angle that is defined by the following expression:

$$\gamma = \frac{164.841101855°}{4\pi^2 + 17} = 2.918656521° \tag{4.12}$$

The angles $\gamma_{\max} = 2{,}9186756521°$ and $\phi_{\max} = 164.841101855°$ are maximal for the gyroscope turn around two axes simultaneously that maintain their ratio. When the gyroscope's internal gimbal with the spinning disc inclined on the angle $\varphi = -74.841101855°$ from the horizontal, the outer gimbal will turn on the angle $\gamma_{\max} = 2.9186756521°$ around vertical axis, and the internal gimbal will reach vertical location, i.e. $\varphi = 90.0°$. The following turn of the outer gimbal does not lead to the turn of the inner gimbal. Equation (4.9) does not have solutions for $\varphi = \pm 90^o$ because there are no precession torques.

The ratio of the gyroscope angular turn around axes is the same as the ratio of its angular velocities and represented by the following equation:

$$\omega_y t = -\left[\frac{2\pi^2 + 8 + (2\pi^2 + 9)\cos\phi}{2\pi^2 + 9 - (2\pi^2 + 8)\cos\phi}\right]\omega_x t \tag{4.13}$$

where t is the time of a turn of the gimbal, other components are as specified above.

Practically, these angular motions are visible on motions of the gyroscopic gimbals. This gyroscope property is validated by the test of the gyroscope with the horizontal location of the spinning disc axis and the turn of the outer and inner

gimbals around axes *oy* and *ox*. The defined angles of the gyroscope turn around axes are validated by the tests on the Super Precision Gyroscope "Brightfusion LTD" (Fig. 4.4) with the spinning disc.

4.1.2 Case Study and Practical Test

The interrelated action of external and inertial torques on a spinning disc shows that all of them come into action simultaneously. This manifestation should be analysed from the standpoint of sequences of the action of the inertial torques on a spinning disc. The external torque generates the system of inertial torques, which action represented by the rotational motions of the spinning disc around axes *ox* and *oy*. The spinning disc with the angular velocity ω located symmetrically regarding its supports of the gimbal 1, which rotates on supports of the gimbal 2 and later one rotates on pivots of the platform 4 (Figs. 4.3a and 4.4). The action of the external torque is applied to outer gimbal 2 of the gyroscope manifests the motions of the inner gimbal 1 around axis *ox* of the coordinate $\sum oxyz$. These motions of the gimbals around axes are expressed by the mathematical model of ratio for the angular velocities (Eq. 4.9). The torque T and inertial torques acting on the spinning disc start to turn the gimbal 2 in the counterclockwise direction around axis *oy* (Fig. 4.3a). The resulting inertial torques ($T_{p\cdot y} - T_{r\cdot x}$) generated by the spinning disc turn intensively the gimbal 1 in the clockwise direction around axis *ox* by the ratio of Eq. (4.10). The turn of the

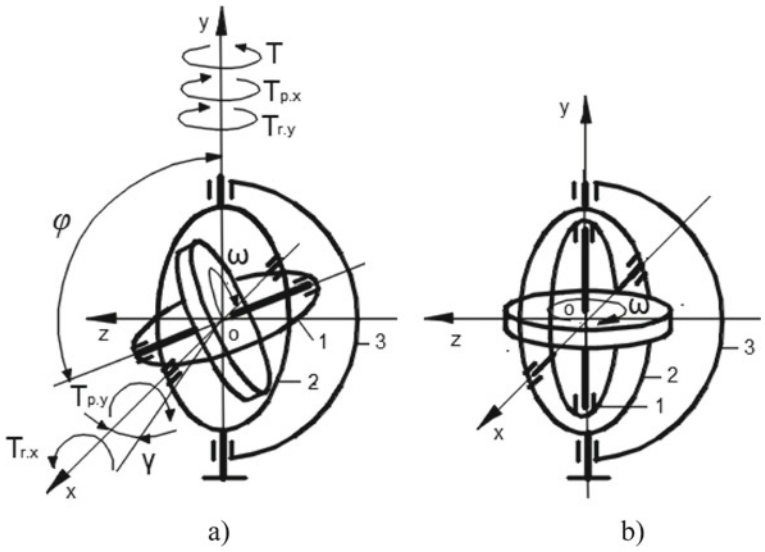

Fig. 4.3 Motions and locations of the spinning disc under the action of the external torque T applied to the gimbal

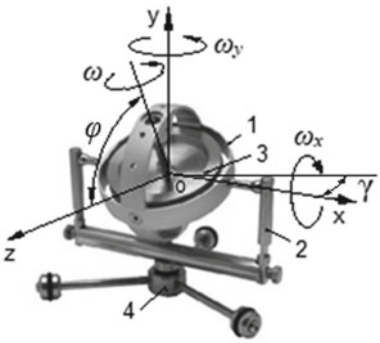

Fig. 4.4 Test stand of Super Precision Gyroscope "Brightfusion LTD"

gimbal 2 on the small angle $\gamma = 2^\circ\ 55'\ 71''$ around axis *oy,* under the action of the resulting torque $(T - T_{\text{p}\cdot x} - T_{\text{r}\cdot y})$, turns the gimbal 1 in the clockwise direction around axis *ox* on the maximal angle $\varphi = 164{,}841101855^\circ$ around axis *ox*. The following turn of the gimbal 2 does not turn the gimbal 1 that keeping the vertical location of the spin axis that coincides with axis *oy*. The final location of the gimbals is represented in Fig. 4.3b.

The practical test of the gimbal motions was conducted for the horizontal location of the spinning disc and its following turn until vertical. At the starting condition, the location of the spinning disc and the outer gimbal represented in Fig. 4.5a. The minor turn of the outer gimbal in the counterclockwise direction around the vertical axis *oy* on the angle γ leads to the big turn of the inner gimbal in the clockwise direction around the horizontal axis ox on the angle φ (Figs. 4.4 and 4.5b).The inner gimbal turns until the vertical location of the spinning disc axis with the minor turn of the outer gimbal on the angle γ (Fig. 4.5c). The following turn of the outer gimbal does not turn the inner gimbal (Fig. 4.5d).

The practical measurement of the angles of the turn for the gimbals by load torque conducted manually by the Mitutoyo Universal Bevel Protractor. The angle of the turn of the inner gimbal on $\omega_y t = 90^\circ$ from horizontal location implements by the minor turn of the outer gimbal on the angle $\omega_x t = \gamma$ and the motion of the inner

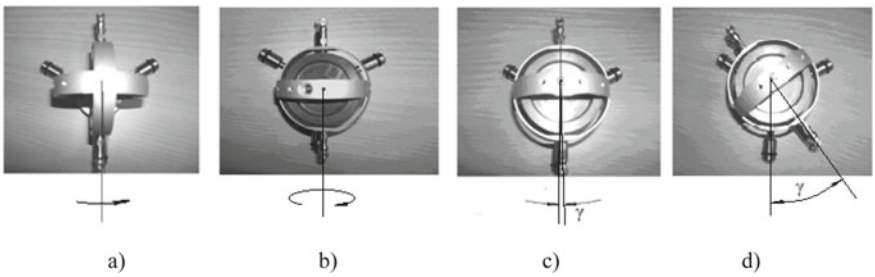

Fig. 4.5 Location of the spinning disc with the inner gimbal at the process of the turn of the outer gimbal

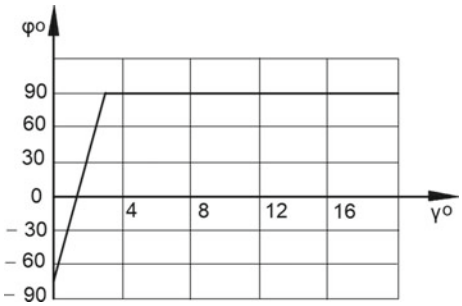

Fig. 4.6 Angular location of the outer gimbal versus the angular location of the spinning disc and the inner gimbal

gimbal on $\varphi = \varphi_{\max} - 90^{o} = 164.841101855^{\circ} - 90^{\circ} = 74.841101855^{\circ}$ that defined by Eq. (4.13).

$$90^{o} = \left[\frac{2\pi^2 + 8 + (2\pi^2 + 9)\cos 74.841101855^{\circ}}{2\pi^2 + 9 - (2\pi^2 + 8)\cos 74.841101855^{\circ}}\right]\gamma \quad \text{and}$$
$$\gamma = 1.641921^{\circ} = 1^{\circ}38'31''$$

The results of measurements yield $\gamma = 1^{\circ}\ 33^{'}$ with an accuracy of ±5 min. The deviation of measurements of the angular sizes is the high sensitivity on the manual turn of the outer gimbal. The turn of the spinning disc axis around axis *ox* on 90° confirmed optically by a template. This practical measurement is a well-matched theoretical result and the validation of the correctness of Eqs. (4.10), (4.12) and (4.13). The measurement of the turn of the inner gimbal around axis ox on $\varphi_{\max} = 164.841101855^{\circ}$ was problematic due to the constructional properties of the gyroscope cage. Figure 4.6 demonstrates the diagram of the change in the angular location of the inner gimbal versus the change in the angular location of the outer gimbal. The obtained results have explained the physics of gyroscopic gimbal motions that was one in the series of unsolved gyroscopic effects.

Analysis of the mathematical models for the inertial torques and angular velocities of gimbal's motions of the gyroscope around axes *ox* and *oy* demonstrates the direct dependency on the value of the external torque applied *T*. Inertial torques are inversely proportionally on the angular velocity of the spinning disc and its mass moment of inertia. The action of these torques is represented in the equations of gyroscope motions that depend on the consideration of the gyroscopic problems. The formulated mathematical models for the resulting resistance and precession torques acting around axes of consideration have manifested in the gimbals motions. The presentation of the action of these torques allows describing the physical processes that result in the gyroscopic effects. New mathematical models for the inertial torques acting on the rotating disc and motions describe the gyroscopic properties and can be useful for modelling the behaviour for the gyroscopic devices that is routing work for practitioners.

4.1.3 *Fundamental Principles of the Theory of Gyroscopic Effects*

Analysis and practical observation of the acting gyroscopic devices with external load torque demonstrate the following properties:

- The permanent external torque and the angular velocity of the spinning disc generate the eight inertial torques acting around axes of gyroscope rotation. The inertial torques indirectly express the mechanical energies of the gyroscope motions that depend on the angular velocity of the spinning disc ω and the angular velocity of precession ω_x around axis ox (Fig. 4.1). The product of these two angular velocities is always constant, $\omega\omega_x = \text{const}$. Increasing or decreasing the angular velocity ω of the spinning disc leads to decreasing or increasing the angular velocity ω_x of precession, respectively. This statement expresses the principle of conservation of mechanical energy.
- The value of the inertial torques and hence the angular velocity of precession ω_x depends on the value of the external torque, the disc's mass moment of inertia J and its angular velocity ω.
- For the given value of the external torque and the angular velocity ω of the spinning disc, there is the limit of the angular velocity of the gyroscope's precession ω_x, i.e. the limit of the kinetic energy of the inertial torques.
- Increasing the value of the external torque acting on a gyroscope, while the angular velocity of the disc is constant, leads to exceeding of the limit the angular velocity of precession ω_x and losing the ratio of the angular velocities of gyroscope's precession around two axes (Eqs. 4.6 and 4.9), i.e. the ratio of the angular velocities is not maintained.
- The resulting torque acting on a gyroscope around axis ox generates the resulting precession torque acting around axis oy and the precession motion around axis, which value of the angular velocity can be significantly different than around axis ox.

The new analytical approach for the inertial torques generated by the rotating mass of the spinning disc describes and represents in the new light the gyroscopic properties. The gyroscopic effects of the spinning object are explained by physical principles and practical validations. These particularities should be taken into account for engineering calculations of the gyroscopic problems. A new analytical approach to the gyroscope theory demonstrates that physics of gyroscopic effects is much more complicated than eighteenth-century scientists could have imagined. Naturally, they could not derive the gyroscope theory because the physical terms of kinetic and potential energies were developed in the middle of the nineteenth century.

The new physical principles of gyroscopic effects based on causative dependencies of the action of interrelated inertial torques can be used for deriving the mathematical models for motions in space of the spinning objects [16–20]. The defined system of interrelated inertial torques and the ratio of the angular velocities of the gyroscope around axes of rotation for the common case is based on the mechanical energy

Table 4.1 Fundamental principles of the gyroscope theory

The basis of the gyroscope theory is the mechanical energy conservation law	
1. Torques acting on the gyroscope around axis ox	
Type of the torque generated by	Equation
Centrifugal forces	$T_{\text{ct}\cdot x} = (2/9)\pi^2 J\omega\omega_x$
Coriolis forces	$T_{\text{cr}\cdot x} = (8/9) J\omega\omega_x$
Inertial forces	$T_{\text{ct}\cdot y} = (2/9)\pi^2 J\omega\omega_y$
Change in angular momentum	$T_{\text{am}\cdot y} = J\omega\omega_y$
2. Torques acting on the gyroscope around axis oy	
Centrifugal forces	$T_{\text{ct}\cdot y} = (2/9)\pi^2 J\omega\omega_y \cos\gamma$
Coriolis forces	$T_{\text{cr}\cdot x} = (8/9) J\omega\omega_y \cos\gamma$
Inertial forces	$T_{\text{ct}\cdot x} = (2/9)\pi^2 J\omega\omega_x \cos\gamma$
Change in angular momentum	$T_{\text{am}\cdot x} = J\omega\omega_x \cos\gamma$
3. The dependency of angular velocities of gyroscope rotation around axes ox and oy	
$\omega_y = \left[\frac{2\pi^2+8+(2\pi^2+9)\cos\gamma}{2\pi^2+9-(2\pi^2+8)\cos\gamma}\right]\omega_x$	

conservation law. The equations of the components of the system are represented in Table 4.1.

Where all parameters are as specified above.

The equations of the components that constitute the fundamental principles of gyroscopic theory (Table 4.1) enable for describing and adequately explaining the physics of gyroscopic effects and will be useful for modelling the behaviour of the gyroscopic devices [17–20]. The new analytical approach represents not only the new method for the analysis of motions of spinning objects but also new challenges for future studies of the dynamics of gyroscopic devices.

In engineering, spinning objects are represented by numerous designs as the parts of the movable machines and mechanisms. Most of the spinning parts and components of mechanisms are designed and represented by the different forms as the sphere, circular cone paraboloid, ellipsoid, propellers, etc. Movable spinning objects of different designs manifest gyroscopic effects under the action of the external forces. The geometry of these types of spinning objects can be described by equations that enable computing their inertial torques by analytical methods described above. The mathematical models for inertial forces generated by the rotating mass of spinning objects depend on their geometry and location of distributed and concentrated masses. This is an obvious statement because the equations of the mass moment of inertia for the spinning objects are different. Such differences in equations of the inertial forces will be also for the expressions of the inertial torques for different designs of the spinning objects. The method of deriving mathematical models for the inertial torques acting on the spinning disc and ring represents a basis for developing the equations of the inertial torques for any spinning objects in engineering.

Applications of the fundamental principles of the gyroscope theory for the typical design of the spinning objects in engineering are presented in Appendixes A and B.

4.2 Mathematical Models for Motions of Gyroscopic Gimbals

New fundamental principles and new mathematical models for the torques acting on the spinning disc enable the formulating of the analytic models for motions of the gyroscope gimbals. The action of external and inertial torques is considered on the example of the spinning disc represented in Fig. 4.1. The mathematical model of motions for gyroscope around axes of gimbals is formulated for the case of the action of the load torque around axis *ox* and frictional torques of the gimbal supports around axes *ox* and *oy*. The frictional torques of supports acting around axes *ox* and *oy* represent the external load torques that change the value of inertial torques of the spinning disc. The frictional torque of supports of the spinning disc acting around axis *oz* does not effect on the gimbal motions. It leads to a decrease in only the angular velocity of the spinning disc. The equations of the gyroscope gimbals motions have formulated by the rules of the interrelations of the inertial torques generated by the spinning disc acting on the gimbals that represented above. The location of the axis of the spinning disc is accepted as horizontal.

The mathematical model for the spinning disc of common motions around the gimbal axes is represented by the differential equations in Euler's forms based on all acting torques summed around two axes *ox* and *oy* (Fig. 4.1). The secondary inertial torques ($T_{\text{ct}\cdot y}$ and $T_{\text{in}\cdot y}$) generated by the common inertial and centrifugal forces acting around axes are removed from the following equations by the processing presented in Eq. (4.5).

$$J_x \frac{\mathrm{d}\omega_x}{\mathrm{d}t} = T - T_{\text{f}\cdot x} - T_{\text{ct}\cdot x} - T_{\text{cr}\cdot x} - T_{\text{am}\cdot y}\eta \tag{4.14}$$

$$J_y \frac{\mathrm{d}\omega_y}{\mathrm{d}t} = (T_{\text{in}\cdot x} + T_{\text{am}\cdot x} - T_{\text{cr}\cdot y})\cos\gamma - T_{\text{f}\cdot y} \tag{4.15}$$

where ω_x and ω_y are the angular velocity of the gyroscope gimbals around axes *ox* and *oy,* respectively; $T_{\text{ct}\cdot x}$, $T_{\text{cr}\cdot x}$, $T_{\text{cr}\cdot y}$, $T_{\text{in}\cdot x,}$ $T_{\text{am}\cdot x}$ and $T_{\text{am}\cdot y}$ are inertial torques generated by the centrifugal, Coriolis, inertial forces and the change in the angular momentum acting around axes *ox* and *oy,* respectively (Table 3.1, Chap. 3); η is the coefficient of the change in the inertial torque due to the action of the frictional torque on the gimbal supports around axis *oy*; $T_{f.x}$ and T_{fy} are the frictional torque acting around axis *ox* and *oy,* respectively; T is the load torque acting on a gimbal around axis *ox*; J_x and J_y are the moment of inertia of the gimbal with the spinning rotor of the gyroscope acting around axis *ox* and *oy,* respectively.

Analysis of the action of the external and inertial torques enables the physical principles of the gyroscope motions around axes to be formulated. The following gyroscope properties were obtained by the analysis, and practical tests are used for the mathematical models of the gyroscope motions around axes with the action of the frictional torques:

(a) The action of the frictional torques on the supports around axis ox of the gyroscope decreases the value of the torque generated by the external load. In turn, the resulting external torque decreases the value of inertial torques acting around axis ox and oy.
(b) The action of the frictional torques on the supports around axis oy of the gyroscope decreases the value of the load inertial torques.
(c) The resulting torques acting around axis oy generate the torque of the angular momentum acting around axis ox.

The presented properties are important for the mathematical modelling of motions of the gyroscope with the action of the frictional torques. The action of the frictional torque decreases the values of the load inertial torques that increase the action of the resulting load torque. The correction coefficient η for the internal torque is considered only for the frictional torques $T_{f.y}$ acting around axis oy. The frictional torques acting around axis oy decrease the value of the precession torques. The resulting torque around axis oy decreases the value of the precession torque acting around axis ox. The frictional torque acting around axis ox decreases the value only of the load torque that generates the inertial resistance torques acting around same axis. From this, the coefficient η expresses the mutual, reciprocal and interrelated action of frictional torque acting around two axes.

The coefficient η is expressed by the ratio of the difference between the precession torques $(T_{\text{in}\cdot x} + T_{\text{am}\cdot x})$ and the frictional torque $T_{\text{f}\cdot y,}$ to the precession torques acting around axis oy. For the common case when the axis of the spinning disc is inclined on the angle γ, the coefficient η is defined by substituting equations of Table 3.1 into the ratio of these torques. Transformation yields the expression of the correction coefficient η.

$$\eta = \frac{(T_{\text{in}\cdot x} + T_{\text{am}\cdot x})\cos\gamma - T_{\text{f}\cdot y}}{(T_{\text{in}\cdot x} + T_{\text{am}\cdot x})\cos\gamma} = 1 - \frac{9T_{\text{f}\cdot y}}{(2\pi^2 + 9)J\omega\omega_x \cos\gamma} \tag{4.16}$$

where η is the coefficient of correction for the action of frictional torques around axis oy; other components are as specified above.

Analysis of Eqs. (4.15) and (4.16) enables for demonstrating the following results. In the case of the absence of the frictional torque $T_{\text{f}\cdot y}$ acting around axes oy, it means the value of correction coefficient of $\eta = 1.0$. In the case, when the frictional torque $T_{\text{f}\cdot y}$ is equal to the precession torques T_{px} acting around axes oy, it means the value of correction coefficient of $\eta = 0$. The gyroscope does not turn around axis oy, and inertial torques of axis ox are deactivated. This statement is validated by practical tests and considered in detail in Chap. 8.

Substituting defined equations for the inertial torques of the gyroscope (Table 3.1), Eqs. (4.9) and (4.16) into Eqs. (4.14) and (4.15) yield the following system of differential equations:

$$J_x \frac{\mathrm{d}\omega_x}{\mathrm{d}t} = T - \left(\frac{2\pi^2+8}{9}\right) J\omega\omega_x - \left[\frac{2\pi^2+8+(2\pi^2+9)\cos\gamma}{2\pi^2+9-(2\pi^2+8)\cos\gamma}\right] J\omega\omega_x \left[1 - \frac{9T_{f.y}}{(2\pi^2+9)J\omega\omega_x\cos\gamma}\right] \tag{4.17}$$

$$J_y \frac{\mathrm{d}\omega_y}{\mathrm{d}t} = \left[\left(\frac{2\pi^2+9}{9}\right) J\omega\omega_x - \left(\frac{8}{9}\right) J\omega\omega_y\right] \cos\gamma - T_{\mathrm{f}\cdot y} \tag{4.18}$$

where all parameters are as specified above.

Analysis of Eqs. (4.17) and (4.18) demonstrates the dependency of the angular velocities of the gyroscope gimbals around axes at the condition of the action of the frictional torques on the gimbal support. In this section, the working example is not considered because the following chapters contain a methodology for solutions of the more complex mathematical models for gyroscope problems that enable us to understand the solution of the simple problem represented by the motions of the gyroscope gimbals.

References

1. Hibbeler, R.C., Yap, K.B.: Mechanics for Engineers—Statics and Dynamics, 13th edn. Prentice Hall, Pearson (2013)
2. Gregory, D.R.: Classical Mechanics. Cambridge University Press, New York (2006)
3. Taylor, J.R.: Classical Mechanics. University Science Books, California (2005)
4. Aardema, M.D.: Analytical Dynamics. Theory and Application. Academic/Plenum Publishers, New York (2005)
5. Jewett, J., Serway, R.A.: Physics for Scientists and Engineers, 10 ed. Cengage Learning, Boston (2018)
6. Knight, R.D.: Physics for Scientists and Engineers: A Strategic Approach with Modern Physics, 4th edn. Pearson, London (2016)
7. Cordeiro, F.J.B.: The Gyroscope. Createspace, Scotts Valley (2015)
8. Greenhill, G.: Report on Gyroscopic Theory. Relink Books, Fallbrook (2015)
9. Scarborough, J.B.: The Gyroscope Theory And Applications. Nabu Press, London (2014)
10. Neil, B.: Gyroscope. The Charles Stark Draper Laboratory, Inc., Cambridge (2014). http://dx.doi.org/10.1036/1097-8542.304100
11. Weinberg, H.: Gyro Mechanical Performance: the most important parameter, Technical Article MS-2158, pp. 1–5. Analog Devices, Norwood, MA (2011)
12. Usubamatov, R.: Properties of inertial torques acting on gyroscopes. Robot. Autom. Eng. J. **2**(4), 555593 (2018)
13. Usubamatov, R.: Inertial forces acting on gyroscope. J. Mech. Sci. Technol. **32**(1), 101–108 (2018)
14. Usubamatov, R.: Mathematical models for gyroscope properties. Math. Eng. Sci. Aerospace **8**(3), 359–371 (2017)

15. Usubamatov, R.: Fundamental principles of gyroscope theory. J. Aeronautics Aerospace Eng. **6**(2) (Suppl) (2017). http://dx.doi.org/10.4172/2168-9792-C1-015
16. Usubamatov, R.: Mathematical models for principles of gyroscope theory. Proc. Am. Inst. Phys. 020133-1–020133-21 (2017). https://doi.org/10.1063/1.4972725
17. Usubamatov, R., Harun, A.B., Fidzwan, M.: Gyroscope mystery is solved. In: International Conference on Advances in Engineering Science and Applied Mathematics (ICAESAM 2013), Cape Town, South Africa, pp. 38–43 (2013)
18. Usubamatov, R.: Gyroscope forces and properties. In: The 2015 World of UAV International Conference (WoUCON 2015), Mahsuri International Exhibition Centre, Langkawi, Kedah, Malaysia, 17–19 Mar 2015, ID-11 (2015)
19. Usubamatov, R.: Gyroscope's internal kinetic energy and properties. In: Proceedings of 5th International Conference on Advanced in Mechanical Aeronautical and Production Techniques (MAPT-2016), Kuala Lumpur, 12–13 Mar 2016, pp. 21–25
20. Usubamatov, R.: Physics and mathematical models for gyroscope properties. In: Proceedings of 4th International Conference and Exhibition on Satellite & Space Missions, Rome, Italy, 18–20 June 2018

Chapter 5
Mathematical Models for Motions of a Gyroscope Suspended from the Flexible Cord

5.1 Inertial Forces Acting on a Gyroscope

Practical tests of the gyroscope suspended from the flexible cord demonstrate unusual properties that are manifested in the form motions [1–3]. Until recent times, the gyroscopic effects for typical gyroscopes with the spinning disc were the most unsolvable and unexplainable problems [4–7]. The new mathematical models for the inertial forces acting on the spinning disc and motions described in previous chapters represent the powerful tool that enables for describing the physics of all gyroscopic effects [8–10]. The mathematical model for motions of the gyroscope with one side support suspended from the flexible cord (Fig. 5.1) represents a favorited example for the lecturers of universities that can explain and describe the physics of acting forces by the principles of classical mechanics [11–14]. The system of the inertial forces, which are centrifugal, common inertial, Coriolis forces, and the change in the angular momentum of the spinning rotor (Chap. 3) are used for formulating the analytic models for the torques and motions of the gyroscope with one side free support. Except these torques are considered the action of centrifugal and Coriolis forces generated by centre mass of the gyroscope [9]. The action of external and inertial torques is considered on the example of the gyroscope suspended from the flexible cord that represented in Fig. 5.2. The one side free support of gyroscope enables avoiding the action of the frictional forces on gimbals and simplifies mathematical models for motions and practical implementation.

The mathematical model of motions for gyroscope with one side free support is formulated for the common case of the gyroscope with the inclined axis on the angle γ. Analysis of the acting forces and motions on the gyroscope is conducted on the base of several rules and regulations. The equations of the gyroscope's motions have accepted the motions in the counterclockwise direction that is positive and in the clockwise direction that is negative. At the starting condition, the action of the gyroscope's weight represents the load torque T with the point of rotation around the support o at the system of coordinates $\Sigma oxyz$ (Fig. 5.2). Analysis of the torques acting on the gyroscope demonstrates the following peculiarities. The external load

© The Editor(s) (if applicable) and The Author(s), under exclusive license to Springer Nature Singapore Pte Ltd. 2020

R. Usubamatov, *Theory of Gyroscopic Effects for Rotating Objects*,
https://doi.org/10.1007/978-981-15-6475-8_5

Fig. 5.1 Running gyroscope with one side support suspended from the flexible cord

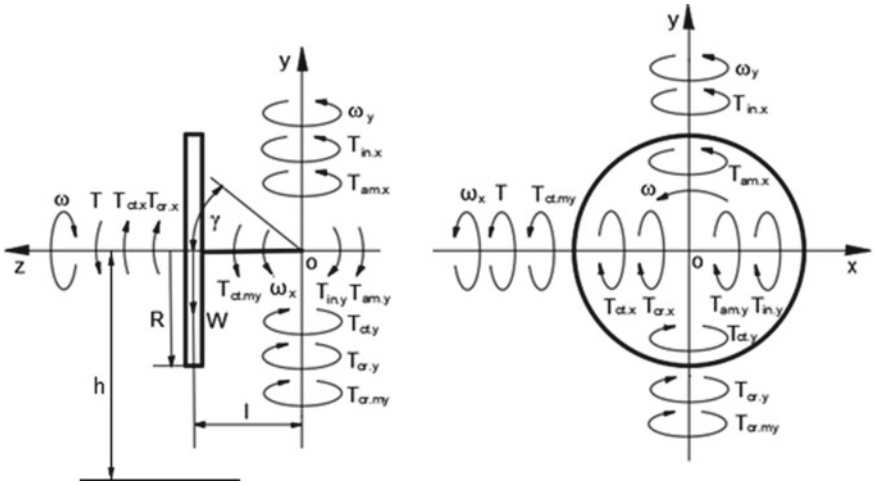

Fig. 5.2 Schematic of acting torques on the gyroscope with one side free support

torque T that is produced by the gyroscope weight W generates the system inertial torques acting around axes ox and oy (Fig. 5.2). These torques are represented by the following interrelated components:

(a) The action of the weight W of the gyroscope produces the system of inertial torques generated by rotating mass of the spinning rotor namely the centrifugal $T_{\text{ct}\cdot i}$ common inertial $T_{\text{in}\cdot i}$ and Coriolis forces $T_{\text{cr}\cdot\text{i}}$ and the change in the angular momentum $T_{\text{am}\cdot i}$ that are components of the resistance $T_{\text{r}\cdot i}$ and procession torques $T_{\text{p}\cdot i}$ acting around axis i;
(b) The resistance torque $T_{\text{r}\cdot x}$ generated by the centrifugal $T_{\text{ct}\cdot x}$ and Coriolis forces $T_{\text{cr}\cdot x}$ acting around axis ox ($T_{\text{r}\cdot x} = T_{\text{ct}\cdot x} + T_{\text{cr}\cdot x}$);
(c) The procession torques $T_{\text{p}\cdot x}$ generated by the inertial forces $T_{\text{in}\cdot x}$ and the change in the angular momentum $T_{\text{am}\cdot x}$ originated on axis ox but acting around axis oy ($T_{\text{p}\cdot x} = T_{\text{in}\cdot x} + T_{\text{am}\cdot x}$);
d) The precession torque $T_{\text{p}\cdot x}$, in turn, generates the resistance torque $T_{\text{r}\cdot y}$ of centrifugal forces $T_{\text{ct}\cdot y}$ and of Coriolis forces $T_{\text{cr}\cdot y}$ acting around axis oy ($T_{\text{r}\cdot y} = T_{\text{ct}\cdot y} + T_{\text{cr}\cdot y}$) that dependant on the procession torque $T_{p\cdot x}$;
(e) The precession $T_{\text{p}\cdot x}$ and resistance $T_{\text{r}\cdot y}$ torques formulating the resulting inertial torques acting around axis oy ($T_{\text{rst}\cdot y} = T_{\text{p}\cdot x} - T_{\text{r}\cdot y}$);
(f) The resulting torque $T_{\text{rst}\cdot y}$, in turn, generates the precession torque $T_{\text{p}\cdot y}$ originated on axis oy but acting around axis ox ($T_{\text{p}\cdot y} = T_{\text{in}\cdot y} + T_{\text{am}\cdot y}$) where the $T_{\text{in}\cdot y}$ is compensated by $T_{\text{ct}\cdot y}$ (d), which justification presented in Chap. 4;
(g) The precession torque $T_{\text{p}\cdot y}$ is added to the resistance torque $T_{\text{r}\cdot x}$ that formulated the resulting resistance torque acting around axis ox ($T_{\text{rst}\cdot x} = T_{\text{r}\cdot x} + T_{\text{p}\cdot y}$);
(h) The resulting torque acting around axis ox ($T_{\text{r}\cdot x} = T - T_{\text{r}\cdot x} - T_{\text{p}\cdot y}$) generates the precession torque acting around axis oy $T^*_{\text{p}\cdot x}$, which value is different from the value pointed in the clause (e).

The action of the external and internal torques on the spinning rotor is looped and expresses the mechanical energy conservation law for the closed system.

Rotation around axes ox and oy of the centre mass of the gyroscope generates the following torques:

(a) The torque generated by the centrifugal force of the rotating gyroscope centre mass around axis oy and acting around axis ox
(b) The torque generated by Coriolis force of the gyroscope centre mass rotating around axes ox and oy and acting around axis oy.

The inertial forces generated by the centre mass can be removed from equations of the gyroscope motions when these torques have small values of a high order.

5.2 Mathematical Models for the Gyroscope Motions

The mathematical model is represented by the differential equations in Euler's forms based on all acting torques summed around two axes ox and oy (Fig. 5.2).

$$J_x \frac{\mathrm{d}\omega_x}{\mathrm{d}t} = T\cos\gamma + T_{\text{ct}\cdot my} - T_{\text{ct}\cdot x} - T_{\text{cr}\cdot x} - T_{\text{am}\cdot y} \tag{5.1}$$

$$J_y \frac{\mathrm{d}\omega_y}{\mathrm{d}t} = T_{\mathrm{in}\cdot x} \cos\gamma + T_{\mathrm{am}\cdot x} \cos\gamma - T_{\mathrm{cr}\cdot y} \cos\gamma - T_{\mathrm{cr}\cdot my} \tag{5.2}$$

where $J_x = J_y$ is the mass moment of gyroscope inertia about axis *ox* and *oy,* respectively, that calculated by the parallel axis theorem; ω_x and ω_y are the angular velocity of precession around axis *ox* and *oy,* respectively; $T = Wl = Mgl$ is the torque generated by the gyroscope weight W around axis *ox; M* is the mass; g is the gravity acceleration; l is overhang distance of the gyroscope centre mass to the free support; $T_{\mathrm{ct},my}$ is the torque generated by the centrifugal forces of the rotating gyroscope centre mass around axis *oy*. $T_{\mathrm{ct}\cdot x}$ and $T_{\mathrm{ct}\cdot y}$ is the resistance torque generated by centrifugal forces around axis *ox* and *oy,* respectively (Table 3.1, Chap. 3); $T_{\mathrm{in}\cdot x}$ and $T_{\mathrm{in}\cdot y}$ is the precession torque generated by inertial forces around axis *ox* and *oy,* respectively (Table 3.1, Chap. 3); $T_{\mathrm{cr}\cdot x}$ and $T_{\mathrm{cr}\cdot y}$ is the resistance torque generated by Coriolis forces around axis *ox* and *oy,* respectively (Table 3.1); $T_{\mathrm{am}\cdot x}$ and $T_{\mathrm{am}\cdot y}$ is the precession and resistance torque that generated by the change in the angular momentum of the spinning rotor around axis *ox* and *oy,* respectively (Table 3.1, Chap. 3); $T_{\mathrm{cr},my}$ is the torque generated by Coriolis force of the rotating gyroscope centre mass around axes *ox* and *oy;* γ is the angle of the spinning disc inclination.

The torques generated by the centrifugal forces of the rotating gyroscope centre mass around axis *oy* defined by the following equation:

$$T_{\mathrm{ct},my} = F_{\mathrm{ct}\cdot my} \times l \sin\gamma = Ml \cos\gamma \omega_y^2 \times l \sin\gamma = Ml^2 \cos\gamma \sin\gamma \omega_y^2 \tag{5.3}$$

where $F_{\mathrm{ct}\cdot my} = Ml \cos\omega_y^2$ is the centrifugal force of the gyroscope centre mass rotating around axis *oy* and ω_y is the angular velocity of the gyroscope around axis *oy*; M is the gyroscope mass; other components are as specified above.

$$\begin{aligned} T_{\mathrm{cr},my} &= F_{\mathrm{cr}\cdot my} \times l \cos\gamma = MV\omega_y l \cos\gamma = Ml\omega_x \sin\gamma \omega_y l \cos\gamma \\ &= Ml^2 \omega_x \omega_y \cos\gamma \sin\gamma \end{aligned} \tag{5.4}$$

where $F_{\mathrm{cr}\cdot my} = Ml\omega_x \sin\gamma\omega_y$ is Coriolis force of the gyroscope centre mass rotating around axes *ox* and *oy*; $V = l\omega_x \sin\gamma$ is the component of the tangential velocity of the gyroscope centre mass around axis *ox*; and ω_x and ω_y is the angular velocity of the gyroscope around axes *ox* and *oy,* respectively; other components are as specified above.

Substituting defined parameters and equations of the inertial torques (Table 3.1, Chap. 3 into Eqs. (5.1) and (5.2) and transformation yield the following system of differential equations:

$$J_x \frac{\mathrm{d}\omega_x}{\mathrm{d}t} = Mgl \cos\gamma + Ml^2 \cos\gamma \sin\gamma \omega_y^2 - \frac{2}{9}\pi^2 J\omega\omega_x - \frac{8}{9} J\omega\omega_x - J\omega\omega_y \tag{5.5}$$

Table 5.1 Mass moments of inertia for the gyroscope components

Title	Equation
The gyroscope mass moment of inertia of the gyroscope about the axis *ox* and *oy*	$J_x = J_y = (MR^2/4) + Ml^2$
The rotor's mass moment of inertia about the axis *ox* and *oy*	$J_x = J_y = (m_r R^2/4)$
The rotor's mass moment of inertia about the axis *oz*	$J = (m_r R^2/2)$

$$J_y \frac{d\omega_y}{dt} = \frac{2}{9}\pi^2 J\omega\omega_x \cos\gamma + J\omega\omega_x \cos\gamma - \frac{8}{9} J\omega\omega_y \cos\gamma - Ml^2\omega_x\omega_y \cos\gamma \sin\gamma \tag{5.6}$$

where parameters of the mass moment of inertia of the gyroscope are represented in Table 5.1; the ratio of the angular velocities of the gyroscope around axes *ox* and *oy* is represented by Eq. (4.9, Chap. 4); and other components are as specified above.

In Table 5.1 m_r is mass of rotating parts, R is the external radius of the disc-type rotor. Practically, gyroscopes have the spinning rotor with complex design, and the external radius of the rotor should be recalculated and represented by its conventional radius R_c. This conventional radius R_c should replace the external radius R of the simple disc-type rotor in equations of Table 5.1.

Equations (5.5) and (5.6) represent acting torques and motions of the spinning rotor around axes *ox* and *oy,* respectively. The location of the gyroscope with one side free support is distinguished from the location with fixed support. The gyroscope with one side support suspended from the flexible cord about the point *o* represents the movable system of free motion at the horizontal plane *xoz* (Fig. 5.2). Analysis of the forces acting on the gyroscope demonstrates the following properties. At the starting condition, the action of the gyroscope weight and the precession torque leads to its turns around axis *ox* and *oy.* At the same time, the resistance torques of the centrifugal and Coriolis forces are counteraction torques around axis *ox* and *oy*. In turn, the gyroscope motion around axis *oy* activates the precession torque of the inertial forces and the rate of change in the angular momentum around axis *ox.* The values of the resistance torques acting around axes *ox* and *oy* are always less than the values of the torques generated by the gyroscope weight and precession torque acting around these axes. At these conditions, the gyroscope receives the angular velocities of precessions around axis *ox* and *oy*.

Analysis of Eqs. (5.5) and (5.6) demonstrates the following peculiarities. Two equations contain two variables, particularly the angular velocities of the gyroscope around two axes. According to the rules of mathematics, to define the solutions of these equations is the simple problem. However, Eqs. (5.5) and (5.6) cannot be resolved by the known methods. The reason for such a situation for solving these equations is explained by the following gyroscope properties:

– The first equation (Eq. 5.5) contains the load torque T that generated by the gyroscope weight W acting around axis *ox.*

– The load torque T produces the several inertial torques around axes ox and oy. Among them, the precession torque $T_{\text{in}\cdot x}$ generated by the common inertial forces acting around axis oy and the resistance torque $T_{\text{ct}\cdot x}$ generated by the centrifugal forces acting around axis ox have the same equation.
– The second equation (Eq. 5.6) does not contain external load torque and cannot be used for solving variables, which are the angular velocities of precessions around axis oy.

Equation (5.6) should be expressed by the component of the load torque T acting around axis ox. The presented gyroscope properties enable for stating the following: Eqs. (5.5) and (5.6) represent specific equations with two variables, which are precessions angular velocities around axes ox and oy. Any change in one equation is reflected by the change in another one. This statement is the result of the interrelations of the inertial torques. The problem is solved by the third equation represented by the equality of the gyroscope's kinetic energies around two axes (Eq. 4.9, Chap. 4). All inertial torques generated by the external torque express the kinetic energies associated with the kinetic energy of the spinning rotor. The kinetic energy of the gyroscope suspended on a flexible cord represents the isolated system. The principle of conservation of mechanical energy states that in an isolated system that is only subject to conservative forces the mechanical energy is constant.

The third equation is represented by Eq. (4.9, Chap. 4), which is the ratio of the angular velocities precessions ω_y and ω_x, around two axes. The final equation of the gyroscope motions is defined by removing the precession torques $T_{\text{in}\cdot y}$ from the first equation of Eq. (5.2) generated by the inertial forces acting around axis ox and resistance torque $T_{\text{ct}\cdot y}$ from the second equation generated by the centrifugal forces acting around axis oy. The equation for the torques $T_{\text{in}\cdot y}$ and $T_{\text{ct}\cdot y}$ is the same that compensates each other in the equation of the internal energy balance (Eq. 4.5). Substituting Eq. (4.9, Chap. 4) into Eqs. (5.5) and (5.6) and transformations yield the following equations:

$$J_x \frac{\mathrm{d}\omega_x}{\mathrm{d}t} = Mgl\cos\gamma + Ml^2\cos\gamma\sin\gamma\omega_y^2 - \left\{\frac{2\pi^2+8}{9} + \left[\frac{2\pi^2+8+(2\pi^2+9)\cos\gamma}{2\pi^2+9-(2\pi^2+8)\cos\gamma}\right]\right\} J\omega\omega_x \tag{5.7}$$

$$J_y \frac{\mathrm{d}\omega_y}{\mathrm{d}t} = \left(\frac{2\pi^2+9}{9}\right) J\omega\omega_x\cos\gamma - \left(\frac{8}{9}\right) J\omega\omega_y\cos\gamma - Ml^2\omega_x\omega_y\cos\gamma\sin\gamma \tag{5.8}$$

where all parameters are as specified above.

Equation (5.8) cannot be used for the direct solving of the gyroscope motion around axis oy because of the precession torques (first component of the right side of Eq. 5.8) contain the sign of the angular velocity ω_x. The expression of ω_x is defined from Eq. (4.9, Chap. 4) and substituted into the expression of the precession torque (Eq. 5.8) which value will be less than the value of the resistance torque generated by

Coriolis forces. This physical discrepancy is expressed by the following inequality:

$$\left[\frac{2\pi^2+9}{9\left[\frac{2\pi^2+8+(2\pi^2+9)\cos\gamma}{2\pi^2+9-(2\pi^2+8)\cos\gamma}\right]}\right]J\omega\omega_y\cos\gamma < \left(\frac{8}{9}\right)J\omega\omega_y\cos\gamma \tag{5.9}$$

The stated inequality contradicts the physical principles of acting torques because of the precession torque generates the resistance torque acting around the same axis. The procession torque (Eq. 5.8) is generated by the action of the resulting torque T_{rs} acting around axis ox that is represented by the right side of Eq. (5.7). The value of the precession torque of Eq. (5.8) should be corrected by the principle of the conservation of the kinetic energy. Since the angular velocity of the gyroscope around axis oy is bigger than around axis ox, then the value of the precession torque should be proportionally increased on the ratio of the angular velocities (Eq. 4.9, Chap. 4) and decreased on the ratio of the precession and resistance torques. This transformation expresses the interdependency of load and inertial torques acting around two axes of the gyroscope. The expression of ω_x is replaced by ω_y (Eq. 4.9, Chap. 4) into the precession torque of Eq. (5.9) and increased on the ratio of the angular velocities, and then, the ratio of the precession and resistance torques is represented by the following:

$$n = \frac{\left[\frac{2\pi^2+8+(2\pi^2+9)\cos\gamma}{2\pi^2+9-(2\pi^2+8)\cos\gamma}\right]\left(\frac{2\pi^2+9}{9}\right)J\omega\omega_y\cos\gamma}{\left[\frac{2\pi^2+8+(2\pi^2+9)\cos\gamma}{2\pi^2+9-(2\pi^2+8)\cos\gamma}\right]} \Bigg/ \left(\frac{8}{9}\right)J\omega\omega_y\cos\gamma = \frac{2\pi^2+9}{8} \tag{5.10}$$

Defined parameters enable the presentation of Eq. (5.8) by the clear physical principles and the direct computing of the angular velocity ω_y of the gyroscope around axis oy. The first component of the right side of Eq. (5.8) is the precession torque $T_{p\cdot x}$ generated by the resulting torque $T_{r\cdot s}$ around axis ox (Eq. 5.7), which is presented by the following expression:

$$T_{r\cdot s} = Mgl\cos\gamma - \left(\frac{2\pi^2+8}{9}\right)J\omega\omega_x - \left[\frac{2\pi^2+8+(2\pi^2+9)\cos\gamma}{2\pi^2+9-(2\pi^2+8)\cos\gamma}\right]J\omega\omega_x \tag{5.11}$$

The angular velocity ω_x is defined from the right side of Eq. (5.11) that is as follows:

$$\omega_x = \frac{Mgl\cos\gamma}{\left\{\frac{2\pi^2+8}{9} + \left[\frac{2\pi^2+8+(2\pi^2+9)\cos\gamma}{2\pi^2+9-(2\pi^2+8)\cos\gamma}\right]\right\}J\omega} \tag{5.12}$$

Equation (5.12) is substituted into an expression of the precession torque (Eq. 5.8), increased on the ratio of the angular velocities (Eq. 4.9, Chap. 4) and decreased on the

ratio of the precession and resistance torques (Eq. 5.10). Then, the modified formula of the precession torque $T_{\mathrm{p}\cdot x}$ is presented by the following expression:

$$T_{\mathrm{p}\cdot x} = \frac{\left[\frac{2\pi^2+8+(2\pi^2+9)\cos\gamma}{2\pi^2+9-(2\pi^2+8)\cos\gamma}\right]\left(\frac{2\pi^2+9}{9}\right)J\omega Mgl\cos^2\gamma}{\left(\frac{2\pi^2+9}{8}\right)\left[\frac{2\pi^2+8}{9}+\left(\frac{2\pi^2+8+(2\pi^2+9)\cos\gamma}{2\pi^2+9-(2\pi^2+8)\cos\gamma}\right)\right]J\omega}$$
$$= \frac{8Mgl\cos^2\gamma}{(2\pi^2+8)\left[\frac{2\pi^2+9-(2\pi^2+8)\cos\gamma}{2\pi^2+8+(2\pi^2+9)\cos\gamma}\right]+9} \tag{5.13}$$

The expression $T_{\mathrm{p}\cdot x}$ (Eq. 5.13) is substituted into Eq. (5.8), and then, the equation for the gyroscope's motion around axis oy is presented by the following equation:

$$J_y\frac{\mathrm{d}\omega_y}{\mathrm{d}t} = \frac{8Mgl\cos\gamma}{\left[(2\pi^2+8)\left[\frac{2\pi^2+9-(2\pi^2+8)\cos\gamma}{2\pi^2+8+(2\pi^2+9)\cos\gamma}\right]+9\right]} - \left(\frac{8}{9}\right)J\omega\omega_y\cos\gamma \tag{5.14}$$

where all components are as specified above.

Equation (5.14) contains the component of the external load torque and enables the direct computing of the angular velocity of gyroscope around axis oy for the gyroscope with one side free support.

5.2.1 *The Limit of the Gyroscope Angular Velocity Around Axis of Motion*

The gyroscope angular velocities around axes are limited by the action of torque produced by the gyroscope weight and the resulting inertial torques. The angular velocities ω_i around axes express the potential and kinetic energies of the gyroscope and the work of the inertial torques. The resulting inertial torque expresses the independent kinetic energy of the spinning disc and the potential and kinetic energies of the gyroscope. The equation of the resulting inertial torque contains the product of the angular velocity ω of the spinning disc and the angular velocity ω_x of precession around axis ox (right component of Eq. 5.9). The value of the product $\omega\omega_x$ is constant for the given data of the gyroscope. The increase in the angular velocity of ω of the spinning disc leads to the decrease of the angular velocity ω_x of the gyroscope and vice versa. The increase in the torque produced by the gyroscope weight does not change in the resulting inertial torque but changes in the location of the gyroscope. This condition is the result of the interrelated action of the inertial torques and angular velocities around axes (Eq. 4.9, Chap. 4). The surplice of the load torque T around axis ox (Fig. 5.2) excesses the value of the resulting resistance inertial torque $T_{\mathrm{r}\cdot x}$ that leads to the fast turn down of the gyroscope. The new location of the gyroscope gives the same value of the torque produced by the gyroscope weight that corresponds to the value of the resulting inertial torque. This circumstance is predetermined by the

law of mechanical energy conservation. The equation of the potential and kinetic energies of the gyroscope and the work of the inertial torques is represented by the following analysis.

For the given example (Fig. 5.2), the location of the gyroscope at the system of coordinate $\Sigma oxyz$ expresses its gravitational potential energy that is a conservative force. The motion of the gyroscope mass expresses its kinetic energy. The action of the inertial resistance expresses the negative work. The datum of energies has accepted the line that below on h of the horizontal location of the gyroscope. The total energies of the gyroscope at any points of the location are remained constant and expressed by the following equation:

$$P_{M1} + K_{1\cdot M} - A_{1\cdot T_i} = P_{M2} + K_{2\cdot M} - A_{2\cdot T_i} \tag{5.15}$$

where $P_{\mathrm{Mi}} = Mgh = Mgl\sin\gamma_i$ is the potential energy of the gyroscope weight $W = Mg$; $K_{i\cdot M} = (1/2)J_x\omega_x^2 + (1/2)M(\omega_x l)^2$ is the kinetic energy of the gyroscope turn and the turn of it's the centre mass around the support. $A_{i\cdot T_i} = DJ\omega\omega_x\gamma$ is the work of the resulting inertial torque on the angle γ of its turn; D is the factor of the resulting inertial torque (Eq. 5.7); other parameters are as specified above.

The equality of the gyroscope energies for the horizontal location ($\gamma = 0$) of the gyroscope that turns in the counterclockwise direction is expressed by the following equation:

$$Mgh = Mgh_1 + \frac{1}{2}J_x\omega_x^2 + \frac{1}{2}M(\omega_x l)^2 - \left(\frac{38\pi^2 + 161}{9}\right)J\omega\omega_x\gamma \tag{5.16}$$

where the index h_1 belongs to the low angular position of the gyroscope, other parameters are as specified above.

The angular velocity of the gyroscope located horizontally is maximal. Increasing the weight of the gyroscope will turn down its axis on the angle where the component of the gyroscope weight is the same as for initial condition.

$$\omega_x = \frac{9Mgl}{\left(38\pi^2 + 161\right)J\omega} \tag{5.17}$$

where all parameters are as specified above.

Equation (5.17) expresses the limit of the angular velocity ω_x and demonstrates the dependency on the potential and kinetic energies of the gyroscope and kinetic energy of the spinning disc. The energies express the action of the torque produced by the gyroscope weight and the resulting resistance torque.

5.3 The Practical Test of Gyroscope Motions

The tests on the angular velocities of gyroscope precessions were conducted on the base of the Super Precision Gyroscope "Brightfusion LTD" with the spinning rotor mounted in the spherical ribbed frame (Fig. 5.3). The gyroscope technical data are represented in Table 5.2. The tests of the gyroscope with one side free support conducted with the application of several devices and instruments. The velocity of the spinning rotor measured by the Optical Multimeter Tachoprobe Model 2108/LSR Compact Instrument Ltd. with a range of measurement 0–60,000.00 rpm. The angular measurements of the location for the gyroscope axis were conducted optically by the angular template with accuracy $\pm$ 1.0°. The time spent on the gyroscope precessions around the flexible cord (axis oy) and axis ox for the suspended gyroscope measured by the stopwatch of Model SKU SW01 with resolution 1/100 s.

The change in the velocity for the spinning rotor per time due to the action of frictional forces on supports and the action of air viscosity is represented in Fig. 5.4. Figure 5.4 demonstrates the angular speed of the spinning rotor is decreasing on average around 67 revolutions per second. The drop in the frequency of the rotor spinning changes the angular velocities of gyroscope precessions and the value of the gyroscope resistance and precession torques.

The gyroscope with one side free support is suspended from the flexible cord. The gyroscope weight generates the load torque T that resulting in the gyroscope precessions about the centre o of coordinate system $\Sigma oxyz$ (Fig. 5.5). The object of the tests is to determine practically the precession angular velocities of the gyroscope around axes ox and oy and validate the mathematical model for the gyroscope motions. Equations (5.5) of the gyroscope motions contain technical parameters and the initial numerical data of the gyroscope components.

The rotor disc mounted on the shaft of the gyroscope and represented the complex form with the different radii of its components. The radius of the location of the centre mass elements and the conventional external radius of the rotor are calculated. The

Fig. 5.3 Super Precision Gyroscope "Brightfusion LTD"

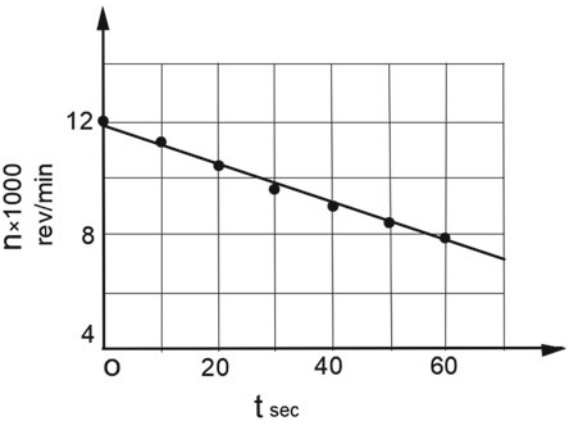

Fig. 5.4 Angular velocity for the spinning rotor versus time

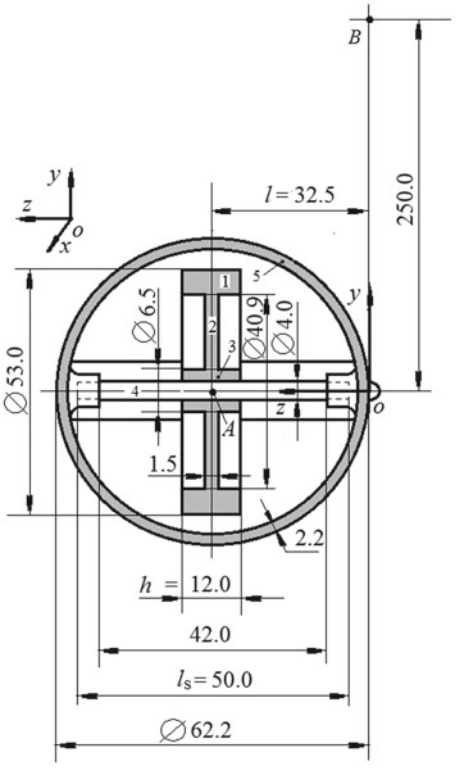

Fig. 5.5 Geometrical parameters of the gyroscope components

components i of the gyroscope are represented by the number 1, …, 5 in Fig. 5.5, which masses are calculated by the following equation:

$$m_i = \rho\pi\left(r_{\text{out}}^2 - r_{\text{in}}^2\right)h \tag{5.18}$$

where ρ is density, r_{in} is the inner radius, r_{out} is the outer radius, h is the length or width, and other parameters are as specified above.

The gyroscope frame is represented the ribbed spherical frame and for simplification is presented as the thin sphere of radius r_5 and mass m_5. The mass moment of inertia of the gyroscope frame about the axis ox or oy is the same and calculated by the following equation:

$$J_{y5} = (2/3)m_5 r_5^2 \tag{5.19}$$

where all parameters are as specified above.

The total mass moment of inertia of the gyroscope components around axis ox or oy is calculated by the following equation of parallel axis theorem of mass moment of inertia:

$$J_y = J_{y5} + J_{yr} = (2/3)m_5 r_5^2 + m_5 l^2 + \left(mR_{\text{c}}^2/4\right) + ml^2 \tag{5.20}$$

where Jy_5 is the mass moment of inertia the frame; J_{yr} is the mass moment of inertia of rotating parts; other parameters are as specified above.

The radius location of the mass element for the gyroscope rotating components is defined by the theorem of location of the centre mass for the complex part by the following equation:

$$r_{\text{m}} = \sum_{i=1}^{n} m_i r_i \Bigg/ \sum_{i=1}^{n} m_i \tag{5.21}$$

where m_{i} is a mass of gyroscope elements, r_{i} is the radius of the location of the mass element.

The radius of the location of the mass element for the rotor's components is calculated by the following equation:

$$r_{mi} = \frac{m_{r\cdot\text{out}} \times (2/3)r_{\text{out}} - m_{r\cdot\text{in}} \times (2/3)r_{\text{in}}}{m_{r\cdot\text{out}} - m_{r\cdot\text{in}}} \tag{5.22}$$

where $m_{\text{r}\cdot i} = \rho\pi r_i^2 h/2\pi = \rho r_i^2 h/2$ is the mass element that is located on i radius.

Substituting defined expression of the mass elements $m_{\text{r.i}}$ and parameters presented in Table 4.3, into Eq. (5.22), and transforming give the following equation:

$$r_{mi} = \frac{2}{3}\left(\frac{r_{i\cdot\text{out}}^3 - r_{i\cdot\text{in}}^3}{r_{i\cdot\text{out}}^2 - r_{i\cdot\text{in}}^2}\right) \tag{5.23}$$

Substituting parameters of the rotor's components from Table 5.3 into Eq. (5.23) is calculated the radii locations of their mass elements:

- the brass disc component 1 (rim)

$$r_{\mathrm{m}\cdot r} = \frac{2}{3}\left(\frac{r_{r\cdot\mathrm{out}}^3 - r_{r\cdot\mathrm{in}}^3}{r_{r\cdot\mathrm{out}}^2 - r_{r\cdot\mathrm{in}}^2}\right) = \frac{2}{3}\left(\frac{0.0265^3 - 0.02045^3}{0.0265^2 - 0.02045^2}\right) = 2.360493 \times 10^{-2}\ \mathrm{m}$$

- the rotor's disc component (tie plate)

$$r_{\mathrm{m}\cdot\mathrm{p}} = \frac{2}{3}\left(\frac{r_{\mathrm{r}\cdot\mathrm{out}}^3 - r_{\mathrm{r}\cdot\mathrm{in}}^3}{r_{\mathrm{r}\cdot\mathrm{out}}^2 - r_{\mathrm{r}\cdot\mathrm{in}}^2}\right) = \frac{2}{3}\left(\frac{0.02045^3 - 0.00325^3}{0.02045^2 - 0.00325^2}\right) = 1.393045 \times 10^{-2}\ \mathrm{m}$$

- the rotor's disc component (bush)

$$r_{\mathrm{m}\cdot\mathrm{b}} = \frac{2}{3}\left(\frac{r_{\mathrm{b}\cdot\mathrm{out}}^3 - r_{\mathrm{b}\cdot\mathrm{in}}^3}{r_{\mathrm{b}\cdot\mathrm{out}}^2 - r_{\mathrm{b}\cdot\mathrm{in}}^2}\right) = \frac{2}{3}\left(\frac{0.00325^3 - 0.002^3}{0.00325^2 - 0.002^2}\right) = 0.267460 \times 10^{-2}\ \mathrm{m}$$

- the shaft 3 $r_{\mathrm{m}\cdot 3} = \frac{2}{3}r = \frac{2}{3} \times 0.002 = 0.133333 \times 10^{-2}$ m

Substituting defined masses (Table 5.2) and radii defined by Eq. (5.23) into Eq. (5.21) is calculated the radius location of the mass element of the gyroscope rotating components

$$r_{\mathrm{m}} = \frac{\sum_{i=1}^{n} m_i r_i}{\sum_{i=1}^{n} m_i} = \frac{\begin{array}{c}0.0926 \times 2.360493 \times 10^{-2} + 0.0166 \times 1.393045 \times 10^{-2} \\ + 0.0021 \times 0.267460 \times 10^{-2} + 0.0047 \times 0.133333 \times 10^{-2}\end{array}}{0.1159}$$
$$= 0.02095725\ \mathrm{m}$$

Defined radius location of the mass element of the gyroscope rotating components enables to defining its conventional external radius of the uniform rotor's disc, which is as follows

$$R_{\mathrm{c}} = (3/2)r_{\mathrm{m}} = (3/2) \times 0.02095725 = 0.0314358\ \mathrm{m}.$$

Defined equations and gyroscope parameters enable to calculating other parameters. For simplicity of calculations, the tests of the gyroscope motions are conducted for the location of the gyroscope axis that close to horizontal (γ =0) with deviations $\pm 10°$.

The torque generated by the gyroscope weight is calculated by the following equation:

$$T = Mgl = 0.146 \times 9.81 \times 0.0325 = 4.654845 \times 10^{-2}\ \mathrm{kg\ m^2/s^2}$$

The mass moment of inertia of the gyroscope components about the axis oy and ox is as follows (Eq. 5.22)

$$\begin{aligned} J_{y\cdot x} &= (2/3)m_5 r_5^2 + m_5 l^2 + \left(m R_c^2/4\right) + ml^2 \\ &= (2/3) \times 0.0294 \times 0.03^2 + 0.0294 \times 0.0325^2 \\ &\quad + \left(0.1159 \times 0.0314358^2/4\right) + 0.1159 \times 0.0325^2 \\ &= 1.9974649 \times 10^{-4} \quad \text{kg m}^2 \end{aligned} \tag{5.24}$$

The mass moment of inertia of the rotating components is as follows

$$J = \left(m_r R_c^2/2\right)\omega = (0.1159 \times 0.0314358^2/2) \times \omega = 0.5726674 \times 10^{-4}\ \omega \text{ kg m}^2 \tag{5.25}$$

The change in the angular momentum of the rotating mass about the axis ox or oy is represented the following equation:

$$T_{\text{a·m}} = J\omega\omega_{\text{p}\cdot i} = 0.5726674 \times 10^{-4}\omega\omega_{\text{p}\cdot i}, \tag{5.26}$$

where ω_i is the angular velocity of precession about the axis i.

All defined gyroscope parameters are represented in Table 5.2 and enable to calculating the torques by the equations that represented in Table 3.1, Chap. 3.

Substituting defined parameters from Table 5.2 into correspondent equations is calculated the resistance and precession torques generated by the centrifugal and common inertial forces, which are as follows:

$$T_{\text{ct}i} = T_{\text{in}ri} = \frac{2}{9}\pi^2 J\omega\omega_{\text{p}\cdot i} = \frac{2}{9}\pi^2 \times 0.5725417 \times 10^{-4}\omega\omega_{\text{p}\cdot i}$$

Table 5.2 Technical data of Super Precision Gyroscope, "Brightfusion LTD"

Mass, kg	Rotor's brass disc, ρ = 8,650 kg/m^3 • Component 1 = 0.0926 • Component 2 = 0.0166 • Component 3 = 0.0021		0.1112
	Steel shaft with washers		0.0047
	Total rotating components		0.1159
	Aluminium casing with bearings and screws		0.0294
	Gyroscope, M		0.146 kg
Mass moment of inertia kgm^2	Around axis oz	Rotating components	0.5726674×10^{-4}
	Around axis ox and oy	Gyroscope	1.9974649×10^{-4}

$$= 1.2560001 \times 10^{-4} \omega \omega_{p.i} \tag{5.27}$$

The resistance torque generated by the Coriolis forces is as follows:

$$T_{\mathrm{cr}i} = \frac{8}{9} J \omega \omega_{\mathrm{p}\cdot i} = \frac{8}{9} \times 0.5726674 \times 10^{-4} \omega \omega_{p\cdot i} = 0.5090377 \times 10^{-4} \omega \omega_{\mathrm{p}\cdot i} \tag{5.28}$$

where all parameters are as specified above.

The tests and measurements of the time motions for the gyroscope with one side free support are conducted for the horizontal location of the gyroscope axis (cos 0° = 1.0, sin 0° = 0.). This condition simplifies the process of measurements of the angular velocities of the gyroscope around axes *ox* and *oy*. The torques generated by the action of the centrifugal (Eq. 5.3) and Coriolis force (Eq. 5.4) of the gyroscope's centre mass for the accepted condition have the zero or small values and are removed from Eqs. (5.7) and (5.8) [9, 10]. Equation (5.7) of gyroscope motion around axis *ox* is simplified and represented by the following expression:

$$J_x \frac{\mathrm{d}\omega_x}{\mathrm{d}t} = Mgl - \left(\frac{38\pi^2 + 161}{9} \right) J \omega \omega_x \tag{5.29}$$

Expression of gyroscope motion around axis *oy* is represented by Eqs. (5.8) and (5.14).

Substituting defined gyroscope parameters represented by Eqs. (5.24)–(5.28) into Eq. (5.29) yields the following differential equation:

$$\begin{aligned} 1.9974649 \times 10^{-4} \frac{\mathrm{d}\omega_x}{\mathrm{d}t} &= 4.654845 \times 10^{-2} \\ &\quad - 59.560551915 \times 0.5726674 \times 10^{-4} \omega \omega_x \end{aligned} \tag{5.30}$$

Simplifications of Eq. (5.30) and transformation bring the following equation:

$$0.0585622 \frac{\mathrm{d}\omega_x}{\mathrm{d}t} = 13.6472155 - \omega \omega_x \tag{5.31}$$

Separating variables and transformation for the differential Eq. (5.31) gives the following equation:

$$\frac{\mathrm{d}\omega_x}{\frac{13.6472155}{\omega} - \omega_x} = 17.0758612 \omega \mathrm{d}t \tag{5.32}$$

Presenting Eq. (5.32) into integral forms at definite limits yields the following integral equations:

$$\int_0^{\omega_x} \frac{\mathrm{d}\omega_x}{\frac{13.6472155}{\omega} - \omega_x} = 17.0758612\omega \int_0^t \mathrm{d}t \tag{5.33}$$

The left integral of Eq. (5.33) is tabulated and represented the integral $\int \frac{\mathrm{d}x}{a-x} = -\ln|a-x| + C$. The right integral is simple, and integrals have the following solution:

$$-\ln\left(\frac{13.6472155}{\omega} - \omega_x\right)\Big|_0^{\omega_x} = 17.0758612\omega t\Big|_0^t$$

that gave rise to the following

$$1 - \frac{\omega_x}{\frac{13.6472155}{\omega}} = \mathrm{e}^{-17.0758612\omega t} \tag{5.34}$$

Solving of Eq. (5.34) gives the equation for the precession angular velocity of the gyroscope around axis *ox*:

$$\omega_x = \frac{13.6472155}{\omega}\left(1 - \mathrm{e}^{-17.0758612\omega t}\right) \tag{5.35}$$

The expression $\mathrm{e}^{-17.0758612\omega t}$ of Eq. (5.35) contains the angular velocity of the spinning rotor, which value can be about $n = 10{,}000$ –30,000 rpm. This expression has a small value and can be neglected. However, analysis of Eq. (5.35) demonstrates the angular velocity is always increased with the change in the time according to the rules of classical mechanics. The calculated angular velocity of the gyroscope precession around axis *ox* for the rotor's speed is accepted $n = 10{,}000.0$ rpm. The practical tests of the gyroscope motion have conducted for the angular velocity of the spinning disc at the range of 10,500–10,000 rpm due to the drop of the angular velocity of 67 revolutions per second (Fig. 5.4). The computed angular velocity of the gyroscope motion around axis *ox* gives the following result:

$$\begin{aligned}\omega_x &= \frac{13.6472155}{\omega} = \frac{13.6472155}{2\pi \times 10,000/60} \\ &= 0.0130321 \text{ rad/s} = 0.746^\circ/\text{s}\end{aligned} \tag{5.36}$$

Substituting Eq. (5.36) into Eq. (4.6, Chap. 4) and transformation yields the following result of the gyroscope precession angular velocity around axis *oy*:

$$\begin{aligned}\omega_y &= (4\pi^2 + 17)\omega_x = (4\pi^2 + 17) \times \frac{13.6472155}{\omega} = \frac{770.773136}{\omega} \\ &= \frac{770.773136}{2\pi \times 10000/60} = 0.7360341 \text{ rad/s} = 42.172^\circ/\text{s}\end{aligned} \tag{5.37}$$

The angular velocity of the gyroscope around axis oy can be computed by Eq. (5.14). Substituting defined gyroscope parameters represented by Eqs. (5.24)–(5.28) into Eq. (5.14) yields the following differential equation:

$$1.9974649 \times 10^{-4} \frac{\mathrm{d}\omega_y}{\mathrm{d}t} = \left(\frac{32\pi^2 + 136}{38\pi^2 + 161}\right) \times 0.146 \times 9.81 \times 0.0325 - \frac{8}{9} \times 0.5726674 \times 10^{-4} \omega\omega_y \tag{5.38}$$

Simplifications of Eq. (5.38) and transformation give the following equation:

$$3.924001981 \frac{\mathrm{d}\omega_y}{\mathrm{d}t} = 770.773136698 - \omega\omega_y \tag{5.39}$$

The following process of solution is the same as represented by Eqs. (5.33)–(5.37), and all comments are omitted.

$$\frac{\mathrm{d}\omega_y}{\frac{770.773136698}{\omega} - \omega_y} = 0.254841869\omega \mathrm{d}t \tag{5.40}$$

$$\int_0^{\omega_x} \frac{\mathrm{d}\omega_y}{\frac{770.773136698}{\omega} - \omega_y} = 0.254841869\omega \int_0^t \mathrm{d}t$$

$$-\ln\left(\frac{770.773136698}{\omega} - \omega_y\right)\Big|_0^{\omega_x} = 0.254841869\omega t\Big|_0^t \tag{5.41}$$

$$1 - \frac{\omega_y}{\frac{770.773136698}{\omega}} = \mathrm{e}^{-0.254841869\omega t} \tag{5.42}$$

$$\omega_y = \frac{770.773136698}{\omega}\left(1 - \mathrm{e}^{-0.254841869\omega t}\right) \tag{5.43}$$

$$\omega_y = \frac{770.773136698}{\omega} = \frac{770.773136698}{2\pi \times 10000/60} = 0.736034128 \text{ rad/s} = 42.172^\circ/\text{s} \tag{5.44}$$

The results of Eqs. (5.37) and (5.44) are the same, which is the validation of the correctness of Eq. (5.19). The time spent on one revolution around axis oy takes $t = 2\pi/\omega_y = 360^\circ/42.172^\circ/\text{s} = 8.536$ s. The precession angular velocity about the axis ox is 0.746° /s. The time spent on the turn of 20° axis ox ($\pm$ 10° about the horizontal location) takes $t = 2\pi/\omega_x = 20^\circ/0.746^\circ/\text{s} = 26.809$ s. The measurement of the time of the gyroscope motion around axis ox is additional and not main due to the drop of the velocity of the spinning disc. Experimental and theoretical results of the gyroscope precession around axes ox and oy are represented in Table 5.3.

Recorded results of the theoretical calculations and practical tests of the gyroscope precessions represented in Table 5.3 are well matched in spite of differences.

Table .5.3 Experimental and theoretical results of the gyroscope precession

Gyroscope average parameters	Test	Theoretical	Difference
Time of precession (one revolution) around the axis *oy*	8.1 s	8.536 s	5.382%
Time of precession around axis *ox* on 20° of the turn about horizontal location	24.5 s	26.809	9.38%
Angular velocity of precession around the axis *ox*	≈1.0°/s	0.746°/s	

This result was obtained by the absence of the friction forces at the free support of the gyroscope. Differences in results can be explained by simplifications in the calculation of geometrical parameters for the gyroscope frame and hence in mechanical properties accepted for the gyroscope. Also, on results have influenced the following factors:

- the accuracy of calculations of the gyroscope technical data,
- the accuracy of measurement,
- the drop of the spinning rotor velocity (Fig. 5.4) for the time of 25 s was around 1500 revolutions that changed the angular precession velocities of the gyroscope around the axes *ox* and *oy* and
- the action of frictional forces on bearings of the spinning rotor.

All these factors have a definite contribution to the calculation of gyroscope motions and in such cases, and theoretical results always will be distinguished from the practical one. The differences in results depend on the quality of calculations of parameters for the mathematical model of the process and the quality of their practice tests that are ordinary components of research. The derived mathematical model for most uncountable gyroscope motions is correct. Expanded tests of the new mathematical model for gyroscope effects can additionally validate its correctness. The study of the acceptable differences of theoretical and practical results represented in publications and recommendations of the experts demonstrate the permissible discrepancy should not exceed 10% [14].

Obtained results enable for defining the resulting torques acting on the gyroscope around axis *ox* and *oy*. The right side components of Eqs. (5.30) and (5.38) represent the resulting torques which expressions are as follows:

$$\begin{aligned} T_x = {} & 4.654845 \times 10^{-2} - 1.2560001 \times 10^{-4}\omega\omega_x \\ & - 0.5090377 \times 10^{-4}\omega\omega_x - (4\pi^2 + 17) \\ & \times 0.5726674 \times 10^{-4}\omega\omega_x \end{aligned} \tag{5.45}$$

$$T_y = \left(\frac{32\pi^2 + 136}{38\pi^2 + 161}\right) \times 4.654845 \times 10^{-2} - \frac{8}{9} \times 0.5726674 \times 10^{-4}\omega\omega_y \tag{5.46}$$

Substituting defined parameters ω, ω_x and ω_y (Eqs. 5.36 and 5.37, Sect. 5.3) into Eqs. (5.45) and (5.46), respectively, and transformation yields the following results:

$$T_x = 4.654845 \times 10^{-2} - 1.2560001 \times 10^{-4} \times \frac{10000 \times 2\pi}{60} \times 0.0130387 - 0.5090377 \times 10^{-4} \times \frac{10000 \times 2\pi}{60} \times 0.0130387 - (4\pi^2 + 17) \times 0.5726674 \times 10^{-4} \times \frac{10000 \times 2\pi}{60} \times 0.0130387 = 1.461887255 \times 10^{-7} \text{ Nm} \quad (5.47)$$

$$T_y = \left(\frac{32\pi^2 + 136}{38\pi^2 + 161}\right) \times 4.654845 \times 10^{-2} - \frac{8}{9} \times 0.5726674 \times 10^{-4} \times \frac{10000 \times 2\pi}{60} \times 0.736034128 = 1.297409209 \times 10^{-11} \text{ Nm} \quad (5.48)$$

The forces acting along axis oz and oy are as follows:

$$\begin{aligned} F_{\text{ct}\cdot mx} &= ml\omega_x^2 = 0.146 \times 0.0325 \times 0.0130387^2 = 8.066865255 \times 10^{-7} \text{ N} \\ F_{\text{ct}\cdot my} &= ml\omega_y^2 = 0.146 \times 0.0325 \times 0.7360341^2 = 2.5705857021 \times 10^{-3} \text{ N} \\ F_z &= F_{\text{ct}\cdot mx} + F_{\text{ct}\cdot my} = 2.571139238 \times 10^{-3} \text{ N} \\ F_{\text{cr}\cdot my} &= ml\omega_x\omega_y \sin 0^o = 0.146 \times 0.0325 \times 0.7360341 \times 0 = 0 \text{ N} \end{aligned} \quad (5.49)$$

Equations (5.47) and (5.48) demonstrate the small values of the resulting torques acting around axis ox and oy. These torques do not generate the sensitive forces acting on the flexible cord. At this condition, the gyroscope rotates with small angular velocities around axes. The forces acting along the axes oz and oy also have small values (Eq. 5.49). Hence, the small values of the frictional torques enable for stating several conclusions. The external torques of small values, like the torque generated by frictional forces of the gyroscope supports, can greatly change in the angular velocities of the gyroscope motions around axes. The total values of the torques acting on the gyroscope are commensurable with values of frictional torques of the supports. Frictional torques acting opposite the load torque are reducing sensitively the values of the gyroscopic inertial torques.

5.3.1 Practical Tests of the Forces Acting on a Gyroscope

The new mathematical model of the internal forces acting on a gyroscope is represented by four components, namely the centrifugal, common inertial and Coriolis forces and the change in the angular momentum of the spinning rotor (Table 3.1). The external torque applied to the gyroscope generates the resistance and precession torques acting about two axes. The tests on the acting forces of gyroscope precession about axis oy were conducted on the base of the Super Precision Gyroscope

"Brightfusion LTD" (Fig. 5.5), which the technical data are represented in Table 5.2. The gyroscope with one side free support is suspended from the flexible cord. The gyroscope weight generates the load torque T that results in the gyroscope precessions about the point o of the support (Fig. 5.5). The defined gyroscope's parameters are represented in Table 5.3 and enable for calculating the value of torques by the equations represented in Table 3.1.

The action of inertial torques is displayed on the motion of the gyroscope suspended from the flexible cord. The equation of gyroscope motion around axis ox at the horizontal location ($\gamma = 0$) is represented by Eq. (5.29) of Sect. 5.3. The weight of the gyroscope and inertial torques are acting on the one side free support of the flexible cord. The picture of the resulting reactions of all forces on the support is demonstrated in Fig. 5.6.

The resulting torques acting around axes ox and oy (Eqs. (5.47) and (5.48), Sect. 5.3), enable to defining the angular accelerations ε_x and ε_y around axes ox and oy of the gyroscope, respectively, by the following equation:

$$T_i = J_i \varepsilon_i \tag{5.50}$$

where $J_x = 1.9974649 \times 10^{-4}$ kgm^2 is the mass moment of the gyroscope inertia around axis ox and oy (Table 5.2), other components are as specified above.

Substituting defined parameters into Eq. (5.50) and transformation yields the following result:

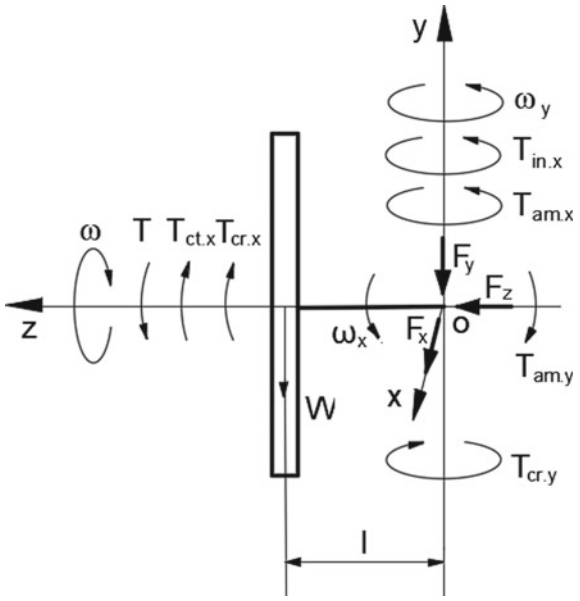

Fig. 5.6 Forces acting on the gyroscope with one side free support

$$\varepsilon_x = \frac{T_x}{J_x} = \frac{1.461887255 \times 10^{-7}/9.81}{1.9974649 \times 10^{-4}} = 7.460461885 \times 10^{-5} \text{ rad/s}^2 \quad (5.51)$$

$$\varepsilon_y = \frac{T_y}{J_y} = \frac{1.297409209 \times 10^{-11}/9.81}{1.9974649 \times 10^{-4}} = 6.621079654 \times 10^{-9} \text{ rad/s}^2 \quad (5.52)$$

The theoretical reactions of the forces F_i acting on the flexible cord along axis oy and ox are calculated by the following formula:

$$F_i = \frac{T_i}{l} \quad (5.53)$$

where $l = 0.0325$ m (Fig. 4.5, Chap. 4), other components are as specified above.

Substituting defined parameters into Eq. (5.53) and transformation gives the following result:

$$F_y = \frac{T_x}{l} = \frac{1.461887255 \times 10^{-7}}{0.0325} = 4.498114630 \times 10^{-6} \text{ N}$$
$$= 4.585234077 \times 10^{-4} \text{ g} \quad (5.54)$$

$$F_x = \frac{T_y}{l} = \frac{1.297409209 \times 10^{-11}}{0.0325} = 3.992028335 \times 10^{-10} \text{ N}$$
$$= 3.992028335 \times 10^{-7} \text{ g} \quad (5.55)$$

The calculated values of the gyroscopic forces acting along axis oy can be measured and validated by the practical test. The test of the gyroscope with one side free support and the measurement of the force acting on the flexible cord were conducted on the stand that represented in Fig. 5.7. The forces were measured by the Compact Digital Scale of the model Taylor TE10FT 5.0 kg with increments 1.0 gr. Figure 5.7a, b represents the photography and the sketch of the stand with the scale and the gyroscope. The gyroscope is suspended from the flexible cord connected with the platform of the scale. The measurement of the force acting along axis ox is practically impossible due to the flexibility of the cord. The tests conducted for the running gyroscope, in which the location of the axis of the spinning rotor was horizontal [9]. The acting parameters of the gyroscope are the same as represented in the previous chapter.

The results of theoretical calculations by Eq. (5.29, Section 5.3) and measurements of practical tests of the acting forces on the support are represented in Table 5.4. The vectorial diagram of the forces acting on the gyroscope is represented in Fig. 5.7.

The results of practical tests and measurement of the gyroscopic forces acting on the flexible cord represent interests for the analysis. The weight of the gyroscope acts on the flexible cord, which reaction demonstrates the digital scale. This gyroscope property can be explained by the following reasons:

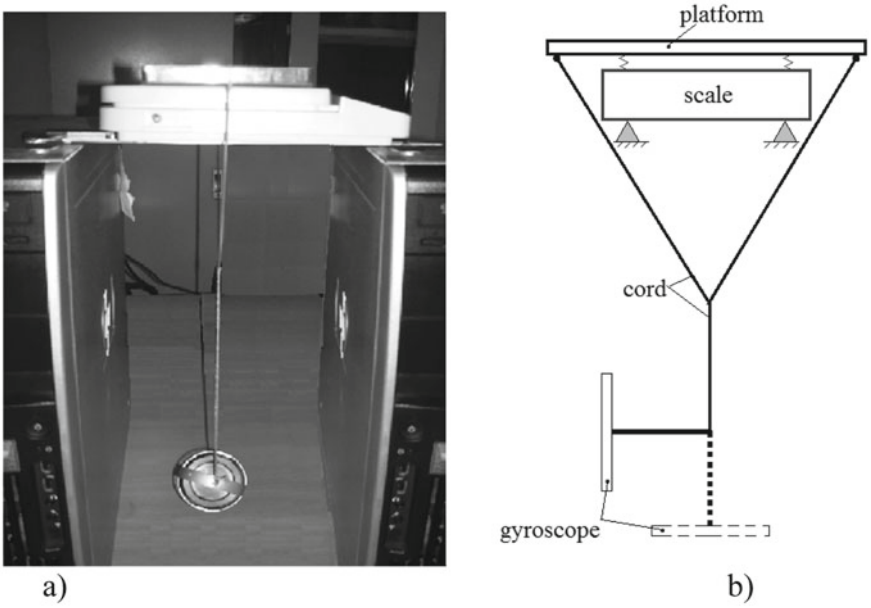

Fig. 5.7 Measurement of the acting forces on the gyroscope with one side free support

Table 5.4 Experimental and theoretical results of the forces acting on the gyroscope with the spinning rotor

Gyroscope parameters	Tests (kg)	Theoretical (kg)
Reaction of the mass, F_{m}	0.146	0.146
Reaction of forces generated by the torque, T_x		4.585×10^{-4}
Total reaction of the free support	0.146	0.1464585

- The inertial torques generated by the centrifugal, inertial, Coriolis forces and the change in the angular momentum are the reactions on the action of the applied or load torque.
- The value of the inertial resistance torques acting around axis *ox* cannot exceed the value of the load torque that can be an external or internal one. The expression of resistance torques contains the angular velocity of the gyroscope around axis *ox*, which direction of the rotation is the same as the direction of the action of the load torque. It means these resistance torques are only restraint torques.
- The value of the resulting reactive force acting on the free support along axis *oy* is very small and can be neglected for the following calculations. This is the reason that the scale demonstrates only the magnitude of the gyroscope weight acting along axis *oy*.

- A similar value of the resulting reactive force acting on the support along with axis *ox,* where the gyroscope precession torque is the load torque acting around axis *oy*.

Described gyroscope property of the action of the inertial torques should be taken into account for calculations of the gyroscopic forces and motions for different gyroscopic mechanisms and devices. The action of the inertial torques is manifesting only in the process of gyroscope motions and disappearing in case of the absent one. The gyroscope suspended from the flexible cord about point *B* represents the movable system with free motion on the horizontal plane *xoz* (Fig. 5.8). At the starting condition, the action of the gyroscope weight and the resistance inertial torques turn the gyroscope around axis *ox* and *oy.* The free horizontal location of the one side support of the suspended gyroscope is having several peculiarities. The resulting torques acting around axis *oy* are shifting the centre of gravity of the gyroscope about point *B* of the cord (Fig. 5.8). The location of the gyroscope relative to the centre axis of system $\Sigma oxyz$ is defined by the action of the gyroscope weight and the inertial torques. The resulting inertial torque acting around axis *oy* shifts the flexible cord

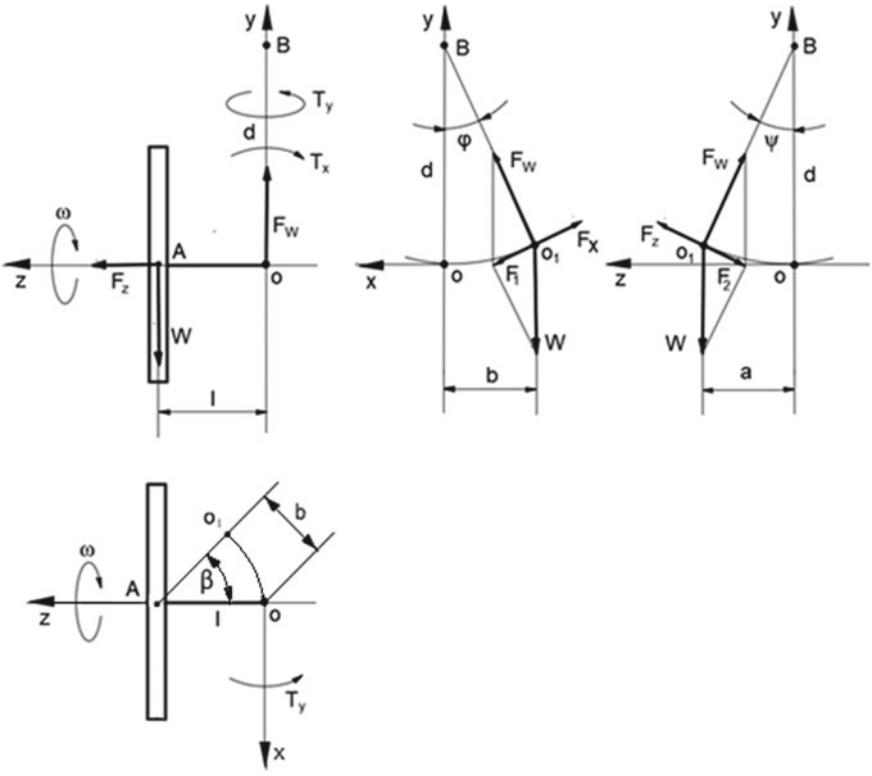

Fig. 5.8 Location of the gyroscope suspended from the flexible cord

and turns the gyroscope on the angle β relative to its centre of gravity A. The end of the gyroscope shaft is shifted on distance b, and the end of the cord o is turned around point B of the suspension on the angle φ. The angles φ and β are restricted by balancing of the force F_1 of the component of the resulting torque acting on the gyroscope around axis ox and by the component force of the gyroscope weight acting around axis oy.

The centrifugal force F_z generated by the rotating gyroscope centre mass around axis oy shifts the end of the gyroscope shaft o on the distance a, and the flexible cord d turns on the angle ψ around point B of the suspension. The angle ψ is restricted by balancing of the force F_2 of the component of resulting torque and by the component force of the gyroscope weight acting around point B. The measurement of the small value of the resulting torques acting on the movable gyroscope suspended on the flexible cord is problematic (Fig. 5.8).

The new location for the end o_1 of gyroscope shaft is defined by the angles β, φ and ψ and by the linear parameter a and b. All these parameters are calculated based on the values of the acting forces and the geometrical parameters of the gyroscope with one side free support. The value of the force F_i is defined by the formula $F_1 = T_y/l$, where l is the overhang of the gyroscope's centre of gravity from the free support o. The value of the force F_2 is defined by the formula $F_2 = Ml\omega_y^2$, M is the gyroscope mass, ω_y is the angular velocity of precession around axis oy, other components are as specified above. The angles φ and ψ are defined by the following formula: $\sin\varphi = F_1/F_m$ and $\sin\psi = F_2/F_m$, (Fig. 5.8). The angle β is calculated by the formula: $\sin\beta = b/l$, where $b = d\sin\varphi$ and d is the length of the flexible cord. The angle ψ is calculated by the formula: $\sin\psi = a/d$.

The new location of the end of the flexible cord o_1 relative to the point B of the suspension is natural for the gyroscope with one side free support. The shifted location of the gyroscope relatively to point B does not have any influence on the formulation of the gyroscope motions. The gyroscope does not manifest the motions of a swinging pendulum. The action of the precession and resistance torques represents the gyroscope as an overdamped or critically damped non-oscillating system. This statement is considered in Chap. 7.

The forces acting on the gyroscope support (point o) are defined by the following scheme. The action of the force F_x, which is a component of the resulting inertial torques T_y acting around axis oy, shifts the end of the flexible cord o on the angle β around the gyroscope centre of gravity A on the horizontal plane xoz and on the angle φ around point B of the suspension (Fig. 5.8). The reactive force F_m and the gyroscope weight W produce the force F_1 that counteracts to the action of the reactive force F_X (Eq. 5.55, Sect. 5.3.1). The balance of the action of two forces ($F_1 = F_x$ and $F_2 = F_z$) enables the angular location φ and ψ about the vertical of the gyroscope to be defined by the following solution:

$$\sin\varphi = \frac{F_1}{F_\mathrm{m}} = \frac{2.589667650 \times 10^{-5}}{0.146 \times 9.81} = 1.808098843 \times 10^{-5}$$

that giving rise to the following

$$\varphi = 0.00103^{\circ} \tag{5.56}$$

The angle φ enables for defining the angle β by the following expressions:

$$\sin\varphi = \frac{b}{d}, \quad \sin\beta = \frac{b}{l} \tag{5.57}$$

Substituting defined parameters into Eqs. (5.57) and transformation yields the following result:

$$1.808098843 \times 10^{-5} = \frac{b}{0.250}, \quad b = 4.520 \times 10^{-6} \quad m = 0.00452\ mm,$$
$$\sin\beta = \frac{4.520 \times 10^{-6}}{0.0325}, \quad \beta = 0.00796^{\circ} \tag{5.58}$$

The end of the gyroscope shaft is shifted on the small distance on the horizontal plane xoz ($b = 0.00452$ mm) and turned on the angle $\beta = 0.00796^{\circ}$ around axis oy.

$$\sin\psi = \frac{F_2}{F_{\mathrm{m}}} = \frac{0.146 \times 0.0325 \times 0.7360341^2}{0.146 \times 9.81} = 0.001794775$$

that giving rise to the following

$$\psi = 0.102^{\circ} \tag{5.59}$$

The angle ψ enables for defining the distance a by the following expressions:

$$\sin\psi = \frac{a}{d}, \tag{5.60}$$

Substituting defined parameters into Eq. (5.60) and transformation yields the following result:

$$0.001794775 = \frac{a}{0.250}, \quad a = 0.00044869\ m = 0.448\ \text{mm}, \tag{5.61}$$

The end of the gyroscope shaft is shifted on the small distance on the horizontal plane xoz ($a = 0.448$ mm) and turned on the angle $\psi = 0.102^{\circ}$ around point B. Defined components have small values and cannot be measured on the movable gyroscope. The vertical location of the cord with the suspended gyroscope is validated by the tests, which demonstrate the non-appreciable declining of the cord from the vertical ($\varphi = = 0.00103^{\circ}$ and $\psi = 0.102^{\circ}$).

References

1. Armenise, M.N., Ciminelli, C., Dell'Olio, F., Passaro, V.M.N.: Advances in Gyroscope Technologies. Springer, Berlin (2010)
2. Deimel, R.F.: Mechanics of the Gyroscope. Dover Publications Inc., New York (2003)
3. Greenhill, G.: Report on Gyroscopic Theory General Books LLC, London (2010)
4. Taylor, J.R.: Classical Mechanics. University Science Books, California (2005)
5. Aardema, M.D.: Analytical Dynamics. Theory and Application. Academic/Plenum Publishers, New York (2005)
6. Knight, R.D.: Physics for Scientists and Engineers: A Strategic Approach with Modern Physics, 4th edn. Pearson, London (2016)
7. Faller, J.E., Hollander, W.J., Nelson, P.G., McHugh, M.P.: Gyroscope-weighing experiment with a null result. Phys. Rev. Lett. **64**(8), 825–826 (1990). http://link.aps.org/doi/10.1103/PhysRevLett.64.825
8. Usubamatov, R.: Gyroscope's torques and motions. Int. J. Advance. Mech. Aeronaut. Eng. **2**(1), 1–5. ISSN: 2372-4153
9. Usubamatov, R.: Inertial Forces Acting on Gyroscope. J. Mech. Sci. Technol. **32**(1), 101–108 (2018)
10. Usubamatov, R.: Gyroscope tests and new effects. Int. J. Mining Metall. Mech. Eng. (IJMMME) **3**(1):1–5
11. Usubamatov, R.: Mathematical models for principles of gyroscope theory. Am. Inst. Phys. **1798**, 020133 (2017). https://doi.org/10.1063/1.4972725
12. Usubamatov, R.: Mathematical model for motions of gyroscope suspended from flexible cord. Cogent Eng. **3**, 1245901 (2016)
13. Usubamatov, R.: Gyroscope's torques and motions. In: Proceedings of the Second International Conference on Advances in Civil, Structural and Mechanical Engineering (CSM 2014), pp. 53–57. Copyright © Institute of Research Engineers and Doctors, USA (2014). All rights reserved. ISBN: 978-1-63248-054 0-5. Doi:10.15224/ 978-1-63248-054-5-50
14. Peters, C. A., Statistics for Analysis of Experimental Data, Princeton University, 2001
15. Scarborough, J.B.: The Gyroscope Theory and Applications. Nabu Press, London (2011)
16. Hibbeler, R.C.: Engineering Mechanics—Statics and Dynamics, 12th edn. Prentice Hall, Pearson (2010)
17. Gregory, D.R.: Classical Mechanics. Cambridge University Press, New York (2006)

Chapter 6
Mathematical Models for Motions of a Gyroscope with One Side Support

6.1 Motions of the Gyroscope with the Action of Frictional Forces

The running gyroscope with one side support demonstrates several properties, which researchers could not explain and describe for a long time [1–4]. The action of the frictional forces on supports and pivot of the gyroscope manifests the intensification of the motions around axes [5–9]. The external torque acting in the direction of precession lifts up the gyroscope [10, 11]. These gyroscopic effects are inconsistent with the known principles of engineering mechanics. The new analytical approach and detailed analysis of the action of the inertial torques on a gyroscope enable explaining their physics [12–15]. The mathematical model for motions around axes of the gyroscope with one side support considers for the gyroscope stand with gimbals that contain supports and pivot. The gyroscope weight and action of the inertial torques generate the reactive forces on the supports and pivot that produce the frictional torques. The frictional torques of the gyroscope's gimbal's supports are represented in the mathematical models of the gyroscope motions around axes. The frictional torques represent the additional external loads. The analytic models for the motions around axes for the gyroscope with the one side support are similar to the mathematical models for the motions of the gyroscope suspended from the flexible cord that represented in Sect. 5.1, Chap. 5 [13]. The frictional torques are added to the external and inertial torques acting on the gyroscope around two axes described in the previous chapter. The interrelations of the inertial and additional external torques are expressed by new peculiarities in equations of the gyroscope motions.

The action of the frictional torques on the gimbal's supports is considered on the test stand for the gyroscope with one side support that is represented in Figs. 6.1 and 6.2. The gyroscope outer gimbal is represented by the construction assembled with the bar, two arms and the centre beam. The gyroscope spherical frame presents the inner gimbal. The technical data of the stand are represented in Table 6.1.

© The Editor(s) (if applicable) and The Author(s), under exclusive license to Springer Nature Singapore Pte Ltd. 2020

R. Usubamatov, *Theory of Gyroscopic Effects for Rotating Objects*,
https://doi.org/10.1007/978-981-15-6475-8_6

Fig. 6.1 Stand of the gyroscope with one side support

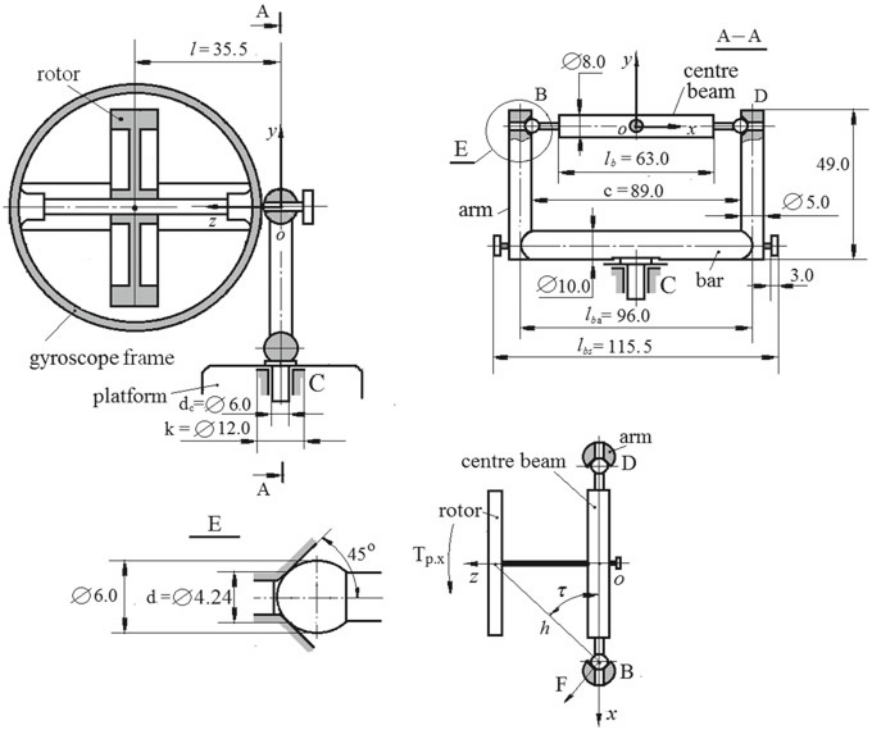

Fig. 6.2 Sketch of the gyroscope test stand

Table 6.1 Technical data of the test stand with Super Precision Gyroscope, "Brightfusion LTD"

Parameters	Mass (kg)	Mass moment of inertia around axis ox and oy (J kg m^2)
Spinning rotor with shaft, m_r	0.1159	$J = m_r R^2/2 = 0.5726674 \times 10^{-4}$ (around axis oz)
Gyroscope, M	0.146	$J_{iM} = (2/3)m_f r_f^2 + m_f l^2 + \left(m_r R_c^2/4\right) + m_r l^2 = 2.284736 \times 10^{-4}$
Centre beam with journals and screw, b	0.028	$J_{bx} = m_b r_b^2/2 = 0.00224 \times 10^{-4}$ (around axis ox) $J_{by} = m_b l_b^2/12 = 0.2105833 \times 10^{-4}$ (around axis oy)
Mass $E = M + b$	0.174	$J_{Ex} = J_{xM} + J_{bx} = 2.286976 \times 10^{-4}$ (around axis ox) $J_{Ey} = J_{xM} + J_{by} = 2.495319 \times 10^{-4}$ (around axis ox)
Bar with screws, b_s	0.067	$J_{bs} = m_{bs} l_{bs}^2/12 = 0.51456 \times 10^{-4}$ (around axis oy)
Arm, a	$2 \times 0.009 = 0.018$	$J_a = m_a r_a^2/2 + m_a l_a^2 = 0.41553 \times 10^{-4}$ (around axis oy)
Total $A = M + b + b_s + a$	0.259	$J_y = J_{yM} + J_b + J_{bs} + J_a = 3.38437 \times 10^{-4}$ (around axis oy)

The mathematical model of motions for the gyroscope with one side support is formulated for the common case when its axle is inclined on the angle γ. The basis of this model is well described in Sect. 5.1, Chap. 5 and is used with modification of mathematical models for motions of the gyroscope with the action of the frictional torques. The changes in the analytical models are represented by the action of the frictional torques on the gyroscope supports and pivot. Besides that, the analysis of the torques and motions acting on the gyroscope with one side support is conducted by the following peculiarities: The values of resulting torques acting on the supports and pivot of the gyroscope are very small (Sect. 5.3.1, Chap. 5); the reactive forces of the supports and pivot do not generate the sensitive frictional torques and can be neglected. This fact should be taken into account when compiling mathematical models of acting torques on the gyroscope and motions.

Analysis of the torques acting on the gyroscope demonstrates the following features. The external load torque T that is produced by the gyroscope weight W generates the frictional and inertial torques acting around axes ox and oy (Fig. 6.3). The inertial torques are represented by the interrelated components that well described in Sect. 5.1, Chap. 5. The action of the frictional torques on the test stand is represented by the following components:

(a) The gyroscope weight W produces the external frictional torques $T_{f.W.x}$ and $T_{f.W.y}$ acting on the supports of the inner gimbal and pivot of the outer gimbal around axes ox and oy, respectively;

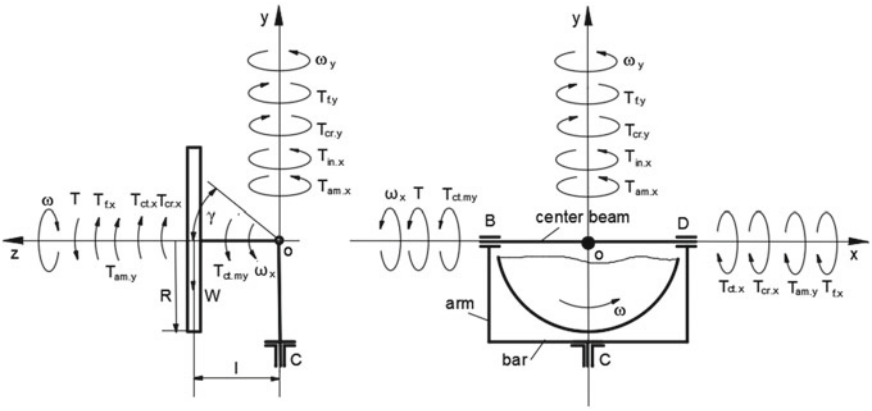

Fig. 6.3 Torques acting on the gyroscope with one side support and motions

(b) The frictional torque $T_{f.W.y}$ decreases the value of the load precession torques $T_{p.x}$, and the resistance torque $T_{cr.y}$ is dependent on the torques $T_{p.x}$;
(c) The change in the value of the precession torques $T_{p.x}$ acting around axis oy changes the value of the precession torque $T_{am.y}$ acting around axis ox. This change is expressed by the coefficient, η;
(d) The action of the frictional torques around axes ox and oy decreases the values of the inertial torques due to their interrelations;
(e) The rotation of the gyroscope around axis oy generates the centrifugal force of the gyroscope centre mass $F_{y.ct.x}$ and $F_{y.ct.y}$ that produces the frictional torques $T_{f.ct.x}$ and $T_{f.ct.y}$ acting on the supports and pivot around axes ox and oy, respectively;
(f) The rotation of the gyroscope around axes oy and ox generates the Coriolis forces of the gyroscope centre mass $F_{y.cr.x}$ and $F_{x.cr.y}$ that produces the frictional torques $T_{f.y.cr.x}$ and $T_{f.x.cr.y}$ acting on the supports and pivot around axes ox and oy, respectively;
(g) The rotation of the gyroscope around axis ox and oy of the test stand has occurred with low angular velocities that give the small values of high order for the inertial forces generated by the gyroscope centre mass that can be neglected;
(h) The decrease in values of inertial torques acting around two axes is equal because the inertial torques express the parts of the kinetic energy of the spinning rotor;
(i) The resulting torques acting on the gyroscope do not generate the sensitive reactive forces on its supports and pivot and can be neglected.

The action of the external and inertial torques on the gyroscope and motions is represented on the diagram of the test stand that represented in Fig. 6.3.

6.2 Mathematical Models for Gyroscope Motions

The action of interrelated external and inertial torques represented in Chaps. 4 (Eq. 4.9) and 5 enables to formulating the mathematical models for the gyroscope motions around two axes that are expressed by the following Euler's differential equations [14, 16, 17]:

$$J_{Ex}\frac{d\omega_x}{dt} = T\cos\gamma + T_{x.ct.y} - T_{f.x} - T_{ct.x} - T_{cr.x} - T_{am.y}\eta \tag{6.1}$$

$$J_{Ey}\frac{d\omega_y}{dt} = T_{in.x}\cos\gamma + T_{am.x}\cos\gamma - T_{cr.y}\cos\gamma - T_{y.cr.y} - T_{f.y} \tag{6.2}$$

$$\omega_y = -\left[\frac{2\pi^2 + 8 + (2\pi^2 + 9)\cos\gamma}{2\pi^2 + 9 - (2\pi^2 + 8)\cos\gamma}\right]\omega_x \tag{6.3}$$

where ω_x and ω_y are the angular velocity of the gyroscope around axes ox and oy, respectively; $T_{ct.x}$, $T_{ct.y,}$ $T_{cr.x,}$ $T_{cr.y}$, $T_{in.x,}$ $T_{in\cdot y}$, $T_{am.x}$ and $T_{am.y}$ are inertial torques generated by the centrifugal, Coriolis, inertial forces and the change in the angular momentum acting around axes ox and oy, respectively (Table 3.1, Chap. 3); η is the coefficient of the change in the inertial torque due to the action of the frictional torques on the pivot; $T_{x.ct.y}$ and $T_{y.ct.y}$ are the torques generated by the centrifugal force of the rotating gyroscope centre mass around axis ox and oy acting around axis ox, respectively; $T_{f.x}$ and $T_{f.y}$ are the frictional torques acting on the supports B and D and the pivot C, respectively; and other components are as specified above.

The running gyroscope produces the system of external and inertial torques acting around two axes of the gyroscope test stand that demonstrated in Fig. 6.3.

The defined external and inertial torques are expressed by the following equations:

(a) The weight W of the gyroscope inclined on the angle γ produces the torque T acting around axis ox in the counterclockwise direction:

$$T = Mgl\cos\gamma \tag{6.4}$$

where M is the gyroscope mass; g is the gravity acceleration, l is the distance between the centre mass of the gyroscope and axis of the centre beam (Fig. 6.3), γ is the angle of the gyroscope axle inclination.

(b) The torque generated by the centrifugal force of the rotating gyroscope centre mass around axis oy acting in the counterclockwise direction around axis ox:

$$T_{x.ct.y} = Ml(\cos\gamma)\omega_y^2(l\sin\gamma) = Ml^2\omega_y^2\cos\gamma\sin\gamma \tag{6.5}$$

where ω_y is the angular velocity of the gyroscope around axis oy and other components are as specified above.

(c) The centrifugal force of the rotating gyroscope centre mass around axis ox acting along the gyroscope axle (Fig. 6.3)

$$F_{z.ct.x} = Ml\omega_x^2 \tag{6.6}$$

where ω_x is the angular velocity of the gyroscope around axis.

(d) The frictional torques acting on the supports B and D are represented by the following equation:

$$T_{f.x} = T_{f.x.E.x} + T_{f.x.cr.y} + +T_{f.z.ct.x} + T_{f.x.ct.y} \tag{6.7}$$

where:

(e) The frictional torque acting on the supports B and D (Fig. 6.2) in the clockwise direction around axis oy generated by the centrifugal force of the rotating gyroscope centre mass around axis oy:

$$T_{f.x.ct.y} = Ml\cos\gamma\omega_y^2\left(\frac{df}{2\cos\delta}\right) \tag{6.8}$$

where d is the diameter of the centre beam; f is the frictional sliding coefficient; $\delta = 45^o$ is the angle of the cone of sliding bearing of the supports (Fig. 6.2), and other components are as specified above.

(f) The frictional torque acting on the supports B and D in the clockwise direction around axis ox generated by the centrifugal force of the rotating gyroscope centre mass around axis ox:

$$T_{f.x.ct.x} = Ml\omega_x^2\left(\frac{df}{2\cos\delta}\right) \tag{6.9}$$

where all components are as specified above.

(g) The frictional torque acting on the supports B and D in the clockwise direction around axis ox generated by the Coriolis force of the rotating gyroscope centre mass around axes oy and ox:

$$T_{f.x.cr.y} = Ml\omega_y\omega_x \sin\gamma\left[\frac{l}{h}\frac{df}{2\cos(\delta-\tau)}\right] \tag{6.10}$$

where $h = 56.925$ mm is the distance between the centre of the gyroscope and the support (Fig. 6.2); $\tau = \arctan[l/(c/2)] = 38.581^{\circ}$ is the angle of the action of Coriolis force on the sliding bearing, and other components are as specified above.

(h) The frictional torque acting on the sliding bearing of the supports B and D in the clockwise direction around axis ox generated by the gyroscope weight with the centre beam E:

$$T_{f.x.E.x} = (Eg\sin\gamma + Ml\omega_x^2)\frac{df}{2\cos\delta} \tag{6.11}$$

(i) where E is the mass of the gyroscope with the centre beam (Table 6.1), $F_{y.ct.x} = Ml\omega_x^2$ is the centrifugal force of the rotating gyroscope centre mass around axis ox acting along axis oy (Fig. 6.3), and other components are as specified above.

The expression of the total frictional torque (Eqs. (6.2)–(6.4)) acting on the supports B and D is represented by the following equation:

$$T_{f.x} = Eg\sin\gamma\frac{df}{2\cos\delta} + Ml\omega_x^2\frac{df}{2\cos\delta} + Ml\omega_y\omega_x(\sin\gamma)\frac{l}{h}\frac{df}{2\cos(\delta-\tau)} + Ml\omega_y^2\cos\gamma\frac{df}{2\cos\delta} \tag{6.12}$$

The torque generated by Coriolis force of the rotating gyroscope centre mass around axes oy and ox and acting in the clockwise direction around axis oy:

$$T_{y.cr.y} = (Ml\omega_y\sin\gamma)(\omega_x l\sin\gamma) = M\omega_y\omega_x(l\sin\gamma)^2 \tag{6.13}$$

where all components are as specified above.

The frictional torques acting on the pivot C are represented by the following equation:

$$T_{f.y} = T_{f.y.F.y} + T_{f.y.cr.y} + T_{f.y.ct.y} + T_{f.y.ct.x} \tag{6.14}$$

where:

(j) The frictional torque acting on the pivot C (Fig. 6.2) in the clockwise direction generated by the centrifugal force of the rotating gyroscope centre mass around axis oy:

$$T_{f.y.ct.y} = Ml\omega_y^2 \cos\gamma\left(\frac{d_c f_c}{2}\right) \tag{6.15}$$

where d_c is the diameter of the pivot; f_c is the frictional sliding coefficient, and other components are as specified above.

(k) The frictional torque acting on the pivot C in the clockwise direction around axis oy generated by the centrifugal force of the rotating gyroscope centre mass around axis ox and acting along axis oz:

$$T_{f.z.ct.x} = Ml\omega_x^2 \cos\gamma\left(\frac{d_c f_c}{2}\right) \tag{6.16}$$

(l) The frictional torque acting on the pivot C generated by Coriolis force of the rotating gyroscope centre mass around axes oy and ox:

$$T_{f.y.cr.y} = Ml\omega_y\omega_x \sin\gamma\left(\frac{d_c f_c}{2}\right) \tag{6.17}$$

(m) The frictional torque acting on the thrust sliding bearing of the pivot C in the clockwise direction around axis oy produced by the weight of the gyroscope's stand and the centrifugal force of the centre mass rotating around axis ox:

$$T_{f.y.F.y} = (Ag - Ml\omega_x^2 \sin\gamma)\left(\frac{d_e + d_c}{4}\right) f_c \tag{6.18}$$

where A is the total mass of the gyroscope stand (Table 6.1); d_e is the external diameter of the thrust sliding bearing of the pivot C; $Ml\omega_x^2 \sin\gamma$ is the centrifugal force of the rotating gyroscope centre mass around axis ox and acting along axis oy; other components are as specified above.

The expression of the total frictional torques (Eqs. 6.15–6.18) acting on the pivot C is represented by the following equation:

$$\begin{aligned} T_{f.y} = {} & (Ag - Ml\omega_x^2 \sin\gamma)\left(\frac{d_e + d_c}{4}\right) f_c + Ml(\sin\gamma)\omega_y\omega_x \frac{d_c f_c}{2} \\ & + Ml\omega_x^2(\cos\gamma)\frac{d_c f_c}{2} + Ml\omega_y^2(\cos\gamma)\frac{d_c f_c}{2} \end{aligned} \tag{6.19}$$

Analysis of the action of the external and inertial torques enables the physical principles of the gyroscope motions around axes to be formulated. The several gyroscope properties were represented in Sect. 4.2 of Chap. 4 where described in detail

the coefficient of the friction and its place in the change in the value of the inertial torque. The technical data of the gyroscope stand (Table 6.1, Figs. 6.2 and 6.3) enable the following information to be used for mathematical modelling of the gyroscope motions. The gyroscope stand generates the frictional torques acting around axes ox and oy. The correction coefficient η for the internal torque is considered for the frictional torques $T_{f.y}$ acting around axis oy. The coefficient η is expressed by the ratio of the difference between the precession torques $(T_{in.x}+ T_{am.x})\cos\gamma$ and the frictional torque $T_{f.y,}$ to the precession torques acting around axis oy. Substituting equations of Table 3.1 and Eqs. (6.7) and (6.13) into the ratio of these torques and transformation yields the expression of the correction coefficient η.

$$\eta = \frac{(T_{in.x} + T_{am.x})\cos\gamma - T_{y.cr.y} - T_{f.y}}{(T_{in.x} + T_{am.x})\cos\gamma} = 1 - \frac{T_{y.cr.y} + T_{f.y}}{(T_{in.x} + T_{am.x})\cos\gamma} =$$

$$1 - \frac{\left[\begin{array}{r} M\omega_y\omega_x(l\sin\gamma)^2 + (Ag - Ml\omega_x^2\sin\gamma)\left(\frac{d_e + d_c}{4}\right)f_c + Ml\omega_y\omega_x(\sin\gamma)\frac{d_c f_c}{2} + \\ Ml\omega_x^2(\cos\gamma)\frac{d_c f_c}{2} + Ml\omega_y^2(\cos\gamma)\frac{d_c f_c}{2} \end{array}\right]}{\left(\frac{2}{9}\pi^2 + 1\right)J\omega\omega_x\cos\gamma} \tag{6.20}$$

where η is the coefficient of correction for the action of frictional torques around axis oy; other components are as specified above.

Substituting defined equations for the inertial torques of the gyroscope (Table 3.1), Eqs. (6.4)–(6.6), (6.12), and (6.13) into Eqs. (6.1) and (6.2) yields the following system of differential equations:

$$J_{Ex}\frac{\mathrm{d}\omega_x}{\mathrm{d}t} = Mgl\cos\gamma + Ml^2\omega_y^2\cos\gamma\sin\gamma - \left[\begin{array}{r} (Eg\sin\gamma + Ml\omega_x^2)\frac{df}{2\cos\delta} + Ml\omega_y\omega_x(\sin\gamma)\frac{l}{h}\frac{df}{2\cos(\delta-\tau)} \\ + Ml\omega_y^2\cos\gamma\frac{df}{2\cos\delta} \end{array}\right] - \left[\frac{2}{9}\pi^2 J\omega\omega_x + \frac{8}{9}J\omega\omega_x + J\omega\omega_y\eta\right] \tag{6.21}$$

$$J_{Ey}\frac{\mathrm{d}\omega_y}{\mathrm{d}t} = \frac{2}{9}\pi^2 J\omega\omega_x\cos\gamma + J\omega\omega_x\cos\gamma - \frac{8}{9}J\omega\omega_y\cos\gamma - M\omega_y\omega_x(l\sin\gamma)^2 \tag{6.22}$$

where all components are as specified above.

Following solutions of Eqs. (6.21) and (6.22) are the same that represented in Sect. 5.1, Chap. 5. Then, for the horizontal $\gamma = 0$ and $\omega_y = (4\pi^2 + 17)\omega_x$ location of the gyroscope, the equations are represented by the following expressions:

$$J_{Ex}\frac{\mathrm{d}\omega_x}{\mathrm{d}t} = Mgl - Ml\omega_x^2\frac{df}{2\cos\delta} - Ml(4\pi^2 + 17)^2\omega_x^2\frac{df}{2\cos\delta} - \left(\frac{2\pi^2+9}{9}\right)J\omega\omega_x - (4\pi^2 + 17)J\omega\omega_x \left\{1 - \frac{\left[Ag\left(\frac{d_e+d_c}{4}\right)f_c + Ml\omega_x^2\frac{d_c f_c}{2} + Ml(4\pi^2 + 17)^2\omega_x^2\frac{d_c f_c}{2}\right]}{\left(\frac{2\pi^2+9}{9}\right)J\omega\omega_x}\right\} \quad (6.23)$$

$$J_{Ey}\frac{d\omega_y}{dt} = \left(\frac{2}{9}\pi^2 + 1\right)J\omega\omega_x - \frac{8}{9}J\omega\omega_y = \left(\frac{2}{9}\pi^2 + 1\right)J\omega\omega_x - Ag\left(\frac{d_e + d_c}{4}\right)f_c - Ml\omega_x^2\frac{d_c f_c}{2} - Ml\omega_y^2\frac{d_c f_c}{2} - \frac{8}{9}J\omega_y \quad (6.24)$$

Equations (6.23) and (6.24) are represented the mathematical models for motions of the gyroscope around axes *ox* and *oy* with the action of the external and inertial torques [14]. Analysis of these equations demonstrates the action of the frictional forces changes the value of the inertial torques that lead to changes in the angular velocities of the gyroscope around axes. The resulting value of the inertial torques acting around axis *ox* is decreased that leads to the increase of the angular velocity under the action of the gyroscope weight. The resulting value of the inertial torques acting around axis *oy* is decreased that leads to the decrease of the gyroscope angular velocity. This statement is confirmed by practical tests.

Equation (6.24) contains the inertial torques acting around axis *oy* generated by the torque of gyroscope weight. These inertial torques can be expressed in the term of the gyroscope weight. The presentation of these inertial torques is the same as described in Sect. 5.2, Chap. 5. Substituting Eq. (4.6), Chap. 4 of the ratio of angular velocities and Eq. (6.19) of the frictional torque into the right side of Eq. (6.23) and transformation yields the expression ω_x that is as follows:

$$\omega_x = \frac{\left(\frac{38\pi^2+161}{9}\right)J\omega}{2\left[9\left(\frac{4\pi^2+17}{2\pi^2+9}\right)\frac{d_c f_c}{2} - \frac{df}{2\cos\delta}\right][1 + (4\pi^2 + 17)^2]Ml} \sqrt{\left\{\frac{\left(\frac{38\pi^2+161}{9}\right)J\omega}{2\left[9\left(\frac{4\pi^2+17}{2\pi^2+9}\right)\frac{d_c f_c}{2} - \frac{df}{2\cos\delta}\right][1 + (4\pi^2 + 17)^2]Ml}\right\}^2 - \frac{Mgl + 9\left(\frac{4\pi^2+17}{2\pi^2+9}\right)Ag\left(\frac{d_e+d_c}{4}\right)f_c}{\left[9\left(\frac{4\pi^2+17}{2\pi^2+9}\right)\frac{d_c f_c}{2} - \frac{df}{2\cos\delta}\right][1 + (4\pi^2 + 17)^2]Ml}} \quad (6.25)$$

The transformation of the precession torque $T_{p.x}$ of Eq. (6.24) is implemented by the solution of Eq. (5.15) of Sect. 5.2, Chap. 5. Equation (6.25) is substituted into an expression of the precession torque (Eq. 6.24), increased on the ratio of the angular velocities (Eq. 4.6) and decreased on the ratio of the precession and resistance torques (Eq. 5.12, Chap. 5). Then, the modified formula of the precession torque $T_{p.x}$ is represented by the following expression:

$$T_{p.x} = \left(\frac{2}{9}\pi^2 + 1\right) J\omega\omega_x = \frac{\left(4\pi^2 + 17\right)\left(\frac{2\pi^2+9}{9}\right) J\omega\omega_x}{\left(\frac{2\pi^2+9}{8}\right)} = \frac{8}{9}\left(4\pi^2 + 17\right) J\omega\omega_x \tag{6.26}$$

where ω_x is represented by Eq. (6.25).

The expression $T_{p.x}$ (Eq. (6.26)) is substituted into Eq. (6.24), and transformation yields the following:

$$J_{Ey}\frac{\mathrm{d}\omega_y}{\mathrm{d}t} = \frac{8}{9}\left(4\pi^2 + 17\right) J\omega\omega_x - Ag\left(\frac{d_e + d_c}{4}\right) f_c - Ml\omega_x^2\frac{d_c f_c}{2} - Ml\omega_y^2\frac{d_c f_c}{2} - \frac{8}{9} J\omega\omega_y \tag{6.27}$$

where ω_x is represented by Eq. (6.25), other components are as specified above.

Equation (6.27) can be used for the direct computing of the angular velocity of the gyroscope motion around axis oy.

6.2.1 Case Study and Practical Tests

The mathematical model for motions of the gyroscope with the action of the frictional torques is considered on the test stand (Fig. 6.2). The practice tests conducted for the horizontal location of the gyroscope spinning axle. The coefficients of the sliding friction of supports and pivots defined empirically $f = 0.1$, $f_c = 0.3$. The speed of the gyroscope's rotor for the tests is accepted 10,000 rpm. The velocity of the spinning rotor measured by the Optical Multimeter Tachoprobe Model 2108/LSR Compact Instrument Ltd. with a range of measurement 0 … 60,000.00 rpm. The spinning rotor demonstrated the permanent drop of 67 revolutions per second. The measurements of the angular location for the gyroscope axle were conducted optically by the angular template with accuracy $\pm 1.0°$. The time of the gyroscope motions around axes measured by the stopwatch of Model SKU SW01 with resolution 1/100 s.

The results of practical tests are represented by the following average data. The time spent on one revolution around axis oy is $t_y = 3.86$ s, and then, the angular velocity is $\omega_y = 360°/3.86\ \text{s} = 93.860°/\text{s}$. The time spent on the gyroscope turn of

20° around axis ox (±10° about horizontal location) is $t_x = 13.9$ s, and then, the angular velocity is $\omega_y = 20°/13.9\text{ s} = 1.43°/\text{s}$.

The numerical solution of the case study.

The gyroscope parameters (Table 6.1, Fig. 6.2) and Eq. (4.6), Chap. 4 are substituted into Eq. (6.23), and transformation yields the following equation of the gyroscope motion around axis ox.

$$J_{Ex}\frac{\mathrm{d}\omega_x}{\mathrm{d}t} = Mgl + Ag9\left(\frac{4\pi^2+17}{2\pi^2+9}\right)\left(\frac{d_e+d_c}{4}\right)f_c - \left(\frac{38\pi^2+161}{9}\right)J\omega\omega_x + \left[9\left(\frac{4\pi^2+17}{2\pi^2+9}\right)d_c f_c - \frac{df}{\cos\delta}\right]\left[\frac{1+(4\pi^2+17)^2}{2}\right]Ml\omega_x^2$$

$$2.286976\times10^{-4}\frac{\mathrm{d}\omega_x}{\mathrm{d}t} = 0.146\times9.81\times0.0355 + 0.259\times9.81\times9 \times\left(\frac{4\pi^2+17}{2\pi^2+9}\right)\left(\frac{0.012+0.006}{4}\right)\times0.3 - \left(\frac{38\pi^2+161}{9}\right)\times0.5726674\times10^{-4}\times10000\times(2\pi/60)\omega_x - \left[9\left(\frac{4\pi^2+17}{2\pi^2+9}\right)\times0.006\times0.3 - \frac{0.00424\times0.1}{\cos45^o}\right] \left[\frac{1+(4\pi^2+17)^2}{2}\right]\times0.146\times0.0355\omega_x^2 \tag{6.28}$$

Following simplification and transformation yield the equation:

$$8.854097609\times10^{-4}\frac{\mathrm{d}\omega_x}{\mathrm{d}t} = 0.431723140 - 13.828417743\omega_x - \omega_x^2 \tag{6.29}$$

Separating variables and transformation for this differential equation gives the following:

$$\frac{d\omega_x}{\omega_x^2 + 13.828417743\omega_x - 0.431723140} = -1129.420573509\mathrm{d}t \tag{6.30}$$

Transformation and presentation of the obtained equation by the integral form with defined limits yield the following:

$$\int_0^{\omega_x}\frac{1}{(\omega_x - 0.031114426)(\omega_x + 13.8595321695)}\mathrm{d}\omega_x = -1129.420573509\int_0^t \mathrm{d}t \tag{6.31}$$

The left integral of Eq. (6.31) is transformed and represented by the two tabulated integrals $\int \frac{dx}{x \mp a} = -\ln|x \mp a| + C$. The right integral is simple, and integrals have the following solution:

$$\frac{1}{13.8906465955} \int_0^{\omega_x} \left(\frac{1}{\omega_x - 0.031114426} - \frac{1}{\omega_x + 13.8595321695} \right) d\omega_x = -1129.420573509 \int_0^t dt \tag{6.32}$$

Solution of Eq. (6.32) is as follows

$$[\ln(\omega_x - 0.031114426) - \ln(\omega_x + 13.8595321695)]\Big|_0^{\omega_x} = -1129.420573509t\Big|_0^t$$

that gave rise to the following

$$(\omega_x - 0.031114426) = -445.437501225(\omega_x + 13.8595321695)e^{-1129.420573509tt} \tag{6.33}$$

The right side Eq. (6.33) has the small value of the high order that can be neglected. Solving of Eq. (6.33) gives the equations of the angular velocity for the gyroscope around axis *ox* and *oy* as the result of the action of the gyroscope weight and the frictional torques.

$$\omega_x = 0.031114426\,\text{rad/s} = 1.782725291^\circ/\text{s} \tag{6.34}$$

$$\omega_y = (4\pi^2 + 17) \times 0.031114426\,\text{rad/s} = 100.685503501^\circ/\text{s} \tag{6.35}$$

The time of one revolution around axis *oy* is

$$t = 360^\circ/\omega_y = 360^\circ/100.685503501^\circ/\text{s} = 3.575\text{s} \tag{6.36}$$

The angular velocity of the precession around axis *oy* can be defined by Eq. (6.27). Numerical solution of Eq. (6.27) is similar as for Eq. (6.23), and all comments are omitted. Substituting initial data (Table 6.1, Fig. 6.2) and Eq. (6.25) into Eq. (6.27) yields the following differential equation:

$$J_{Ey}\frac{d\omega_y}{dt} = \frac{8}{9}(4\pi^2 + 17)J\omega\omega_x - Ag\left(\frac{d_e + d_c}{4}\right)f_c - Ml\omega_x^2\frac{d_c f_c}{2} - Ml\omega_y^2\frac{d_c f_c}{2} - \frac{8}{9}J\omega\omega_y \tag{6.37}$$

where ω_x is computed by Eq. (6.25)

$$\omega_x = \frac{\left(\frac{38\pi^2+161}{9}\right) \times 0.5726674 \times 10^{-4} \times 10000 \times (2\pi/60)}{2\left[9\left(\frac{4\pi^2+17}{2\pi^2+9}\right)\frac{0.006\times 0.3}{2} - \frac{0.00424\times 0.1}{2\cos\delta}\right][1+(4\pi^2+17)^2] \times 0.146 \times 0.0355}$$
$$- \sqrt{\left\{\frac{\left(\frac{38\pi^2+161}{9}\right) \times 0.5726674 \times 10^{-4} \times 10000 \times (2\pi/60)}{2\left[9\left(\frac{4\pi^2+17}{2\pi^2+9}\right)\frac{0.006\times 0.3}{2} - \frac{0.00424\times 0.1}{2\cos\delta}\right][1+(4\pi^2+17)^2] \times 0.146 \times 0.0355}\right\}}$$
$$- \sqrt{\frac{0.146 \times 9.81 \times 0.0355 + 9\left(\frac{4\pi^2+17}{2\pi^2+9}\right)0.259 \times 9.81 \times \left(\frac{0.012+0.006}{4}\right) \times 0.3}{\left[9\left(\frac{4\pi^2+17}{2\pi^2+9}\right)\frac{0.006\times 0.3}{2} - \frac{0.00424\times 0.1}{2\cos\delta}\right][1+(4\pi^2+17)^2] \times 0.146 \times 0.0355}}$$
$$= 0.031125678 \tag{6.38}$$

$$2.286976 \times 10^{-4}\frac{d\omega_y}{dt} = \frac{8(4\pi^2+17)}{9} \times 0.5726674 \times 10^{-4} \times 10.000$$
$$\times (2\pi/60) \times 0.031125678 - 0.259 \times 9.81$$
$$\times \left(\frac{0.012+0.006}{4}\right) \times 0.3 - 0.146$$
$$\times 0.0355 \times 0.031125678^2 \times \frac{0.006 \times 0.3}{2} - 0.146$$
$$\times 0.0355 \times \frac{0.006 \times 0.3}{2}\omega_y^2 - \frac{8}{9} \times 0.5726674 \times 10^{-4}$$
$$\times 10000 \times (2\pi/60)\omega_y \tag{6.39}$$

The right side of Eq. (6.39) contains third and fourth components of small value of high order that can be neglected.

The solution and simplifications of Eq. (6.39) bring the following equation

$$4.2902545423 \times 10^{-3}\frac{d\omega_y}{dt} = 1.7579290418 - \omega_y \tag{6.40}$$

The solution of Eq. (6.40) is similar as Eq. (5.23) of Sect. 5.3 that yields the following result:

$$\omega_y = 1.7579290418\,\text{rad/s} = 100.721914^\circ/\text{s} \tag{6.41}$$

that is almost same as the result of Eq. (6.8).

The obtained result is a validation of the correctness of Eq. (6.27) that can be used for the right computing of the angular velocity of precession around axis *oy*. Experimental and theoretical results of the gyroscope precessions around two axes with the action of load and frictional torques on supports are represented in Table 6.2.

Analysis of the results of the theoretical calculations and practical tests for the gyroscope precessions demonstrates acceptable discrepancies between them. The difference of times around axis *ox* is explained by the drop of the revolutions of the

Table 6.2 Experimental and theoretical results of the gyroscope precessions

Gyroscope average parameters	Tests	Theoretical	Difference (%)
Time of one revolution around axis *oy* (s)	3.77	3.575	5.45
Time of precession of the gyroscope motion around axis *ox* on 20° (from +10° to −10°) of the turn about horizontal location around axis *ox* (s)	14.46	15.35	6.15

spinning disc around 1000 revolutions. Obtained data enable for stating the theoretical and practical results are well coincided and mathematical models for the forces acting on the gyroscope and its motions are acceptable for engineering applications in practice. A clear confirmation of the results obtained can be seen from the data for the motion of a gyroscope suspended from a flexible cord where there are no friction forces.

The test results are a validation of the analytic statement that the action of the frictional forces on supports and pivots of the gyroscope gimbals decreases the values of the inertial torques. This circumstance increases the action of the load torque and explains the increase of the angular velocity of precession around axis *ox*. The value of the load inertial torque acting around axis *oy* and hence the angular velocity is also increased. The mathematical model for the external and inertial torques acting on the gyroscope explains the physics of its motions. Differences in theoretical and practical results are explained by the reasons represented in Sect. 5.3, Chap. 5.

6.3 Physics of the Gyroscope "Anti-gravity" Effects

The physics of the gyroscope "anti-gravity" effects are explained by the mathematical model for the gyroscope motions around two axes with two load torques [18]. The analytical model considers the action of the torques on the stand with the gyroscope of one side support (Figs. 6.1 and 6.2). The first load torque T is represented by the gyroscope weight that acts around axis *ox*. The external torque acting around axis *oy* represents the second torque *Ty*. The action of two external torques on the gyroscope generates the combination of the inertial and external torques and the new motions. The mathematical models for the gyroscope motions formulated by the interrelated action of the internal and external torques. The analytical approach for modelling of the gyroscope motions with two external loads is similar to the model for the gyroscope motions represented in Sect. 5.1, Chap. 5. The action of the inertial torques generated by two external torques is expressed by the complicated mathematical models for motions of the gyroscope. The two external torques acting around different axes on a gyroscope and its motions are considered for the horizontal location of the spinning rotor. The action of the frictional forces on the supports and pivot is omitted with the aim to remove the cumbersome expressions. Removing of the frictional forces from consideration does not misrepresent the mathematical models for the physics of the gyroscope "anti-gravity" effects.

Mathematical models for gyroscope motions are examined for two types of load torques acting in counter and clockwise directions around axis *oy*. These two approaches provide a clear picture of the interrelated actions of two external and several inertial torques resulting in gyroscope motions. Two models consider the action of the external torque T_y in the counterclockwise and clockwise direction around axis *oy,* respectively, and the action of the torque T of the gyroscope weight. The action of two loads changes in values of inertial torques that depend on the values of external torques applied to axes. The changes in values of the inertial torques acting around axis *ox* and *oy* are interrelated with the values of the external torques. These changes are expressed in the mathematical models for the motions of the gyroscope around two axes. The analysis of the torques and motions acting on the gyroscope with one side support is conducted by the regulations described in Chap. 5.

6.3.1 Case Study 1

The mathematical model for the motions of the gyroscope considers the action of the load torque T_y around axis *oy* in a counterclockwise direction. The load torque $T = Mgl$ is generated by the weight W of the gyroscope around axis *ox*. The action of the external load torque T_y generates the following system of inertial torques acting around axes of the gyroscope (Fig. 6.4):

(a) The resistance torque $T_{r.y} = T_{ct.y} + T_{cr.y}$ generated by the centrifugal $T_{ct.y}$ and Coriolis forces $T_{cr.y}$ around axis *oy* is acting in a clockwise direction (i.e. in the opposite direction of the action of load torque T_y).

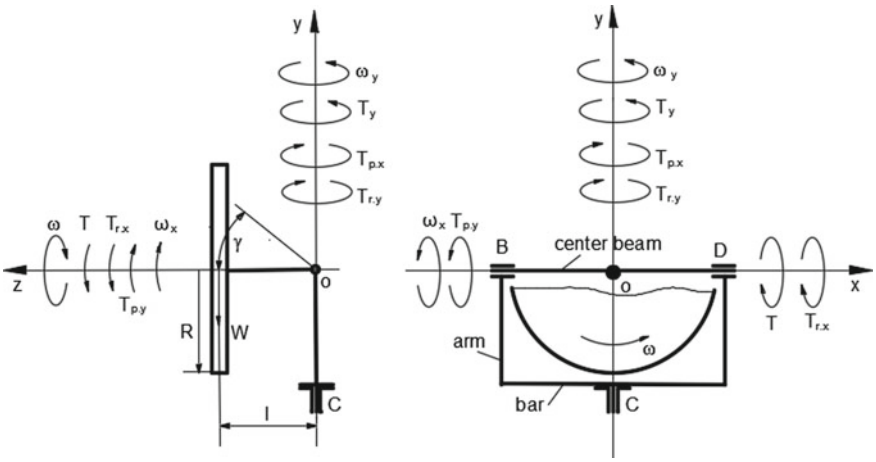

Fig. 6.4 Internal torques and motions when the load torque T_y acts in the counterclockwise direction around axis *oy*

(b) The procession torque $T_{p.y} = T_{in.y} + T_{am.y}$ generated by the common inertial forces $T_{in.y}$ and the change in the angular momentum of the spinning rotor $T_{am.y}$ originated on axis *oy* but acting around axis *ox* in a clockwise direction (i.e. in the opposite direction of the action of the gyroscope weight T). The value of the torque produced by the gyroscope weight T is lower than the value of the resulting inertial torques $T_{rstx} = T_{p.y} - T_{r.x} - T$ acting around axis *ox*. The latter (T_{rstx}) causes the upward motion of the gyroscope.

(c) The procession torque $T_{p.y}$ around axis *ox,* in turn, generates the resistance torque $T_{r.x} = T_{ct.x} + T_{cr.x}$ of centrifugal $T_{ct.x}$ and Coriolis forces $T_{\mathrm{cr.x}}$ around axis *ox*. The torque $T_{r.x}$ acting in a counterclockwise direction and added to the action of the gyroscope weight *T.* The resulting torque around axis *ox* is as follows $T_{rst.x} = T_{p.y}$ - $T_{r.x}$ - T

(d) The action of the resulting torque $T_{rst.x}$ around axis *ox* produces the precession torque $T_{p.x} = T_{in.x} + T_{am.x}$ generated by the common inertial forces $T_{in.x}$ and the change in the angular momentum $T_{am.x}$ originated on axis *ox* but acting around axis *oy* and added to the resistance torque $T_{r.y}$ around axis *oy*, which results in the resistance torque $T_{rst.y} = T_{r.y} + T_{p.x}$. The resulting torque around axis *oy* is as follows $T_{rst.y} = T_y - T_{ct.y} - T_{cr.y} - T_{am.x}$

The actions of load torque T_y and T change the values of interrelated inertial torques acting around two axes. The action of the external torque T_y generates precession torque $T_{p.y}$ acting around axis *ox*, which is opposite to the action of the gyroscope weight T. This situation leads to a decrease in the value of the resulting inertial torque $T_{rst.x}$ and the precession torque $T_{p\cdot x}$ acting around axis *oy*. The change in the value of the precession torque $T_{p\cdot x}$ is expressed by the coefficient of the change in the inertial torques around axis *oy*:

$$\eta = \left| \frac{T_{p.y} - T}{T_{p.y}} \right| = \left| 1 - \frac{T}{T_{p.y}} \right| = \left| 1 - \frac{9Mgl\cos\gamma}{(2\pi^2 + 9)J\omega\omega_y} \right| \tag{6.42}$$

where expressions of the inertial torques (Table 4.1, Chap. 4) and the torque produced by the gyroscope weight are substituted into Eq. (6.42). All components are as specified above.

The coefficient η represents the decrease in the value of precession torque acting around axis *oy* when the value of inertial torque around axis *ox* decreases. This dependency expresses the interrelation of the inertial torques acting around two axes. An analysis of Eq. (6.42) yields the following values of the coefficient η:

- The absence of the load torque T acting around axis *ox* means that the coefficient is $\eta = 1.0$ (i.e. there is no change in the value of the inertial torques acting around two axes).
- The action of the load torque T means that the coefficient is $\eta < 1.0$ (i.e. the values of the inertial acting torques around two axes decrease due to the interrelation).
- When the load torque is equal to the precession torque ($T = T_{p.y}$), the coefficient is $\eta = 0$ (i.e. the gyroscope does not turn around axis *oy* but instead turns around axis *ox* under only the action of the gyroscope weight).

This peculiarity should be represented in equations of the gyroscope motions around two axes. A mathematical model has been developed to assess a gyroscope's motions that are caused by the action of the external and internal torques. This model corrected due to the interrelated action of the inertial and external torques and is presented by the following Euler's differential equations:

$$J_y \frac{d\omega_y}{dt} = T_y - T_{ct.y} \cos\gamma - T_{cr.y} \cos\gamma - T_{am.x} \cos\gamma\eta \tag{6.43}$$

$$J_x \frac{d\omega_x}{dt} = -T_{in.y} - T_{am.y} + T_{cr.x} + T\cos\gamma \tag{6.44}$$

where ω_x and ω_y are the angular velocities of the gyroscope around axes ox and oy, respectively; $T_{ct.y}$, $T_{cr.x}$, $T_{cr.y}$, $T_{in.y}$, $T_{am.x}$, $T_{am.y}$ and $T_{am.y}$ are the inertial torques generated by the centrifugal, Coriolis and common inertial forces and the change in the angular momentum acting around axes ox and oy, respectively (Table 4.6). All other components are as specified above.

The equations of inertial torques (Table 4.1, Chap. 4), Eq. (6.42) and modified Eq. (4.9), Chap. 4 due to the change in the indices of axes are substituted into Eqs. (6.42) and (6.44). The simplification and modification of these equations are similar to the solution presented in Sect. 5.2, Chap. 5 and Sect. 6.2, wherein this process is justified in detail. Modified equations presented by the following system:

$$\begin{aligned} J_y \frac{\mathrm{d}\omega_y}{\mathrm{d}t} &= T_y - \left(\frac{2\pi^2+8}{9}\right) J\omega\omega_y \cos\gamma \\ &\quad - \left[\frac{2\pi^2+8+(2\pi^2+9)\cos\gamma}{2\pi^2+9-(2\pi^2+8)\cos\gamma}\right] J\omega\omega_y \cos\gamma \left[1 - \frac{9Mgl\cos\gamma}{(2\pi^2+9)J\omega\omega_y}\right] \end{aligned} \tag{6.45}$$

$$J_x \frac{\mathrm{d}\omega_x}{\mathrm{d}t} = -\left(\frac{2\pi^2+9}{9}\right) J\omega\omega_y + \left(\frac{8}{9}\right) J\omega\omega_x + Mgl\cos\gamma \tag{6.46}$$

where all parameters are as specified above.

Defined parameters enable the presentation of Eq. (6.45) by the direct computing of the angular velocity ω_x of the gyroscope around axis ox. The first component of the right side of Eq. (6.46) is the precession torque $T_{p.y}$ generated by the resulting torque $T_{r.y}$ around axis oy, which is presented by the following expression:

$$\begin{aligned} T_{r.y} &= T_y - \left(\frac{2\pi^2+8}{9}\right) J\omega\omega_y \cos\gamma \\ &\quad - \left[\frac{2\pi^2+8+(2\pi^2+9)\cos\gamma}{2\pi^2+9-(2\pi^2+8)\cos\gamma}\right] J\omega\omega_y \cos\gamma \left[1 - \frac{9Mgl\cos\gamma}{(2\pi^2+9)J\omega\omega_y}\right] \end{aligned} \tag{6.47}$$

The angular velocity ω_y is defined from the right side of Eq. (6.47) that is as follows:

$$\omega_y = \frac{\frac{T_y}{\cos\gamma} + \left[\frac{2\pi^2+8+(2\pi^2+9)\cos\gamma}{2\pi^2+9-(2\pi^2+8)\cos\gamma}\right]\left(\frac{9Mgl\cos\gamma}{2\pi^2+9}\right)}{\left[\frac{2\pi^2+8}{9} + \frac{2\pi^2+8+(2\pi^2+9)\cos\gamma}{2\pi^2+9-(2\pi^2+8)\cos\gamma}\right]J\omega} \tag{6.48}$$

Equation (6.48) is substituted into an expression of the precession torque (Eq. 6.46), which increased on the ratio of the angular velocities (Eq. 4.9, Chap. 4), and decreased on the ratio of precession and resistance torques (Eq. 5.11, Chap. 5). Then, the precession torque $T_{p.y}$ is represented by the following modified expression:

$$\begin{aligned} T_{p.y} &= -\frac{\left(\frac{2\pi^2+8+(2\pi^2+9)\cos\gamma}{2\pi^2+9-(2\pi^2+8)\cos\gamma}\right)\left(\frac{2\pi^2+9}{9}\right)J\omega\cos\gamma\times}{\left(\frac{2\pi^2+9}{8}\right)} \\ &= -\frac{8\left\{T_y+\left[\frac{2\pi^2+8+(2\pi^2+9)\cos\gamma}{2\pi^2+9-(2\pi^2+8)\cos\gamma}\right]\left(\frac{9Mgl\cos^2\gamma}{2\pi^2+9}\right)\right\}}{(2\pi^2+8)\left[\frac{2\pi^2+9-(2\pi^2+8)\cos\gamma}{2\pi^2+8+(2\pi^2+9)\cos\gamma}\right]+9} \end{aligned} \tag{6.49}$$

The expression $T_{p.y}$ (Eq. 6.49) is substituted into Eq. (6.46), and transformation yields the following:

$$J_x\frac{d\omega_x}{dt} = -\frac{8\left\{T_y + \left[\frac{2\pi^2+8+(2\pi^2+9)\cos\gamma}{2\pi^2+9-(2\pi^2+8)\cos\gamma}\right]\left(\frac{9Mgl\cos^2\gamma}{2\pi^2+9}\right)\right\}}{(2\pi^2+8)\left[\frac{2\pi^2+9-(2\pi^2+8)\cos\gamma}{2\pi^2+8+(2\pi^2+9)\cos\gamma}\right]+9} + \left(\frac{8}{9}\right)J\omega\omega_x \tag{6.50}$$

where the torque generated by the gyroscope weight (Eq. 6.46) is removed because the modified precession torque $T_{p.y}$ contains it, other components are as specified above.

Equation (6.50) can be used for the direct computing of the angular velocity of the gyroscope lift up motion around axis ox.

For the horizontal location of the gyroscope, Eqs. (6.45) and (6.46) are represented by the following:

$$J_y\frac{\mathrm{d}\omega_y}{\mathrm{d}t} = T_y - \left(\frac{2\pi^2+8}{9}\right)J\omega\omega_y - (4\pi^2+17)J\omega\omega_y\left[1 - \frac{9Mgl}{(2\pi^2+9)J\omega\omega_y}\right] \tag{6.51}$$

$$J_x\frac{\mathrm{d}\omega_x}{\mathrm{d}t} = -\left(\frac{2\pi^2+9}{9}\right)J\omega\omega_y + \left(\frac{8}{9}\right)J\omega\omega_x + Mgl \tag{6.52}$$

The following consideration is the same as represented above, and all comments are omitted.

$$T_{r.y} = T_y - \left(\frac{2\pi^2+8}{9}\right) J\omega\omega_y - (4\pi^2+17) J\omega\omega_y \left[1 - \frac{9Mgl}{(2\pi^2+9) J\omega\omega_y}\right] \tag{6.53}$$

$$\omega_y = \frac{9}{(38\pi^2+161) J\omega}\left[T_y + 9\left(\frac{4\pi^2+17}{2\pi^2+9}\right) Mgl\right] \tag{6.54}$$

$$J_x \frac{\mathrm{d}\omega_x}{\mathrm{d}t} = -8\left(\frac{4\pi^2+17}{38\pi^2+161}\right)\left[T_y + 9\left(\frac{4\pi^2+17}{2\pi^2+9}\right) Mgl\right] + \left(\frac{8}{9}\right) J\omega\omega_x \tag{6.55}$$

where the torque of the gyroscope weight (Eq. 6.52) is removed because the modified precession torque $T_{p.y}$ contains it, other components are as specified above.

6.3.1.1 Working Example

The gyroscope with one side support and horizontal location ($\gamma = 0°$) turns under the action of the two external torques T_y and T, which act around axes oy and ox, respectively. The value of the first torque T_y is half of the value of torque T (i.e. T_y=0.05 Wgl). The actions of the torques and motions are presented in Fig. 6.4. The technical data related to the gyroscope are presented in Table 6.1 and Fig. 6.2. The angular velocity of the sinning rotor is 10,000 rpm. All Eqs. (6.52)–(6.55) are modified because $\gamma = 0°$. Equation (6.55) expresses the gyroscope motion around axis ox. Substituting the initial data of the gyroscope (Table 6.1) into Eq. (6.55) for horizontal location of the gyroscope yields the following equation:

$$\begin{aligned} 3.38437 \times 10^{-4} \frac{\mathrm{d}\omega_x}{\mathrm{d}t} = &-8\left(\frac{4\pi^2+17}{38\pi^2+161}\right) \\ &\left[0.05 + 9 \times \left(\frac{4\pi^2+17}{2\pi^2+9}\right) \times 0.146 \times 9.81 \times 0.0355\right] \\ &+ \left(\frac{8}{9}\right) \times 0.5726674 \times 10^{-4} \times 10000 \times (2\pi/60)\omega_x \end{aligned} \tag{6.56}$$

Equation (6.56) is simplified and yields the following:

$$0.0119102458 \frac{\mathrm{d}\omega_x}{\mathrm{d}t} = -15.010400235 + \omega_x \tag{6.57}$$

The following solutions are similar as represented in Sect. 6.2.1. The results of the angular velocities of the gyroscope around axes ox and oy are as follows:

$$\omega_x = -15.010400235 \text{ rad/s} \tag{6.58}$$

$$\omega_y = -\frac{\omega_x}{4\pi^2 + 17} = -\frac{15.010400235}{4\pi^2 + 17} = -0.2657723228 \text{ rad/s} \tag{6.59}$$

The torque T_y acting around axis oy leads to slow counterclockwise rotation around axis oy and causes the intensive precessed clockwise rotation of the gyroscope around axis ox. The gyroscope moves upward from its horizontal location. This effect serves as practical evidence of the absence of the anti-gravity property. The obtained result of the gyroscope upward motion is the action of the inertial torques generated by the spinning rotor. The value of the load torque is limited by the value of the resulting resistance inertial torques that should not exceed the capacity of their kinetic energy. The surplus load torque leads to losing the ratio of the gyroscope angular velocities around axes that expresses their equality of the kinetic energies.

6.3.2 Case Study 2

The mathematical model for the gyroscope's motions is considered for the same gyroscope stand and technical parameters presented in case study 6.3.1. The difference is the clockwise action of the load torque T_y around axis oy. Under this condition, the actions of the gyroscope internal torques and motions are as follows:

- The load torque T_y generates the resistance torque T_{ry}, which acts in a counterclockwise direction around axis oy and the precession torque T_{py}, which acts around axis ox in a counterclockwise direction. This coincides with the action of the load torque T.
- The action of the torque produced by the gyroscope weight T generates the resistance T_{rx} and precession T_{px} torques. The resistance torque T_{rx} acts in a clockwise direction around axis ox. The precession torque T_{px} acts in a counterclockwise direction around axis oy as the torque T.

All acting torques and motions of the gyroscope with one side support are illustrated in Fig. 6.5.

For the simplification of the computation is accepted the horizontal location of the gyroscope ($\gamma = 0°$). The equations of the gyroscope torques and motions around axes ox and oy are represented by the following expressions:

$$J_y \frac{d\omega_y}{dt} = -T_y + T_{ct.y} + T_{cr.y} + T_{am.x}\eta \tag{6.60}$$

$$J_x \frac{d\omega_x}{dt} = T + T_{in.y} + T_{am.y} - T_{cr.x} \tag{6.61}$$

where the sign (−) indicates clockwise movement. All other components are as specified above.

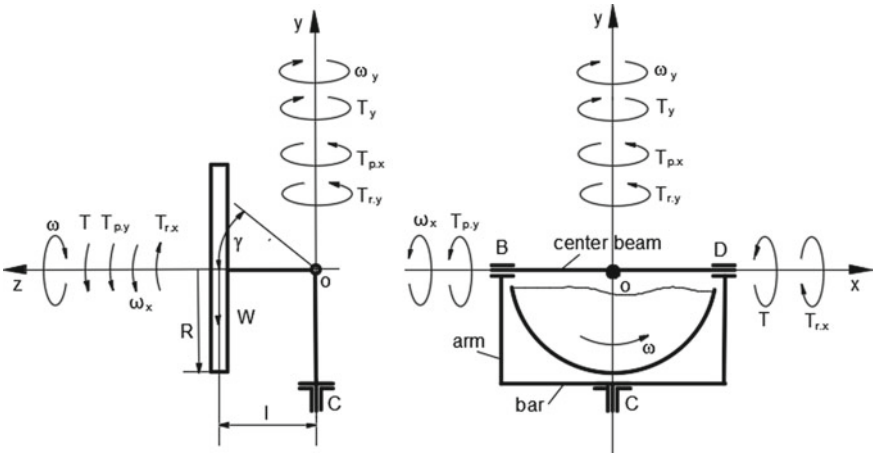

Fig. 6.5 Internal torques and motions when the load torque T_y acts in the clockwise direction around axis oy

The coefficient η represents the increase of the precession torque $T_{p.x}$ around axis oy. The coefficient η is expressed as the ratio of the sum of the precession $T_{p.y}$ and load T torques to the precession $T_{p.y}$ torque, which acts around axis ox. The expression η is obtained in a similar way as in Eq. (6.42) and is represented by the following equation:

$$\eta = \frac{T_{p.y} + T}{T_{p.y}} = 1 + \frac{T}{T_{p.y}} = \left[1 + \frac{Wgl}{\left(\frac{2\pi^2+9}{9}\right) J\omega\omega_y}\right] \tag{6.62}$$

where η is the coefficient of the increase of the value of the precession torque $T_{p.x}$ acting around axis oy. All other parameters are as specified above.

The coefficient η denotes the increase in precession torque $T_{p.x}$ around axis oy when the value of the resulting torque $T_{r.x}$ around axis ox also increases. Equation (6.52) demonstrates the following values of the coefficient η:

- The absence of the load torque T acting around axis ox means that the coefficient $\eta = 1.0$ (i.e. there is no change in the values of the inertial torques acting around two axes).
- The action of the load torque T means that the coefficient is $\eta > 1.0$ (i.e. the values of the inertial torques acting around two axes increase).
- When the load torque of the gyroscope weight is equal to the precession torque ($T = T_{p.y}$), the coefficient $\eta = 2$ (i.e. there is an increase in the value of the resulting resistance torque $T_{rtst.y}$ acting around axis oy.

Equation (6.62) are substituted into Eqs. (6.60) and (6.61) transformed in the same manner as Eqs. (6.51) and (6.52):

$$J_y \frac{d\omega_y}{dt} = -T_y + \left(\frac{2\pi^2 + 8}{9}\right) J\omega\omega_y + (4\pi^2 + 17) J\omega\omega_y \times \left[1 + \frac{Mgl}{\left(\frac{2\pi^2+9}{9}\right) J\omega\omega_y}\right] \tag{6.63}$$

$$J_x \frac{d\omega_x}{dt} = T + \left(\frac{2\pi^2 + 9}{9}\right) J\omega\omega_y - \frac{8}{9} J\omega\omega_x \tag{6.64}$$

Transformation of Eq. (6.64) yields the following equation:

$$T_{r.y} = -T_y + \left(\frac{2\pi^2 + 8}{9}\right) J\omega\omega_y + (4\pi^2 + 17) J\omega\omega_y \left[1 + \frac{9Mgl}{(2\pi^2 + 9) J\omega\omega_y}\right] \tag{6.65}$$

$$\omega_y = \frac{9}{(38\pi^2 + 161) J\omega} \left[T_y - 9\left(\frac{4\pi^2 + 17}{2\pi^2 + 9}\right) Mgl\right] \tag{6.66}$$

$$J_x \frac{d\omega_x}{dt} = 8\left(\frac{4\pi^2 + 17}{38\pi^2 + 161}\right) \left[T_y - 9\left(\frac{4\pi^2 + 17}{2\pi^2 + 9}\right) Mgl\right] - \left(\frac{8}{9}\right) J\omega\omega_x \tag{6.67}$$

where the torque of the gyroscope weight (Eq. 6.64) is removed because the modified precession torque $T_{p.y}$ contains it, other components are as specified above.

Equation (6.65) can be used for the direct computing of the angular velocity of the gyroscope motion down around axis *ox*.

6.3.2.1 Working Example

The motions of the gyroscope with one side support are conducted under the clockwise action of the load torque T_y around axis *oy*. The sketch of the action of the torques and motions is represented in Fig. 6.2. Equation (6.67) represents the gyroscope motion around axis *oy*. The angular velocities of precessions around two axes should be defined. Substituting the initial data of the gyroscope represented in Sect. 6.3.1.1 into Eq. (6.67) and making transformations yields the following equation:

$$3.38437 \times 10^{-4} \frac{\mathrm{d}\omega_x}{\mathrm{d}t} = 8\left(\frac{4\pi^2 + 17}{38\pi^2 + 161}\right) \left[0.05 - \frac{9(4\pi^2 + 17)}{2\pi^2 + 9} \times 0.146 \times 9.81 \times 0.0355\right] - \left(\frac{8}{9}\right) \times 0.5726674 \times 10^{-4} \times 10000 \times (2\pi/60)\omega_y \tag{6.68}$$

Equation (6.68) is simplified. Then, the steps of solutions similar to the steps presented in Sect. 6.3.1.1, and case study I is carried out. All comments related to the solutions of the equations are omitted.

$$6.348911602 \times 10^{-3} \frac{\mathrm{d}\omega_y}{\mathrm{d}t} = -14.792720132 - \omega_y \tag{6.69}$$

$$\omega_y = 14.792720132\,\text{rad/s} \tag{6.70}$$

$$\omega_y = -\frac{\omega_x}{4\pi^2 + 17} = -\frac{14.792720132}{4\pi^2 + 17} = -0.261918105\,\text{rad/s} \tag{6.71}$$

The torque T_y acting around axis oy leads to slow clockwise rotation around axis oy (the sign $(-)$ of Eq. (6.71)) and causes the intensive precessed counterclockwise rotation of the gyroscope around axis ox. The gyroscope moves downward from its horizontal location.

References

1. Armenise, M.N., Ciminelli, C., Dell'Olio, F., Passaro, V.M.N.: Advances in Gyroscope Technologies. Berlin and Heidelberg GmbH & Co. KG, Berlin, Springer-Verlag (2010)
2. Deimel, R.F.: Mechanics of the Gyroscope. Dover Publications Inc., New York (2003)
3. Greenhill, G.: Report on Gyroscopic Theory General Books LLC, London (2010)
4. Scarborough, J.B.: The Gyroscope Theory and Applications. Nabu Press, London (2011)
5. Hibbeler, R.C.: Engineering Mechanics—Statics and Dynamics, 12th edn. Prentice Hall, Pearson, Singapore (2010)
6. Gregory, D.R.: Classical Mechanics. Cambridge University Press, New York (2006)
7. Taylor, J.R.: Classical Mechanics. University Science Books, California, USA (2005)
8. Aardema, M.D.: Analytical Dynamics. Theory and Application. Academic/Plenum Publishers, New York (2005)
9. Jewett, J., Serway, R.A.: Physics for Scientists and Engineers, Cengage Learning, 10 ed. USA, Boston (2018)
10. Hayasaka, H., Tackeuchi, S.: Anomalous weight reduction on a gyroscope's right rotations around the vertical axis on the earth. Phys. Rev. Lett. **63**(25), 2701–2704 (1989)
11. Hayasaka, H.: Possibility for the existence of anti-gravity: evidence from a free-fall experiment using a spinning gyro. In: Speculations in Science and Technology, vol. 20, pp. 173–181 http://www.keelynet.com

12. Usubamatov, R.: Inertial forces acting on gyroscope. J. Mech. Sci. Technol. **32**(1), 101–108 (2018)
13. Usubamatov, R.: Mathematical model for motions of gyroscope suspended from flexible cord. Cogent Eng. **3**, 1245901 (2016)
14. Usubamatov, R.: Properties of gyroscope motion about one axis. Int. J. Adv. Mech. Aeronaut. Eng. **2**(1), 39–44 (2014)
15. Usubamatov, R.: Analysis of motions for gyroscope with one side support. Scholar J. Appl. Sci. Res. **1:3**(4), pp. 95–113 (2018)
16. Usubamatov, R.: Properties of gyroscope motion about one axis. In: 8th MUCET 2014, Date: 10–11 November 2014, Melaka, Malaysia
17. Usubamatov, R.: Physics of gyroscope motion about one axis. Int. J. Adv. Mech. Aeronaut. Eng. **2**(1) (2015), pp. 55–60. ISSN: 2372-4153
18. Usubamatov, R.: Physics of gyroscope's "anti-gravity effect". Math. Probl. Eng. Article ID 4197863 (2019)

Chapter 7
Mathematical Models for the Top Motions and Gyroscope Nutation

7.1 The Top Motions

A manifestation of gyroscopic effects depends on the type of gyroscopic devices and how they work at different conditions [1–4]. Fundamental principles of classical mechanics enable for describing and formulating physical parameters of any objects in motions [5–10]. The top represents the simplest gyroscopic device in which acting torques and motions researchers could not describe exactly for the long-time. The known publications about top motions represented by simplified mathematical models that not well-matched with practical tests and the physics of their motions represented indistinctly [11, 12]. The new mathematical models for the system inertial torques acting on of spinning objects enable for describing the top motions [13–19]. The typical design of tops is represented in Fig. 7.1. The external load torque, which presented by the action of the top weight, generates inertial resistance and precession torques acting around axes of the top. Observation of an inclined fast-spinning top demonstrates the spiral motion of its leg on the flat surface with following asymptotically motion to the vertical position of its axis. The spinning top stabilizes itself, and its spin axis preserves a vertical position until the minimal angular velocity that leads to the wobbling and then to side fall. This phenomenon of the top's motion is the result of the action of inertial torques generated by the spinning mass elements and the centre mass. The spiral motion of the top on the flat surface is the result of the action of the frictional force on the spherical surface of the tip of the top's leg. The mathematical models for the well-balanced top motions are considered by the interrelated action of the inertial torques (Table 3.1, Chap. 3).

The spiral motion of the top is being considered in terms of machine dynamics. The acting forces on the top are its weight, frictional force of the leg's tip at the point of contact the leg with the horizontal surface and the system of inertial forces mentioned above. The analysis of top motions is conducted using the example of a top that is tilted and spinning in a counterclockwise direction. The motion of the top spinning in a counterclockwise direction is considered around the point of support O that demonstrated in Fig. 7.2. If the axis of a top is adjusted on the angle γ to

© The Editor(s) (if applicable) and The Author(s), under exclusive license to Springer Nature Singapore Pte Ltd. 2020

R. Usubamatov, *Theory of Gyroscopic Effects for Rotating Objects*,
https://doi.org/10.1007/978-981-15-6475-8_7

Fig. 7.1 Typical designs of the tops

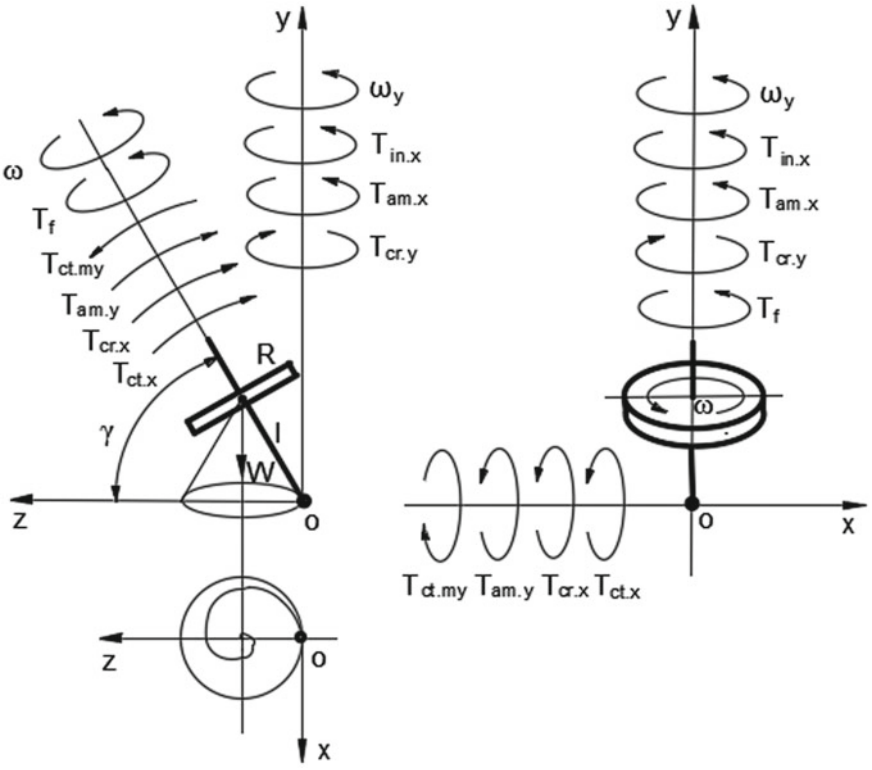

Fig. 7.2 Torques acting on a spinning top

the horizontal and released, then, under the action of the weight of the top, frictional force and inertial torques, the top's axis will begin to presses at about the vertical and horizontal. The frictional force acting on the tip of the leg starts to move the top around its gravity centre, and the top's axis describes a conical surface. The action of external and inertial torques leads to the decrease of the angular velocity of the top's spin. Hence, the values of inertial torques are decreasing gradually, while the precession velocities correspondingly increase. When the angular velocity of the top becomes smaller, the internal torques become weaker. In this case, the

tip of the top's leg describes a visible spiral curve with a decrease of its radius of curvature. This situation leads to the vertical approach of the top axis that manifests its stabilization. This situation leads to the vertical approach of the top's axle that manifests its stabilization.

The motion of a spinning top that inclined to a horizontal flat surface is complex. The equation of motion is formulated by the action of several forces and torques on the top that is as follows: the external torque generated by action of the weight of an inclined top; the torque generated by the centrifugal force of the rotating top's centre mass around axis *oy*; the external torque generated by the frictional force acting on the top's leg and around its axis. Other acting inertial torques are generated by the rotating masses mentioned above and represented in several publications (Table 3.1, Chap. 3). All forces and torques acting on the top are demonstrated in Fig. 7.2.

The parameters defined above allow for the formulation of a mathematical model for a top's motion around axes ox and oy in Euler's form. The torques acting on the top are similar to the torques acting on the gyroscope suspended from a flexible cord (Chap. 5). Both models consider the motion of the spinning disc with one side support. As such, the mathematical model for a top's motion is represented by the following system of equations:

$$J_x \frac{\mathrm{d}\omega_x}{\mathrm{d}t} = T + T_{\mathrm{ct.my}} - T_{\mathrm{ctx}} - T_{\mathrm{crx}} - T_{\mathrm{amy}}\eta \tag{7.1}$$

$$J_y \frac{\mathrm{d}\omega_y}{\mathrm{d}t} = (T_{\mathrm{inx}} + T_{\mathrm{amx}} - T_{\mathrm{cry}})\cos\,\gamma + T_f \tag{7.2}$$

$$\omega_y = \left(\frac{2\pi^2 + 8 + (2\pi^2 + 9)\cos\,\gamma}{2\pi^2 + 9 - (2\pi^2 + 8)\cos\,\gamma}\right)\omega_x \tag{7.3}$$

where $J_i = (MR^2/4) + ml^2$ is the top's mass moment of inertia around axis i [3]; M is the top's mass; is the external torque generated by action of the top weight; g is the gravity acceleration, l is the length of the leg; $F_{\mathrm{ct.mx}} = Ml\omega_x^2 \sin\gamma\cos\gamma$ is the force generated by the centrifugal force of the rotating top's centre mass around axis ox; $T_{\mathrm{f}} = Mgfl\cos\gamma$ is the torque generated by the frictional force acting on the tip and turns the top around its centre mass in the counterclockwise direction; f is the coefficient of the sliding friction between the leg and flat surfaces; $T_{\mathrm{ct\cdot my}} = F_{\mathrm{ct\cdot my}} l\sin\gamma = Ml\cos\gamma\omega_y^2 l\sin\gamma = Ml^2\cos\gamma\sin\gamma\omega_y^2$ is the torque generated by the centrifugal force of the rotating top's centre mass around axis *oy*; ω_y is the precession velocity of the top around axis *oy*; η is the coefficient of the change in the value of the inertial torques; other expressions are as specified above.

The mathematical model for the top motions considers the action of the frictional torque, centrifugal forces of the top centre mass, inertial forces generated by the mass elements of the disc and weight of the top. The rotation of the top is accepted in the counterclockwise direction around axes *oy* and *ox,* respectively. At this condition, the actions of the gyroscope external and internal torques and motions are demonstrated

in Fig. 7.2. The action of the frictional torque T_f turns the top around axis oy and added to the action of the precession torques ($T_{p.x} = T_{\text{in}.x} + T_{\text{am}.x}$) generated by the top's weight. The value of the precession torque $T_{\text{am}.y}$ acting around axis ox also decreases due to the interrelated the actions of the inertial and frictional torques around axes. This action is expressed by the coefficient η of the change in the precession torque $T_{\text{am}.y}$ that is presented by the following equation:

$$\eta = \frac{T_{p.x}\cos\gamma + T_f\cos\gamma}{T_{p.x}\cos\gamma} = 1 + \frac{9Mgf}{(2\pi^2+9)J\omega\omega_x} \tag{7.4}$$

where $T_{p,x}$ is the precession torques originated on axis ox but acting around axis oy and represented by the equation in Table 3.1, Chap. 3, and other components are as specified above.

The methodology towards a solution for Eqs. (7.1)–(7.2) by adding the ratio of the precession velocities of a top around axes (Eq. (7.3)) is represented in Chap. 5 and 6. Substituting Eq. (7.4) and inertial torques (Table 3.1) into Eq. (7.5) and simplification yield the following equation of the top's motion around axis ox:

$$\begin{aligned} J_x\frac{\mathrm{d}\omega_x}{\mathrm{d}t} &= Mgl\cos\gamma + Ml^2\cos\gamma\sin\gamma\omega_y^2 \\ &\quad -\left(\frac{2\pi^2+8}{9}\right)J\omega\omega_x - J\omega\omega_y\left[1+\frac{9Mgf}{(2\pi^2+9)J\omega\omega_x}\right] \end{aligned} \tag{7.5}$$

Substituting Eq. (7.3) into Eq. (7.6) and simplification yield the following equation of the top's motion around axis ox:

$$\begin{aligned} J_x\frac{\mathrm{d}\omega_x}{\mathrm{d}t} &= Mgl\cos\gamma + Ml^2\cos\gamma\sin\gamma\left[\left(\frac{2\pi^2+8+(2\pi^2+9)\cos\gamma}{2\pi^2+9-(2\pi^2+8)\cos\gamma}\right)\omega_x\right]^2 \\ &\quad -\left[\left(\frac{2\pi^2+8}{9}\right)+\left(\frac{2\pi^2+8+(2\pi^2+9)\cos\gamma}{2\pi^2+9-(2\pi^2+8)\cos\gamma}\right)\right]J\omega\omega_x \\ &\quad -\left(\frac{9}{2\pi^2+9}\right)\left(\frac{2\pi^2+8+(2\pi^2+9)\cos\gamma}{2\pi^2+9-(2\pi^2+8)\cos\gamma}\right)Mgf \end{aligned} \tag{7.6}$$

Separating variables and transformation of Eq. (7.6) gives the following equation:

$$\begin{aligned} &\frac{J_x\mathrm{d}\omega_x}{Mgl\cos\gamma + Ml^2\cos\gamma\sin\gamma\left[\left(\frac{2\pi^2+8+(2\pi^2+9)\cos\gamma}{2\pi^2+9-(2\pi^2+8)\cos\gamma}\right)\omega_x\right]^2} = \mathrm{d}t \\ &\quad -\left[\left(\frac{2\pi^2+8}{9}\right)+\left(\frac{2\pi^2+8+(2\pi^2+9)\cos\gamma}{2\pi^2+9-(2\pi^2+8)\cos\gamma}\right)\right]J\omega\omega_x \\ &\quad -\left(\frac{9}{2\pi^2+9}\right)\left(\frac{2\pi^2+8+(2\pi^2+9)\cos\gamma}{2\pi^2+9-(2\pi^2+8)\cos\gamma}\right)Mgf \end{aligned} \tag{7.7}$$

where all parameters are as specified above.

Self-stabilization. Observation of a fast-spinning top shows that it preserves the vertical position of the axis, remains steady on the supporting pivot and avoids tilting or falling to the ground. If the axis of a spinning top is inclined from the vertical axis under the action of an external torque, the axis starts to describe the vertical circular cone of the precessed motion. Then, the spinning top stabilizes itself, and its spin axis goes to a vertical position. A tilted, well-balanced spinning top with a high angular velocity proves its capacity for self-stabilization. The axis of the tilted spinning top goes to the vertical position by the action of the inertial torques generated by the rotating mass elements, in which values are bigger than torques generated by the top's weight and inertial torque generated by the centre mass. The necessary condition for a top's self-stabilization is formulated by separating variables of the torques produced by the centrifugal forces and the centre mass of the top and by the inertial torques generated by the rotating mass elements of the top. These two types of torques are represented on the right side of Eq. (7.7) and expressed by the following equation:

$$\begin{aligned} & Mgl\cos\gamma + Ml^2\cos\gamma\sin\gamma\left[\left(\frac{2\pi^2+8+(2\pi^2+9)\cos\gamma}{2\pi^2+9-(2\pi^2+8)\cos\gamma}\right)\omega_x\right]^2 \\ & = \left|\begin{array}{l} -\left[\left(\frac{2\pi^2+8}{9}\right)+\left(\frac{2\pi^2+8+(2\pi^2+9)\cos\gamma}{2\pi^2+9-(2\pi^2+8)\cos\gamma}\right)\right]J\omega\omega_x \\ -\left(\frac{9}{2\pi^2+9}\right)\left(\frac{2\pi^2+8+(2\pi^2+9)\cos\gamma}{2\pi^2+9-(2\pi^2+8)\cos\gamma}\right)Mgf \end{array}\right| \end{aligned} \tag{7.8}$$

Analysis of Eq. (7.8) shows the equilibrium of the acting torques depends on three main variable components, i.e. the angular velocity ω of the top, the velocity of precession ω_x, the angle γ of its inclination and the length of the top's leg. The stabilization process is intensive when the value of the inertial torques of the right side equation is big, and also, the length of the top's leg should be short, and, i.e. the centre mass of the top is located towards the tip of the leg. The spinning top with a long leg and a small radius of the disc manifests less stability. The top of high spinning velocity generates the high value of the inertial torques represented on the right side of Eq. (7.8). The border condition of the top motions is represented by the following:

- When the value of the resulting torque on the right side of Eq. (7.8) is bigger than the value of the resulting torques on the left side, this is a condition of the top self-stabilization. The running top starts to wobble when the speed of the top is always close to zero that reduces the value of the inertial torques of the mass elements and loose of its stability.
- When the value of the resulting torque on the right side of Eq. (7.8) is equal or less than the value of the resulting torques on the left side, this is a condition of the top turn down.

Equation (7.8) is transcendental. The conditions of self-stabilization and turn down of the running top are defined by graphical solutions of multiparametric Eq. (7.8).

7.1.1 Working Example

The example considers the motion of a disc-type top whose technical data are represented in Table 7.1. The centre mass of the top is located on the plane of the thin disc. The spinning top initially possesses an inclined axle and rotating around a vertical axis (Fig. 7.2).

Substituting initial data into Eq. (7.7) and transformation brings the following equation:

$$\frac{1.1125 \times 10^{-5} \mathrm{d}\omega_x}{0.02 \times 0.02^2 \cos 75^\circ \sin 75^\circ \left[\frac{2\pi^2+8+(2\pi^2+9)\cos 75^\circ}{2\pi^2+9-(2\pi^2+8)\cos 75^\circ}\right]^2 \omega_x^2} = \mathrm{d}t$$
$$-\left[\frac{2\pi^2+8}{9}+\frac{2\pi^2+8+(2\pi^2+9)\cos 75^\circ}{2\pi^2+9-(2\pi^2+8)\cos 75^\circ}\right] \times 0.625 \times 10^{-5} \times 1000 \times \frac{2\pi}{60}\omega_x$$
$$+0.02 \times 9.81 \times \left\{0.02\cos 75^\circ - \left(\frac{9}{2\pi^2+9}\right)\left[\frac{2\pi^2+8+(2\pi^2+9)\cos 75^\circ}{2\pi^2+9-(2\pi^2+8)\cos 75^\circ}\right] \times 0.1\right\} \tag{7.9}$$

Simplification of Eq. (7.10) and transformation yields the following solution:

$$\frac{\mathrm{d}\omega_x}{\omega_x^2 - 579.4358672398\omega_x - 1692.107224935} = 0.4785977324\,\mathrm{d}t \tag{7.10}$$

Table 7.1 Technical data of the top

Parameter	Data
Angular velocity, ω	1000 rpm
Radius of the disc, R	0.025 m
Length of the leg, l	0.02 m
Angle of tilt, γ	75.0°
Mass, M	0.02 kg
Coefficient of friction, f	0.1
Mass moment of inertia, kgm^2	
Around axis oz, $J = MR^2/2$	0.625×10^{-5}
Around axes ox and oy of the centre mass, $J = MR^2/4$	0.3125×10^{-5}
Around axes ox and oy, $J_x = J_y = MR^2/4 + Ml^2$	1.1125×10^{-5}

The denominator on the left side of Eq. (7.10) represents the quadratic equation with the following expression:

$$\frac{\mathrm{d}\omega_x}{(\omega_x + 2.9056954429)(\omega_x - 582.3415626827)} = 0.4785977324\,\mathrm{d}t \tag{7.11}$$

Equation (7.11) is converted into integral forms with definite limits that yields the following equation:

$$-\frac{1}{585.2472581256}\int_0^{\omega_x}\left(\frac{1}{\omega_x + 2.9056954429} - \frac{1}{\omega_x - 582.3415626827}\right)\mathrm{d}\omega_x$$
$$= 0.4785977324\int_0^t \mathrm{d}t \tag{7.12}$$

Integrals of Eq. (7.12) are tabulated and presented the integrals $\int \frac{\mathrm{d}x}{x \pm a} = \ln|a \pm x| + \mathrm{C}$ with the following solutions:

$$\ln(\omega_x + 2.9056954429)\Big|_0^{\omega_x} - \ln(\omega_x - 582.3415626827)\Big|_0^{\omega_x} = -280.098010632t\Big|_0^t$$

giving rise to the following:

$$\ln\left(\frac{\omega_x + 2.9056954429}{2.9056954429}\right) - \ln\left(\frac{\omega_x - 582.3415626827}{-582.3415626827}\right) = -280.0980106t \tag{7.13}$$

The next transformation of Eq. (7.13) yields the following result:

$$\omega_x + 2.9056954429 = -\mathrm{e}^{-280.0980106\,t} \times (\omega_x - 582.3415626827)/200.4138334957 \tag{7.14}$$

The right component of Eq. (7.14) has a small value of a high order that can be neglected. The solution of Eqs. (7.14) and (7.3) yields the following values of the precession angular velocities for the top around axes *ox* and *oy:*

$$\omega_x = -2.9056954429\,\mathrm{rad/s} \tag{7.15}$$

$$\omega_y = \left[\frac{2\pi^2 + 8 + (2\pi^2 + 9)\cos 75^\circ}{2\pi^2 + 9 - (2\pi^2 + 8)\cos 75^\circ}\right] \times 2.9056954429 = 4.741005101\,\mathrm{rad/s} \tag{7.16}$$

where the sign (−) for ω_x means the turn of the top axel in the clockwise direction towards the vertical location.

Self-stabilization. The presented data of a tilted spinning top allow the condition for its self-stabilization to be checked. Substituting the defined data above and from Table 7.1 into Eq. (7.8) yields the following result:

$$
\begin{aligned}
&0.02 \times 9.81 \times 0.02 \times \cos 75^\circ + 0.02 \times 0.02 \cos 75^\circ \sin\ 75^\circ \\
&\quad \times \left[\left[\frac{2\pi^2 + 8 + (2\pi^2 + 9)\cos 75^\circ}{2\pi^2 + 9 - (2\pi^2 + 8)\cos 75^\circ}\right](-2.9056954429)\right]^2 \\
&= \left[\frac{2\pi^2 + 8}{9} + \frac{2\pi^2 + 8 + (2\pi^2 + 9)\cos 75^\circ}{2\pi^2 + 9 - (2\pi^2 + 8)\cos 75^\circ}\right] \\
&\quad \times 0.625 \times 10^{-5} \times 1000 \times \frac{2\pi}{60} \times (-2.9056954429) \\
&\quad - \left(\frac{9}{2\pi^2 + 9}\right)\left[\frac{2\pi^2 + 8 + (2\pi^2 + 9)\cos 75^\circ}{2\pi^2 + 9 - (2\pi^2 + 8)\cos 75^\circ}\right] \times 0.02 \times 9.81 \times 0.1
\end{aligned}
\tag{7.17}
$$

Solution of Eq. (7.17) yields the following result:

$$0.003263318 < 0.018989562 \tag{7.18}$$

The right component of Eq. (7.17) is bigger than the left one. It means the system of interrelated inertial torques acting on the top turns up to vertical with the spiral motion on the horizontal surface. The inclined spinning top with given data (Table 7.1) will come to vertical. Equation (7.8) enables to define the other parameters for the top equilibrium, i.e. the top will have motions without self-stabilization. For example, it is defined the mass of the top that keeps the equilibrium of motion. For this case, the left side of Eq. (7.8) should be equal to the right side.

$$
\begin{aligned}
&M \times 9.81 \times 0.02 \times \cos 75^\circ + M \times 0.02 \times \cos 75^\circ \sin 75^\circ \\
&\quad \times \left[\left[\frac{2\pi^2 + 8 + (2\pi^2 + 9)\cos 75^\circ}{2\pi^2 + 9 - (2\pi^2 + 8)\cos 75^\circ}\right](-2.9056954429)\right]^2 \\
&\quad - \left(\frac{9}{2\pi^2 + 9}\right)\left[\frac{2\pi^2 + 8 + (2\pi^2 + 9)\cos 75^\circ}{2\pi^2 + 9 - (2\pi^2 + 8)\cos 75^\circ}\right] \times M \times 9.81 \times 0.1 \\
&= \left\{\frac{2\pi^2 + 8}{9} + \left[\frac{2\pi^2 + 8 + (2\pi^2 + 9)\cos 75^\circ}{2\pi^2 + 9 - (2\pi^2 + 8)\cos 75^\circ}\right]\right\} \\
&\quad \times 0.625 \times 10^{-5} \times 1000 \times \frac{2\pi}{60} \times (-2.9056954429)
\end{aligned}
\tag{7.19}
$$

Solution of Eq. (7.19) yields the following mass of the top:

$$M = 0.165213821\,\text{kg} \tag{7.20}$$

Similar method enables to define the length of the top leg, the angular velocity of the top and other parameters that can keep the top equilibrium. The obtained mathematical model for the top's motions enables for the describing physical principles of acting forces and the gyroscopic effect of the top for self-stabilization. The application of new mathematical models for the top's motions effectively demonstrates the principles of the top's properties. In that regard, this is also a good example of educational processes for engineering mechanics.

7.2 The Top Nutation

The well-balanced gyroscopic devices and a top with high angular velocities do not display the process of the nutation because they belong to the overdamped or critically damped systems according to the theory of vibration. A gyroscope with low angular velocity manifests the nutation and represents a simple damped system. However, the top can demonstrate the steady and unsteady nutation processes for different reasons. The nature of the top's steady nutation is represented if its centre mass is displaced from the axis of rotation and the imperfect surface geometry of the tip of the top leg, etc. The action of the displaced centre mass of the spinning top represents the continuing existence of a disturbing force that generates a forced oscillation.

The unsteady top's nutation is manifested in case of the shocking displacement of the centre mass generated by the short time action of an external force to the axis of a spinning top. The top receives the free oscillation of the periodic complex motion and reveals itself as fast shivering of the precessing axis. This phenomenon of the top nutation represents the fast and short time oscillations process with a small amplitude about its mean position. The reason for such short time nutation is the top's property for the self-stabilization descried above. The oscillations for a well-balanced top are subjects to asymptotically rapid decay. In most cases, the nutation of a well-balanced top is quickly damped by the action of inertial resistance forces and frictional forces on the bearing, leaving uniform precession. This makes it possible to neglect nutation in solving most engineering problems.

The nutation process is considered in terms of machine dynamics and vibration analysis. The acting forces on the top are its weight and the force generated by centrifugal forces of the displaced top centre mass, torques generated by the system of inertial torques of the rotating mass elements. The simulation of a free nutation process is represented by modelling it with a damping process and energy losses in the oscillation of a not so well-balanced spinning top. Vibration analysis often takes into account the energy losses using a single factor called the damping factor. The nutation model of the spinning top consists of a not so well-balanced mass and a damper that represents the action of the top weight and several internal torques. In the case of the free nutation process, the action of the single short time action torque on a spinning top represents one period of oscillation with a short time for a

single cycle. The damping resistance torques decay the action of one shock torque, resulting in the inclination of only the spinning top axis.

For a top that possesses an eccentric rotating mass, i.e. the centre mass is displaced on some small distance from the top axle, the nutation is a regular process. The centrifugal force of the offset mass is asymmetric, which causes an angular displacement of the top axle. The spinning top is constantly being displaced and moved by these asymmetric forces. The eccentric rotating mass of the top represents harmonic nutation, which means that the top is forced to nutate at the frequency of excitation. A plot using the nutation amplitude along one axis and the forcing frequency along the other axis is then described as a performance or response curve for the system. The eccentric rotation of the mass at about the top axis is modelled as a sinusoidal wave, as shown in Fig. 7.3. Here, the function $y = e\sin\alpha$ denotes the displacement of the eccentric mass that represents the excitation input, where e is the eccentricity of mass location. The frequency of this sine wave is also the frequency at which nutation occurs.

The analysis of gyroscope motions and nutation is conducted using the example of a tilted top on the angle γ to the horizontal that is not well-balanced. The analysis of the top motions is conducted for its rotation around the support point O in the counterclockwise direction. The top's leg has the sharpened tip, in which, frictional torque acting on the leg is neglected (Fig. 7.4). If the axis of a top is released, then the force of gravity should tilt its axis in the direction of the action of this force. As a result, the top axis will begin to precess at about the vertical and horizontal. The motions of the top are accompanied by a visually undetectable nutational process, which decays rapidly according to the action of the inertial torques. Because of the inertial resistance torques, the proper rotation of the top gradually slows down, while the precession velocities correspondingly increase. In the case of a slowly rotating top, the nutation is noticeable and manifests a substantial change in the pattern of the top axial movement. The end of the top axis can describe a clearly visible wavy or looped curve alternately departing from the vertical. In the case of a highly rotating top, the nutation can decrease and manifest the stabilization of the top axial movement. The top axis approaches the vertical.

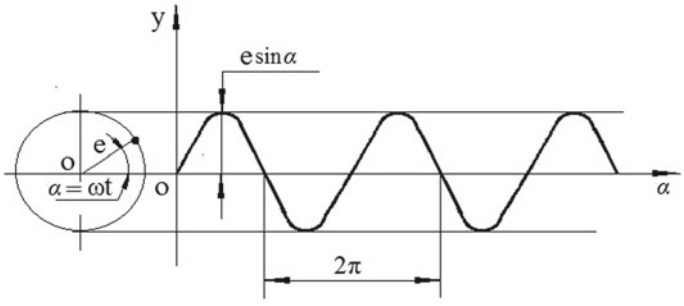

Fig. 7.3 Diagram of gyroscope eccentric rotation by a sinusoidal law

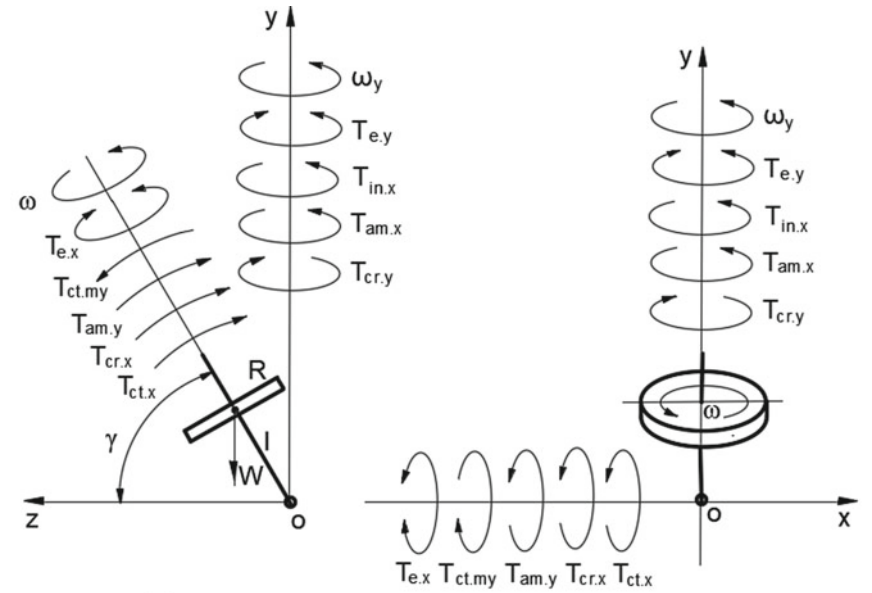

Fig. 7.4 Torques acting on a spinning top with eccentricity of mass

The motions of a not well-balanced spinning top are complex. The equation of nutation is formulated by the action of the system of inertial torques on the top generated by the action of external and internal forces. These forces represent the top weight, the centrifugal forces of eccentric mass and centre mass, and the centrifugal, common inertial forces and Coriolis forces generated by the rotating mass elements, and the change in the angular momentum. These forces are demonstrated in Fig. 7.4 and formulated by the equations represented in Table 3.1, Chap. 3.

The centrifugal force of the eccentric mass generates the variable torque represented by the following equation.

$$T_{ex} = Fl = Me\omega^2 l \sin\alpha \quad \text{by axis } ox \tag{7.21}$$

$$T_{ey} = Fl = Me\omega^2 l \cos\gamma \cos\alpha \quad \text{by axis } oy \tag{7.22}$$

where $F = Me\omega^2$ is the centrifugal force generated by the rotating eccentric mass M, l is the length of the top toy's leg, γ is the tilt angle of the top axis, α is the angle that is used for calculating the maximum magnitude, while T_{ex} and T_{ey} are the torques acting around axes ox and oy, respectively.

The weight W of a top generates torque, for which the equation is as follows: $T = Wl = Mgl\cos\gamma \cdot T_{\text{ct.my}}$ is the torque generated by the centrifugal force of the rotating top centre mass m around axis oy. Other acting inertial torques are presented in Table 3.1, Chap. 3. The data defined above allow for the formulation

of a mathematical model for a top motion around axes *ox* and *oy* in Euler's form. The torques acting on the top with eccentric mass are similar to the torques acting on the top represented in Sect. 7.1. Both models consider the top with one-sided support to be equal except for the added torque generated by the centrifugal force of the eccentric rotating mass. For simplicity, the motion of the top with eccentric mass does not consider the spiralled motion of its leg's tip. The torques acting on the not well-balanced top are presented in Fig. 7.4.

As such, the mathematical model for a top motion around axes *ox* and *oy* is represented by the following system of equations:

$$J_x \frac{\mathrm{d}\omega_x}{\mathrm{d}t} = T + T_{\mathrm{ct.my}} \pm T_{ex} - T_{ctx} - T_{\mathrm{crx}} - T_{\mathrm{amy}} \tag{7.23}$$

$$J_y \frac{\mathrm{d}\omega_y}{\mathrm{d}t} = (\pm T_{\mathrm{ey}} + T_{\mathrm{inx}} + T_{\mathrm{amx}} - T_{\mathrm{cry}}) \cos\,\gamma \tag{7.24}$$

where $J_i = (MR^2/4) + Ml^2$ is the top mass moment of inertia around axis *i*, while the sign (±) denotes (+) and (−) as the positive and negative directions of the action, respectively, for the torque generated by the eccentric mass.

The torques generated by the centrifugal forces of the rotating centre mass around axis *oy* is defined by the following equation:

$$T_{\mathrm{ct,my}} = F_{\mathrm{ct.my}} \times l \sin\gamma = Ml^2 \cos\gamma\, \sin\gamma\, \omega_y^2 \tag{7.25}$$

where $F_{\mathrm{ct.my}} = Ml\cos\omega_y^2$ is the centrifugal force of the top centre mass rotating around axis *oy*, and ω_y is the angular velocity of the top around axis *oy;* other components are as specified above.

The methodology towards a solution for Eqs. (7.23) and (7.24) by adding the ratio of the angular velocities of a gyroscope around axes $\omega_y = f(\omega_x)$ is presented in (Sect. 7.3.1). Substituting the defined parameters (Eqs. (7.23)–(7.25) and Table 7.1) into Eqs. (7.23) and (7.24) and transformation yield the equations of the top motions as follows:

$$J_x \frac{\mathrm{d}\omega_x}{\mathrm{d}t} = Mgl\cos\gamma + Ml^2 \sin\gamma\cos\gamma\omega_y^2 \pm Me\omega^2 l \sin\alpha - \left(\frac{2\pi^2+8}{9}\right) J\omega\omega_x - J\omega\omega_y \cos\gamma \tag{7.26}$$

$$J_y \frac{\mathrm{d}\omega_y}{\mathrm{d}t} = \left[\pm Me\omega^2 l\cos\alpha + \left(\frac{2\pi^2+9}{9}\right) J\omega\omega_x - \frac{8}{9} J\omega\omega_y\right] \cos\gamma \tag{7.27}$$

$$\omega_y = -\left[\frac{2\pi^2+8+(2\pi^2+9)\cos\gamma}{2\pi^2+9-(2\pi^2+8)\cos\gamma}\right]\omega_x \tag{7.28}$$

where all parameters are as specified above.

Solving of Eqs. (7.26)–(7.28) yields the maximum and minimum angular precessions ω_x and ω_y, which allow for defining the nutation amplitudes around axes ox and oy, respectively. Changes in the angular velocities of precessions around two axes make it possible to depict the trajectory of a top centre mass nutation. The mathematical model for the motions of a tilted top is derived from Eqs. (7.26)–(7.28). Substituting the expression ω_y from Eq. (7.5) into Eq. (7.26) and transformation yield the following equation:

$$J_x \frac{d\omega_x}{dt} = Mgl\cos\gamma + Ml^2 \tan\gamma \times \left[\frac{2\pi^2 + 8 + (2\pi^2 + 9)\cos\gamma}{2\pi^2 + 9 - (2\pi^2 + 8)\cos\gamma}\right]^2 \times \omega_x^2 \pm Me\omega^2 l \sin\alpha - \left\{\frac{2\pi^2 + 8}{9} + \left[\frac{2\pi^2 + 8 + (2\pi^2 + 9)\cos\gamma}{2\pi^2 + 9 - (2\pi^2 + 8)\cos\gamma}\right]\right\} J\omega\omega_x \tag{7.29}$$

where all parameters are as specified above.

7.2.1 Working Example

The example considers the nutation process of a disc-type top whose data are represented in Table 7.2. The centre mass of the top is located at the plane of the disc (Fig. 7.4). The top initially possesses a displaced mass, while spinning around a vertical axis is conducted with nutation. The top moves around axis oy without the action of the frictional force on the support.

The torque generated by the top weight W is as follows:

Table 7.2 Technical data of a top

Parameter	Data
Angular velocity, ω	1000 rpm
Radius of the disc, R	0.025 m
Length of the leg, l	0.02 m
Eccentricity of the centre mass, e	0.001 m
Angle of tilt, γ	75.0°
Mass, M	0.02 kg
Mass moment of inertia, kgm²	
Around axis oz, $J = mR^2/2$	0.625×10^{-5}
Around axes ox and oy of the centre mass, $J = mR^2/4$	0.3125×10^{-5}
Around axes ox and oy at the point of support, $J_x = J_y = mR^2/4 + ml^2$	1.1125×10^{-5}

$$T = Mgl\cos\gamma = 0.02 \times 9.81 \times 0.02 \times \cos 75.0^\circ = 1.015605932 \times 10^{-3}\,\mathrm{N\,m} \tag{7.30}$$

The torque generated by the centrifugal force of the top centre mass rotation around axis oy is as follows:

$$\begin{aligned} T_{ct.my} &= M^2 l\cos\gamma\sin\gamma\omega_y^2 \\ &= 0.02 \times 0.02^2 \times \cos 75^\circ \times \sin 75^\circ \times \left[\frac{2\pi^2 + 8 + (2\pi^2 + 9)\cos 75^\circ}{2\pi^2 + 9 - (2\pi^2 + 8)\cos 75^\circ}\right]^2 \times \omega_x^2 \\ &= 5.324399773 \times 10^{-6} \times \omega_x^2\,\mathrm{N\,m} \end{aligned} \tag{7.31}$$

The value $T_{ct.my}$ is small of high order and can be neglected.

The maximal torque generated by the centrifugal forces of the eccentric rotating centre mass around axis ox is as follows:

$$\begin{aligned} T_{ex} &= \pm Me\omega^2 l\sin\alpha = \pm 0.02 \times 0.001 \times (1000 \times 2\pi/60)^2 \times 0.02 \times \sin 90.0^\circ \\ &= \pm 4.3864908449 \times 10^{-3}\,\mathrm{N\,m} \end{aligned} \tag{7.32}$$

where all parameters are as specified above.

Substituting the defined parameters (Table 7.2, Eqs. (7.30), (7.31)) into Eq. (7.29) and then transformation yield the following differential equation:

$$\begin{aligned} 1.1125 \times 10^{-5}\frac{\mathrm{d}\omega_x}{\mathrm{d}t} &= 1.015605932 \times 10^{-3} \pm 4.3864908449 \times 10^{-3} \\ &\quad - \left[\frac{2\pi^2 + 8}{9} + \frac{2\pi^2 + 8 + (2\pi^2 + 9)\cos 75^\circ}{2\pi^2 + 9 - (2\pi^2 + 8)\cos 75^\circ}\right] \\ &\quad \times 0.625 \times 10^{-5} \times 1000 \times 2\pi/60 \times \omega_x \end{aligned} \tag{7.33}$$

After simplification and transformation of Eq. (7.33) yield the following equation:

$$0.00360598\frac{\mathrm{d}\omega_x}{\mathrm{d}t} = 0.329191943 \pm 1.421808793 - \omega_x \tag{7.34}$$

Separating variables and transformation for the differential Eq. (7.34) and presenting by the integral form with defined limits give the following expression:

$$\int_0^{\omega_x} \frac{\mathrm{d}\omega_x}{\omega_x - 0.329191943 \pm 1.421808793} = -277.316692488 \int_0^{\mathrm{t}} \mathrm{d}t \tag{7.35}$$

The left integral of Eq. (7.35) is tabulated and presented the integral $\int \frac{\mathrm{dx}}{x-a} = \ln|a-x| + \mathrm{C}$. The integrals have the following solution:

$$\begin{aligned} &\ln(\omega_x - 0.329191943 \pm 1.421808793)\big|_0^{\omega_x} \\ &\quad - \ln(-0.329191943 \pm 1.421808793)\big|_0^{\omega_x} \\ &= -277.316692488t\big|_0^t \end{aligned}$$

giving rise to the following:

$$\ln\left(\frac{\omega_x - 0.329191943 \pm 1.421808793}{-0.329191943 \pm 1.421808793}\right) = -277.316692488\,t \tag{7.36}$$

The next transformation yields the following result:

$$\omega_x - 0.329191943 \pm 1.421808793 = (-0.329191943 \pm 1.421808793)\mathrm{e}^{-277.316692488\,t} \tag{7.37}$$

The right component of Eq. (7.37) has the small value of a high order that can be neglected.

$$\omega_x = 0.329191943 \pm 1.421808793 \tag{7.38}$$

Solving of Eq. (7.38) gives the maximal and minimal value of the precession angular velocity for the top around axis *ox:*

$$\omega_{x.\max} = +1.751000736 \text{ rad/s} \tag{7.39}$$

$$\omega_{x.\min} = -1.09261685 \text{ rad/s} \tag{7.40}$$

where the signs (+) and (−) represent motion in a counterclockwise and clockwise direction, respectively.

Equation (7.38) enables the angular velocity of a well-balanced top toy precession around axes *ox* and *oy* to be defined, as represented by the following results:

$$\omega_x = 0.329191943 \text{ rad/s} \tag{7.41}$$

$$\omega_y = \left[\frac{2\pi^2 + 8 + (2\pi^2 + 9)\cos 75^\circ}{2\pi^2 + 9 - (2\pi^2 + 8)\cos 75^\circ}\right] \times 0.329191943 = 0.537117778 \text{ rad/s} \tag{7.42}$$

The precession's linear velocities of a balanced top centre mass around axes ox and oy have the following values:

$$V_x = \omega_x l \cos\gamma = 0.329191943(\text{rad/s}) \times 20\,\text{mm} \times \cos 75.0^\circ = 1.7040228868\ \text{mm/s} \tag{7.43}$$

$$V_y = \omega_y l \cos\gamma = 0.537117778\ (\text{rad/s}) \times 20\,\text{mm} \times \cos 75.0^\circ = 2.780326210\ \text{mm/s} \tag{7.44}$$

The time spent on a half oscillation is as follows:

$$t = \frac{\pi}{n} = \frac{\pi}{2000 \times 2\pi/60} = 0.015\,\text{s} \tag{7.45}$$

The distance of precessed motion for the centre mass of a balanced top per nutation of half oscillation time is as follows:

$$a_x = \mathrm{V}_y t = 2.780326210 \times 0.015 = 0.04170489\,\text{mm} \tag{7.46}$$

The maximal and minimal values of the linear velocity of the top centre mass around axis ox have the following values:

$$V_{x\,\max} = \omega_{x\,\max} l = 1.751000736(\text{rad/s}) \times 20\,\text{mm} \times \cos 75^\circ = 9.063844822\ \text{mm/s} \tag{7.47}$$

$$V_{x\,\min} = \omega_{x\,\min} l = -1.09261685(\text{rad/s}) \times 20\,\text{mm} \times \cos 75^\circ = -5.655800995\ \text{mm/s} \tag{7.48}$$

The maximal and minimal value of the amplitudes of centre mass nutation around axis ox as well as the location of a balanced top are as follows:

$$a_y\,\max = \mathrm{V}_{x\,\max} t = 9.063844822(\text{mm}/s) \times 0.015\,s = 0.135957672\ \text{mm} \tag{7.49}$$

$$a_y\,\min = V_{x\,\min} t = -5.655800995(\text{mm/s}) \times 0.015\,\text{s} = -0.084837014\ \text{mm} \tag{7.50}$$

$$a_y = V_x t = 1.7040228868(\text{mm/s}) \times 0.015\,\text{s} = 0.02556034\ \text{mm} \tag{7.51}$$

The total amplitude of oscillation around axis ox is as follows:

$$a_y = a_y\,\max + \left|a_y\,\min\right| = 0.135957672 + 0.084837014 = 0.220794686\ \text{mm} \tag{7.52}$$

The maximal and minimal values of the angular velocity for top precession around axis oy are defined by Eq. (7.5). Substituting the parameters defined above (Eq. (7.40)

and (7.41)) and from Table 7.2 into Eq. (7.43) and then transformation yield the following results:

$$\omega_{y.}\max = \left[\frac{2\pi^2 + 8 + (2\pi^2 + 9)\cos 75^\circ}{2\pi^2 + 9 - (2\pi^2 + 8)\cos 75^\circ}\right] \times 1.751000736 = 2.856976439\,\text{rad/s} \tag{7.53}$$

$$\omega_{y.}\min = \left[\frac{2\pi^2 + 8 + (2\pi^2 + 9)\cos 75^\circ}{2\pi^2 + 9 - (2\pi^2 + 8)\cos 75^\circ}\right] \times (-1.09261685) = -1.782740882\,\text{rad/s} \tag{7.54}$$

The maximal and minimal values of the linear velocities of the top centre mass around axis *oy* indicate the following values:

$$\begin{aligned} V_{y\max} &= \omega_{y\max} l\cos\gamma = 2.856976439(\text{rad/s}) \times 20\text{mm} \times \cos 75.0^\circ \\ &= 14.788798276\ \text{mm/s} \end{aligned} \tag{7.55}$$

$$\begin{aligned} V_{y\min} &= \omega_{y\min} l\cos\gamma = 1.782740882(\text{rad/s}) \times 20\text{mm} \times \cos 75.0^\circ \\ &= -9.228145859\ \text{mm/s} \end{aligned} \tag{7.56}$$

The maximal and minimal values of the amplitudes of the centre mass nutation around *oy* as well as the location of a balanced top (Eq. (7.44)) are as follows:

$$a_x\max = V_y\max t = 14.788798276(\text{mm/s}) \times 0.015\,\text{s} = 0.22183197\ \text{mm} \tag{7.57}$$

$$a_x\min = V_y\min t = -9.228145859(\text{mm/s}) \times 0.015\,\text{s} = -0.138422187\ \text{mm} \tag{7.58}$$

The total amplitude of oscillation around axis *oy* is as follows:

$$a_{xt} = a_x\max + |a_x\min| = 0.22183197 + 0.138422187 = 0.360254157\,\text{mm} \tag{7.59}$$

The positive and negative values of the angular velocities around axes *ox* and *oy* (Eqs. (7.41), (7.53) and (7.54)), respectively, mean the rotation in counterclockwise and clockwise directions. Hence, the linear motions of the top centre mass will be in negative and positive directions along the axes. This situation is expressed in the diagrams of nutation amplitudes. This diagram of the top nutation loop is represented in Fig. 7.5 and contains two coordinate systems. The system with asterisks is accepted for the motions of a balanced top. Figure 7.5 demonstrates that the actual loop of amplitudes for top centre mass has stretched down along the axis *oy*. This is a natural result because any action of the centrifugal force in the direction of the action of the top weight increases the amplitude. Any action in the opposite direction decreases the amplitude of nutation.

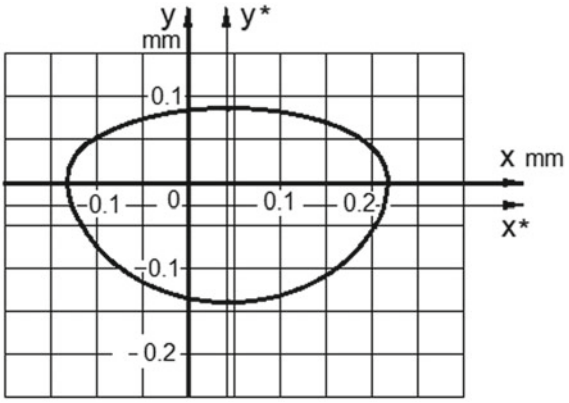

Fig. 7.5 Nutation's amplitudes of a top centre mass

The values of precessed motion's distance (Eq. (7.46)) and the amplitudes of oscillations around axes *ox* (Eq. (7.58)) and *oy* (Eq. (7.50)) make it possible for diagrams of top nutation to be depicted. The distance of the centre mass motion along axis *ox* is less than the minimal value of the amplitude. It means that the deployed diagram of top nutation has loops of oscillated motions. The following represents the half cyclic nutation of the top along the axis *ox*:

$$a_{xc.}\max = a_x + a_{x.}\max = 0.04170489 + 0.22183197 = 0.26353686 \text{ mm} \quad (7.60)$$

$$a_{xc.}\min = a_x - a_{x.}\min = 0.04170489 - 0.138422187 = -0.096717297 \text{ mm} \quad (7.61)$$

Deployed diagram of top nutation is illustrated in Fig. 7.6.

The deployed diagram of top nutation can be without loops if the positive amplitude of oscillation along axis *ox* is bigger than the distance of top motion for the

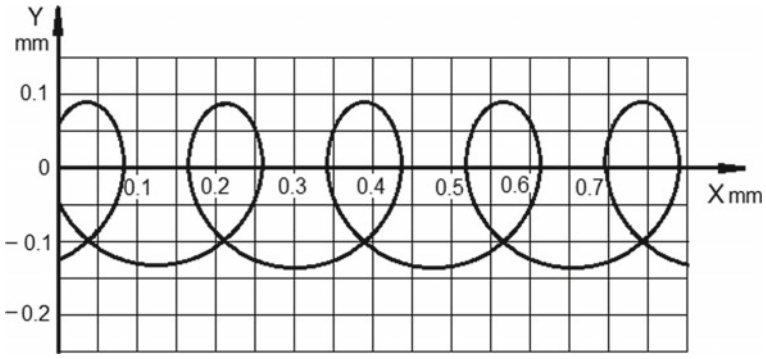

Fig. 7.6 Deployed diagram of top nutation

same precessing time. Equations of top motions with the given and calculated data of nutation parameters demonstrate that the amplitude and frequency of nutation are cyclic. The cycles are different because the centrifugal force of top eccentric centre mass acts at the first semicircle of rotation in the direction of precessed motions and at the second semicircle in a direction opposite to the precessed motions. The result of this example demonstrates the axis of a spinning top precesses with a rapid tremor of small amplitude. For the top with a big, eccentric, rotating centre mass, the tremor can be visible; however, for small eccentrics, this can hardly be noticeable to the naked eye. The presented diagram of top nutation demonstrates a short time of the process of top motion with precessing around axis oy (Fig. 7.6). Practically, the inclined top motion is going with self-stabilization, and the top axis comes to the vertical position. The resistance torque of top inertial forces acting around axis ox turns up the top to the vertical position. However, the rotation of the top at a vertical position occurs with a nutation described above. The conducted analysis and computing a data of the top nutation under the action of the system of external and inertial torques describe the physics of this process [20].

7.3 The Gyroscope Nutation

Fundamental principles of classical mechanics enable for describing and formulating physical parameters of any rotating objects [5–10]. The gyroscope nutation was a mostly unsolved problem in engineering mechanics. This section considers the gyroscope nutation that solved by the new mathematical models for the system of the interrelated inertial torques and principles of potential and kinetic energy conservation law [16–19]. The gyroscope nutation is represented in terms of machine dynamics and vibration analysis. The process of nutation of a gyroscope should be analytically described in detail by principles of conservation of potential, kinetic energies and work of a force. The gyroscope nutation is considered as the object of the classical viscous damped vibration with the constant action of the damping forces. Nevertheless, the peculiarities of acting inertial torques demonstrate the following differences in the gyroscope nutation:

– The equations of the inertial torques contain the product of $\omega\omega_{x,}$ which is constant and expresses the total (kinetic, potential and work of forces) energy of the spinning rotor (Table 3.1, Chap. 3). The increase of the angular velocity ω of the rotor leads to the decrease in the angular velocity ω_x of the gyroscope precession and the decrease of ability for the gyroscope nutation and vice versa.
– The angular velocity ω_x depends on the stand centre mass M and ω. Their variations and the relationship demonstrate the amplitude of the gyroscope nutation. The big value of ω_x leads to the big amplitude of the gyroscope nutation, and the small value of ω_x leads to the overdamped condition. The effect of overdamping is strong. After the action of the single input torques, the gyroscope system does

not return to its original position. The gyroscope nutation does not have a critically damped condition. Its nutation with the action of the frictional forces is dynamically irreversible and presents a monotonically damping process.
– The action of the gyroscopic inertial torques at the process of nutation is variable, and hence, the nutation is variable.
– The inertial torques of the spinning rotor do not possess the property of the spring's torque and do not have the index of torsional stiffness or the spring constant that described in the theory of the vibration.
– Practice demonstrates the blocking of the gyroscope motion around one axis and its high angular velocity ω_x leads to the partial deactivation of the inertial torques generated by the rotating mass element. The ratio of the angular velocities of a gyroscope around axes (Eq. 4.9, Chap. 4) is not maintained. The physics of this phenomenon is not described. For the small value of the spinning of the rotor, the gyroscope nutation is implemented around two axes of rotation.

This peculiarity represents the specific properties of the action of the inertial torques, and the gyroscope damped nutation is described by the terms that differ from the known classical theory for the viscously damped vibration [7, 8].

The nutation process of the gyroscope has been studied on the stand of Super Precision Gyroscope, "Brightfusion LTD". The test stand with the gyroscope is demonstrated in Figs. 6.1 and 6.2, in which the technical data of the test stand are presented in Table 6.1 of Chap. 6. The gyroscope tests conducted for conditions of the gyroscope turn around axis ox on the centre beam. The test's aim is to demonstrate and validate the mathematical model for the gyroscope motion under the action of the external and inertial torques. Recorded results are represented in the form of the gyroscope time motions and the magnitude of forces acting on the gyroscope.

The mathematical models for acting torques on the gyroscope stand and motions around two axes are processed and the same as for the gyroscope motion with one side support (Chaps. 5 and 6). The mathematical models for the gyroscope nutation with the action of the load, inertial and frictional forces are represented by the cumbersome expressions for the damping process. The computing process of such cumbersome models is tedious, and the physics of the gyroscope nutation is considered by the action of only inertial forces and the gyroscope weight. This condition and the absence of the frictional forces represent the undamped gyroscope nutation.

The analysis of the gyroscope nutation is implemented on a base of the acting torques and their mathematical models. The mathematical model of the gyroscope nutation deals with the quantification of the amount of its potential and kinetic energies that express a function tending to the change between extremes. The acting forces and torques on the gyroscope stand are represented by the following components. The weight of the gyroscope components produces the external torque in which expression is as follows:

$$T = Mgl_m \cos\gamma \tag{7.62}$$

where W is the gyroscope mass; g is the gravity acceleration; l is the distance of location the centre gravity of the gyroscope.

The nutation process considers the short time action of the single impact torque around axis ox that leads to the deactivation of some inertial torques. Such condition leads to the change in the balance of its potential and kinetic energies and the change in the values and direction of inertial torques and the angular velocities around axes. The action of the single input torque increases the angular velocity and the value of the resulting resistance inertial torques of the gyroscope. This peculiarity of the gyroscope nutation process considers the several steps of its motions. The starting condition for the short time action of the single input torque on the gyroscope is considered for its horizontal position. The action of the extra input torque leads to the increasing of ω_x of the inertial resistance torques and their kinetic energy, and the gyroscope turns back. The action of inertial torques, the change in the potential and kinetic energies and the gyroscope motions are considered by consistent steps of the change in their values and directions around axes. Such analysis enables for demonstrating the changes in the nutation.

The kinetic energy action of the single input torque on the gyroscope is converted into its potential energy of the location. At the process of the gyroscope nutation, the potential energy is converted into kinetic energy stored in the rotational gyroscope that is described by the moment of inertia J_x, mass M, the angular and linear velocities ω_x and $v = \omega_x l_{m,}$ respectively. The parameters of the gyroscope nutation are depended on the time of action of external and inertial torques and the steps of consideration. The motions up and down of the gyroscope nutation are represented by four mathematical models, in which conditions are described at sections below. The motion from low to the upper position is presented by two equations, in which conditions are defined at sections a_1 and a_2. The motion from the upper point to the down position is also presented by two equations that described at sections b_1 and $b_{2.}$ Following gyroscope motions from low to upper position and back are repeated.

Practice demonstrates the following peculiarities of the gyroscope motions. The short time action of the external torque deactivates the ratio of the angular velocities of the gyroscope around axes due to the high inertia of the system. The following fast motion of a gyroscope around axis ox does not demonstrate the oscillation around axis oy because the action of the precessed torques is opposite direction around axis oy. The action of the inertial masses does not maintain the ratio of the gyroscope angular velocities. For the motion down, the action of the precession torques does not contradict to gyroscope motion. The ratio of the gyroscope angular velocities is maintained. For the low speed of motions, the gyroscope manifests an oscillation around two axes. The action of the inertial torques generated by the spinning rotor on the gyroscope is variable and considered with the action of the gyroscope mass by the principle of energy conservation. The following steps of the gyroscope nutation are described by the detailed analysis of the action of its inertia torque and mass. The gyroscope nutation is considered for the two parts, namely the turn-up and down.

($a_{1.}$) The first phase of the action of inertial torque is started by removing the short time action of the input torque. The gyroscope locates at the angle $\gamma_{l.1.}$ The surplus

inertial resistance torques $T_{r.x}$ of the gyroscope activate around axis ox in the clockwise direction, and the action of the gyroscope weight T is in the counterclockwise direction. The precession torque $T_{p.y}$ is absent because the gyroscope does not turn around axis oy. The value of the surplus resulting resistance torques $T_{r.x}$ is decreased to zero ($T_{r.x} = 0$) at some angular position of $\gamma_{e.1}$. The gyroscope passes the angle of $\gamma_{e.1}$ under the action of the kinetic energy of the gyroscope centre mass.

($a_{2.}$) The second phase describes the action of the resistance torque $T_{r.x}$ in which direction is changed in the counterclockwise and added to the action of the precession torque $T_{p.y}$. The action of the excess kinetic energy of the gyroscope centre mass continues to turn up the gyroscope in the clockwise direction and to change the value of the inertial resistance torques, which act in the counterclockwise direction. The actions of the resulting mass of the gyroscope, inertial resistance torques $T_{r.x}$, the precession torque $T_{p.y}$ decrease the kinetic energy of the gyroscope mass that manifest the damping of the gyroscope motion. The gyroscope stops at an upper position γ_u with the high potential energies of the gyroscope mass and the resistance inertial torque $T_{r.x}$ precession torques $T_{p.y}$ that act in the counterclockwise direction.

($b_{1.}$) From the upper point of location γ_u, gyroscope turns down. At this condition, the gyroscope motion is represented by two phases. The first one describes the action of the gyroscope weight, resulting in resistance torques $T_{r.x}$ that acting in the counterclockwise direction, and the precession torque $T_{p.y}$ that act in the clockwise direction. The action of $T_{p.y}$ torques continues until the angular position $\gamma_{e.2}$ where the value of the $T_{r.x}$ is decreased to zero.

($b_{2.}$) The second phase describes the action of all components of the gyroscope after passing the angle $\gamma_{e.2}$. At this condition, the action of the inertial resistance torques $T_{r.x}$ is changed in the clockwise direction and added to the action of the precession torques $T_{p.y.}$ The action of the excess kinetic energy of the gyroscope mass continues to turn down the gyroscope in the counterclockwise direction and to change in the value of the inertial resistance torques $T_{r.x}$. The gyroscope stops at a low position $\gamma_{l.2}$ with the minimal potential energy and the high value of inertial resistance torques $T_{r.x}$ and precession torques $T_{p.y}$ that act in the clockwise direction.

The gyroscope starts to turn up under the action of surplus resistance inertial torques around axis ox in the clockwise direction. The following actions of external and internal torques are the same as described in sections ($a_{1,}$ a_2) and (b_1, b_2). The gyroscope nutation is repeated with the continuous action of changeable inertial torques. The action of the external and internal torques on the gyroscope for the conditions described above is presented in Fig. 7.7.

The gyroscope motions are presented by the corresponding equations that are described in several publications [13, 14]. The equations for stages (a_1, a_2 and b_1, b_2) of the gyroscope nutation are presented below.

(a_1) The equation for the gyroscope motion from the low position to the angle where the resistance torque resets to zero ($T_{r.x} = 0$) is as follows (Chaps. 5 and 6):

$$J_x \frac{d\omega_x}{dt} = Mgl_m \cos\gamma - \left(\frac{2\pi^2 + 8}{9}\right) J\omega\omega_x + \left(\frac{2\pi^2 + 9}{9}\right) J\omega\omega_y \qquad (7.63)$$

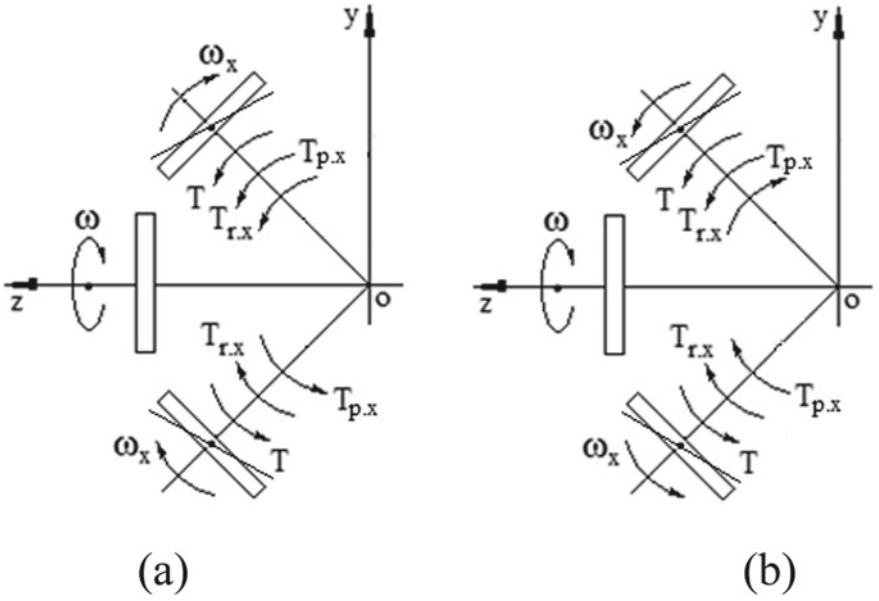

Fig. 7.7 Torques and angular velocities of the gyroscope motions around axis *ox* in clockwise (**a**) and counterclockwise (**b**) directions

$$J_y \frac{\mathrm{d}\omega_y}{\mathrm{d}t} = -\left(\frac{2\pi^2+9}{9}\right) J\omega\omega_x \cos\,\gamma + \left(\frac{2\pi^2+8}{9}\right) J\omega\omega_y \cos\,\gamma \tag{7.64}$$

where all parameters are as specified above.

Inertial torques action around axes *ox* and *oy* express their kinetic energies that are equal and presented by the following equation:

$$\begin{aligned} &-\left(\frac{2\pi^2+8}{9}\right) J\omega\omega_x + \left(\frac{2\pi^2+9}{9}\right) J\omega\omega_y \\ &= -\left(\frac{2\pi^2+9}{9}\right) J\omega\omega_x \cos\gamma + \left(\frac{2\pi^2+8}{9}\right) J\omega\omega_y \cos\gamma \end{aligned} \tag{7.65}$$

in which simplification yields the following expression:

$$\omega_y = \left[\frac{(2\pi^2+9)\cos\gamma - (2\pi^2+8)}{(2\pi^2+8)\cos\gamma - (2\pi^2+9)}\right]\omega_x \tag{7.66}$$

Substituting ω_y (Eq. (7.65) into Eq. (7.63) simplification and transformations [18] yield the following:

$$J_x \frac{d\omega_x}{dt} = Mgl_m \cos\gamma - \left[\frac{2\pi^2+8}{9} - \frac{(2\pi^2+9)\cos\gamma - (2\pi^2+8)}{(2\pi^2+8)\cos\gamma - (2\pi^2+9)}\right] J\omega\omega_x \tag{7.67}$$

The mathematical models for the motion of the gyroscope after the action of the short time impulse torque should be considered for the two cases. The first model describes the gyroscope motion with the low angular velocity of the spinning rotor (Eq. (7.67)). The second model describes the gyroscope motion with the high angular velocity of the spinning rotor. The impulse torque of the short time action deactivates the ratio of the angular velocities of the gyroscope around two axes. At this condition, the gyroscope motion is described by the known equations of classical mechanics.

(a_2) The equation for the gyroscope motion up from the angle of the reset to zero of the resistance torque ($T_{r.x} = 0$) to the upper position is as follows:

$$J_x \frac{d\omega_x}{dt} = Mgl_m \cos\gamma + \left(\frac{2\pi^2+8}{9}\right) J\omega\omega_x + \left(\frac{2\pi^2+9}{9}\right) J\omega\omega_y \tag{7.68}$$

$$J_y \frac{d\omega_y}{dt} = -\left(\frac{2\pi^2+9}{9}\right) J\omega\omega_x \cos\gamma + \left(\frac{2\pi^2+8}{9}\right) J\omega\omega_y \cos\gamma \tag{7.69}$$

Following steps of the analysis are the same as presented in the section (a_1), and all comments are omitted.

$$\left(\frac{2\pi^2+8}{9}\right) J\omega\omega_x + \left(\frac{2\pi^2+9}{9}\right) J\omega\omega_y = -\left(\frac{2\pi^2+9}{9}\right) J\omega\omega_x \cos\gamma + \left(\frac{2\pi^2+8}{9}\right) J\omega\omega_y \cos\gamma \tag{7.70}$$

$$\omega_y = \left[\frac{(2\pi^2+9)\cos\gamma + (2\pi^2+8)}{(2\pi^2+8)\cos\gamma - (2\pi+9)}\right] \omega_x \tag{7.71}$$

$$-J_x \frac{d\omega_x}{dt} = Mgl_m \cos\gamma + \left[\frac{2\pi^2+8}{9} + \frac{(2\pi^2+9)\cos\gamma + (2\pi^2+8)}{(2\pi^2+8)\cos\gamma - (2\pi+9)}\right] J\omega\omega_x \tag{7.72}$$

(b_1) The equation for the gyroscope motion down from the upper position to the angle of the reset to zero of the resistance torque ($T_{r.x} = 0$) is as follows:

$$J_x \frac{d\omega_x}{dt} = Mgl_m \cos\gamma + \left(\frac{2\pi^2+8}{9}\right) J\omega\omega_x - \left(\frac{2\pi^2+9}{9}\right) J\omega\omega_y \tag{7.73}$$

$$J_y \frac{d\omega_y}{dt} = \left(\frac{2\pi^2+9}{9}\right) J\omega\omega_x \cos\gamma - \left(\frac{2\pi^2+8}{9}\right) J\omega\omega_y \cos\gamma \tag{7.74}$$

$$\left(\frac{2\pi^2+8}{9}\right)J\omega\omega_x - \left(\frac{2\pi^2+9}{9}\right)J\omega\omega_y$$
$$= \left(\frac{2\pi^2+9}{9}\right)J\omega\omega_x\cos\gamma - \left(\frac{2\pi^2+8}{9}\right)J\omega\omega_y\cos\gamma \tag{7.75}$$

$$\omega_y = \left[\frac{(2\pi^2+8)-(2\pi^2+9)\cos\gamma}{(2\pi^2+9)-(2\pi^2+8)\cos\gamma}\right]\omega_x \tag{7.76}$$

$$J_x\frac{\mathrm{d}\omega_x}{\mathrm{d}t} = Mgl_m\cos\gamma + \left[\frac{2\pi^2+8}{9} - \frac{(2\pi^2+8)-(2\pi^2+9)\cos\gamma}{(2\pi^2+9)-(2\pi^2+8)\cos\gamma}\right]J\omega\omega_x \tag{7.77}$$

(b_2) The equation for the gyroscope motion down from the angle of the reset to zero of the resistance torque ($T_{r.x} = 0$) to the low position is as follows:

$$J_x\frac{\mathrm{d}\omega_x}{\mathrm{d}t} = Mgl_m\cos\gamma - \left(\frac{2\pi^2+8}{9}\right)J\omega\omega_x - \left(\frac{2\pi^2+9}{9}\right)J\omega\omega_y \tag{7.78}$$

$$J_y\frac{\mathrm{d}\omega_y}{\mathrm{d}t} = \left(\frac{2\pi^2+9}{9}\right)J\omega\omega_x\cos\gamma - \left(\frac{2\pi^2+8}{9}\right)J\omega\omega_y\cos\gamma \tag{7.79}$$

$$- \left(\frac{2\pi^2+8}{9}\right)J\omega\omega_x - \left(\frac{2\pi^2+9}{9}\right)J\omega\omega_y$$
$$= \left(\frac{2\pi^2+9}{9}\right)J\omega\omega_x\cos\gamma - \left(\frac{2\pi^2+8}{9}\right)J\omega\omega_y\cos\gamma \tag{7.80}$$

$$\omega_y = -\left[\frac{(2\pi^2+8)+(2\pi^2+9)\cos\gamma}{(2\pi^2+9)-(2\pi^2+8)\cos\gamma}\right]\omega_x \tag{7.81}$$

$$J_x\frac{\mathrm{d}\omega_x}{\mathrm{d}t} = Mgl_m\cos\gamma - \left[\frac{2\pi^2+8}{9} + \frac{(2\pi^2+8)+(2\pi^2+9)\cos\gamma}{(2\pi^2+9)-(2\pi^2+8)\cos\gamma}\right]J\omega\omega_x \tag{7.82}$$

where all parameters are as specified above.

The angles of the gyroscope position, the potential and kinetic energies of the gyroscope and the work of the inertial torques at some points of the nutation are defined by the rules of the law of mechanical energy conservation. The position of the resulting gyroscope weight expresses the gravitational potential energy of a gyroscope that is a conservative force. The action of the inertial torques that depends on the angles of the gyroscope turn and the direction of action expresses the negative or positive work. The motion of the gyroscope mass expresses the kinetic energy for the intermediate position and the potential energy for its low and upper points of location and the work of the inertial torques. The datum of energies is accepted the horizontal location of the gyroscope. The total energies of the gyroscope at any points of the nutation are equalized, and this fact is expressed by the following equation:

$$P_{M1} + K_{1.M} \pm A_{1.T_i} = P_{M2} + K_{2.M} \pm A_{2.T_i} \tag{7.83}$$

where $P_{Mi} = Mgl_m \sin\gamma_i$ is the potential energy of the resulting gyroscope weight M; $K_{i.M} = (1/2)J_x\omega_x^2 + (1/2)M(\omega_x l_m)^2$ is the kinetic energy of the gyroscope turn and the linear motion of it is the centre mass of location on the radius l_m about the centre of rotation. $A_{i.T_i} = D_i J\omega\omega_x\gamma$ is the work of the resulting inertial torque on the angle γ of its turn; D_i is the factor of each resulting inertial torque (Table 3.1); the sign ($\pm$) is applied for the work that coincides or opposite to the action of the gyroscope weight; other parameters are as specified above.

The first step (section (a_1)) is considered the equation of the equality of the gyroscope energies for the low point and angular position (γ_e) of the gyroscope that turns in the clockwise direction. Substituting Eq. (7.62), equations of inertial torques (Table 3.1, Chap. 3) into Eq. (7.81), and transformation yield the following equation:

$$Mgl_m \sin(-\gamma_{l.1}) = Mgl_m \sin\gamma_e + \frac{1}{2}J_x\omega_{x.e}^2 + \frac{1}{2}M(\omega_{x.e}l_m)^2 - \left[\frac{2\pi^2+8}{9} - \frac{(2\pi^2+9)\cos\gamma_e - (2\pi^2+8)}{(2\pi^2+8)\cos\gamma_e - (2\pi^2+9)}\right]J\omega\omega_{x.l}(\gamma_{e.1} - \gamma_{l.1}) \tag{7.84}$$

where the indices l and $e.1$ belong to the low and the angular position (for $T_{r.x} = 0$) of the gyroscope, respectively, other parameters are as specified above.

The second step (section (a_2)) considers the equation of the equality of the gyroscope energies for the angular position γ_e of the reset to zero of the resistance torques ($T_{r.x} = 0$) and the upper point of location γ_u of the gyroscope (Eqs. (7.62) and (7.71)).

$$Mgl_m \sin\gamma_u = Mgl_m \sin\gamma_{e.1} + \frac{1}{2}J_x\omega_{x.e}^2 + \frac{1}{2}M(\omega_{x.e}l_m)^2 - \left[\frac{2\pi^2+8}{9} + \frac{(2\pi^2+9)\cos\gamma + (2\pi^2+8)}{(2\pi^2+8)\cos\gamma - (2\pi+9)}\right]J\omega\omega_x(\gamma_u - \gamma_{e.1}) \tag{7.85}$$

where $\gamma_{e.1}$ and γ_u are the angle of the gyroscope at the reset to zero of the resistance torques ($T_{r.x} = 0$) and the upper position, respectively, other parameters are as specified above.

The angular velocity of the gyroscope motion down is presented by Eq. (7.76). The first step (section (b_1)) considers the equation of the equality of the gyroscope energies for the upper γ_u and γ_e positions of the reset to zero of the resistance torques ($T_{r.x} = 0$) that turns down the gyroscope in the counterclockwise direction (Eqs. (7.62) and (7.76)).

$$Mgl_m \sin\gamma_u = Mgl_m \sin(-\gamma_{e.2}) + \frac{1}{2}J_x\omega_{x.e}^2 + \frac{1}{2}M(\omega_{x.e}l_m)^2$$

$$+\left[\frac{2\pi^2+8}{9}-\frac{(2\pi^2+8)-(2\pi^2+9)\cos\gamma}{(2\pi^2+9)-(2\pi^2+8)\cos\gamma}\right]J\omega\omega_{x.u}(\gamma_u-\gamma_{e.2}) \tag{7.86}$$

where all parameters are as specified above.

The second step (section (b_2)) considers the equation of the equality of the gyroscope energies for the angular position ($\gamma_{e.2}$) of the reset to zero of the resistance torques ($T_{r.x}=0$) and low point ($\gamma_{l.2}$) of location of the gyroscope that turns down in the counterclockwise direction (Eqs. (7.62) and (7.80)).

$$Mgl_m\sin(-\gamma_{l.2})=Mgl_m\sin(-\gamma_{e.2})+\frac{1}{2}J_x\omega_{x.e}^2+\frac{1}{2}M(\omega_{x.e}l_m)^2 -\left[\frac{2\pi^2+8}{9}+\frac{(2\pi^2+8)+(2\pi^2+9)\cos\gamma}{(2\pi^2+9)-(2\pi^2+8)\cos\gamma}\right]J\omega\omega_{e.x}(\gamma_{e.2}-\gamma_{l.2}) \tag{7.87}$$

where all parameters are as specified above.

The time of the gyroscope nutation is defined by the expression $t=\gamma/\omega_x$. Following gyroscope nutation is repeated with the change in the numerical data of processes.

7.3.1 Case Study and Practical Tests

The mathematical model for the nutation of the gyroscope with the one side support is based on the technical parameters of the test stand (Figs. 6.1, 6.2 and Table 6.1, Chap. 6). The practical solution of the gyroscope nutation is considered for the conditions of action of the weight of the gyroscope components, single input torque, and inertial torques. The angular velocity of the spinning rotor is accepted $\omega=4000$ rpm. The nutation process is started by the action of the single input torque which time action is $t=0.5$ s and the value of the angular velocity is $\omega_s=0.7$ rad/s. The single input torque turns down the gyroscope on the angle: $\gamma_{l.1}=\omega_s t=0.35\times(180^\circ/\pi)\times 1.0=-20.053522^\circ$, where the sign (−) means, the negative angle from the horizontal datum of the gyroscope. The geometrical parameters of the gyroscope $h=0.0569254$ m, $\tau=38.581266^o$. Numerical solution of the gyroscope amplitude from horizontal versus time of the motion used mathematical models for the gyroscope nutation (Eqs. (7.22), (7.27), (7.32), (7.37), (7.39)–(7.42)) and represented in Appendix, in Table 7.3 and Fig. 7.8. The gyroscope nutation is implemented with the high velocity of the oscillation. In such case the ratio of the angular velocities (Eq. 4.9, Chap. 4) is not maintained and this component is removed from equations pointed above.

In order to elucidate all particular steps of the nutation process, computations have been performed using calculus; all numerical operations have been performed manually by a simple calculator. The computation processes have been represented

Table 7.3 Numerical solution of the gyroscope amplitude from horizontal versus time of the motion

Nutation	First		Second		Third	
	Up	Down	Up	Down	Up	Down
Angular location, γ^{o}	16.272	−16.942	16.25	−16.856	16.26	−16.87
Time of motion, t (s)	0.05	0.028	0.026	0.027	0.027	0.027
Amplitude, γ^{o}	33.21		33.11		33.13	

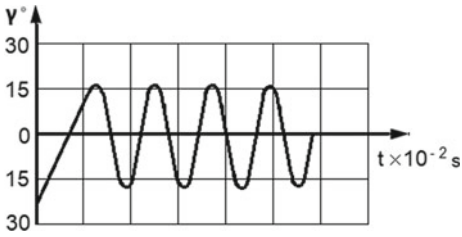

Fig. 7.8 The gyroscope nutation around axis ox

for the first oscillation, the following processes duplicate the first one and did not include in the section.

Figure 7.8 demonstrates the gyroscope nutation process generated by the action of the surplus inertial torques of the spinning rotor. Practical observation confirms the presented diagram.

Appendix

A. **Solution**. The gyroscope parameters and data of the case study [18] are used for several Euler's form equations of the gyroscope undamped nutation. Solutions of gyroscope nutation are based on the action of the system of inertial torques, the gyroscope weight, and the principle of the law of energy conservation. The gyroscope nutation is defined by substituting initial gyroscope parameters (Table 7.3) into basic Eq. (7.37) that accepted for the datum.

A. ***First nutation***. After the short time action of the single input torque, the gyroscope turns up in the clockwise direction until the upper position of the nutation. The motion of the gyroscope is considered for the four stages that are presented by Eqs. (7.21), (7.26), (7.31) and (7.35) by substituting data defined above into corresponding equations:

(a_1) The first stage is the gyroscope motion up from the low position until the value of the resistance torque rests to zero ($T_{r.x} = 0$), thus according to Eq. (7.22) we have

$$2.286976 \times 10^{-4} \frac{\mathrm{d}\omega_x}{\mathrm{d}t} = 0.146 \times 9.81 \times 0.0355 \cos\gamma - \left(\frac{2\pi^2 + 8}{9}\right) \times 0.5726674 \times 10^{-4} \times 4000 \times \left(\frac{2\pi}{60}\right)\omega_x \tag{A1}$$

Separating variables and transformation of Eq. (A1) yields the following:

$$\frac{\mathrm{d}\omega_x}{0.687713\cos\gamma - \omega_x} = 323.281594\,\mathrm{d}t \tag{A2}$$

The differential Eq. (A2) is represented by the integral form of defined limits and yields the following:

$$\int_{-0.7}^{-\omega_{e.1}} \frac{\mathrm{d}\omega_x}{0.687713\cos\gamma - \omega_x} = 323.281594 \int_0^t \mathrm{d}t \tag{A3}$$

The left integral of Eq. (A3) is tabulated and represented the integral $\int \frac{\mathrm{d}x}{a-x} = -\ln|a-x| + \mathrm{C}$. Solving of the integral Eq. (A3) yields the following expression:

$$-\ln(0.687713\cos\gamma - \omega_x)\Big|_{-0.7}^{-\omega_{e.1}} = 323.281594\,t\Big|_0^t$$

giving rise to the following expression:

$$\left(\frac{0.687713\cos\gamma + \omega_x}{0.687713\cos\gamma + 0.7}\right) = \mathrm{e}^{-323.281594\,t} \tag{A4}$$

The right side of Eq. (A4) has the small value of the high order that can be neglected. Solving Eq. (A4) yields the equation of the dependency ω_x in γ:

$$\omega_{e.1} = -0.687713\cos\gamma \tag{A5}$$

where the sign $(-)$ means the motion in the clockwise direction.

The first derivative of Eq. (A5), transformation and the following integral equation with definite limits enables for defining the expression of ω_x

$$\mathrm{d}\omega_{e.1} = 0.687713\sin\gamma d\gamma \tag{A6}$$

$$\int_{-0.7}^{-\omega_{e.1}} \mathrm{d}\omega_x = 0.687713 \int_{-20.053522^\circ}^{\gamma_{e.1}} \sin\gamma d\gamma \tag{A7}$$

Solving of the integral Eq. (A7) brings the following:

$$\omega_x\Big|_{-0.7}^{-\omega_{e.1}} = -0.687713 \times \cos\gamma\Big|_{-20.053522^\circ}^{\gamma_{e.1}}$$

giving rise to the following result:

$$\begin{aligned}\omega_{e.1} &= 0.687713 \times [-\cos\gamma_{e.1} + \cos(-20.053522^\circ)] + 0.7\\ &= 0.687713(1.942783 - \cos\gamma_{e.1})\end{aligned} \tag{A8}$$

Equation (7.39) of the equality of the gyroscope energies for the low point and the equilibrium position of the resisting torque enables for expressing the angular velocity and position of the gyroscope. The gyroscope does not rotate around axis *oy* due to high velocity of the precession and inertia of the system. The precession torques are absence. Substituting the gyroscope data [18] and the result of Eq. (A8) into modified Eq. (7.39) yields the following expression:

$$\begin{aligned}0.146 \times 9.81 \times 0.0355 \times \sin(-20.053522^\circ) &= 0.146 \times 9.81 \times 0.0355 \times \sin\gamma_{e.1}\\ &+ \left(\frac{1}{2}\right) \times 2.286976 \times 10^{-4}\\ &\times [0.687713(1.942783\\ &- \cos\gamma_{e.1})]^2 + \left(\frac{1}{2}\right) \times 0.146\\ &\times [0.687713(1.942783 - \cos\gamma_{e.1})\\ &\times 0.0355]^2 - \left(\frac{2\pi^2 + 8}{9}\right) \times 0.5726674\\ &\times 10^{-4} \times 4000 \times \left(\frac{2\pi}{60}\right) \times 0.687713\\ &(1.942783 - \cos\gamma_{e.1}) \times (\gamma_{e.1}\\ &+ 20.053522^\circ) \times \left(\frac{\pi}{180^\circ}\right)\end{aligned} \tag{A9}$$

Simplification and transformation of Eq. (A9) bring the following transcendental equation:

$$\begin{aligned}-19.646523 = 57.295570\sin\gamma_{e.1} &+ 9.759166 \times 10^{-5} \times (1.9427834 - \cos\gamma_{e.1})^2\\ &- (1.9427834 - \cos\gamma_{e.1})(\gamma_{e.1.} + 20.053522^\circ)\end{aligned} \tag{A10}$$

Numerical solution of Eq. (A10) yields the following result:

$$\gamma_{e.1} = 16.262^\circ \tag{A11}$$

Substituting Eq. (A10) into Eq. (A8) and transformation yields the following angular velocity of the gyroscope:

$$\omega_{e.1} = 0.687713(1.942783 - \cos 16.262^\circ) = 0.675878 \text{ rad/s} \tag{A12}$$

Defined information enables for calculating the time of the gyroscope turn up until equilibrium. The angle of the gyroscope turn in the clockwise direction is $\gamma_{1+}\gamma_{e.1} = \left|-20.053522^{\circ}\right| + 16.262^{\circ} = 36.315^{\circ}$, and the time of gyroscope motion is defined by the expression $t = \gamma/\omega_x$. Substituting $\omega_{e.1}$ (Eq. (A8)), the value of 36.315° into the expression *t,* derivation and integration giving rise to the following result:

$$t_1 = \frac{36.315^{\circ} \times (\pi/180^{\circ})}{0.687713(1.9427834 - \cos\gamma_{e.1})} \tag{A13}$$

$$\mathrm{d}t_1 = \frac{(|-20.053522^{\circ}\} + 16.262^{\circ})(\pi/180^{\circ})\sin\gamma_{e.1}}{(1.9427834 - \cos\gamma_{e.1})^2}\mathrm{d}\gamma \tag{A14}$$

$$\int_0^{t_1} dt_1 = -0.025378 \int_{-20.053522^{o}}^{0} \frac{|-20.053522^{o}|\sin\gamma_e}{(1.9427834 - \cos\gamma_{e.1})^2} d\gamma$$
$$-0.025378 \int_0^{16.262^{o}} \frac{16.262^{o}\sin\gamma_e}{(1.9427834 - \cos\gamma_{e.1})^2} d\gamma \tag{A15}$$

$$t_1\Big|_0^{t_1} = \frac{0.508933}{1.9427834 - \cos\gamma_{e.1}}\Big|_{|-20.053522^{o}|}^{0} + \frac{0.412697}{1.9427834 - \cos\gamma_{e.1}}\Big|_0^{16.262^{o}} =$$

$$t_1 = 0.05\,\mathrm{s}. \tag{A16}$$

(a_2) The second stage is the motion of the gyroscope from the equilibrium until the upper position, (Eq. (7.27)). Following steps of solutions are similar as for the first stage presented above. For the simplification of mathematical processing all comments are omitted:

$$2.286976 \times 10^{-4}\frac{\mathrm{d}\omega_x}{\mathrm{d}t} = 0.146 \times 9.81 \times 0.0355\ \cos\gamma$$
$$+\left(\frac{2\pi^2 + 8}{9}\right) \times 0.5726674 \times 10^{-4}$$
$$\times 4000 \times \left(\frac{2\pi}{60}\right)\omega_x \tag{A17}$$

$$\frac{\mathrm{d}\omega_x}{0.687713\cos\gamma\ - \omega_x} = 323.281594\,\mathrm{d}t \tag{A18}$$

$$\int_{-0.675878}^{-\omega_u} \frac{\mathrm{d}\omega_x}{0.687713\cos\gamma\ - \omega_x} = 323.281594\int_0^t \mathrm{d}t \tag{A19}$$

$$-\ln(0.687713\ \cos\gamma - \omega_x)\Big|_{-0.675878}^{-\omega_u} = 323.281594\,t\Big|_0^t \tag{A20}$$

$$\left(\frac{0.687713\cos\gamma+\omega_u}{0.687713\cos\gamma+0.675878}\right)=\mathrm{e}^{-323.281594\,t} \tag{A21}$$

$$\omega_u=-0.687713\cos\gamma \tag{A22}$$

$$\mathrm{d}\omega_u=0.687713\sin\gamma d\gamma \tag{A23}$$

$$\int_{-0.675878}^{-\omega_u}\mathrm{d}\omega_x=0.687713\int_{16.262^\circ}^{\gamma_u}\sin\gamma d\gamma \tag{A24}$$

$$\omega_x\big|_{-0.675878}^{-\omega_u}=-0.687713\times\cos\gamma\big|_{16.262^\circ}^{\gamma_u}$$

$$\begin{aligned}\omega_u&=0.687713\times[-\cos\gamma_u+\cos(-16.262^\circ)]+0.675878\\&=0.687713(1.942782-\cos\gamma_u)\end{aligned} \tag{A25}$$

$$\begin{aligned}0.146\times9.81\times0.0355\times\sin16.262^\circ&=0.146\times9.81\times0.0355\times\sin(\gamma_u)\\&\quad+\frac{1}{2}\times2.286976\times10^{-4}\times[0.687713(1.942782\\&\quad-\cos\gamma_u)]^2+\frac{1}{2}\times0.146\times[0.687713(1.942782\\&\quad-\cos\gamma_u)\times0.0355]^2-\left(\frac{2\pi^2+8}{9}\right)\times0.5726674\\&\quad\times10^{-4}\times4000\times\left(\frac{2\pi}{60}\right)\times0.687713(1.942782\\&\quad-\cos\gamma_u)\times(\gamma_u-16.262)\times\frac{\pi}{180^\circ}\end{aligned} \tag{A26}$$

$$\begin{aligned}16.044482&=57.295570\sin\gamma_u+9.759166\times10^{-5}\times(1.942782-\cos\gamma_u)^2\\&\quad-(1.942782-\cos\gamma_u)(\gamma_{e.1}-16.262^\circ)\end{aligned} \tag{A27}$$

$$\gamma_u=16.272^\circ \tag{A28}$$

$$\omega_u=0.687713(1.942782-\cos16.272^\circ)=0.675911\ \mathrm{rad/s} \tag{A29}$$

The time of the gyroscope turn from equilibrium to the upper position is determined as follows. The angle of the gyroscope turn in the clockwise direction is γ_u - $\gamma_e = 16.272^\mathrm{o} - 16.262^\mathrm{o} = 0.01^\mathrm{o}$ that is a small value. Then, the time of gyroscope motion

($t=\gamma/\omega_u$) can be computed by the value of average angular velocity (A20).

$$t_2 = \frac{0.01^\circ \times (\pi/180^\circ)}{0.687713(1.942782 - \cos 16.272^\circ)} = 2.582185 \times 10^{-4}\text{s} \tag{A30}$$

The total time of the gyroscope motion up is as:

$$t_u = t_1 + t_2 = 0.05 + 2.582185 \times 10^{-4} = 0.0502\,\text{s}. \tag{A31}$$

(b_1) The gyroscope turns down from the upper position to the equilibrium that leads to change in the direction of the action for the inertial torque (Eq. (7.32). Substituting initial data into Eq. (7.32) and transformation yields the following equation:

$$2.286976 \times 10^{-4}\frac{\mathrm{d}\omega_x}{\mathrm{d}t} = 0.146 \times 9.81 \times 0.0355\,\cos\gamma + \left(\frac{2\pi^2+8}{9}\right) \times 0.5726674 \times 10^{-4} \times 4000 \times \left(\frac{2\pi}{60}\right)\omega_x \tag{A32}$$

$$\frac{\mathrm{d}\omega_x}{0.687713\cos\gamma\ + \omega_x} = 323.281594\,\mathrm{d}t \tag{A33}$$

$$-\int_{0.675911}^{\omega_{e.2}} \frac{\mathrm{d}\omega_x}{-0.687713\cos\gamma\ - \omega_x} = 323.281594\int_0^t \mathrm{d}t \tag{A34}$$

$$\ln(-0.687713\ \cos\gamma - \omega_x)\big|_{0.675911}^{\omega_{e.2}} = -323.281594\,t\big|_0^t$$

$$\left(\frac{-0.687713\cos\gamma - \omega_{e.2}}{-0.687713\cos\gamma - 0.675911}\right) = \mathrm{e}^{-323.281594\,t} \tag{A35}$$

$$\omega_{e.2} = -0.687713\cos\gamma \tag{A36}$$

$$\mathrm{d}\omega_{e.2} = 0.687713\sin\gamma d\gamma \tag{A37}$$

$$\int_{0.675911}^{\omega_{e.2}} \mathrm{d}\omega_x = 0.687713\int_{16.272^\circ}^{\gamma_{e.2}} \sin\gamma d\gamma \tag{A38}$$

$$\omega_x\big|_{0.675911}^{\omega_{e.2}} = -0.687713 \times \cos\gamma\big|_{16.272^\circ}^{\gamma_{e.2}}$$

$$\omega_{e.2} = 0.687713 \times [-\cos\gamma_{e.2} + \cos(16.272^\circ)] + 0.675911$$
$$= 0.687713(1.942781 - \cos\gamma_{e.2}) \tag{A39}$$

The equality of the gyroscope energies for the upper position and the reset to zero of the resisting torque enables for expressing the angular velocity and position of the gyroscope (Eq. (7.41)).

$$\begin{aligned}0.050845\sin(16.272^\circ) = 0.05084\sin(-\gamma_{e.2}) + \frac{1}{2}\times 2.286976\times 10^{-4}\times[0.687713(1.942781\\ -\cos\gamma_{e.2})]^2 + \frac{1}{2}\times 0.146\times[0.687713(1.942781-\cos\gamma_{e.2})\times 0.0355]^2\\ -\left(\frac{2\pi^2+8}{9}\right)\times 0.5726674\times 10^{-4}\times 4000\times\left(\frac{2\pi}{60}\right)\times 0.687713(\cos\gamma_{e.1}\\ -0.430440)\times(1.942781-\cos\gamma_{e.2})\frac{\pi}{180^\circ}\end{aligned} \tag{A40}$$

$$\begin{aligned}16.054082 = 57.295570(-\sin\gamma_{e.2}) + 9.759166\times 10^{-5}\times(1.942781-\cos\gamma_{e.1})^2\\ +(1.942781-\cos\gamma_{e.1})(16.272^\circ-\gamma_{e.2})\end{aligned} \tag{A41}$$

$$\gamma_{e.2} = -16.897^\circ \tag{A42}$$

$$\omega_{e.2} = 0.687713(1.942781-\cos 16.897^\circ) = 0.67742\ \text{rad/s} \tag{A43}$$

Defined information enables for calculating the time of the gyroscope turn down until equilibrium. The angle of the gyroscope turn in the counter clockwise direction is $\gamma_{e.2+}\gamma_{u=}|-16.897^\circ|+16.272^\circ = 33.169^\circ$ and the time of gyroscope motion is defined by the expression $t=\gamma/\omega_x$. Substituting $\omega_{e.2}$ (Eq. (A36)), into the expression t, derivation and integration giving rise to the result.

$$t = \frac{33.1269^\circ\times(\pi/180^\circ)}{0.687713(1.942781-\cos\gamma_{e2})} \tag{A44}$$

$$\mathrm{d}t = \frac{(|-16.897^\circ|+16.272^\circ)\times 0.025378\sin\gamma_{e2}}{1.942781-\cos\gamma_{e2}}\mathrm{d}\gamma \tag{A45}$$

$$\int_0^{t_3} dt = -0.025378\int_{16.272^o}^{0}\frac{16.272^o\sin\gamma_{e2}}{(1.942781-\cos\gamma_{e2})^2}d\gamma$$

$$-0.025378\int_0^{-16.897^o}\frac{|-16.897^o|\sin\gamma_{e2}}{(1.942781-\cos\gamma_{e2})^2}d\gamma$$

$$t_1\Big|_0^{t_1} = \frac{0.412950816}{1.942781-\cos\gamma_{e2}}\Big|_{16.272^\circ}^{0} - \frac{0.428812066}{1.942781-\cos\gamma_{e2}}\Big|_0^{|-16.897^\circ|} \tag{A46}$$

$$t_1 = 0.027\ \text{s}. \tag{A47}$$

(b_2) The next step is to define the angle of the gyroscope location at the lower point and the time of the turn down. Substituting initial data into Eq. (7.37) and transformation yields the following equation:

$$2.286976 \times 10^{-4} \frac{\mathrm{d}\omega_x}{\mathrm{d}t} = 0.146 \times 9.81 \times 0.0355 \cos\gamma - \left(\frac{2\pi^2 + 8}{9}\right) \times 0.5726674 \times 10^{-4} \times 4000 \times \left(\frac{2\pi}{60}\right)\omega_x \tag{A48}$$

The solution of Eq. (A48) is similar to Eq. (A1):

$$\frac{\mathrm{d}\omega_x}{0.687713\cos\gamma - \omega_x} = 323.281594\mathrm{d}t \tag{A49}$$

$$\int_{0.67742}^{\omega_{l.2}} \frac{\mathrm{d}\omega_x}{0.687713\cos\gamma - \omega_x} = 323.281594 \int_0^t \mathrm{d}t \tag{A50}$$

$$-\ln(0.687713\cos\gamma - \omega_x)\Big|_{0.67742}^{-\omega_{l.2}} = 323.281594\, t\Big|_0^t$$

$$\left(\frac{0.687713\cos\gamma + \omega_{l.2}}{0.687713\cos\gamma + 0.67742}\right) = \mathrm{e}^{-323.281594\, t} \tag{A51}$$

$$\omega_{l.2} = -0.687713\cos\gamma \tag{A52}$$

$$\mathrm{d}\omega_{l.2} = -0.687713\sin\gamma d\gamma \tag{A53}$$

$$\int_{0.67742}^{-\omega_{l.2}} \mathrm{d}\omega_x = 0.687713 \int_{-16.897^\circ}^{-\gamma_{l.2}} \sin\gamma d\gamma \tag{A54}$$

$$\omega_x\Big|_{-0.67742}^{-\omega_{l.2}} = -0.687713 \times \cos\gamma\Big|_{-16.897^\circ}^{-\gamma_{l.2}}$$

$$\begin{aligned}\omega_{l.2} &= 0.687713 \times [-\cos\gamma_{l.2} + \cos(-16.897^\circ)] + 0.67742 \\ &= 0.687713(1.942781 - \cos\gamma_{l.2})\end{aligned} \tag{A55}$$

Equation (7.42) of the equality of the gyroscope energies for the equilibrium and the resisting torque of the low position enabled for expressing the angular velocity and position of the gyroscope.

$$\begin{aligned}0.050845\sin(-16.897^\circ) = {} & 0.05084\sin(-\gamma_{l.2}) + \frac{1}{2} \times 2.286976 \times 10^{-4} \\ & \times [0.687713(1.942781 - \cos\gamma_{l.2})]^2 + \frac{1}{2} \times 0.146 \\ & \times [0.687713(1.942781 - \cos\gamma_{l.2}) \times 0.0355]^2 \\ & - \left(\frac{2\pi^2 + 8}{9}\right) \times 0.5726674 \times 10^{-4} \times 4000 \times \left(\frac{2\pi}{60}\right)\end{aligned}$$

$$\times 0.687713(\cos\gamma_{l.2} - 0.430440) \times (1.942781 - \cos\gamma_{l.2}) \times \frac{\pi}{180^{\circ}} \tag{A56}$$

$$-16.653076 = 57.295570\sin(-\gamma_{l.2}) + 9.759166 \times 10^{-5} \times (1.942781 - \cos\gamma_{l.2})^2 - (1.942781 - \cos\gamma_{l.2})(-16.897^{\circ} - \gamma_{l.2}) \tag{A57}$$

$$\gamma_{l.2} = -16.942^{\circ} \tag{A58}$$

$$\omega_{l.2} = 0.687713(1.942781 - \cos 16.942^{\circ}) = 0.6782 \text{ rad/s} \tag{A59}$$

The time of the gyroscope turn from equilibrium to the lower position is determined as follows. The angle of the gyroscope turn in the counter clockwise direction is $\gamma_{l.2} - \gamma_{e.2} = -16.942^{\circ} - 16.897^{\circ} = 0.045^{\circ}$ that is a small value. Then, the time of gyroscope motion ($t = \gamma/\omega_l$) can be computed by the value of average angular velocity (A50).

$$t_4 = \frac{0.047^{\circ} \times (\pi/180^{\circ})}{0.687713(1.942781 - \cos\gamma_{e2})} = 0.0012s \tag{A60}$$

The total time of the gyroscope motion down is as:

$$t_l = t_3 + t_4 = 0.027 + 0.0012 = 0.028\,\text{s}. \tag{A61}$$

The first nutation of the gyroscope is terminated with the surplus kinetic energy of the inertial torques. The value of the angular velocity of the gyroscope is the same as the angular velocity of the initial condition for gyroscope's nutation, i.e., the gyroscope will continue the nutation. The minor differences in the result of the angular locations and the time of motions are explained by the rough manual computing. The parameters computed for the following nutation demonstrate the same results that represented above by Eqs. (A1)–(A61). The validation of the mathematical model for the gyroscope nutation presented above needs the high-tech instrumentation for the measurement of the short time action and value of the input torque.

References

1. Armenise, M.N., Ciminelli, C., Dell'Olio, F., Passaro, V.M.N.: Advances in Gyroscope Technologies. Berlin and Heidelberg GmbH and Co. KG, Berlin, Springer (2010)
2. Deimel, R.F.: Mechanics of the Gyroscope. Dover Publications Inc., New York (2003)
3. Greenhill, G.: Report on Gyroscopic Theory General Books LLC, London (2010)
4. Scarborough, J.B.: The Gyroscope Theory and Applications. Nabu Press, London (2011)
5. Hibbeler, R.C.: Engineering Mechanics-Statics and Dynamics, 12th edn. Prentice Hall, Pearson, Singapore (2010)
6. Gregory, D.R.: Classical Mechanics. Cambridge University Press, New York (2006)
7. Taylor, J.R.: Classical Mechanics. University Science Books, California, USA (2005)

8. Aardema, M.D.: Analytical Dynamics. Theory and Application. Academic/Plenum Publishers, New York (2005)
9. Jewett, J., Serway, R.A.: In: Physics for Scientists and Engineers, Cengage Learning, 10 ed. USA, Boston (2018)
10. Knight, R.D.: Physics for Scientists and Engineers: A Strategic Approach with Modern Physics, Pearson, 4th edn. UK, London (2016)
11. Perry, J.: Spinning Tops and Gyroscopic Motions, Literary Licensing, LLC, NV USA
12. Klein, F., Sommerfeld, A.: The Theory of the Top. I–IV. pp. 2008–2014, Springer, Birkhäuser, New York, NY (2008)
13. Usubamatov, R.: Inertial forces acting on gyroscope. J. Mech. Sci. Technol. **32**(1), 101–108 (2018)
14. Usubamatov, R.: Mathematical model for motions of gyroscope suspended from flexible cord. Cogent Eng. **3**, 1245901 (2016)
15. Usubamatov, R., Omorova, A.: A mathematical model for top nutation based on inertial forces of distributed masses. Mathemat. Problems Eng. **2018**(6132891), 10 (2018). https://doi.org/10.1155/2018/6132891
16. Omorova, A., Usubamatov, R.: A mathematical model for top motions, advances in theoretical and computational. Physics **2**(4), 1–6 (2019)
17. Usubamatov, R.: Gyroscope's torques and motions. Int. J. Adv. Mech. Aeronaut. Eng. **2**(1), 1–5. ISSN: 2372-4153
18. Usubamatov,bR.: Gyroscope's internal kinetic energy and properties. In: Proceedings of 5th International Conference on Advanced in Mechanical Aeronautical and Production Techniques, MAPT-2016, March 12–13, Kuala Lumpur, pp. 21–25 (2016)
19. Usubamatov, R.: Physics of gyroscope nutation. AIP Adv. **9**, 105101 (2019). https://doi.org/10.1063/1.5099647
20. Cross, R.: Why does a spinning egg rise? Eur. J. Phys. **39**(2). http://doi.org/10.1088/1361-6404/aa997b

Chapter 8
Gyroscopic Effects of Deactivation of Inertial Forces

8.1 Deactivation of Gyroscopic Inertial Forces

The complex gyroscope motions in space, interrelation of the system inertial torques generated by the distributed masses and centre mass of the spinning objects demonstrate several unusual physical effects [1–4]. The complexity of the action of the interrelated inertial torques and external forces on the rotating objects is still unclear [5–10]. The new mathematical models for the inertial torques and methods for computing of gyroscopic effects enable to solve gyroscope problems [11–13]. The interrelated inertial torques acting on the rotating objects demonstrate the deactivation of most parts of the inertial torques at the time of the motion around one axis [14, 15]. The nature of these gyroscopic effects contradicts principles of classical mechanics at first sight. However, the following analysis enables for describing gyroscopic properties by known principles of classical mechanics. The new inertial forces acting on spinning disc and their origin presented in previous chapters are used for the following study and discussion of the physics of deactivation of inertial forces.

Inertial torques generated by spinning objects under the action of the external torque are separated into two groups. The first group is the inertial torque generated by the rotating centre mass presented by the change in the angular momentum of the spinning objects. The second group is the several inertial torques generated by the rotating mass elements or distributed mass and acting around axes of the spinning objects. All gyroscopic inertial torques are interrelated and acted around three axes of the accepted coordinate system of the gyroscope. One specific property is represented by the following condition. The mass elements of the spinning object generate the resistance torque T_{ct} of the centrifugal forces and precession torque T_{in} of the common inertial forces are acted around different axes but described by one equation, which contains the angular velocity ω_x of precession around one axis (Chap. 3 and Table 3.1) [11–14]. The resistance T_{ct} and precession T_{in} torques have direct interdependent action. If the resistance torque is deactivated, then the precession torque also should be deactivated. This statement needs validation by the practical tests. These two torques are compensated at the process of mathematical transformations

© The Editor(s) (if applicable) and The Author(s), under exclusive license to Springer Nature Singapore Pte Ltd. 2020

R. Usubamatov, *Theory of Gyroscopic Effects for Rotating Objects*,
https://doi.org/10.1007/978-981-15-6475-8_8

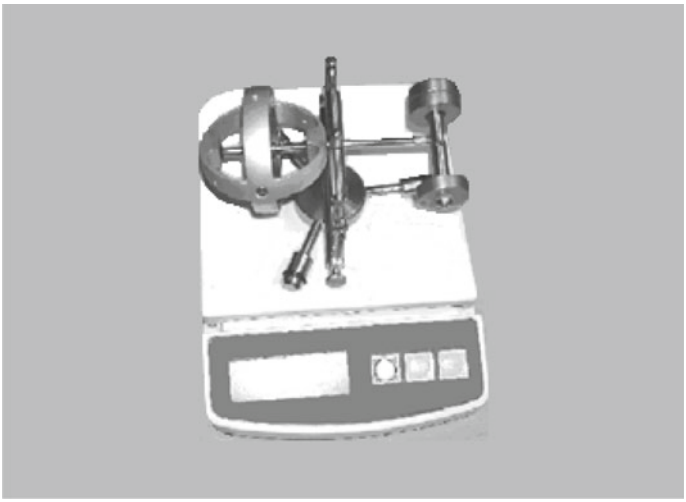

Fig. 8.1 Test stand of the gyroscope with the counterweight

of the equations for gyroscope motions around axes. The compensation of the inertial torques cannot be accepted by the rules of physics but accepted by rules of abstract mathematics.

The practical tests of the gyroscope motions around two axes demonstrate the deactivation of inertial torques when its precession motion around one axis is blocked. At this condition, the gyroscope demonstrates several new properties represented by the mathematical models and validated by the practical tests. The physical phenomena of the deactivation of inertial torques contradict known principles of classical mechanics and need deep analytical and practical analysis. The tests of the deactivation of gyroscopic inertial torques are conducted on the stand assembled with the high precession gyroscope and the counterweight. The test stand with Super Precision Gyroscope "Brightfusion LTD" is demonstrated in Figs. 8.1 and 8.2, and the technical data are represented in Table 8.1. The mass of the counterweight is selected with the aim to have the slow gyroscope turn around axis ox and to have the ability to record the time of motions. The location of the centre mass is near the centre o of the coordinate system $\Sigma oxyz$, and the difference between masses left and right sides is small. The gyroscope with one side support connected with the counterweight G by the axle s. The axle s is fixed on the centre beam b with the ability to free rotation around axis ox. The spherical journals B and D of the centre beam are located on the supports of conical surfaces on the vertical arms of the frame. The centre beam is assembled with the frame that contains two arms mounted on the horizontal bar b_s. This assembled construction presents the gyroscope gimbal. The gimbal has the ability to free rotation about the fixed pivot C (vertical axis oy) on the platform.

Table 8.1 contains the following symbols: $J_{x\cdot W} = J_{y\cdot W} = (MR_c^2/4) + Ml^2$ is the mass moment of the movable gyroscope component inertia around axes ox and oy,

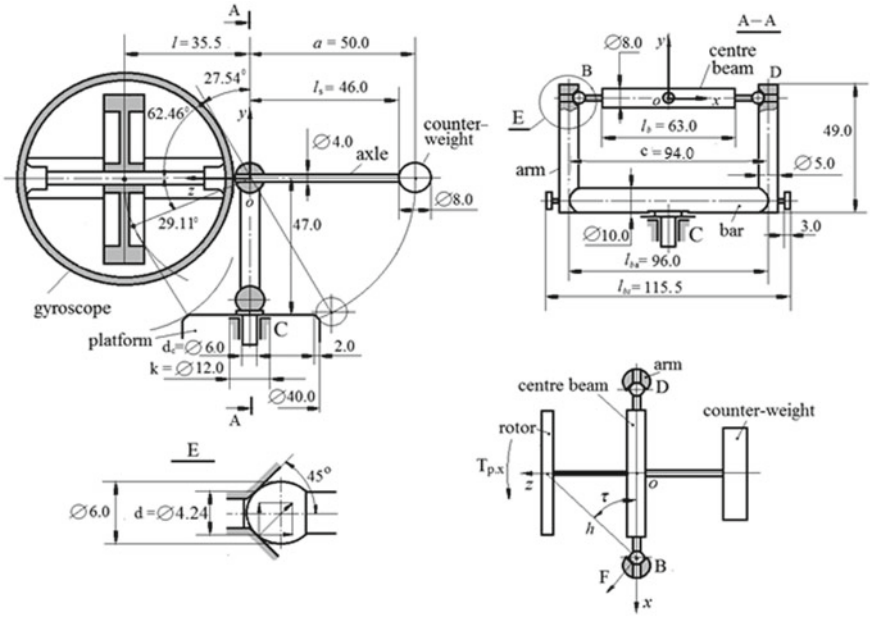

Fig. 8.2 Scheme of the gyroscope's stand with the counterweight

Table 8.1 Technical data of the test stand with Super Precision Gyroscope, "Brightfusion LTD"

Parameters	Mass (kg)	Mass moment of inertia (J kg m^2)	Around axis
Spinning rotor	0.1159	$J = mR_c^2/2 = 0.5726674 \times 10^{-4}$	*oz*
Gyroscope with rotor, *M*	0.146	$J_{i\,W} = (2/3)m_5 r_5^2 + m_5 l^2 + (m R_c^2/4) + ml^2 = 2.284736 \times 10^{-4}$	*ox*, *oy*
Axle, *s*	0.005	$J_s = m_s l_s^2/3 = 0.0352666 \times 10^{-4}$	*ox*, *oy*
Centre beam with journals and screw, *b*	0.028	$J_b = m_b r_b^2/2 = 0.00224 \times 10^{-4}$	*ox*
		$J_b = m_b l_b^2/12 = 0.2105833 \times 10^{-4}$	*oy*

respectively; l is the overhang of the centre of mass of the gyroscope from the centre beam; M is the mass of the movable gyroscope component; $J_{r\cdot x} = J_{r\cdot y} = (mR_c^2/4/4)$ is the rotor's mass moment of inertia around axis *ox* and *oy;* R_c is the conditional radius of the rotor; $J = (mR_c^2/4/2)$ is the rotor's mass moment of inertia around axis *oz.* The computed mass moments of the gyroscope's components inertia around axes *ox* and *oy* are presented in Chap. 5.

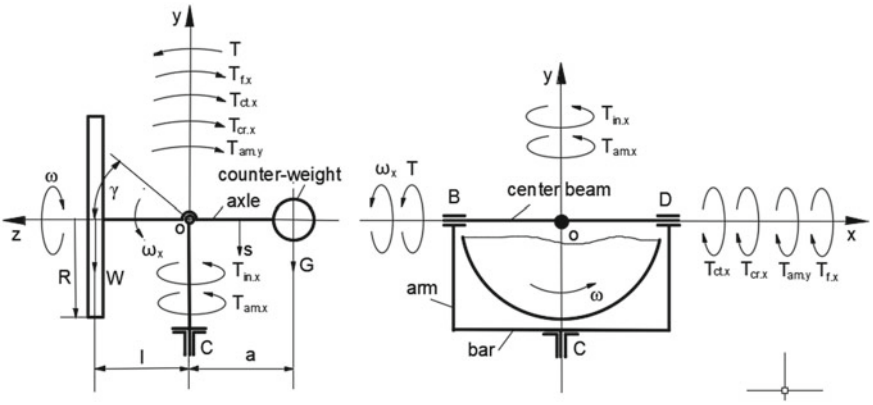

Fig. 8.3 Forces and torques acting on the gyroscope with the counterweight

The gyroscope tests conducted for conditions of the gyroscope turn around axis *ox* and blocking of its turn around vertical axis *oy*. The object of the tests is to demonstrate the deactivation of the gyroscopic inertial torques and validate the mathematical model. The analytical and practical results of the tests are represented by the gyroscope time motions and the value of the precessed torque converted to the force acting on the digital scale. The mathematical model for the gyroscope motion around axis *ox* is similar to the model for the gyroscope suspended from a flexible cord [14]. The difference of the equation for the gyroscope motion is the absence of the action of the precession torques originated around axis *oy* and acting around axis *ox* (Figs. 8.1 and 8.2). Figure 8.3 represents the action of the external and inertial torques on the gyroscope stand. These technical data enable for formulating of the hypothetical mathematical model for the motion of the gyroscope under the action of the external and inertial torques by the following Euler's differential equation:

$$J_x \frac{\mathrm{d}\omega_x}{\mathrm{d}t} = T - T_{\mathrm{fx}} - T_{\mathrm{ct}\cdot x} - T_{\mathrm{cr}\cdot x} \tag{8.1}$$

where ω_x is the angular velocity of the gyroscope around axes *ox*; T is the resulting torque generated by the weight of the gyroscope components; $T_{\mathrm{ct}\cdot x}$, $T_{\mathrm{cr}\cdot x,}$ are inertial torques generated by the centrifugal and Coriolis forces acting around axis *ox* (Table 3.1); T_{fx} is the frictional torques acting on gyroscope's supports and pivot, respectively; other components are as specified above.

The expressions for inertial torques of Eq. (8.1) are represented in Table 3.1, Chap. 3. The load torque T acting around axis *ox* is generated by the weight of gyroscope components and represented by the following expression:

$$T = (Ml - sa/2 - Ga)g\cos\gamma \tag{8.2}$$

where M is the gyroscope mass; s is the axle mass; G is the mass of the counterweight; g is the gravity acceleration; l is the distance of location of the centre mass of the gyroscope; a is the length of the axle and the distance of location of the centre mass of the counterweight; γ is the angle of the axle inclination.

Analysis of components of Eq. (8.1) shows the acting torque T is variable and depends on the angle γ of the gyroscope inclination. The several external and inertial torques acting on the gyroscope generate the frictional forces on the supports of the gimbal. Frictional toques generated by the weight of the gyroscope components acting on the supports B and D are represented by the following equations:

$$T_{\mathrm{fA}} = (M + s + b + G)gf\frac{d}{2\cos\delta} = Ag\frac{fd}{2\cos\delta} \tag{8.3}$$

where b is the mass of the centre beam; f is the coefficient of friction of sliding supports; d is the diameter of the supports B and D; $\delta = 45°$ is the angle of the conical surface of the sliding bearing; other parameters are as specified above.

The rotation of the gyroscope around axis generates the centrifugal forces produced by the centre mass, and hence, the frictional torque acting on the sliding supports B and D is expressed by the following equation:

$$T_{\mathrm{fm}} = m_{\mathrm{r}}l_{\mathrm{m}}\frac{fd}{2\cos\delta}\omega_x^2 \tag{8.4}$$

where m_{r} is resulting load mass: l_{m} is the location of resulting load mass (Table 8.1; Fig. 8.2); other parameters are as specified above.

The load torque T produces the resistance torques of the centrifugal T_{ct} and Coriolis T_{cr} forces acting around axis ox and precession torques of the common inertial forces T_{in}, and the change in the angular momentum T_{am} around axis oy. The precession torques produce the additional load on the supports B and D. Then, the frictional torque generated by the precession torque is represented by the following equation:

$$T_{\mathrm{fp}\cdot x} = T_{\mathrm{am}\cdot x} = \frac{fd\cos(\delta - \tau)}{2h\cos\delta}J\omega\omega_x \tag{8.5}$$

where $T_{\mathrm{p}\cdot x}$ is the precession torque (Table 3.1, Chap. 3); h is the distance from the centre mass of the gyroscope to the centre of the spherical journal of the centre beam with supports B and D; τ is the constructive angle (Fig. 8.2); other parameters are as specified above.

The total frictional torque acting on supports of the gyroscope stand is represented by the following equations:

$$T_{\mathrm{fx}} = T_{\mathrm{fA}} + T_{\mathrm{fm}} + T_{\mathrm{fpx}} = Ag\frac{fd}{2\cos\delta} + m_{\mathrm{r}}l_{\mathrm{m}}\frac{fd}{2\cos\delta}\omega_x^2 + \frac{fd\cos(\delta - \tau)}{2h\cos\delta}J\omega\omega_x \tag{8.6}$$

where all parameters are as specified above.

Substituting defined equations for the external and inertial torques of the gyroscope (Eqs. 8.2–8.6) into Eq. (8.1) yields the following differential equation:

$$J_x \frac{\mathrm{d}\omega_x}{\mathrm{d}t} = \left(Ml - s\frac{a}{2} - Ga\right) g\cos\gamma - \left[(Ag + m_\mathrm{r} l_\mathrm{m} \omega_x^2)\frac{fd}{2\cos\delta} + \frac{fd\cos(\delta - \tau)}{2h\cos\delta} J\omega\omega_x\right] - \left(\frac{2\pi^2 + 8}{9}\right) J\omega\omega_x \tag{8.7}$$

where all parameters are as specified above.

Practical observation of the motion for the running gyroscope around axis ox manifests the following properties. The blocking of the gyroscope motion around axis oy demonstrates its fast turn down under the action of the gravity and frictional forces. It means the resistance torques T_ct and T_cr are deactivated. For this condition, the equation of the gyroscope motion around axis ox is represented by the following:

$$J_{x1} \frac{\mathrm{d}\omega_x}{\mathrm{d}t} = \left(Wl - s\frac{a}{2} - Ga\right) g\cos\gamma - \left[Ag\frac{fd}{2\cos\delta} + m_\mathrm{r} l_\mathrm{m} \frac{fd}{2\cos\delta}\omega_x^2 + \frac{fd\cos(\delta - \tau)}{2h\cos\delta} J\omega\omega_x\right] \tag{8.8}$$

In the case, when the rotor of the gyroscope does not spin, there is no precession torque around axis oy (Eq. 8.5). Then, the equation for the gyroscope motion around axis ox is as follows:

$$J_x \frac{\mathrm{d}\omega_x}{\mathrm{d}t} = \left(Ml - s\frac{a}{2} - Ga\right) g\cos\gamma - \left[Ag + m_\mathrm{r} l_\mathrm{m} \omega_x^2\right]\frac{fd}{2\cos\delta} \tag{8.9}$$

where all parameters are as specified above.

Equations (8.8) and (8.9) enable for computing of the angular velocities of the gyroscope motions around axis ox and the times of motions. The time of the gyroscope turn with the spinning rotor should be bigger than the time of the turn when the rotor does not spin. This statement is confirmed, and practical tests have validated the deactivation of the resistance torques around axis ox and the action of the precession torque around axis oy.

8.1.1 Case Study and Practical Tests

Equation (8.8) represents the mathematical model of the gyroscope motion with the spinning rotor when its motion around axis oy is blocked. The case study and first practical tests were conducted for the condition of the gyroscope turn on the angle $\gamma = 91.57°$, which calculated by the geometrical parameters of the stand. At the starting condition, the gyroscope counterweight has contacted with the surface of

the platform. At the end of the turn, the spherical frame of the gyroscope has contacted the platform (Fig. 8.2). The surfaces of sliding support of the arm and spherical ball of the beam polished and handbooks give the value of the dry frictional coefficient, $f = 0.15$–0.18, [16–18]. The parameter $l = 35.5$ mm (Fig. 8.2), the angular velocity of the spinning rotor is $\omega = 10{,}000$ rpm, other parameters represented in Table 8.1 and Fig. 8.2. Substituting defined data into Eq. (8.8) and transformation yields the following expression:

$$\begin{aligned} 4.780082 \times 10^{-4} \frac{\mathrm{d}\omega_x}{\mathrm{d}t} &= (0.146 \times 0.0355 - 0.005 \times 0.025 - 0.098 \times 0.05) \\ &\times 9.81 \cos\gamma - \frac{0.277 \times 9.81 \times 0.16 \times 0.00424}{2 \cos 45^\circ} \\ &- 0.043 \times 0.03674418 \times \left(\frac{0.16 \times 0.00424}{2 \cos 45^\circ} \right) \omega_x^2 \\ &- \left[\frac{0.16 \times 0.00424 \times \cos(45^\circ - 38.581266^\circ)}{2 \times 0.0569254 \cos 45^\circ} \right] \\ &\times 0.5726674 \times 10^{-4} \times 10.000 \times \left(\frac{2\pi}{60} \right) \omega_x \end{aligned} \tag{8.10}$$

Simplification and transformation of Eq. (8.10) give the following expression:

$$\begin{aligned} 4.780082 \times 10^{-4} \times \frac{\mathrm{d}\omega_x}{\mathrm{d}t} &= 1.54998 \times 10^{-3} \cos\gamma - 1.303525758 \times 10^{-3} \\ &- 7.5792783504 \times 10^{-7} \omega_x^2 - 5.021862882 \times 10^{-4} \end{aligned} \tag{8.11}$$

The right component $7.5792783504 \times 10^{-7}\ \omega_x^2$ of Eq. (8.11) has the small value of high order that can be neglected. Separating variables and transformation for differential Eq. (8.11) gives the following equation:

$$\frac{\mathrm{d}\omega_x}{3.086464199 \cos\gamma - 2.595701613 - \omega_x} = 1.050580906 \mathrm{d}t \tag{8.12}$$

Equation (8.12) is represented by the integral forms at definite limits that yields the following expression:

$$\int_0^{\omega_x} \frac{\mathrm{d}\omega_x}{3.086464199 \cos\gamma - 2.595701613 - \omega_x} = 1.050580906 \int_0^t \mathrm{d}t \tag{8.13}$$

The left integral of Eq. (8.13) is tabulated and represented the integral $\int \frac{\mathrm{d}x}{a-x} = -\ln|a - x| + C$. The right integral is simple, and the integral equation has the following solution:

$$-\ln(3.086464199\cos\gamma - 2.595701613 - \omega_x)\Big|_0^{\omega_x} = 1.050580906t\Big|_0^t$$

that gave rise to the following

$$1 - \frac{\omega_x}{3.086464199\cos\gamma - 2.595701613} = \mathrm{e}^{-1.050580906t} \tag{8.14}$$

Solving of Eq. (8.14) gives the expression of the angular velocity for the gyroscope around axis ox as the result of the action of the gyroscope weight and frictional torques:

$$\omega_x = (3.086464199\cos\gamma - 2.595701613)(1 - \mathrm{e}^{-1.050580906t}) \tag{8.15}$$

The angular velocity of the gyroscope around axis ox is variable and depends on the angle γ of location of the gyroscope and the time of the motion. The time of gyroscope turn on angle γ is derived from the following equation:

$$t = \frac{\gamma}{\omega_x} \tag{8.16}$$

where t is the time of the gyroscope turn, γ is the angle of the turn.

The change in the time of the gyroscope motion with the change in its angle of location is represented by the following differential equation:

$$\mathrm{d}t = \frac{\mathrm{d}\gamma}{\omega_x} \tag{8.17}$$

Substituting Eq. (8.15) into Eq. (8.17), transformation and separating variables enable for representing the integral form of Eq. (8.17) that is as follows:

$$\int_0^t \left(1 - \mathrm{e}^{-1.050580906t}\right)\mathrm{d}t = 0.32399533 \int_0^\gamma \frac{\mathrm{d}\gamma}{\cos\gamma - 0.840995211} \tag{8.18}$$

The right integral is converted to the integral of the rational function using the versatile trigonometric substitution $x = \tan(\gamma/2)$, which the derivative is $\mathrm{d}x = \frac{\mathrm{d}\gamma}{2\cos^2(\gamma/2)}$. Using the trigonometric identities $\cos\gamma = \frac{1-\tan^2(\gamma/2)}{1+\tan^2(\gamma/2)}$, $\cos^2\frac{\gamma}{2} = \frac{1+\cos\gamma}{2}$, substituting into Eq. (8.18), and transformation yield the following integral equation:

$$\int_0^t \left(1 - \mathrm{e}^{-1.050580906t}\right)\mathrm{d}t = -0.351978460 \int_0^x \frac{\mathrm{d}x}{x^2 - 0.293885915^2} \tag{8.19}$$

The right integral of Eq. (8.19) is tabulated and presented the integral: $\int \frac{\mathrm{d}t}{x^2-a^2} = \frac{1}{2a}\ln\left|\frac{x-a}{x+a}\right|$. Solving of the integral Eq. (8.19) brings the following equation:

$$\left(t+\frac{\mathrm{e}^{-1.050580906t}}{1.050580906}\right)\Big|_0^t=-\frac{0.351978460}{2\times 0.293885915}\times\ln\left|\frac{x-0.0.293885915}{x+0.293885915}\right|\Big|_0^x \tag{8.20}$$

Substituting of the parameters x represented by the trigonometric expression into Eq. (8.20), changing the limits and transformation yield the following equation:

$$\left(t+\frac{\mathrm{e}^{-1.050580906t}}{1.050580906}\right)\Big|_0^t=-0.59883519\times\ln\left|\frac{\tan(\gamma/2)-0.293885915}{\tan(\gamma/2)+0.293885915}\right|\Big|_{-29.11^\circ}^{62.46^\circ} \tag{8.21}$$

that gave rise to the following

$$\begin{aligned}\left(t+\frac{\mathrm{e}^{-1.050580906t}}{1.050580906}\right)=&-0.59883519\\&\times\left[\ln\left|\frac{\tan(62.46^\circ/2)-0.293885915}{\tan(62.46^\circ/2)+0.293885915}\right|\right.\\&\left.-\ln\left|\frac{\tan(-29.11^\circ/2)-0.293885915}{\tan(-29.11^\circ/2)+0.293885915}\right|\right]\end{aligned} \tag{8.22}$$

Solving of Eq. (8.22) yields the following expression:

$$\left(t+\frac{\mathrm{e}^{-1.050580906t}}{1.050580906}\right)==2.299 \tag{8.23}$$

Numerical solution of transcendental Eq. (8.23) gives the following result:

$$t=2.205\ \mathrm{s}$$

For the gyroscope, which rotor does not spin, the time of the gyroscope turn is calculated by Eq. (8.9) that is the typical example from the textbooks of the engineering mechanics. The solution of Eq. (8.9) yields the angular velocity of the gyroscope turn, which value is less than for the gyroscope turn with the spinning rotor (Eq. 8.8). The left component of Eq. (8.9) is represented by the form $\mathrm{d}\omega_x/\mathrm{d}t=\varepsilon_{x,}$ which is the acceleration of the gyroscope turn. Substituting defined parameters above into Eq. (8.9) and transformation yields the following result:

$$4.780082\times 10^{-4}\times\varepsilon_x=1.54998\times 10^{-3}\cos\gamma-1.303525758\times 10^{-3} \tag{8.24}$$

Simplification and transformation of Eq. (8.24) bring the following expression:

$$\varepsilon_x=3.242580357\cos\gamma-2.726994553 \tag{8.25}$$

The acceleration ε_x is variable due to the change in the angle γ. The change in the acceleration is defined by the first derivative of Eq. (8.25)

$$\mathrm{d}\varepsilon_x = -3.242580357 \sin\gamma \mathrm{d}\gamma \tag{8.26}$$

Equation (8.26) is represented by the integral form with defined limits:

$$\int_0^{\varepsilon_x} \mathrm{d}\varepsilon_x = -3.242580357 \int_{62.46^\circ}^{-29.11^\circ} \sin\gamma \mathrm{d}\gamma,$$

that gave rise to the following

$$\varepsilon_x = 3.242580357 \times [\cos(-29.11^\circ) - \cos 62.46^\circ] = 1.333736781 \text{ rad/s}^2 \tag{8.27}$$

The time of the gyroscope turn on the angle $\gamma = 91.57^\circ$ is defined by the following:

$$\gamma = \frac{\varepsilon_x t^2}{2} \tag{8.28}$$

Substituting defined parameters above into Eq. (8.28) and solving yield the following result

$$t = \sqrt{\frac{2\gamma}{\varepsilon_x}} = \sqrt{\frac{2 \times 91.57^\circ \times \pi}{180^\circ \times 1.333736781}} = 1.54 \text{ s} \tag{8.29}$$

The final computing is conducted for Eq. (8.7) to define the time of the gyroscope motion around axis ox with the hypothetical action of the resistance inertial torques. The comparative analysis of the results of practical tests and the analytical model validate the deactivation of the inertial torques. Substituting defined parameters presented in Table 8.1 and Fig. 8.2 into Eq. (8.7), transformation and simplification yield the following equation:

$$\begin{aligned} 4.780082 \times 10^{-4} \times \frac{\mathrm{d}\omega_x}{\mathrm{d}t} &= (0.146 \times 0.0355 - 0.005 \times 0.025 - 0.098 \times 0.05) \\ &\times 9.81 \times \cos\gamma - 0.277 \times 9.81 \times 0.16 \\ &\times \frac{0.00424}{2\cos 45^\circ} - \left[2\left(\frac{\pi}{3}\right)^2 + 1\right] \\ &\times \frac{0.16 \times 0.00424}{2 \times 0.056925} \times \cos(45^\circ - 38.581^\circ) \times 0.5726674 \\ &\times 10^{-4} \times 10.000 \times \frac{2\pi}{60}\omega_x - \left[2\left(\frac{\pi}{3}\right)^2 + \frac{8}{9}\right] \\ &\times 0.5726674 \times 10^{-4} \times 10.000 \times \frac{2\pi}{60}\omega_x \end{aligned} \tag{8.30}$$

Simplification of Eq. (8.30) brings the following expression:

$$4.780082 \times 10^{-4} \times \frac{\mathrm{d}\omega_x}{\mathrm{d}t} = 1.54998 \times 10^{-3} \cos\gamma - 1.303525758 \times 10^{-3} - 0.186437934\omega_x \tag{8.31}$$

The following steps of computing are the same as presented in Eqs. (8.10)–(8.23), and all comments are omitted.

$$\frac{\mathrm{d}\omega_x}{8.313651416 \times 10^{-3} \cos\gamma - 6.991741031 \times 10^{-3} - \omega_x} = 390.030829414\mathrm{d}t \tag{8.32}$$

$$\int_0^{\omega_x} \frac{\mathrm{d}\omega_x}{8.313651416 \times 10^{-3} \cos\gamma - 6.991741031 \times 10^{-3} - \omega_x} = 390.030829414 \int_0^t \mathrm{d}t \tag{8.33}$$

$$\begin{aligned} &- \ln\left(8.313651416 \times 10^{-3} \cos\gamma - 6.991741031 \times 10^{-3} - \omega_x\right)\Big|_0^{\omega_x} \\ &= 390.030829414t\Big|_0^t \\ &1 - \frac{\omega_x}{8.313651416 \times 10^{-3} \cos\gamma - 6.991741031 \times 10^{-3}} \\ &= \mathrm{e}^{-390.030829414t} \end{aligned} \tag{8.34}$$

$$\omega_x = \left(8.313651416 \times 10^{-3} \cos\gamma - 6.991741031 \times 10^{-3}\right)\left(1 - \mathrm{e}^{-390.030829414t}\right) \tag{8.35}$$

$$\omega_x = 8.313651416 \times 10^{-3} \cos\gamma - 6.991741031 \times 10^{-3} \tag{8.36}$$

$$t = \frac{\gamma}{\omega_x} \quad \text{and} \quad \mathrm{d}t = \frac{\mathrm{d}\gamma}{\omega_x} \tag{8.37}$$

$$\int_0^t \mathrm{d}t = 120.28409058 \int_0^{\gamma} \frac{\mathrm{d}\gamma}{\cos\gamma - 0.840995211} \tag{8.38}$$

$$\int_0^t \mathrm{d}t = -130.672898942 \int_0^{\gamma} \frac{\mathrm{d}x}{x^2 - 0.293885915^2} \tag{8.39}$$

$$t\Big|_0^t = -\frac{130.672898942}{2 \times 0.293885915} \ln\left|\frac{x - 0.293885915}{x + 0.293885915}\right|\Big|_0^x \tag{8.40}$$

Table 8.2 Experimental and theoretical results of the time of the gyroscope turn

Parameters	Time of the gyroscope turn on 91.57° (s)		Difference, %
	Test	Theoretical	
The rotor is spun, (Eq. 8.8)	2.1	2.205	5.0
The rotor is stopped, (Eq. 8.9)	1.44	1.54	6.94
The rotor is spun, (Eq. 8.7)		853.926	

$$
\begin{aligned}
t &= -222.319090967 \\
&\times \left[\ln \left| \frac{\tan(62.46^\circ/2) - 0.293885915}{\tan(62.46^\circ/2) + 0.293885915} \right| \right. \\
&\left. - \ln \left| \frac{\tan(-29.11^\circ/2) - 0.293885915}{\tan(-29.11^\circ/2) + 0.293885915} \right| \right] \\
&= 853.926 \text{ s}
\end{aligned} \tag{8.41}
$$

Obtained result $t = 853.926$ s is not appropriate and gives the answer for the solution and proves the inertial resistance torques acting around axis ox are deactivated. The results of practical tests and theoretical calculation of the time motion of the gyroscope at defined conditions recorded and presented in Table 8.2.

Analysis of the results of the theoretical calculations and practical tests for the gyroscope motions demonstrate discrepancies between them. This divergence is explained by the several factors that are the accuracy of calculations for the gyroscope technical data, the accuracy of test measurement, the drop of the spinning rotor velocity and variable values of the coefficient of friction in supports. The mathematical model (Eq. 8.8) used the coefficient of friction $f = 0.16$ [16–19]. Other values of the coefficient give bigger discrepancies in the time of the turn but also validate the accepted analytical model. The short time of the gyroscope motion resulted in the accuracy of the measurement, which is less of the limit of 10%. This divergence in theoretical and practical results is accepted and recommended by most researchers, but some of them prefer the limit of 5%. The exact percentage of the accepted limit of divergence in theoretical and practical results is an absence in scientific publications. These data and obtained results of the test and theoretical model are well coincided and enable for stating that the mathematical model for the gyroscope motions can be accepted for engineering practice [20].

Practical tests of the gyroscope motion around one axis are conducted on the stand with sliding supports of the gimbal, which give the sensitive value of the frictional forces. The rolling supports of the gimbal with ball bearings give a hundred times less the value of the frictional forces acting on the supports. In such a case, the resistance torques generated by the frictional forces of the precession torque will have a small value. Then, the time of the running gyroscope motion at the condition of the blocking of the motion around one axis will not have a big difference from the

short time of the motion with the stopped rotor of the gyroscope. This is the reason that tests of the gyroscope design with ball bearings of the support are not necessary.

Conducted tests for the gyroscope with the spinning rotor and recorded time of its motion are the validation of the accepted mathematical model. The blocking of the motion of the gyroscope around axis *oy* deactivates all inertial torques generated by the rotating mass elements of the spinning rotor. However, at this condition, the torque of the change in the angular momentum generated by the centre mass is acting on a gyroscope. The hypothetical time ($t = 853.926$ s) of the gyroscope turn with the action of the resistance inertial torques around axis *ox* when the motion around axis *oy* is blocked is not validated by the practical tests. The gyroscope turns under the action of the gravity, frictional forces and the action of the precession torque yield the increased time of the turn ($t = 2.1$ s). The time of the turn around axis *ox* for the gyroscope with the stopped rotor is shorter ($t = 1.44$ s) < ($t = 2.1$ s) because the precession torque is absent and does not produce the frictional torque. This result is the validation of the action of the precession torque (the change in the angular momentum) on the running gyroscope. The results of the deactivation of the inertial forces present a new direction in the study of the physics for the complex action of inertial torques generated by the rotating objects [20].

8.1.2 Test of the Gyroscope on the Action of the Precession Torque

The blocking of the gyroscope rotation around axis *oy* deactivates all inertial torques generated by the rotating mass elements of the spinning rotor. However, this blocking does not lead to the deactivation of the precession torque of the change in the angular momentum acting around axis *oy*. The validation of the action of the precession torque and the measure of its value is conducted on the stand that represented in Fig. 8.4. The gyroscope stand additionally equipped with the angular rocker that transfers the action of the precession torque to the digital scale. The sketch of the stand is represented in Fig. 8.5. The bar of the gimbal is contacted with the angular rocker that presses the platform of the digital scale of Model TS-SF 400A with division one gr. The digital scale has demonstrated the value of the force generated by the precession torque. The practical result is compared with the theoretical value of the force of the precession torque computed for the horizontal location of the running gyroscope. The torque and forces acting on the gyroscope stand are represented in Fig. 8.5. The basic geometrical parameters of the stand are represented in Table 8.1, Fig. 8.2 and in Sect. 8.1.

The value of the velocity is changed with the change in the angle of the gyroscope turn and time of motion. The force of the precession torque is varied with the change of the angular velocity and the time of the motion of the gyroscope. The expression of the precession torque for the horizontal location ($\gamma = 0°$) of the gyroscope is represented by substituting ω_x (Eq. 6) into $T_{\text{am}} = J\omega\omega_x$:

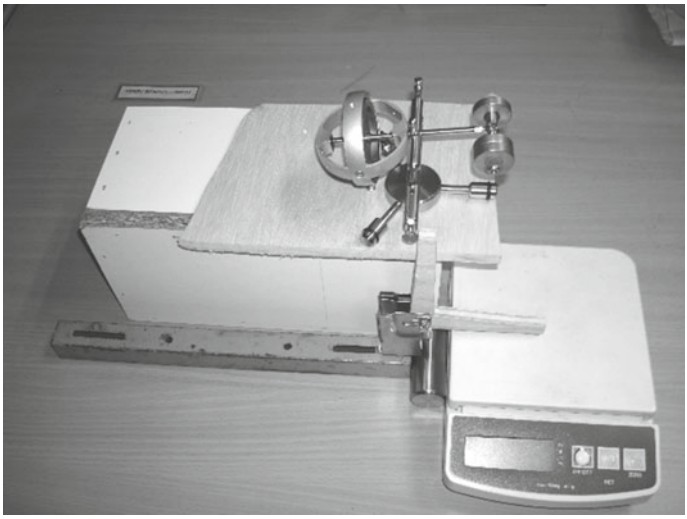

Fig. 8.4 Stand for measurement of the precession torque acting around axis *oy*

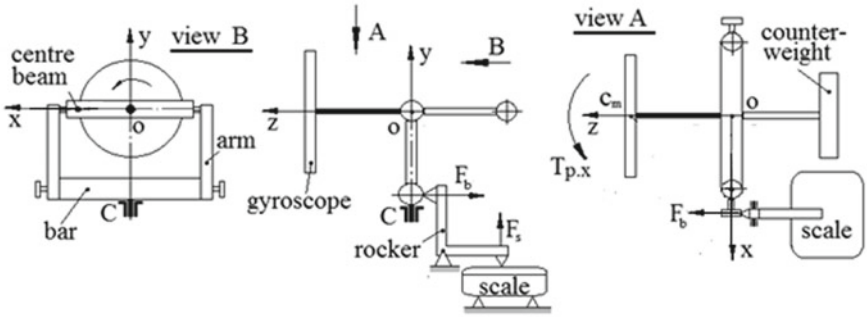

Fig. 8.5 Schematic of measurement value of the precession torque

$$\begin{aligned} T_{\text{am}} &= J\omega \times (3.086464199\cos 0^\circ - 2.595701613)\left(1 - \mathrm{e}^{-1.050580906t}\right) \\ &= 0.490762586 J\omega\left(1 - \mathrm{e}^{-1.050580906t}\right) \end{aligned} \tag{8.42}$$

where all parameters are as specified above.

The precession torque produces the reactive forces F_s of the digital scale (Fig. 8.5) that represented by the following equation:

$$F_{\text{s}} l_{\text{h}} = \frac{T_{\text{am}} l_{\text{v}}}{l_{\text{b}}/2} - \frac{T_{\text{am}}(d_{\text{r}}/2) f_{\text{r}}}{l_{\text{b}}/2} \quad \text{or} \quad F_{\text{s}} = \frac{2T_{\text{am}}}{l_{\text{h}} l_{\text{b}}}\left(l_{\text{v}} - \frac{d_{\text{r}} f_{\text{r}}}{2}\right) \tag{8.43}$$

where $l_{\text{h}} = 90.0$ mm, $l_{\text{v}} = 80.0$ mm and $l_{\text{b}} = 115.5$ mm is the length of the rocker's horizontal and vertical arm and the bar of the gimbal, respectively; $d_{\text{r}} = 4.0$ mm is

the diameter of the rocker's pivot; $f_r = 0.5$ is the friction coefficient in the rocker's pivot (wood-steel) [21]; other parameters are as specified above.

Substituting Eqs. (8.42) into Eq. (8.43) and transformation yield the following equation:

$$F_s = \frac{0.981525172}{l_h l_b}\left(l_v - \frac{d_r f_r}{2}\right) J\omega\left(1 - e^{-1.050580906t}\right) \tag{8.44}$$

where all parameters are as specified above and in Table 7.3.

The value of the force acting on the scale is calculated for the condition of the free turn of the gyroscope. The data calculated above and from the previous test (Table 7.3) are substituted into Eq. (8.35). The numerical value of the force acting on the scale is represented by the following expression:

$$F_s = \frac{0.981525172}{0.09 \times 0.1155}\left(0.08 - \frac{0.004 \times 0.5}{2}\right) 0.5726674 \times 10^{-4} \times 10{,}000 \times \frac{2\pi}{60}\left(1 - e^{-1.050580906t}\right) \tag{8.45}$$

Simplification of Eq. (8.45) yields the following result:

$$F_s = 0.447337306\left(1 - e^{-1.050580906t}\right) \tag{8.46}$$

The time of the gyroscope turn down is short, and the value of the force acting on the scale is computed for the time $t = 0.\ 2, 0.3, 0.4$ s because there are minor clearances between elements of the gimbal, rocker and its support. In such a condition, the manual measurement of the short time action of the gyroscope is problematic. The value of the force computed by Eq. 8.21 is represented by the following results proportional to the accepted time t of the gyroscope turn, respectively: $F_s = 0.084$; 0.120; 0.153 kg. The digital scale demonstrated similar values of the force. The value of the combined precession torque ($T_{inx} + T_{am}$) will be bigger than the value of the torque of the change in the angular momentum, T_{am}. The result obtained by the test of the precession torque confirms the correctness of the analytical solution that the blocking of the gyroscope rotation around axis oy deactivates all inertial torques generated by the rotating mass elements of the rotor. Also, this result validates the action of the precession torque of the change in the angular momentum of the spinning rotor which formula based on the expression of the centre mass.

8.2 Physics of Deactivation of Gyroscopic Inertial Forces

The equations of the inertial torques generated by the rotating masses of the spinning rotor (Table 3.1) are presented by the following expression:

$$T_i = D_i J \omega \omega_x \tag{8.47}$$

where D_i is the factor that depends on the type inertial torque, i.e. generated by the centrifugal, common inertial, Coriolis and the change in the angular momentum; other components are as specified above.

Equation (8.47) contains two variable components ω and ω_x which the product $\omega\omega_x = \varepsilon_y$ represents the acceleration around axis oy. The angular velocity of the spinning disc ω around axis oz is accepted as constant and does not change the value. The precession angular velocity of the gyroscope ω_x around axis ox is variable. The running gyroscope under the action of the external torque rotates around three axes ox, oy and oz. These motions express the work of the potential energy of the gyroscope weight and kinetic energy of the spinning disc along axes of motions. The kinetic energy of the spinning disc is expressed by the action of the change in the angular momentum around axis oz and by the action of the inertial torques generated by the centrifugal, common inertial and Coriolis forces around axes ox and oy. The action of all inertial torques around axes is interrelated. The vectorial diagram of the angular velocities and acceleration of the spinning disc and the gyroscope around axes are presented in Fig. 8.6. All rotational motions of the gyroscope around axes are in the counterclockwise directions if considered from the tips of the coordinate axes.

The blocking of the turn of the running gyroscope around axis oy causes rotation to stop the acceleration and rotation around this axis, i.e. $\omega\omega_x = \varepsilon_y = 0$. Since the angular velocity of the spinning disc ω is constant, the angular velocity of the precession around axis ox is an absence $\omega_x = 0$. It means all inertial torques (Eq. 8.47) have the zero values $T_i = 0$, i.e. they are deactivated formally for the accepted condition and should be proofed physically. The gyroscope starts to turn down under the action of

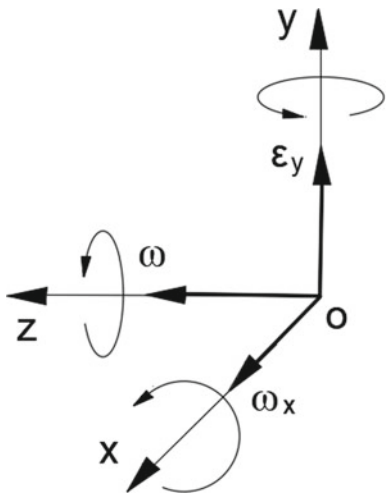

Fig. 8.6 Vectorial diagram of the velocities and acceleration of the gyroscope with spinning disc

the gyroscope weight and frictional forces acting on the supports that confirmed by the practical tests.

The new condition of the gyroscope motion around axis *ox* with the high angular velocity should generate the new values of inertial torques and frictional forces generated by the rotating mass of the spinning rotor. However, practice demonstrates their absence, except the action of the precession torque, which is carried out according to the principles of classical mechanics. Other inertial torques generated by the rotating mass elements of the spinning disc are deactivated and at the first blush contradicted to the laws of physics.

Analysis of the external and inertial torques acting on a gyroscope yields the following. The torques acting on the gyroscope and its motions around three axes are results of the work of potential and kinetic energies. The potential energy is expressed by the location of the gyroscope weight. The kinetic energy is expressed by the spinning of the disc around axis *oz* and gyroscope rotation around axes *ox* and *oy*. Analysis of the action of torques around three axes enables the formulation of the following principles:

- The kinetic energy of the spinning disc maintains its motion around axis *oz*;
- The external load torque generates the inertial torques acting around axis *ox* and *oy* that express the work of the potential and kinetic energies of the gyroscope around axes *ox* and *oy*;
- The kinetic energy of the spinning disc is redistributed along the axes proportionally to the ratio of angular velocities of the gyroscope by the principle of energy conservation.

Kinetic energies of the gyroscope along the axes of motions are manifested by the action of the angular momentums. The vectorial diagram of the angular momentum of the spinning disc and its changing at a starting condition under the action of the external torque on the gyroscope represented in Fig. 8.7.

The action of the external load torque T around axis *ox* on the spinning disc leads to the change in the location of the vector of the angular momentum H on the small angle γ_x that represented by the vector H_1. The value of H_1 is less than value H on the value of the change in the angular momentum ΔH_x. The latter is acting around

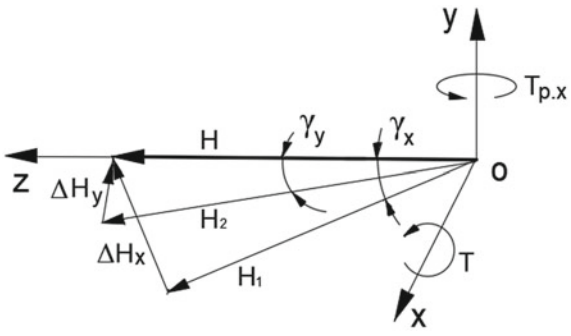

Fig. 8.7 Vectorial diagram of the components of the angular momentum of the spinning rotor

axis oy and changes in the location of the vector H on the angle γ_y. The value of the new vector H_2 is less than vector H on the value of the ΔH_y. The action of the torques ΔH_x and ΔH_y is simultaneous and expresses the changes in the values of the angular momentum of the spinning disc around axes ox and oy. This simple example demonstrates the redistribution of the value of the angular momentum of the spinning disc along the axes ox and oy of the rotation by the principle of the conservation of the angular momentum. These principles are confirmed by the following statements. The absence of the spin of the gyroscope's disc means the absence of its kinetic energy and hence the inertial torques around axes.

The gyroscope rotates around axes under the action of the system of the inertial torques that consume the part of the potential and kinetic energies of the spinning disc. The total value of the kinetic energies of the gyroscope about axes is constant according to principles of energy conservation. The interrelations of the kinetic energies along the axes indirectly express the ratio of the angular velocities $\omega_y = (4\pi^2 + 17)\omega_x$ of the gyroscope motions around axes (Chap. 4). The absence of the rotation of the gyroscope around axis oy ($\omega_y = 0$) means $\omega_x = 0$, i.e. the absence of kinetic energies and the inertial torques acting around these axes. The angular velocities ω_y and ω_x express the kinetic energies of the gyroscope rotation that are parts of the kinetic energy of the spinning disc.

From the previous discussion, the angular velocity ω_x of the gyroscope is the result of the action of the resisting resulting torque ($\Sigma T_{\text{r}} = (T_{\text{ct}\cdot x} + T_{\text{cr}\cdot x} + T_{\text{in}\cdot y} + T_{\text{am}\cdot y}$) and external torques T and T_{fx}. The angular velocity is a component of the inertial torques and when its value $\omega_x = 0$ means the resulting torque $\Sigma T_r = 0$ is absent. Then, the spinning rotor rotates around axis ox under the action only of the external load and frictional torques. The ratio of angular velocities around two axes $\omega_y = (4\pi^2 + 17)\omega_x$ is not maintained. This is the reason that the rotation of the spinning disc under the action of the external loads around axis ox does not generate new inertial torques that demonstrated the practical tests. The deactivation of the gyroscopic inertial torques is taking place according to the physical principle of the kinetic energy conservation for the rotating objects. The blocking of the motion of the gyroscope around axis oy does not lead to stopping of the rotation of the spinning disc around axis oz. The kinetic energy of the spinning rotor along axis oz is conserved, and the action of the external torque activates the change in the angular momentum at any conditions. The partial deactivation of the inertial torques is demonstrated on the example of the gyroscope nutation (Sect. 7.3, Chap. 7). The input torque of the short time action deactivates precession torques around two axes but the resistance torques are active. The resistance torques are active with the excess kinetic energy and deactivate at the example described in this chapter. Physics and conditions of the action and deactivation of the resistance torques of the gyroscope are not described and not explained. The conducted analysis partially explains the physics of the deactivation of the inertial torques generated by the rotating mass elements of the spinning disc and confirms the principle of the conservation of its angular momentum.

The phenomena of the deactivation of the gyroscopic inertial torques are very difficult to perceive against the background of generally accepted knowledge of

classical mechanics. The rejection of the deactivation of inertial forces is explained by the traditional examples in known publications that consider simple mechanisms and schemes of acting inertial forces on some objects. The motions of the gyroscope around three axes is not simple, and this is the reason that the solutions for its acting inertial forces and motions researchers could not find during the centuries. Presented above the explanation of the deactivation of the gyroscopic inertial torques also is not ordinary and needs deep analysis and comprehension. Nevertheless, the described physics of the deactivation of the inertial torques does not claim to be the ultimate truth and represents the challenge for the researchers in the area of dynamics of rotating objects.

The numerous publications for the computing of the inertial forces acting on the spinning objects consider examples with motions of the object around one axis. These examples are fitted for the simple solution by the action of the change in the angular momentum. The authors of these publications did know about the complexity of the action of the inertial torques on spinning objects and about the deactivation of them but presented the correct solutions. However, the publications that consider the complex motions of the gyroscopic devices represent wrong solutions for the action of the inertial torques. The action of the system interrelated inertial torques should be used for the solutions of the complex gyroscopic problems in engineering. A solution to such examples represents a good educational process for the course of engineering mechanics in the part of the dynamics of rotating objects.

References

1. Deimel, R.F.: Mechanics of the Gyroscope. Dover Publications Inc., New York (2003)
2. Greenhill, G.: Report on Gyroscopic Theory. General Books LLC, London (2010)
3. Scarborough, J.B.: The Gyroscope Theory and Applications. Nabu Press, London (2011)
4. Weinberg, H.: Gyro Mechanical Performance: The Most Important Parameter, pp. 1–5. Technical Article MS-2158, Analog Devices, Norwood, MA (2011)
5. Hibbeler, R.C.: Engineering Mechanics—Statics and Dynamics, 12th edn. Prentice Hall, Pearson (2010)
6. Gregory, D.R.: Classical Mechanics. Cambridge University Press, New York (2006)
7. Taylor, J.R.: Classical Mechanics. University Science Books, California (2005)
8. Aardema, M.D.: Analytical Dynamics. Theory and Application. Academic/Plenum Publishers, New York (2005)
9. Jewett, J., Serway, R.A.: Physics for Scientists and Engineers, 10 ed. Cengage Learning, Boston (2018)
10. Knight, R.D.: Physics for Scientists and Engineers: A Strategic Approach with Modern Physics, 4th edn. Pearson, London (2016)
11. Usubamatov, R.: Inertial forces acting on gyroscope. J. Mech. Sci. Technol. **32**(1), 101–108 (2018)
12. Usubamatov, R.: Properties of gyroscope motion about one axis. Int. J. Adv. Mech. Aeronautical Eng. **2**(1), 39–44 (2014)
13. Usubamatov, R.: Physics of gyroscope motion about one axis. Int. J. Adv. Mech. Aeronautical Eng. **2**(1), 55–60 (2015). ISSN: 2372-4153
14. Usubamatov, R.: Mathematical model for motions of gyroscope suspended from flexible cord. Cogent Eng. **3**, 1245901 (2016)

15. Usubamatov, R.: Deactivation of gyroscopic inertial forces. AIP Adv. **8**, 115310 (2018). https://doi.org/10.1063/1.5047103
16. Engineering ToolBox, Friction and Friction Coefficients for various Materials (2004). Available at: https://www.engineeringtoolbox.com/friction-coefficients-d_778.html
17. Machinery's Handbook 29th Edition—Large Print 29 Indexed Edition by Oberg, Erik published by Industrial Press (2012)
18. Sliding friction coefficients of smoothly processed (polished) non-lubricated surfaces. Physical Handbook, TehTab.ru (2014)Technical Tables. https://vk.com/tehtab
19. Peters, C.A.: Statistics for Analysis of Experimental Data. Princeton University (2001)
20. Usubamatov, R.: Deactivation of the gyroscope's inertial forces is the physical phenomena. In: Proceedings of 4th International Conference and Exhibition on Satellite & Space Missions, Rome, Italy, 18–20 June 2018
21. Usubamatov, R.: Theory of gyroscopic effects, deactivation of gyroscopic inertial forces. In: Proceedings of 3rd International Conference on Astronomy and Space Physics, London, UK, 2–3 May 2019

Appendix A
Mathematical Models for Inertial Forces Acting on Spinning Objects

The spinning objects in engineering are presented by numerous designs as the parts of the movable machines and mechanisms [1–5]. All rotating objects manifest gyroscopic effects which should be computed on the action of inertial forces and to receive the real dynamical parameters of the moving objects [6–11]. The rotating parts and components of the mechanisms can have different geometries where some of them are simple design as a disc, ring, cylinder [12]. The inertial torques of these mechanical parts are computed by known simple equations [13, 14]. Other rotating objects can have a complex form like a sphere, circular cone, paraboloid, propellers, etc. The mathematical models for inertial torques generated by the spinning objects of complex geometry should be defined for engineering mechanics. The derived method for computing of the inertial torques of the spinning disc (Chap. 3) contains several steps with detailed explanations of solutions [14–15]. This analytical approach is universal and can be used for the computing of inertial torques for rotating objects of different designs. The mathematical models for the inertial forces depend on the geometry of the spinning objects and different from for the flat spinning disc. The mass elements of the rotating objects are located on the surfaces that correspond to their geometries. Appendix A considers the application of the derived analytical method for computing the inertial torques for the several designs of rotating objects that are typical in engineering [16–18]. The steps for computing of the inertial torques acting on the spinning disc are used for others spinning objects. For new rotating objects, these steps are omitted with the aim do not repeat computing and pointed out the references to the sources.

© The Editor(s) (if applicable) and The Author(s), under exclusive license to Springer Nature Singapore Pte Ltd. 2020

R. Usubamatov, *Theory of Gyroscopic Effects for Rotating Objects*,
https://doi.org/10.1007/978-981-15-6475-8

A.1 Inertial Forces and Torques Acting on a Spinning Sphere

A.1.1 Centrifugal Forces Acting on a Spinning Sphere

The inertial forces acting on of the spinning sphere are generated by its centre mass and mass elements that distributed on the sphere. The mass elements of the spinning sphere rotate separately with different acceleration in uniform circular motions. This rotation of mass elements generates the centrifugal forces acting strictly perpendicular to axis *oz* of the spinning sphere.

The analytical approach for the modelling of the action of the centrifugal forces of the spinning sphere is similar to the spinning disc represented in Chap. 3. The rotating mass elements of the spinning sphere are located on the surface of the 2/3 sphere radius. The analysis of the acting inertial forces generated by the mass element of the sphere is considered on the arbitrary planes that parallel to the plane of the maximal diameter of the sphere (Fig. A.1) that is the same as the plane of the thin disc represented in Fig. 3.2 of Chap. 3. The plane of the mass elements generates the change in the vector's components $f_{\text{ct.}z}$, whose directions are parallel to the spinning sphere axle *oz*. The integrated product of components for the vector's change in the centrifugal forces $f_{\text{ct.}z}$ and their variable radius of location relative to axis *ox* generate the resistance torque T_{ct} acting opposite to the external torque.

The resistance torque ΔT_{ct} produced by the centrifugal force of the mass element of the sphere is expressed by the following equation:

$$\Delta T_{\text{ct}} = -f_{\text{ct.}z}\, y_{\text{m}} \tag{A.1.1}$$

where $f_{\text{ct.}z}$ is the axial component of the centrifugal force; and y_{m} is the distance of the location of the mass element along axis *oy*.

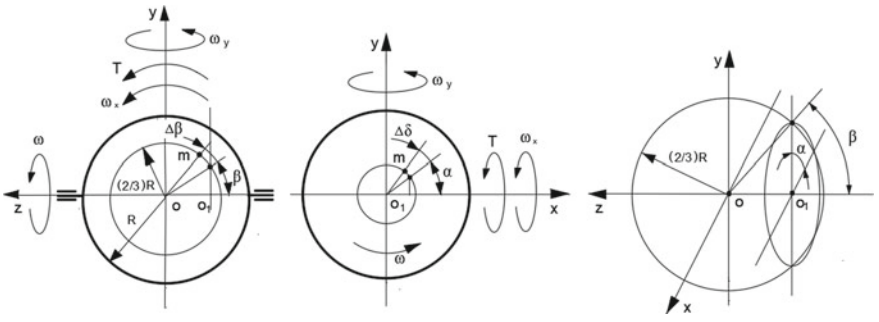

Fig. A.1 Schematic of the spinning sphere

The axial component of the mass element's centrifugal force for arbitrarily chosen plane at the semisphere is represented by the following equation:

$$f_{\text{ct}.z} = f_{\text{ct}} \sin\beta \sin\alpha \sin\Delta\gamma = mr\omega^2 \sin\beta \sin\alpha \sin\Delta\gamma$$
$$= \left[\frac{M(2/3)R\sin\alpha \sin\beta\omega^2}{4\pi}\Delta\delta\Delta\beta\right]\sin\Delta\gamma = \frac{MR\omega^2}{6\pi}\Delta\delta\Delta\gamma\sin\alpha\sin\beta \tag{A.1.2}$$

where $f_{\text{ct}} = mr\sin\alpha\sin\beta\omega^2 = \left[\frac{M(2/3)R\omega^2\sin\alpha\sin\beta}{4\pi}\Delta\delta\right]$ is the centrifugal force of the mass element m; $m = \frac{M}{4\pi[(2/3)R]^2}\Delta\delta[(2/3)R]^2 = \frac{M}{4\pi}\Delta\delta$, M is the mass of the sphere; 4π is the spherical angle; $\Delta\delta$ is the spherical angle of the mass element's location; $r = (2/3)R\sin\alpha\sin\beta$ is the radius of the mass elements location; R is the external radius of the sphere; ω is the constant angular velocity of the sphere; α is the angle of the mass element's location on the plane that parallel to plane xoz; β is the angle of the mass element's location on the plane pass axis oz; $\Delta\gamma$ is the angle of turn for the sphere's plane around axis ox ($\sin\Delta\gamma = \Delta\gamma$ for the small values of the angle) (Fig. 3.2, Chap. 3).

Substituting the defined parameters into Eq. (A.1.1) yields the following equation:

$$\Delta T_{\text{ct}} = -\frac{MR\omega^2}{6\pi}\Delta\delta\Delta\gamma\sin\alpha\sin\beta \times y_{\text{m}}$$
$$= -\frac{MR\omega^2}{6\pi}\Delta\delta\Delta\gamma\sin\alpha\sin\beta \times \frac{2}{3}R\sin\alpha\sin\beta$$
$$= -\frac{MR^2\omega^2}{9\pi}\Delta\delta\Delta\gamma\sin^2\alpha\sin^2\beta \tag{A.1.3}$$

where $y_{\text{m}} = (2/3)R\sin\alpha\sin\beta$ (Fig. A.1) is the distance of the mass element's location on the sphere's plane relative to axis ox, other components are as specified above.

The action of the centrifugal forces' $f_{\text{ct}.z}$ axial components represents the distributed load where the sphere's mass elements are located (Fig. 3.2, Chap. 3). The resultant torque is the product of the resultant centrifugal forces and the centroid at the semicircle. The location of the resultant force of the one plane is the centroid (point A, Fig. 3.2, Chap. 3) that is defined by the expression y_{m}. For the hemisphere, the centroid is defined by the following expression:

$$y_{\text{A}} = \frac{\int_{\alpha=0}^{\pi}\int_{\beta=0}^{\pi} f_{\text{ct}.z}\, y_{\text{m}}\,\text{d}\alpha\,\text{d}\beta}{\int_{\alpha=0}^{\pi}\int_{\beta=0}^{\pi} f_{\text{ct}.z}\,\text{d}\alpha\,\text{d}\beta} = \frac{\int_{\alpha=0}^{\pi}\frac{MR\omega^2}{6\pi}\Delta\delta\Delta\gamma\frac{2}{3}R\sin^2\alpha\,\text{d}\alpha\int_0^{\pi}\sin\beta^2\,\text{d}\beta}{\int_{\alpha=0}^{\pi}\frac{MR\omega^2}{6\pi}\Delta\delta\Delta\gamma\sin\alpha\,\text{d}\alpha\int_0^{\pi}\sin\beta\,\text{d}\beta}$$
$$= \frac{\frac{MR\omega^2}{6\pi}\Delta\delta\Delta\gamma\int_{\alpha=0}^{\pi}\frac{2}{3}R\sin^2\alpha\,\text{d}\alpha\int_0^{\pi}\sin\beta^2\,\text{d}\beta}{\frac{MR\omega^2}{6\pi}\Delta\delta\Delta\gamma\int_{\alpha=0}^{\pi}\sin\alpha\,\text{d}\alpha\int_0^{\pi}\sin\beta\,\text{d}\beta}$$

$$= \frac{R\int_0^{\pi}(1-\cos 2\alpha)\mathrm{d}\alpha \int_0^{\pi}(1-\cos 2\beta)\mathrm{d}\beta}{6\int_0^{\pi}\sin\alpha\mathrm{d}\alpha \int_0^{\pi}\sin\beta\mathrm{d}\beta} \tag{A.1.4}$$

where the expression $\frac{MR\omega^2}{6\pi}\Delta\delta\Delta\gamma$ is accepted at this stage of computing as constant for Eq. (A.1.4); the expression $\sin^2\alpha = (1-\cos 2\alpha)/2$ is a trigonometric identity that replaced in the equation for α and β, and other parameters are as specified above.

Equation (A.1.3) and its components are expressed for integration by a differential form where $\sin^2\alpha = \int_0^{\pi} 2\sin\alpha\cos\alpha\mathrm{d}\alpha$ and$\sin^2\beta = \int_0^{\pi} 2\sin\beta\cos\beta\mathrm{d}\beta$; defined components is substituted into Eq. (A.1.3) and represented by the integral form. The solution to the integral is considered for the hemisphere. The upper limit for $\mathrm{d}\delta$ is represented by the area of the hemisphere. Substituting defined parameters and expressing by the integral forms, the following equation emerges:

$$\begin{aligned}\int_0^{T_{\mathrm{ct}}}\mathrm{d}T_{\mathrm{ct}} &= -\frac{MR\omega^2}{9\pi}\int_0^{\pi}\mathrm{d}\delta\int_0^{\gamma}\mathrm{d}\gamma\times\int_0^{\pi}2\sin\alpha\cos\alpha\mathrm{d}\alpha\int_0^{\pi}2\sin\beta\cos\beta\mathrm{d}\beta\\ &\times\frac{R\int_0^{\pi}(1-\cos 2\alpha)\mathrm{d}\alpha\int_0^{\pi}(1-\cos 2\beta)\mathrm{d}\beta}{6\int_0^{\pi}\sin\alpha\mathrm{d}\alpha\int_0^{\pi}\sin\beta\mathrm{d}\beta}\\ &= -\frac{MR^2\omega^2}{54\pi}\int_0^{\pi}\mathrm{d}\delta\int_0^{\gamma}\mathrm{d}\gamma\times\int_0^{\pi}2\sin\alpha\mathrm{d}\sin\alpha\int_0^{\pi}2\sin\beta\mathrm{d}\sin\beta\\ &\times\frac{\int_0^{\pi}(1-\cos 2\alpha)\mathrm{d}\alpha\int_0^{\pi}(1-\cos 2\beta)\mathrm{d}\beta}{\int_0^{\pi}\sin\alpha\mathrm{d}\alpha\int_0^{\pi}\sin\beta\mathrm{d}\beta}\end{aligned} \tag{A.1.5}$$

Solving integral Eq. (A.1.5) yields the following result:

$$\begin{aligned}T_{\mathrm{ct}}\Big|_0^{T_{\mathrm{ct}}} &= -\frac{MR^2\omega^2}{54\pi}\times\left(\delta\Big|_0^{\pi}\right)\times\left(\gamma\Big|_0^{\gamma}\right)\times 2\left(\sin^2\alpha\Big|_0^{\pi/2}\right)\times 2\left(\sin^2\beta\Big|_0^{\pi/2}\right)\\ &\times\quad\frac{\left(\alpha-\frac{1}{2}\sin 2\alpha\right)\Big|_0^{\pi/2}\times\left(\beta-\frac{1}{2}\sin 2\beta\right)\Big|_0^{\pi/2}}{-\cos\alpha\Big|_0^{\pi}\times(-)\cos\beta\Big|_0^{\pi}}\end{aligned}$$

The change of the upper limit for the trigonometric expression sinus is compensated by increasing the result twice. For the expressions $\sin 2\alpha$ and $\sin 2\beta$, the limit is the same due to the symmetrical location of the centroid. The solution of the expression yields the following:

$$\begin{aligned}T_{\mathrm{ct}} &= -4\times\frac{MR^2\omega^2}{54\pi}\times(\pi-0)\times(\gamma-0)\times 2(1-0)\\ &\times 2(1-0)\times\frac{\left(\frac{\pi}{2}-0\right)\times\left(\frac{\pi}{2}-0\right)}{(-1-1)\times(-1-1)} = \frac{MR^2\omega^2\pi^2}{54}\gamma\end{aligned} \tag{A.1.6}$$

The following steps of a solution are the same as represented in Sect. 3.1 of Chap. 3, which comments are omitted.

$$\frac{\mathrm{d}T_{\mathrm{ct}}}{\mathrm{d}t} = -\frac{MR^2\omega^2\pi^2}{54}\frac{\mathrm{d}\gamma}{\mathrm{d}t} \tag{A.1.7}$$

$t = \frac{\alpha}{\omega}$, $\mathrm{d}t = \frac{\mathrm{d}\alpha}{\omega}$, $\frac{\mathrm{d}\gamma}{\mathrm{d}t} = \omega_x$

$$\frac{\omega \mathrm{d}T_{\mathrm{ct}}}{\mathrm{d}\alpha} = -\frac{MR^2\omega^2\omega_x\pi^2}{54} \tag{A.1.8}$$

$$\mathrm{d}T_{\mathrm{ct}} = -\frac{MR^2\pi^2\omega\omega_x}{54}\mathrm{d}\alpha. \tag{A.1.9}$$

$$\int_0^{T_{\mathrm{ct}}} \mathrm{d}T_{\mathrm{ct}} = -\int_0^{\pi} \frac{MR^2\pi^2\omega\omega_x}{54}\mathrm{d}\alpha \tag{A.1.10}$$

$$T_{\mathrm{ct}}\Big|_0^{T_{\mathrm{ct}}} = -\frac{MR^2\pi^2\omega\omega_x}{54}\alpha\Big|_0^{\pi} \tag{A.1.11}$$

The centrifugal forces act on the upper and lower sides of the sphere's plane, then the total resistance torque T_{ct} is obtained when the result of Eq. (A.1.11) is increased twice:

$$T_{\mathrm{ct}} = -\frac{2\pi^3 MR^2\omega\omega_x}{54} = -\frac{5}{54}\pi^3 J\omega\omega_x \tag{A.1.12}$$

where $J = 2MR^2/5$ is the sphere mass moment of inertia; other parameters are as specified above.

A.1.2 Common Inertial Forces Acting on a Spinning Sphere

The modelling of the action of the common inertial forces generated by the mass elements of the spinning sphere is the same as represented for the spinning disc in Sect. 3.2 of Chap. 3. The equation for the precession torque generated by the common inertial forces is the same as for the resistance torque generated by the centrifugal forces of the spinning sphere that presented Eq. (A.1.12):

$$T_{\mathrm{in}} = \frac{5}{54}\pi^3 J\omega\omega_x \tag{A.1.13}$$

where all components are represented in Sect. A.1.1.

A.1.3 Coriolis Forces Acting on a Spinning Sphere

The modelling of the action of Coriolis forces generated by the mass elements of the spinning sphere is the same as represented for the spinning disc in Sect. 3.3 of Chap. 3. Similar Coriolis forces are generated by the rotating mass elements located on parallel planes of the sphere. The resistance torque ΔT_{cr} generated by Coriolis force of the mass elements f_{cr} of the spinning sphere is expressed by the following equation:

$$\Delta T_{\mathrm{cr}} = f_{\mathrm{cr}} y_{\mathrm{m}} = m a_z y_{\mathrm{m}} \tag{A.1.14}$$

where $y_{\mathrm{m}} = (2/3)R\ \sin\alpha\ \sin\beta$ is the distance to the mass element's location along axis *oy;* other components are represented in Eq. (A.1.2) of Sect. A.1.1.

The expression for a_{z} is represented by the following equation:

$$\alpha_z = \frac{\mathrm{d}V_z}{\mathrm{d}t} = \frac{\mathrm{d}(V\cos\alpha\sin\Delta\gamma)}{\mathrm{d}t} = -V\cos\alpha\frac{\mathrm{d}\gamma}{\mathrm{d}t} = -\frac{2}{3}R\omega\omega_x\cos\alpha\sin\beta \tag{A.1.15}$$

where $a_{\mathrm{z}} = \mathrm{d}V_{\mathrm{z}}/\mathrm{d}t$ is Coriolis acceleration of the mass element along axis *oz*; $V_{\mathrm{z}} = V\ \cos\alpha\ \sin\Delta\gamma = (2/3)R\omega\ \cos\alpha\ \sin\beta\ \sin\Delta\gamma$ is the change in the tangential velocity V of the mass element; other components are represented in Sect. A.1.1.

Substituting defined data into the expression of Coriolis force (Eq. 1.14) is represented by the following expression:

$$f_{\mathrm{cr}} = \frac{M\Delta\delta}{4\pi}\frac{2}{3}R\omega\omega_x\cos\alpha\sin\beta = \frac{MR\Delta\delta}{6\pi}\omega\omega_x\cos\alpha\sin\beta \tag{A.1.16}$$

Substituting defined parameters into Eq. (1.16) and transforming yield the following equation:

$$\Delta T_{\mathrm{cr}} = \frac{MR\omega\omega_x\Delta\delta}{6\pi}\cos\alpha\sin\beta\times y_{\mathrm{m}} \tag{A.1.17}$$

The location of the resultant force is the centroid (point *C*, Fig. 3.4, Chap. 3) of the area under the Coriolis force's curve calculated by Eq. (A.1.4), but with symbols of the sphere. The centroid point *C* is defined for the resultant force acting around axis *oz*.

$$y_{\mathrm{C}} = \frac{\int_{\alpha=0}^{\pi}\int_{\beta=0}^{\pi} f_{\mathrm{cr}} y_{\mathrm{m}}\mathrm{d}\alpha\mathrm{d}\beta}{\int_{\alpha=0}^{\pi}\int_{\beta=0}^{\pi} f_{\mathrm{cr}}\mathrm{d}\alpha\mathrm{d}\beta} = \frac{\int_{\alpha=0}^{\pi}\int_{\beta=0}^{\pi}\frac{MR\omega\omega_x\Delta\delta}{6\pi}\cos\alpha\sin\beta\times\frac{2}{3}R\sin\alpha\sin\beta\mathrm{d}\alpha\mathrm{d}\beta}{\int_{\alpha=0}^{\pi}\int_{\beta=0}^{\pi}\frac{MR\omega\omega_x\Delta\delta}{6\pi}\cos\alpha\sin\beta\mathrm{d}\alpha\mathrm{d}\beta}$$
$$= \frac{\frac{MR\omega\omega_x\Delta\delta}{6\pi}\int_{\alpha=0}^{\pi}\frac{2}{3}R\sin\alpha\cos\alpha\mathrm{d}\alpha\times\int_0^{\pi}\sin^2\beta\mathrm{d}\beta}{\frac{MR\omega\omega_x\Delta\delta}{6\pi}\int_{\alpha=0}^{\pi}\cos\alpha\mathrm{d}\alpha\times\int_0^{\pi}\sin\beta\mathrm{d}\beta}$$

$$= \frac{\frac{2}{3}R\int_0^{\pi}\sin\alpha \mathrm{d}\sin\alpha \times \int_0^{\pi}\sin^2\beta \mathrm{d}\beta}{\int_0^{\pi}\cos\alpha \mathrm{d}\alpha \times \int_0^{\pi}\sin\beta \mathrm{d}\beta}$$
$$= \frac{\frac{2}{3}R\int_0^{\pi}\sin\alpha \mathrm{d}\sin\alpha \times \frac{1}{2}\int_0^{\pi}(1-\cos 2\beta)\mathrm{d}\beta}{\int_0^{\pi}\cos\alpha \mathrm{d}\alpha \times \int_0^{\pi}\sin\beta \mathrm{d}\beta} \tag{A.1.18}$$

where the expression $\frac{MR\omega\omega_x\Delta\delta}{6\pi}$ is accepted as constant and the expression $\sin^2\beta = \frac{1}{2}(1-\cos 2\beta)$is represented by the trigonometric identity for Eq. (A.1.18).

The expression of y_C (Eq. A.1.18) is substituted into Eq. (A.1.17) where $\cos\alpha = \int_0^{\pi} -\sin\alpha \mathrm{d}\alpha$, $\sin\beta = \int_0^{\pi}\cos\beta \mathrm{d}\beta$ and represented by the integral form.

$$\int_0^{T_{cr}} \mathrm{d}T_{cr} = \frac{MR\omega\omega_x}{6\pi} \times \int_0^{\pi}\mathrm{d}\delta \times \int_0^{\pi} -\sin\alpha d\alpha \int_0^{\pi}\cos\beta \mathrm{d}\beta$$
$$\times \frac{\frac{2}{3}R\int_0^{\pi}\sin\alpha \mathrm{d}\sin\alpha \times \frac{1}{2}\int_0^{\pi}(1-\cos 2\beta)\mathrm{d}\beta}{\int_0^{\pi}\cos\alpha \mathrm{d}\alpha \times \int_0^{\pi}\sin\beta \mathrm{d}\beta} \tag{A.1.19}$$

where the limits of integration for the trigonometric expression of sinus are taken for the quarter and half of the circle and result are increased twice; for the y_C is no change because the location of the centroid is symmetrical; other components integrated for the hemisphere.

Solving integral Eq. (A.1.19) yields the following result:

$$T_{cr}\Big|_0^{T_{cr}} = \frac{MR\omega\omega_x}{6\pi} \times \left(\delta\Big|_0^{\pi}\right) \times \left(\cos\alpha\Big|_0^{\pi}\right) \times 2\left(\sin\beta\Big|_0^{\pi/2}\right)$$
$$\times \frac{\frac{1}{3}R\sin^2\alpha\Big|_0^{\pi/2} \times \frac{1}{2}(\beta - \frac{1}{2}\sin 2\beta)\Big|_0^{\pi/2}}{\sin\alpha\Big|_0^{\pi/2} \times \left(-\cos\beta\Big|_0^{\pi}\right)}$$

that giving the rise to the following

$$T_{cr} = \frac{MR^2\omega\omega_x}{6\pi} \times (\pi - 0) \times (-1-1) \times 2(1-0)$$
$$\times \frac{\frac{1}{3}R(1-0) \times \frac{1}{2}\left(\frac{\pi}{2}-0\right)}{(1-0)\times[-(-1-1)]} = \frac{MR^2\pi\omega\omega_x}{36} \tag{A.1.20}$$

When Coriolis forces act on the left and right sides of the quarter-sphere, then the total resistance torque T_{cr} is obtained when the result of Eq. (A.1.20) is increased four times:

$$T_{cr} = \frac{4MR^2\pi\omega\omega_x}{36} = \frac{5}{18}\pi J\omega\omega_x \tag{A.1.21}$$

where $J = 2MR^2/5$ is the sphere mass moment of inertia; other parameters are as specified above.

A.1.4 Attributes of the Inertial Torques Acting on the Spinning Sphere

The total initial precession torque acting around axis oy of the spinning sphere has represented a sum of the precession torques generated by the common inertial forces of the mass elements and the change in the angular momentum ($T_{\text{am}} = J\omega\omega_x$) whose equation is as follows:

$$T_{\text{r}} = T_{\text{in}} + T_{\text{am}} = \left(\frac{5}{54}\pi^3 + 1\right) J\omega\omega_x \tag{A.1.22}$$

where T_{p} is the total precession torque acting around axis *oy* of the spinning sphere. Other components are as specified above.

The total initial resistance torque T_{r} acting around axis ox has represented a sum of the resistance torques generated by the centrifugal and Coriolis forces of the sphere's mass elements whose equation is as follows:

$$T_r = T_{ct} + T_{cr} = \left(\frac{5}{54}\pi^3 + \frac{5}{18}\pi\right) J\omega\omega_x = \frac{5}{18}\pi\left(\frac{\pi^2}{3} + 1\right) J\omega\omega_x \tag{A.1.23}$$

where all components are as specified above.

The mathematical models for internal torques acting on the spinning sphere are represented in Table A.1.

The equations for the inertial torques acting on the spinning sphere [13] are different than for the spinning disc.

Table A.1 Equations of the internal torques acting on the spinning sphere

Type of the torque generated by	Equation
Centrifugal forces	$T_{\text{ct}} = T_{\text{in}} = \frac{5}{54}\pi^3 J\omega\omega_x$
Inertial forces	
Coriolis forces	$T_{\text{cr}} = \frac{5}{18}\pi J\omega\omega_x$
Change in an angular momentum	$T_{\text{am}} = J\omega\omega_x$
Resistance torque $T_{\text{r}} = T_{\text{ct}} + T_{\text{cr}}$	$T_r = \frac{5}{18}\pi\left(\frac{\pi^2}{3} + 1\right) J\omega\omega_x$
Precession torque $T_{\text{p}} = T_{\text{in}} + T_{\text{am}}$	$T_{\text{p}} = \left(\frac{5}{54}\pi^3 + 1\right) J\omega\omega_x$

A.1.5 Working Example

The sphere has a mass of 1.0 kg, a radius of 0.1 m and spinning at 3000 rpm. An external torque acts on the sphere, which rotates with an angular velocity of 0.05 rpm. It is determined by the value of the resistance and precession torques acting on the spinning sphere (Fig. A.1). Substituting the initial data into equations of Table A.1 and transforming yield the following result:

- Resistance torque T_{r}

$$T_r = \tfrac{5}{18}\pi\left(\tfrac{\pi^2}{3}+1\right)J\omega\omega_x = \tfrac{5}{18}\pi\left(\tfrac{\pi^2}{3}+1\right)\times\tfrac{2MR^2}{5}J\omega\omega_x = \tfrac{5}{18}\pi\left(\tfrac{\pi^2}{3}+1\right)\times\tfrac{2}{5}\times 1.0\times 0.1^2\times\tfrac{3000\times 2\pi}{60}\times\tfrac{0.05\times 2\pi}{60} = 0.024632\ \text{Nm}$$

- Precession torque T_{p}

$$T_p = \left(\tfrac{5}{54}\pi^3+1\right)J\omega\omega_x = \left(\tfrac{5}{54}\pi^3+1\right)\times\tfrac{2}{5}\times 1.0\times 0.1^2\times\tfrac{3000\times 2\pi}{60}\times\tfrac{0.05\times 2\pi}{60} = 0.025469\ \text{Nm}$$

where all parameters are as specified above.

A.2 Inertial Forces Acting on a Spinning Circular Cone

A.2.1 Centrifugal Forces Acting on a Spinning Cone

The inertial forces acting on of the spinning cone are generated by its centre mass and mass elements that distributed on the line forming the cone. In uniform circular motions, the rotation of mass elements generates the centrifugal forces, which act strictly perpendicular to the axis oz of the spinning cone (Fig. 3.1, Chap. 3). The action of an external torque on the spinning cone inclines the plane of the rotating centrifugal forces that resist the action of the external torque. The circular cone's mass elements m are located on the cone whose arbitrary radius is r and the length b, creating their rotating cone around axes oz.

The analytical approach for the modelling of the action of the centrifugal forces generated by the mass elements of the spinning cone is the same as represented for the spinning disc in Sect. 3.1, Chap. 3. The rotating mass elements of the spinning cone are located on the cone surface which maximal radius is the 2/3 radius of the base of the cone. The analysis of the acting inertial forces generated by the mass element of the cone is considered on the arbitrary planes that parallel to the plane of the base of

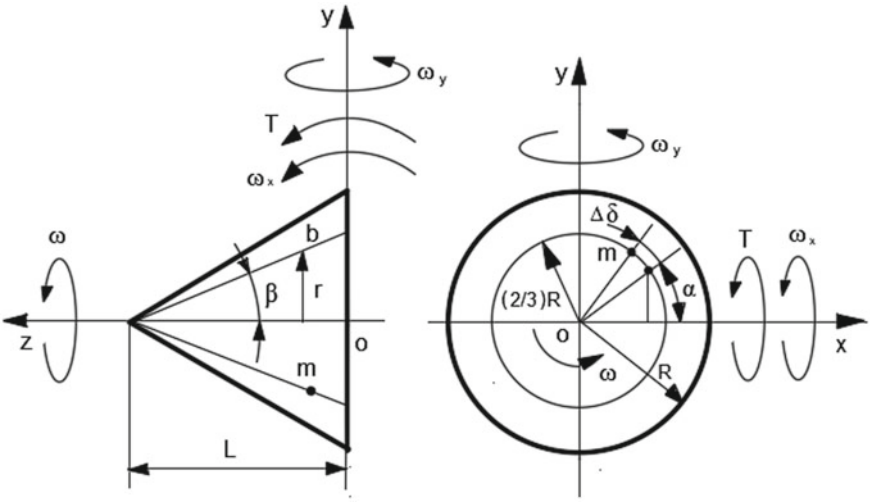

Fig. A.2 Schematic of the spinning cone

the cone (Fig. A.2) that is the same as the plane of the thin disc represented in Fig. 3.2 of Chap. 3. Similar resistance torques are generated by the mass elements located on the planes of the cone that parallel to the plane *xoy*. The resistance torque ΔT_{ct} produced by the centrifugal force of the mass element is expressed by the following equation:

$$\Delta T_{ct} = f_{ct.z} y_m \tag{A.2.1}$$

where is $f_{ct.z}$ is the axial component of the centrifugal force; $y_m = (2/3)(2/3)R \sin\alpha = (4/9)R \sin\alpha$ is the distance of the location of the cone's plane of the centre mass and mass element along axis *oz* and relatively to axis *ox*.

The equation for the axial component of the centrifugal force for the arbitrarily chosen plane of the cone is presented by the following:

$$f_{ct.z} = f_{ct} \sin\alpha \sin\Delta\gamma = mr\omega^2 \sin\alpha \sin\Delta\gamma \tag{A.2.2}$$

where $f_{ct} = mr \sin\alpha\omega^2$ is the centrifugal force of the mass element m; $m = (M/2\pi b)\Delta\delta\Delta b$, M is the mass of the cone; $b = [(2/3)R]/\sin\beta$ is the line that forms the cone surface of the mass element's location, R and L is the radius and height of the cone, respectively, $\Delta\delta$ is the sector's angle of the mass element's location on the plane that parallel to the plane *xoy*; $\Delta b = \Delta r/\sin\beta$ is the line part of the mass element's location, r is the radius of the arbitrary circle plane of the cone where the mass elements located; ω is the constant angular velocity of the cone; β is the angle of the mass element's location on the cone forming line (Fig. A.2); $\Delta\gamma$ is the angle of turn for the cone's plane around axis *ox* ($\sin\Delta\gamma = \Delta\gamma$ for the small values of the angle).

Substituting the defined parameters into Eq. (A.2.2) yields the following equation:

$$f_{\mathrm{ct}.z} = \left[\frac{Mr\omega^2 R\sin\beta\sin\alpha}{2\pi(2/3)R\sin\beta}\right]\Delta r\Delta\delta\Delta\gamma = \frac{3M\omega^2}{4\pi R}\Delta\delta\Delta\gamma r\Delta r\sin\alpha \tag{A.2.3}$$

where all components are as specified above.

Equation (A.2.3) contains variable parameters whose incremental components are independent and represented by different symbols. The action of the centrifugal forces' axial components presents the distributed load applied across the length of the line forming the cone. The distributed loads are equated with a concentrated load applied at a specific point along axis *oy*, which is the centroid at the semicircle and the triangle of the cone. The centroid y_{A} is defined by the expression y_{m} that represented by the following equation:

$$\begin{aligned} y_{\mathrm{A}} &= \frac{\int_{\alpha=0}^{\pi}\int_{r=0}^{(2/3)R} f_{\mathrm{ct}.z}\, y_{\mathrm{m}}\mathrm{d}\alpha\mathrm{d}r}{\int_{\alpha=0}^{\pi}\int_{r=0}^{(2/3)R} f_{\mathrm{ct}.z}\mathrm{d}\alpha\mathrm{d}r} \\ &= \frac{\int_{\alpha=0}^{\pi}\frac{3M\omega^2}{4\pi R}\Delta\gamma\Delta\delta\times\frac{4}{9}R\sin\alpha\sin\alpha\mathrm{d}\alpha\int_0^{(2/3)R} r\mathrm{d}r}{\int_{\alpha=0}^{\pi}\frac{3M\omega^2}{4\pi R}\Delta\gamma\Delta\delta\sin\alpha\mathrm{d}\alpha\int_0^{(2/3)R} r\mathrm{d}r} \\ &= \frac{\frac{M\omega^2}{3\pi}\Delta\gamma\Delta\delta\int_{\alpha=0}^{\pi}\sin^2\alpha\mathrm{d}\alpha}{\frac{3M\omega^2}{4\pi R}\Delta\gamma\Delta\delta\int_{\alpha=0}^{\pi}\sin\alpha\mathrm{d}\alpha} = \frac{2R\int_0^{\pi}(1-\cos 2\alpha)\mathrm{d}\alpha}{9\int_0^{\pi}\sin\alpha\mathrm{d}\alpha} \end{aligned} \tag{A.2.4}$$

where the expression $\frac{3M\omega^2}{4\pi R}\Delta\delta\Delta\gamma$ is accepted at this stage of computing as constant for Eq. (A.2.4); the expressionsin$^2\alpha = (1-\cos 2\alpha)/2$is a trigonometric identity that replaced in the equation, and other parameters are as specified above.

Substituting Eqs. (A.2.4) and (A.2.3) into Eq. (A.2.1) and replacing $\sin\alpha = \int_0^{\pi}\cos\alpha\mathrm{d}\alpha$ by the integral expression with defined limits and representing other components by the integral forms and transformation, the following equation emerges:

$$\begin{aligned} \int_0^{T_{\mathrm{ct}}}\mathrm{d}T_{\mathrm{ct}} = \frac{3M\omega^2}{4\pi R}\times\int_0^{\pi}\mathrm{d}\delta\times\int_0^{\pi}\cos\alpha\mathrm{d}\alpha\times\int_0^{\gamma}\mathrm{d}\gamma\times\int_0^{(2/3)R} r\mathrm{d}r \\ \times\frac{2R\int_0^{\pi}(1-\cos 2\alpha)\mathrm{d}\alpha}{9\int_0^{\pi}\sin\alpha\mathrm{d}\alpha} \end{aligned} \tag{A.2.5}$$

where the limits of integration for the trigonometric expression of sinus are taken for the quarter of the circle and result are increased twice.

Following steps of solutions are the same as presented in Sect. A.1.1 of Appendix A.

$$T_{\mathrm{ct}}\Big|_0^{T_{\mathrm{ct}}} = \frac{3M\omega^2}{4\pi R} \times \delta\Big|_0^{\pi} \times 2\left(\sin\alpha\Big|_0^{\pi/2}\right) \times (\gamma) \times \left(\frac{r^2}{2}\Big|_0^{(2/3)R}\right) \times \frac{2R\left(\alpha - \frac{1}{2}\sin 2\alpha\right)\Big|_0^{\pi}}{-9\cos\alpha\Big|_0^{\pi}}$$

$$T_{\mathrm{ct}} = \frac{3M\omega^2}{4\pi R} \times \pi \times 2(1-0) \times (\gamma - 0) \times \left(\frac{2}{9}R^2 - 0\right) \times \frac{2R(\pi - 0)}{-9(-1-1)} = \frac{MR^2\pi\omega^2}{27} \times \gamma \tag{A.2.6}$$

$$\frac{\mathrm{d}T_{\mathrm{ct}}}{\mathrm{d}t} = \frac{MR^2\pi\omega^2}{27}\frac{\mathrm{d}\gamma}{\mathrm{d}t} \tag{A.2.7}$$

$t = \frac{\alpha}{\omega}$, $\mathrm{d}t = \frac{d\alpha}{\omega}$, $\frac{\mathrm{d}\gamma}{\mathrm{d}t} = \omega_x$

$$\frac{\omega \mathrm{d}T_{\mathrm{ct}}}{\mathrm{d}\alpha} = \frac{MR^2\pi\omega^2\omega_x}{27} \tag{A.2.8}$$

$$\mathrm{d}T_{\mathrm{ct}} = \frac{MR^2\pi\omega\omega_x}{27}\mathrm{d}\alpha \tag{A.2.9}$$

$$\int_0^{T_{\mathrm{ct}}} \mathrm{d}T_{\mathrm{ct}} = \int_0^{\pi} \frac{MR^2\pi\omega\omega_x}{27}\mathrm{d}\alpha \tag{A.2.10}$$

$$T_{\mathrm{ct}}\Big|_0^{T_{\mathrm{ct}}} = \frac{MR^2\pi\omega\omega_x}{27}\alpha\Big|_0^{\pi}$$

$$T_{\mathrm{ct}} = \frac{MR^2\pi^2\omega\omega_x}{27} \tag{A.2.11}$$

The change in centrifugal forces acts on the upper and lower sides of the cone's, then the total resistance torque T_{ct} is obtained when the result of Eq. (A.2.11) is increased twice.

$$T_{\mathrm{ct}} = \frac{2MR^2\pi^2\omega\omega_x}{27} = \frac{20}{81}\pi^2 J\omega\omega_x \tag{A.2.12}$$

where $J = 3MR^2/10$ is the cone's mass moment of inertia. The other parameters are as specified above.

A.2.2 Common Inertial Forces Acting on a Spinning Cone

The modelling of the acting common inertial forces generated by the mass elements of the spinning cone is the same as represented in Sect. A.2.1. The equation of the precession torque generated by the common inertial forces acting on the cone is the same as for the resistance torque generated by the centrifugal forces and presented Eq. (A.2.12):

$$T_{in} = \frac{20}{81}\pi^2 J\omega\omega_x \tag{A.2.13}$$

where all components are represented in Sect. A.2.1.

A.2.3 Coriolis Forces Acting on a Spinning Cone

The resulting action of Coriolis force, generated by the mass elements of the spinning cone, is expressed as the integrated resistance torque acting opposite to the action of the external torque. The resistance torque generated by the Coriolis force of the mass elements of the cone is expressed by the following equation:

$$\Delta T_{\mathrm{cr}} = f_{\mathrm{cr}} y_{\mathrm{m}} = m a_z y_{\mathrm{m}} \tag{A.2.14}$$

where ΔT_{cr} is the torque generated by the Coriolis force f_{cr} of the spinning cone's mass element $m = \frac{3M\Delta\delta\Delta r}{4\pi R}$, (Eq. A.2.2); $y_{\mathrm{m}} = (4/9)R\ \sin\alpha$ is the distance to the mass element's location along axis oy, and other components are represented in Eq. (A.2.1).

The expression for a_{z} is represented by the following equation:

$$\alpha_z = \frac{\mathrm{d}V_z}{\mathrm{d}t} = \frac{\mathrm{d}(V\cos\alpha\sin\Delta\gamma)}{\mathrm{d}t} = V\cos\alpha\frac{\mathrm{d}\gamma}{\mathrm{d}t} = r\omega\omega_x\cos\alpha \tag{A.2.15}$$

where $a_{\mathrm{z}} = \mathrm{d}V_{\mathrm{z}}/\mathrm{d}t$ is the Coriolis acceleration of the mass element along with axis oz; $V_{\mathrm{z}} = V\ \cos\alpha\ \sin\Delta\gamma$ is the change in the tangential velocity $V = r\omega\ \cos\alpha$ of the mass element; $\omega_{\mathrm{x}} = \Delta\gamma/\mathrm{d}t$, and other parameters are as specified above.

Substituting defined parameters into the expression of Coriolis force fcr and transforming yield the following expression:

$$f_{\mathrm{cr}} = \frac{3M}{4\pi R}\omega\omega_x\Delta\delta r\Delta r\cos\alpha = \frac{3M}{4\pi R}\omega\omega_x r\Delta r\Delta\delta\cos\alpha \tag{A.2.16}$$

Substituting these defined parameters into Eq. (A.2.14) and transforming yield the following equation:

$$\Delta T_{\text{cr}} = \frac{3M\omega\omega_x}{4\pi R}\cos\alpha \times r\Delta r\Delta\delta \times y_C \tag{A.2.17}$$

The Coriolis forces represent the distributed load applied along the length of the circle and the cone forming line where the cone's mass elements are located. The location of the resultant force is the centroid (point C, Fig. 3.4, Chap. 3) of the area under the Coriolis force's curve calculated by Eq. (A.2.4), but with its own symbols. The centroid is expressed by the following equation:

$$y_C = \frac{\int_{\alpha=0}^{\pi}\int_{r=0}^{(2/3)R} f_{cr}\, y_m\, d\alpha dr}{\int_{\alpha=0}^{\pi}\int_{r=0}^{(2/3)R} f_{cr}\, d\alpha dr} = \frac{\int_{\alpha=0}^{\pi}\frac{3M\omega^2}{4\pi R}\Delta\delta\Delta\gamma\times\cos\alpha\times\frac{4}{9}R\sin\alpha\cos\alpha d\alpha\times\int_{r=0}^{(2/3)R} r dr}{\int_{\alpha=0}^{\pi}\frac{3M\omega^2}{4\pi R}\Delta\delta\Delta\gamma\cos\alpha d\alpha\times\int_{r=0}^{(2/3)R} r dr} =$$
$$\frac{\frac{3M\omega^2}{4\pi R}\Delta\delta\Delta\gamma\cos\alpha\times\int_{r=0}^{(2/3)R} r dr\times\frac{4}{9}R\int_{\alpha=0}^{\pi}\sin\alpha\cos\alpha d\sin\alpha}{\frac{3M\omega^2}{4\pi}\Delta\delta\Delta\gamma\times\int_{r=0}^{(2/3)R} r dr\times\int_{\alpha=0}^{\pi}\cos\alpha d\alpha} = \frac{4R\int_0^{\pi}\sin\alpha\cos\alpha d\sin\alpha}{9\int_0^{\pi}\cos\alpha d\alpha} \tag{A.2.18}$$

where the expression $\frac{3M}{4\pi R}\omega\omega_x\Delta\delta$ is accepted as constant for Eq. (A.2.18) and other parameters are as specified above.

Equation (A.2.18) is substituted into Eq. (A.2.17), and replacing $\cos\alpha = -\int_0^{\pi}\sin\alpha d\alpha$ by the integral expression with defined limits before, the following equation emerges

$$\int_0^{T_{\text{cr}}} dT_{\text{cr}} = \frac{3M\omega\omega_x}{4\pi R}\times\int_0^{\pi} d\delta\times\int_0^{(2/3)R} r dr$$
$$\times\int_0^{\pi} -\sin\alpha d\alpha\times\frac{2R\int_0^{\pi}\sin\alpha\cos^2 d\alpha}{9\int_0^{\pi}\cos\alpha d\alpha} \tag{A.2.19}$$

The solution of the integral

$\int\sin\alpha\cos^2\alpha d\alpha = \int\sin^p\alpha\cos^q\alpha d\alpha = -\frac{\sin^{p-1}\alpha\cos^{q+1}\alpha}{p+q} + \frac{p-1}{p+q}\int\sin^{p-2}\alpha\cos^q\alpha d\alpha$

$= -\frac{\cos^3\alpha}{3}$ is presented in [12].

Following solution is the similar as presented in Sect. A.1.3 of Appendix A.

$$T_{\text{cr}}\Big|_0^{T_{\text{cr}}} = \frac{3M\omega\omega_x}{4\pi R}\times\left(\delta\Big|_0^{\pi}\right)\times\left(\frac{r^2}{2}\Big|_0^{(2/3)R}\right)$$
$$\times\left(-\cos\alpha\Big|_0^{\pi}\right)\times\frac{2R\cos^3\alpha\Big|_0^{\pi}}{9\times\sin\alpha\Big|_0^{\pi/2}} \tag{A.2.20}$$

Coriolis forces act on the upper and lower sides of the cone's plane, then the total resistance torque T_{cr} is obtained when the result of Eq. (A.2.20) is increased twice:

$$T_{cr} = \frac{4MR^2\omega\omega_x}{27} = \frac{40}{81}J\omega\omega_x \tag{A.2.21}$$

where $J = 3MR^2/10$ is the cone's mass moment of inertia, and other parameters are as specified above.

A.2.4 Attributes of the Inertial Torques Acting on a Spinning Cone

The total initial precession torque T_p acting on the cone around axis oy has represented a sum of the precession torques generated by the inertial forces of the mass elements and the change in the angular momentum whose equation is as follows:

$$T_p = T_{in} + T_{am} = \left(\frac{20}{81}\pi^2 + 1\right)J\omega\omega_x \tag{A.2.22}$$

The total initial resistance torque T_r acting around axis ox has presented a sum of the resistance torques generated by the centrifugal and Coriolis forces of the cone's mass elements whose equation is as follows:

$$T_r = T_{ct} + T_{cr} = \left(\frac{20}{81}\pi^2 + \frac{40}{81}\right)J\omega\omega_x = \frac{20}{81}\left(\pi^2 + 2\right)J\omega\omega_x \tag{A.2.23}$$

where all components are as specified above.

The mathematical models for internal torques acting on the spinning cone are represented in Table A.2.

Analysis of the inertial torques acting on the spinning cone demonstrates differences in the results compare with other spinning objects.

Table A.2 Equations of the internal torques acting in the spinning cone

Type of the torque generated by	Equation
Centrifugal forces	$T_{ct} = T_{in} = \frac{20}{81}\pi^2 J\omega\omega_x$
Inertial forces	
Coriolis forces	$T_{cr} = \frac{40}{81}J\omega\omega_x$
Change in an angular momentum	$T_{am} = J\omega\omega_x$
Resistance torque $T_r = T_{ct} + T_{cr}$	$T_r = \frac{20}{81}\left(\pi^2 + 2\right)J\omega\omega_x$
Precession torque $T_p = T_{in} + T_{am}$	$T_p = \left(\frac{20}{81}\pi^2 + 1\right)J\omega\omega_x$

A.2.5 Working Example

The cone has a mass of 1.0 kg; a radius of 0.1 m at about the spin axis and spinning at 3000 rpm. External torque acts on the cone, which rotates with an angular velocity of 0.05 rpm. It is determined by the value of the resistance and precession torques generated by the centrifugal, common inertial and Coriolis forces, as well as the change in the angular momentum of the spinning cone (Fig. A.2). The value of the resistance and precession torques acting on the spinning cone is defined by equations of Table A.2. Substituting the initial data into defined equations and transforming yield the following result:

$$T_r = T_{ct} + T_{cr} = \frac{20}{81}\left(\pi^2 + 2\right) J\omega\omega_x = \frac{20}{81}\left(\pi^2 + 2\right)\frac{3MR^2}{10}\omega\omega_x$$

$$= \frac{20}{81}\left(\pi^2 + 2\right) \times \frac{3.0 \times 1.0 \times 0.1^2}{10} \times \frac{3000 \times 2\pi}{60} \times \frac{0.05 \times 2\pi}{60}$$
$$= 0.0144627 \text{ Nm}$$

$$T_p = T_{in} + T_{am} = \left(\frac{20}{81}\pi^2 + 1\right) J\omega\omega_x = \left(\frac{20}{81}\pi^2 + 1\right)\frac{3MR^2}{10}\omega\omega_x$$

$$= \left(\frac{20}{81}\pi^2 + 1\right) \times \frac{3.0 \times 1.0 \times 0.1^2}{10} \times \frac{3000 \times 2\pi}{60} \times \frac{0.05 \times 2\pi}{60}$$
$$= 0.0169606 \text{ Nm}$$

where T_r and T_p are, respectively, the initial resistance and precession torques generated by the mass elements and centre mass of the spinning cone.

A.3 Inertial Forces Acting on a Spinning Paraboloid of Revolution

A.3.1 Centrifugal Forces Acting on a Spinning Paraboloid

The paraboloid's mass elements m are located on the arbitrary radius r which forming the rotating paraboloid around axes oz. The focus of the parabola locates at the point o of the system coordinate $\Sigma oxyz$. The rotating mass elements of the spinning paraboloid are located on the paraboloid surface which maximal radius is the 2/3 radius of the base of the paraboloid. The analysis of the acting inertial forces generated by the mass element of the paraboloid is considered on the arbitrary planes that parallel to the plane of the base of the paraboloid (Fig. A.3) that is the same as the plane of the thin disc represented in Fig. 3.2 of Chap. 3. The rotating centrifugal

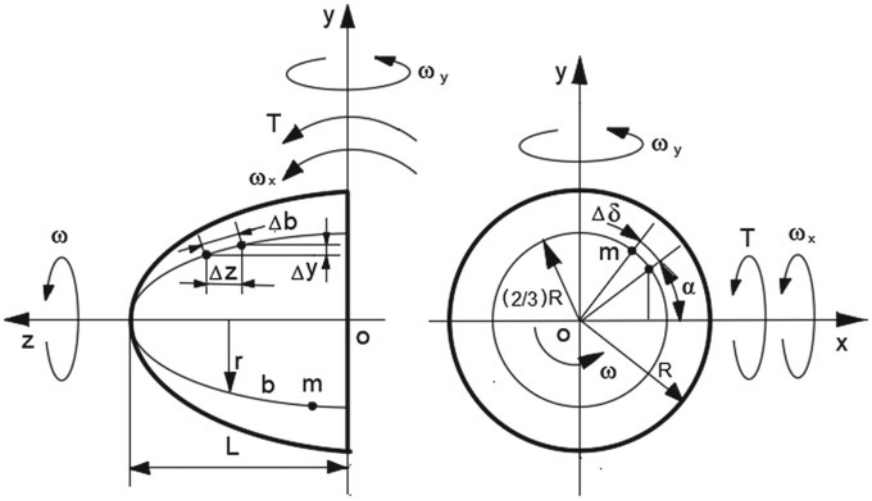

Fig. A.3 Schematic the spinning paraboloid of revolution

forces of the paraboloid's mass elements is declined and resisted opposite to the action of external torque.

The analytical approach for the modelling of the acting centrifugal forces generated by the mass elements of the spinning paraboloid is the same as represented for the spinning cone in Sect. A.2.4. Similar resistance torques are generated by the mass elements located on the planes of the paraboloid that parallel to the plane *xoy* (Fig. A.3). The resistance torque ΔT_{ct} produced by the centrifugal force $f_{\text{ct}.z}$ of the paraboloid's mass element is expressed by the following equation:

$$\Delta T_{\text{ct}} = f_{\text{ct}.z} y_{\text{m}} \tag{A.3.1}$$

where y_{m} is the distance of the paraboloid's mass element's location at the arbitrary plane relatively to axis *ox*.

The equation for the axial component of the centrifugal force for the arbitrarily chosen plane of the paraboloid is as follows:

$$f_{\text{ct}.z} = f_{\text{ct}} \sin\alpha \sin\Delta\gamma = mr\omega^2 \sin\alpha \sin\Delta\gamma \tag{A.3.2}$$

where $f_{\text{ct}} = mr \sin\alpha\omega^2$ is the centrifugal force of the mass element m; $m = (M/2\pi b)\Delta\delta\Delta b$, M is the mass of the paraboloid; b is the length of the line that forms the paraboloid surface of the mass element's location; Δb is the line part of the mass element's location; $\Delta\delta$ is the sector's angle of the mass element's location on the plane that parallel to plane *xoy*; r is the radius of the arbitrary circle plane of the paraboloid where the mass elements located; ω is the constant angular velocity of the paraboloid; other components as specified above.

Substituting defined parameters into Eq. (A.3.2) yields the following equation:

$$f_{\mathrm{ct}.z} = \frac{M}{2\pi b} r\omega^2 \sin\alpha \Delta\delta \Delta b \Delta\gamma \tag{A.3.3}$$

The simple equation of the parabola, $y^2 = z$. The maximal radius of the paraboloid is as follows: $y = R = \sqrt{z} = \sqrt{L}$, where $L = R^2$ (Fig. A.3). The equation for the parabola line of mass elements is as follows $(2/3)y = \sqrt{z}$ where (2/3) is the factor of the mass elements location or $y = (3/2)\sqrt{z}$. The maximal radius of the parabola line of mass elements is as follows $y = r = (2/3)R$.

The length b of the parabola line where the mass elements locate is computed by the following equation [10] and by substituting parameters defined above:

$$b = \int_0^L \sqrt{1 + y'^2(z)}\mathrm{d}z \tag{A.3.4}$$

The derivative of $y = (3/2)\sqrt{z}$is as follows: $y' = \frac{3}{4\sqrt{z}}$, and then substituting into Eq. (A.3.4) and transforming emerges in the following expression:

$$b = \int_0^L \sqrt{1 + \frac{9}{16z}}\mathrm{d}z = \int_0^{L=R^2} \sqrt{\frac{9/16 + z}{0 + z}}\mathrm{d}z \tag{A.3.5}$$

Integral Eq. (A.3.5) presents the tabulated one [10].

$\int \sqrt{\frac{a+x}{b+x}}\mathrm{d}x = \sqrt{(a+x)(b+x)} + (a-b)\ln\left|\sqrt{a+x} + \sqrt{b+x} + C\right|$ with the following solution:

$$b = \sqrt{\left(\frac{9}{16} + z\right)z} + \frac{9}{16}\ln\left|\sqrt{\frac{9}{16} + z} + \sqrt{z}\right|\Big|_0^{L=R^2}$$

giving rise for the following result

$$\begin{aligned} b &= \sqrt{\left(\frac{9}{16} + R^2\right)R^2} + \frac{9}{16}\ln\left(\sqrt{\frac{9}{16} + R^2} + \sqrt{R^2}\right) - \frac{9}{16}\ln\frac{3}{4} \\ &= R\sqrt{\frac{9}{16} + R^2} + \frac{9}{16}\ln\left[\frac{4}{3}\left(\sqrt{\frac{9}{16} + R^2} + R\right)\right] \end{aligned} \tag{A.3.6}$$

The part of the line Δb (Fig. A.3) for the mass element m is expressed by the following equation:

$$\Delta b = \sqrt{(\Delta z)^2 + (\Delta y)^2} = \sqrt{\left(\frac{8}{9} y \Delta y\right)^2 + (\Delta y)^2}$$
$$= \Delta y \sqrt{\left(\frac{8}{9} y\right)^2 + 1} = \Delta r \sqrt{\left(\frac{8}{9} r\right)^2 + 1} \tag{A.3.7}$$

where Δz is expressed from the equation $(4/9)y^2 = z$ by the following solution (Fig. A.3): $(4/9)y^2 - (4/9)(y - \Delta y)^2 = (z + \Delta z) - z$, which solving yields $\Delta z = (8/9)y\Delta y$, where $y = r$, and $(\Delta y)^2 = 0$ is accepted due to the small value.

Substituting the defined parameters into Eq. (A.3.3) and transforming yield the following equation:

$$f_{\text{ct.}z} = \left(\frac{M\omega^2 \sin\alpha}{2\pi b}\right) \Delta\delta\Delta\gamma \left(\sqrt{\left(\frac{8}{9} r\right)^2 + 1}\right) r\Delta r \tag{A.3.8}$$

where all components are as specified above.

The centre mass of the paraboloid locates at the distance $z_{\text{cm}} = (2/3)L$ from its vertex [10]. The radius of the paraboloid plan of mass elements passes through the centre mass and presented by the expression $y = r = \sqrt{(2/3)}R$ that is defined from proportion $R = y^2 = L$ and $r = y_r^2 = (2/3)L$. y_{m} is the distance of the location of the paraboloid's mass elements at the plane of the centre mass along with axis oz, and relative the axis ox (Fig. A.3) is presented by the following expression:

$$y_m = \sqrt{\frac{2}{3}} \times \frac{2}{3} R \sin\alpha. \tag{A.3.9}$$

Substituting Eqs. (A.3.7), (A.3.8) and (A.3.9) and all defined components above and transforming yield the following equation:

$$y_A = \frac{\int_{\alpha=0}^{\pi} \int_{r=0}^{(2/3)R} f_{\text{ct.}z} y_m \mathrm{d}\alpha \mathrm{d}r}{\int_{\alpha=0}^{\pi} \int_{r=0}^{(2/3)R} f_{\text{ct.}z} \mathrm{d}\alpha \mathrm{d}r}$$
$$= \frac{\int_{\alpha=0}^{\pi} \int_{0}^{(2/3)R} \left(\frac{M\omega^2 \sin\alpha}{2\pi b}\right) \Delta\delta\Delta\gamma \left(\sqrt{\left(\frac{8}{9} r\right)^2 + 1}\right) r\Delta r \times \sqrt{\frac{2}{3}} \frac{2}{3} R \sin\alpha \mathrm{d}\alpha \mathrm{d}r}{\int_{\alpha=0}^{\pi} \int_{0}^{(2/3)R} \left(\frac{M\omega^2 \sin\alpha}{2\pi b}\right) \Delta\delta\Delta\gamma \left(\sqrt{\left(\frac{8}{9} r\right)^2 + 1}\right) r\Delta r}$$
$$= \frac{\frac{M\omega^2}{2\pi b} \Delta\delta\Delta\gamma}{\frac{M\omega^2}{2\pi b} \Delta\delta\Delta\gamma} \times \frac{\int_{r=0}^{(2/3)R} \left(\sqrt{\left(\frac{8}{9} r\right)^2 + 1}\right) r\Delta r \mathrm{d}r}{\int_{r=0}^{(2/3)R} \left(\sqrt{\left(\frac{8}{9} r\right)^2 + 1}\right) r\Delta r \mathrm{d}r} \times \frac{\sqrt{\frac{2}{3}} \frac{2}{3} R \int_{\alpha=0}^{\pi} \sin^2\alpha \mathrm{d}\alpha}{\int_{\alpha=0}^{\pi} \sin\alpha \mathrm{d}\alpha}$$
$$= \frac{\sqrt{\frac{2}{3}} \frac{2}{3} R \int_{\alpha=0}^{\pi} \sin^2\alpha \mathrm{d}\alpha}{\int_{\alpha=0}^{\pi} \sin\alpha \mathrm{d}\alpha} \tag{A.3.10}$$

where the expression $\frac{M\omega^2}{\pi b}\Delta\gamma$ is accepted at this stage of computing as constant for Eq. (A.3.10), and other parameters are as specified above.

Replacing expressionssin$^2\alpha = (1-\cos 2\alpha)/2$by a trigonometric identity and $\sin\alpha = \int_0^{\pi}\cos\alpha\mathrm{d}\alpha$ by the integral expression with defined limits in Eq. (A.3.4), and representing other components by the integral forms with transformation, and substituting into Eq. (A.3.1), the following equation emerges:

$$\Delta T_{\mathrm{ct}} = \frac{M\omega^2}{2\pi b}\Delta\delta\Delta\gamma\left(\sqrt{\left(\frac{8}{9}r\right)^2+1}\right)r\Delta r\int_0^{\pi}\cos\alpha\mathrm{d}\alpha \times \frac{\sqrt{\frac{2}{3}}\frac{R}{3}\int_{\alpha=0}^{\pi}(1-\cos 2\alpha)\mathrm{d}\alpha}{\int_{\alpha=0}^{\pi}\sin\alpha\mathrm{d}\alpha} \tag{A.3.11}$$

Equation (A.3.11) is transformed and expressed by the integral form

$$\int_0^{T_{\mathrm{ct}}}\mathrm{d}T_{\mathrm{ct}} = \frac{M\omega^2}{2\pi b}\times\int_0^{\pi}\mathrm{d}\delta\times\int_0^{\pi}\cos\alpha\mathrm{d}\alpha\times\int_0^{\gamma}\mathrm{d}\gamma \times\int_0^{(2/3)R}\left(\sqrt{\left(\frac{8}{9}r\right)^2+1}\right)r\mathrm{d}r\times\frac{\sqrt{\frac{2}{3}}\frac{R}{3}\int_0^{\pi}(1-\cos 2\alpha)\mathrm{d}\alpha}{\int_0^{\pi}\sin\alpha\mathrm{d}\alpha} \tag{A.3.12}$$

The integral $\int_0^{(2/3)R}\left(r\sqrt{\left(\frac{8}{9}r\right)^2+1}\right)\mathrm{d}r = \frac{8}{9}\int_0^{(2/3)R}\left(r\sqrt{r^2+\left(\frac{9}{8}\right)^2}\right)\mathrm{d}r$ presents the following tabulated integral $\int x\sqrt{x^2+a^2}dx = \frac{1}{3}\sqrt{(x^2+a^2)^3}+C$. Solving integral Eq. (A.3.12) yields the following result

$$T_{\mathrm{ct}}\Big|_0^{T_{\mathrm{ct}}} = \frac{M\omega^2}{2\pi b}\times\delta\Big|_0^{\pi}\times\left(\sin\alpha\Big|_0^{\pi/2}\right)\times(\gamma)\Big|_0^{\pi} \times\frac{8}{27}\left\{\sqrt{\left[r^2+\left(\frac{9}{8}\right)^2\right]^3}\right\}\Big|_0^{(2/3)R}\times\frac{\sqrt{\frac{2}{3}}\frac{R}{3}\left(\alpha-\frac{1}{2}\sin 2\alpha\right)\Big|_0^{\pi}}{-\cos\alpha\Big|_0^{\pi}}$$

where the limits of integration for the trigonometric expression of sinus are taken for the quarter of the circle and result are increased twice, thus giving rise to the following:

$$T_{\mathrm{ct}} = \frac{M\omega^2}{2\pi b}\times(\pi-0)\times 2(1-0)\times(\gamma-0)$$

$$\times \left[\frac{8}{27} \left(\sqrt{\left[\left(\frac{4}{9}R \right)^2 + \left(\frac{9}{8} \right)^2 \right]^3} - \left(\frac{9}{8} \right)^3 \right) \right] \times \sqrt{\frac{2}{3}} \frac{R}{3} \frac{(\pi - 0)}{[-(-1-1)]}$$

$$= \frac{4}{81} \left\{ \sqrt{\left[\left(\frac{4}{9}R \right)^2 + \left(\frac{9}{8} \right)^2 \right]^3} - \left(\frac{9}{8} \right)^3 \right\} \sqrt{\frac{2}{3}} R \frac{M\pi\omega^2}{b} \times \gamma \qquad \text{(A.3.14)}$$

where all parameters are as specified above.

Following steps of solutions are the same as presented in Sect. A.2.1 of the Appendix

$$\frac{\mathrm{d}T_{\mathrm{ct}}}{\mathrm{d}t} = \frac{4}{81} \left\{ \sqrt{\left[\left(\frac{4}{9}R \right)^2 + \left(\frac{9}{8} \right)^2 \right]^3} - \left(\frac{9}{8} \right)^3 \right\} \sqrt{\frac{2}{3}} \frac{RM\pi\omega^2}{b} \frac{\mathrm{d}\gamma}{\mathrm{d}t} \qquad \text{(A.3.15)}$$

$t = \frac{\alpha}{\omega}, \mathrm{d}t = \frac{d\alpha}{\omega}, \frac{\mathrm{d}\gamma}{\mathrm{d}t} = \omega_x$

$$\frac{\omega \mathrm{d}T_{\mathrm{ct}}}{\mathrm{d}\alpha} = \frac{4}{81} \left\{ \sqrt{\left[\left(\frac{4}{9}R \right)^2 + \left(\frac{9}{8} \right)^2 \right]^3} - \left(\frac{9}{8} \right)^3 \right\} \sqrt{\frac{2}{3}} \frac{RM\pi\omega^2\omega_x}{b} \qquad \text{(A.3.16)}$$

$$\mathrm{d}T_{\mathrm{ct}} = \frac{4}{81} \left\{ \sqrt{\left[\left(\frac{4}{9}R \right)^2 + \left(\frac{9}{8} \right)^2 \right]^3} - \left(\frac{9}{8} \right)^3 \right\} \sqrt{\frac{2}{3}} \frac{RM\pi\omega\omega_x}{b} \mathrm{d}\alpha \qquad \text{(A.3.17)}$$

$$\int_0^{T_{\mathrm{ct}}} \mathrm{d}T_{\mathrm{ct}} = \int_0^{\pi} \frac{4}{81} \left\{ \sqrt{\left[\left(\frac{4}{9}R \right)^2 + \left(\frac{9}{8} \right)^2 \right]^3} - \left(\frac{9}{8} \right)^3 \right\} \sqrt{\frac{2}{3}} \frac{RM\pi\omega\omega_x}{b} \mathrm{d}\alpha \qquad \text{(A.3.18)}$$

$$T_{\mathrm{ct}} \Big|_0^{T_{\mathrm{ct}}} = \frac{4}{81} \left\{ \sqrt{\left[\left(\frac{4}{9}R \right)^2 + \left(\frac{9}{8} \right)^2 \right]^3} - \left(\frac{9}{8} \right)^3 \right\} \sqrt{\frac{2}{3}} \frac{RM\pi\omega\omega_x}{b} \alpha \Big|_0^{\pi}$$

$$T_{\mathrm{ct}} = \frac{4}{81} \left\{ \sqrt{\left[\left(\frac{4}{9}R \right)^2 + \left(\frac{9}{8} \right)^2 \right]^3} - \left(\frac{9}{8} \right)^3 \right\} \sqrt{\frac{2}{3}} \frac{RM\pi^2\omega\omega_x}{b} \qquad \text{(A.3.19)}$$

The change in centrifugal forces acts on the upper and lower sides of the paraboloid's, substituting the expression b (Eq. A.3.6) then the total resistance torque T_{ct} is obtained when the result of Eq. (A.3.19) is increased twice.

$$T_{\mathrm{ct}} = \frac{\frac{8}{81}\left\{\sqrt{\left[\left(\frac{4}{9}R\right)^2 + \left(\frac{9}{8}\right)^2\right]^3} - \left(\frac{9}{8}\right)^3\right\}\sqrt{\frac{2}{3}}}{R\sqrt{\frac{9}{16} + R^2} + \frac{9}{16}\ln\left[\frac{4}{3}\left(\sqrt{\frac{9}{16} + R^2} + R\right)\right]} \times MR\pi^2\omega\omega_x \tag{A.3.20}$$

where all parameters are as specified above.

The mass moment of paraboloid inertia is computed by the following solution. The change in the mass moment of inertia of the arbitrary micro-disc that perpendicular to axis of the paraboloid is presented by the following equation:

$$\mathrm{d}J = \frac{1}{2}y^2\mathrm{d}m \tag{A.3.21}$$

where y is the arbitrary radius of the paraboloid external surface (Fig. A.4), $\mathrm{d}m = \rho\mathrm{d}V$,$\mathrm{d}V = \pi y^2\mathrm{d}z$, where m is the mass, ρ is the density, V is the volume of the paraboloid, respectively.

Substituting defined parameters into Eq. (A.3.21) and transforming yield the following:

$$\mathrm{d}J = \frac{1}{2}y^2\rho\pi y^2\mathrm{d}z = \frac{1}{2}y^4\rho\pi\,\mathrm{d}z \tag{A.3.22}$$

Equation (A.3.22) is represented by the integral form and $\mathrm{d}z = 2y\mathrm{d}y$, $y = \sqrt{z}$; transforming and solving yield the following result:

$$\int_0^J \mathrm{d}J = \int_0^L \frac{1}{2}y^4\rho\pi 2y\mathrm{d}y \tag{A.3.23}$$

giving rise to the following result:

$$J = \frac{1}{6}\rho\pi y^6 = \frac{1}{6}\rho\pi y^2y^2y^2 = \frac{1}{6}(\rho\pi R^2L)R^2 = \frac{1}{6}MR^2 \tag{A.3.24}$$

where $y^2 = z = L$, $y = R$, $M = \rho\pi R^2L$,, and other parameters are as specified above.

Then, the resistance torque generated by the rotating mass element of the paraboloid emerges as follows:

$$T_{\mathrm{ct}} = \frac{16\left\{\sqrt{\left[\left(\frac{4}{9}R\right)^2 + \left(\frac{9}{8}\right)^2\right]^3} - \left(\frac{9}{8}\right)^3\right\}\sqrt{\frac{2}{3}}}{27\left\{R\sqrt{\frac{9}{16} + R^2} + \frac{9}{16}\ln\left[\frac{4}{3}\left(\sqrt{\frac{9}{16} + R^2} + R\right)\right]\right\}R} \times J\pi^2\omega\omega_x \tag{A.3.25}$$

where all parameters are as specified above.

A.3.2 Common Inertial Forces Acting on a Spinning Paraboloid

The modelling of the acting common inertial forces generated by the mass elements of the spinning paraboloid is the same as represented in Sect. 3.1. The equation of the precession torque generated by the common inertial forces acting on the paraboloid is the same as for the resistance torque generated by the centrifugal forces and presented Eq. (A.3.25)

$$T_{\mathrm{ct}} = \frac{16\left\{\sqrt{\left[\left(\frac{4}{9}R\right)^2 + \left(\frac{9}{8}\right)^2\right]^3} - \left(\frac{9}{8}\right)^3\right\}\sqrt{\frac{2}{3}}}{27\left\{R\sqrt{\frac{9}{16} + R^2} + \frac{9}{16}\ln\left[\frac{4}{3}\left(\sqrt{\frac{9}{16} + R^2} + R\right)\right]\right\}R} \times J\pi^2\omega\omega_x \qquad \text{(A.3.26)}$$

where all components are represented in Sect. A.3.1.

The change in the angular momentum represents a precession torque generated by the centre mass of the spinning paraboloid and expressed by the well-known equation $T_{\mathrm{am}} = J\omega\omega_{x.}$

A.3.3 Coriolis Forces Acting on a Spinning Paraboloid

The resulting action of Coriolis force, generated by the mass elements of the spinning paraboloid is expressed as the integrated resistance torque acting opposite to the action of the external torque. The resistance torque ΔT_{cr} generated by the Coriolis force f_{cr} of the mass elements of the paraboloid is expressed by the following equation:

$$\Delta T_{\mathrm{cr}} = f_{\mathrm{cr}} y_{\mathrm{m}} = m a_z y_{\mathrm{m}} \qquad \text{(A.3.27)}$$

where y_{m} is the distance to the mass element's location along axis *oy;* other components are represented in Eq. (A.3.1) of the Appendix.

The expression for a_{z} is represented by the following equation:

$$\alpha_z = \frac{\mathrm{d}V_z}{\mathrm{d}t} = \frac{\mathrm{d}(V\cos\alpha\sin\Delta\gamma)_-}{\mathrm{d}t} = V\cos\alpha\frac{\mathrm{d}\gamma}{\mathrm{d}t} = r\omega\omega_x\cos\alpha \qquad \text{(A.3.28)}$$

where $a_{\mathrm{z}} = \mathrm{d}V_z/\mathrm{d}t$ is the Coriolis acceleration of the mass element along with axis *oz*; $V_{\mathrm{z}} = V\ \cos\alpha\ \sin\Delta\gamma$ is the change in the tangential velocity $V = r\omega\ \cos\alpha$ of the mass element; r is the arbitrary radius of the paraboloid's circle with mass elements location; $\omega_x = \Delta\gamma/\mathrm{d}t$; other parameters are as specified above.

Defined parameters enable for the expression Coriolis force generated by the mass elements:

$$f_{\mathrm{cr}} = \frac{M}{2\pi b}\Delta\delta\Delta b r\omega\omega_x \cos\alpha = \frac{M\omega\omega_x}{2\pi b}\Delta\delta\Delta r\left(\sqrt{\left(\frac{8}{9}r\right)^2 + 1}\right) r\cos\alpha \quad \text{(A.3.29)}$$

where Δb is presented by Eq. (A.3.7)

Substituting Eq. (A.3.29) into Eq. (A.3.27) and transforming yield the following equation:

$$\Delta T_{\mathrm{cr}} = \frac{M\omega\omega_x}{2\pi b}\cos\alpha \times \left(\sqrt{\left(\frac{8}{9}r\right)^2 + 1}\right) r\Delta r\Delta\delta\Delta b \times y_{\mathrm{m}} \quad \text{(A.3.30)}$$

where $\Delta\delta$ and Δb is the angular and axial location of the mass element, y_{C} is presented by Eq. (A.3.10) (Sect. A.3.1, Appendix A).

The location of the resultant force is the centroid (point C, Fig. 3.4, Chap. 3) of the area under the Coriolis force's curve calculated by Eq. (A.3.4) of Chap. 3, but with its own symbols. The centroid point C is defined for the resultant force by the following equation:

$$\begin{aligned} y_{\mathrm{C}} &= \frac{\int_{\alpha=0}^{\pi}\int_{r=0}^{(2/3)R} f_{\mathrm{cr}} y_m \mathrm{d}\alpha\mathrm{d}r}{\int_{\alpha=0}^{\pi}\int_{r=0}^{(2/3)R} f_{\mathrm{cr}}\mathrm{d}\alpha\mathrm{d}r} \\ &= \frac{\int_{\alpha=0}^{\pi}\frac{M\omega\omega_x}{2\pi b}\Delta\delta\cos\alpha \times \left(\sqrt{\left(\frac{8}{9}r\right)^2+1}\right) r\Delta r \times \sqrt{\frac{2}{3}}\frac{2}{3}R\sin\alpha\mathrm{d}\alpha\mathrm{d}r}{\int_{\alpha=0}^{\pi}\frac{M\omega\omega_x}{2\pi b}\Delta\delta\cos\alpha\left(\sqrt{\left(\frac{8}{9}r\right)^2+1}\right) r\mathrm{d}r\mathrm{d}\alpha} \\ &= \frac{\frac{M\omega\omega_x}{2\pi b}\Delta\delta \times \int_{r=0}^{(2/3)R}\left(\sqrt{\left(\frac{8}{9}r\right)^2+1}\right) r\mathrm{d}r \times \sqrt{\frac{2}{3}}\frac{2}{3}R\sin\alpha\cos\alpha\mathrm{d}\alpha}{\frac{M\omega\omega_x}{2\pi b}\Delta\delta\int_{r=0}^{(2/3)R}\left(\sqrt{\left(\frac{8}{9}r\right)^2+1}\right) r\mathrm{d}r\int_{\alpha=0}^{\pi}\cos\alpha\mathrm{d}\alpha} \\ &= \frac{\int_{\alpha=0}^{\pi}\sqrt{\frac{2}{3}}\frac{2}{3}R\sin\alpha\cos\alpha\mathrm{d}\alpha}{\int_{\alpha=0}^{\pi}\cos\alpha\mathrm{d}\alpha} = \frac{\int_{\alpha=0}^{\pi}\sqrt{\frac{2}{3}}\frac{R}{3}\sin 2\alpha\mathrm{d}\alpha}{\int_{\alpha=0}^{\pi}\cos\alpha\mathrm{d}\alpha} \end{aligned} \quad \text{(A.3.31)}$$

where the expression $\frac{M\omega\omega_x}{2\pi b}\Delta\delta$ is accepted as constant for Eq. (A.3.31), the expression $2\sin\alpha\cos\alpha = \sin 2\alpha$ is a trigonometric identity that is replaced in Eq. (A.3.31), and the other parameters are as specified above.

Expression $\cos\alpha = \int_0^{\pi} -\sin\alpha\mathrm{d}\alpha$ of Eq. (A.3.31) is presented by the integral form with defined limits and substituted into Eq. (A.3.30) that transformed into the integral form with defined limits and the following equation emerges:

$$\int_0^{T_{cr}} dT_{cr} = \frac{M\omega\omega_x}{2\pi b}\int_0^{\pi} d\delta \times \int_0^{\pi} -\sin\alpha d\alpha \times \int_{r=0}^{(2/3)R}\left(\sqrt{\left(\frac{8}{9}r\right)^2+1}\right) r dr \times \frac{\int_{\alpha=0}^{\pi}\sqrt{\frac{2}{3}}\frac{R}{3}\sin 2\alpha d\alpha}{\int_{\alpha=0}^{\pi/2}\cos\alpha d\alpha} \tag{A.3.32}$$

The solution of the integral $\int_{r=0}^{(2/3)R}\left(\sqrt{\left(\frac{8}{9}r\right)^2+1}\right) r dr$ is presented by Eq. (A.3.12); expression of b presented by Eq. (A.3.6) and solving integral Eq. (A.3.32) yield the following result:

$$T_{cr}\Big|_0^{T_{cr}} = \frac{M\omega\omega_x}{2\pi b} \times \left(\delta\Big|_0^{\pi}\right) \times \left(-\cos\alpha\Big|_0^{\pi}\right) \times \frac{8}{27}\left\{\sqrt{\left[r^2+\left(\frac{9}{8}\right)^2\right]^3}\right\}\Big|_0^{(2/3)R} \times \frac{-\sqrt{\frac{2}{3}}\frac{R}{6}\cos 2\alpha\Big|_0^{\pi/2}}{\sin\alpha\Big|_0^{\pi/2}}$$

giving rise to the following solution:

$$\begin{aligned} T_{cr} &= -\frac{M\omega\omega_x}{2\pi\left\{R\sqrt{\frac{9}{16}+R^2}+\frac{9}{16}\ln\left[\frac{4}{3}\left(\sqrt{\frac{9}{16}+R^2}+R\right)\right]\right\}} \times (\pi-0) \times [-(-1-1)] \\ &\times \frac{8}{81}\left\{\sqrt{\left[\left(\frac{4}{9}R\right)^2+\left(\frac{9}{8}\right)^2\right]^3}-\left(\frac{9}{8}\right)^3\right\}\sqrt{\frac{2}{3}} \times \frac{R}{6}\frac{[-(-1-1)]}{(1-0)} \\ &= \frac{\frac{8}{243}\left\{\sqrt{\left[\left(\frac{4}{9}R\right)^2+\left(\frac{9}{8}\right)^2\right]^3}-\left(\frac{9}{8}\right)^3\right\}\sqrt{\frac{2}{3}}}{R\sqrt{\frac{9}{16}+R^2}+\frac{9}{16}\ln\left[\frac{4}{3}\left(\sqrt{\frac{9}{16}+R^2}+R\right)\right]} \times MR\omega\omega_x \end{aligned} \tag{A.3.33}$$

Coriolis forces act on the upper and lower sides of the paraboloid's parts, and then, the resistance torque T_{cr} is obtained when the result of Eq. (A.3.33) is increased twice. The mass moment of paraboloid inertial presented by Eq. (A.3.24) is embedded into Eq. (A.3.33) that yields the following equation:

$$T_{cr} = \frac{32\left\{\sqrt{\left[\left(\frac{4}{9}R\right)^2+\left(\frac{9}{8}\right)^2\right]^3}-\left(\frac{9}{8}\right)^3\right\}\sqrt{\frac{2}{3}}}{81\left\{R\sqrt{\frac{9}{16}+R^2}+\frac{9}{16}\ln\left[\frac{4}{3}\left(\sqrt{\frac{9}{16}+R^2}+R\right)\right]\right\}R} \times J\omega\omega_x \tag{A.3.34}$$

where all parameters are as specified above.

A.3.4 Attributes of the Inertial Torques Acting on the Spinning Paraboloid

The total initial precession torque T_{p} acting on the paraboloid around axis oy has represented a sum of the precession torques generated by the inertial forces of the mass elements and the change in the angular momentum whose equation is as follows:

$$T_{\mathrm{ct}} = \left(\frac{16\left\{\sqrt{\left[\left(\frac{4}{9}R\right)^2 + \left(\frac{9}{8}\right)^2\right]^3} - \left(\frac{9}{8}\right)^3\right\}\sqrt{\frac{2}{3}}}{27\left\{R\sqrt{\frac{9}{16} + R^2} + \frac{9}{16}\ln\left[\frac{4}{3}\left(\sqrt{\frac{9}{16} + R^2} + R\right)\right]\right\}R} \right) \times J\pi^2\omega\omega_x \quad \text{(A.3.35)}$$

The total initial resistance torque T_{r} acting around axis ox has represented a sum of the resistance torques generated by the centrifugal (Eq. A.3.14) and Coriolis forces (Eq. A.3.34) of the paraboloid's mass elements whose equation is as follows:

$$T_{\mathrm{r}} = T_{\mathrm{ct}} + T_{\mathrm{cr}} = \left(\frac{16}{27}\pi^2 + \frac{32}{81}\right) \times \frac{\left\{\sqrt{\left[\left(\frac{4}{9}R\right)^2 + \left(\frac{9}{8}\right)^2\right]^3} - \left(\frac{9}{8}\right)^3\right\}\sqrt{\frac{2}{3}}}{\left\{R\sqrt{\frac{9}{16} + R^2} + \frac{9}{16}\ln\left[\frac{4}{3}\left(\sqrt{\frac{9}{16} + R^2} + R\right)\right]\right\}R} \times J\omega\omega_x \quad \text{(A.3.36)}$$

where all components are as specified above.

The mathematical models for inertial torques acting on the spinning paraboloid are represented in Table A.3.

Analysis of the inertial torques acting on the spinning paraboloid demonstrates differences in the results compare with other spinning objects.

A.3.5 Working Example

The paraboloid has a mass of 3.0 kg, the radius of 0.1 m at the end and the length of 0.2 m. The paraboloid is spinning at 3000 rpm. An external torque acts on the paraboloid, which rotates with an angular velocity of 0.05 rpm. These data are used to determine the value of the resistance and precession torques generated by the centrifugal, common inertial and Coriolis forces, as well as the change in the angular momentum of the spinning paraboloid (Fig. A.3). Solving this problem is based on the equations in Table A.3. Substituting the initial data into the aforementioned equations and transforming yield the following result:

Table A.3 Equations of the internal torques acting on the spinning paraboloid

Type of the torque generated by	Equation
Centrifugal forces Inertial forces	$T_{\mathrm{ct}} = T_{\mathrm{in}} = \dfrac{16\left\{\sqrt{\left[\left(\frac{4}{9}R\right)^2+\left(\frac{9}{8}\right)^2\right]^3}-\left(\frac{9}{8}\right)^3\right\}\sqrt{\frac{2}{3}}}{27\left\{R\sqrt{\frac{9}{16}+R^2}+\frac{9}{16}\ln\left[\frac{4}{3}\left(\sqrt{\frac{9}{16}+R^2}+R\right)\right]\right\}R}\times J\pi^2\omega\omega_x$
Coriolis forces	$T_{\mathrm{cr}} = \dfrac{32\left\{\sqrt{\left[\left(\frac{4}{9}R\right)^2+\left(\frac{9}{8}\right)^2\right]^3}-\left(\frac{9}{8}\right)^3\right\}}{243\left\{R\sqrt{\frac{9}{16}+R^2}+\frac{9}{16}\ln\left[\frac{4}{3}\left(\sqrt{\frac{9}{16}+R^2}+R\right)\right]\right\}R}J\omega\omega_x$
Change in angular momentum, M is mass, R is radius	$T_{\mathrm{am}} = J\omega\omega_x = \frac{MR^2}{6}\omega\omega_x$
Resistance torque $T_{\mathrm{r}} = T_{\mathrm{ct}} + T_{\mathrm{cr}}$	$T_{\mathrm{r}} = T_{\mathrm{ct}} + T_{\mathrm{cr}} =$ $\left(\frac{16}{27}\pi^2+\frac{32}{81}\right)\times\dfrac{\left\{\sqrt{\left[\left(\frac{4}{9}R\right)^2+\left(\frac{9}{8}\right)^2\right]^3}-\left(\frac{9}{8}\right)^3\right\}\sqrt{\frac{2}{3}}}{\left\{R\sqrt{\frac{9}{16}+R^2}+\frac{9}{16}\ln\left[\frac{4}{3}\left(\sqrt{\frac{9}{16}+R^2}+R\right)\right]\right\}R}\times J\omega\omega_x$
Precession torque $T_{\mathrm{p}} = T_{\mathrm{in}} + T_{\mathrm{am}}$	$T_{\mathrm{p}} = T_{\mathrm{in}} + T_{\mathrm{am}} =$ $\left(\dfrac{16\left\{\sqrt{\left[\left(\frac{4}{9}R\right)^2+\left(\frac{9}{8}\right)^2\right]^3}-\left(\frac{9}{8}\right)^3\right\}\sqrt{\frac{2}{3}}\pi^2}{27\left\{R\sqrt{\frac{9}{16}+R^2}+\frac{9}{16}\ln\left[\frac{4}{3}\left(\sqrt{\frac{9}{16}+R^2}+R\right)\right]\right\}R}+1\right)J\omega\omega_x$

$$T_{\mathrm{r}} = \left(\frac{16}{27}\pi^2+\frac{32}{81}\right)\times\frac{\left\{\sqrt{\left[\left(\frac{4}{9}R\right)^2+\left(\frac{9}{8}\right)^2\right]^3}-\left(\frac{9}{8}\right)^3\right\}\sqrt{\frac{2}{3}}}{\left\{R\sqrt{\frac{9}{16}+R^2}+\frac{9}{16}\ln\left[\frac{4}{3}\left(\sqrt{\frac{9}{16}+R^2}+R\right)\right]\right\}R}\times J\omega\omega_x$$

$$= \left(\frac{16}{27}\pi^2+\frac{32}{81}\right)\times\frac{\left\{\sqrt{\left[\left(\frac{4}{9}\times 0.1\right)^2+\left(\frac{9}{8}\right)^2\right]^3}-\left(\frac{9}{8}\right)^3\right\}\sqrt{\frac{2}{3}}}{\left\{0.1\sqrt{\frac{9}{16}+0.1^2}+\frac{9}{16}\ln\left[\frac{4}{3}\left(\sqrt{\frac{9}{16}+0.1^2}+0.1\right)\right]\right\}0.1}$$

$$\times\frac{3.0\times 0.1^2}{6}\times\frac{3000\times 2\pi}{60}\times\frac{0.05\times 2\pi}{60} = 0.0143410\,\mathrm{Nm}$$

$$T_{\mathrm{p}} = \left(\frac{16\left\{\sqrt{\left[\left(\frac{4}{9}R\right)^2+\left(\frac{9}{8}\right)^2\right]^3}-\left(\frac{9}{8}\right)^3\right\}\sqrt{\frac{2}{3}}\pi^2}{27\left\{R\sqrt{\frac{9}{16}+R^2}+\frac{9}{16}\ln\left[\frac{4}{3}\left(\sqrt{\frac{9}{16}+R^2}+R\right)\right]\right\}R}+1\right)J\omega\omega_x$$

$$= \left(\frac{16\left\{\sqrt{\left[\left(\frac{4}{9}\times 0.1\right)^2+\left(\frac{9}{8}\right)^2\right]^3}-\left(\frac{9}{8}\right)^3\right\}\sqrt{\frac{2}{3}}\pi^2}{27\left\{0.1\sqrt{\frac{9}{16}+0.1^2}+\frac{9}{16}\ln\left[\frac{4}{3}\left(\sqrt{\frac{9}{16}+0.1^2}+0.1\right)\right]\right\}0.1}+1 \right)$$
$$\times \frac{3.0\times 0.1^2}{6}\times\frac{3000\times 2\pi}{60}\times\frac{0.05\times 2\pi}{60}=0.018828\,\text{Nm}$$

where T_r and T_p are, respectively, the resistance and precession torques generated by the mass elements and centre mass of the spinning paraboloid.

A.4 Inertial Forces Acting on Spinning Propellers

In aerospace and ship engineering, the aircraft's, helicopter's and ships propellers are represented by several designs which manifest the gyroscopic effects at the time of moving in space and action of the external force. The typical design of a propeller is represented by the several relatively narrow blades mounted on the cylindrical hub. Practically, the number of propeller blades of engines is mostly presented from two to six. The inertial forces acting on the propeller are generated by the centre mass of the hub and centre mass of the blades, whose locations and actions are different. The several blades mounted on a hub are considered as one holistic object spinning around the axel.

The action of inertial forces generated by the blade's and the hub masses is considered on a propeller running. The blade's mass m is located on the defined distance r on the propeller, and the mass centre of the propeller's hub is m_h. The blades of the propellers of the different design numbered as I, II, III, IV, V and VI that presented in Fig. A.4. The design of the propeller is complex, and to define its mass moment of inertia around the centre of rotation is the special problem. For simplicity for the following analysis, the design of propeller is presented by the blades mounted on the cylindrical hub. The mass moments of inertia for propellers with several blades are represented by the common expression $J_p = nJ + J_h$, where J is the mass moments of inertia of the blade, n is the number of the blades, and J_h is the mass moments of inertia of the hub. This approach enables avoiding the cumbersome presentations of equations for inertial forces acting on the propeller. The mathematical models for inertial forces acting on the propeller's blade are derived by the methods presented in Sect. 3.1, Chap. 3. Nevertheless, there is a difference in the analytical approaches. The blade of the propeller is considered a narrow design, which concentrated mass, locates on a defined radius of rotation.

The mathematical models for inertial torques generated by the masses of the propeller hub are the same as for the spinning disc described in Chap. 3. This is the reason to omit the cumbersome equations of the inertial torques generated by the propeller's hub, but its equations of the inertial torques are added to the mathematical models of total inertial torques acting on a spinning propeller. The inertial

torques of the blade's mass are generated when the propeller turns around axes that perpendicular to axis of the hub.

A.4.1 Centrifugal Forces Acting on a Spinning Propeller

The first analysis considers the action of the centrifugal force of the rotating propeller's blade.

The reactive resistance torque T_{ct} of the centrifugal force $f_{ct.z}$ of the blade's mass is expressed by the following equation:

$$T_{ct} = f_{ct.z} y_m \tag{A.4.1}$$

where $y_m = r\sin\alpha$ is the distance of the location of the blade's mass along axis *oy, r* is the radius of the location of the blade's mass.

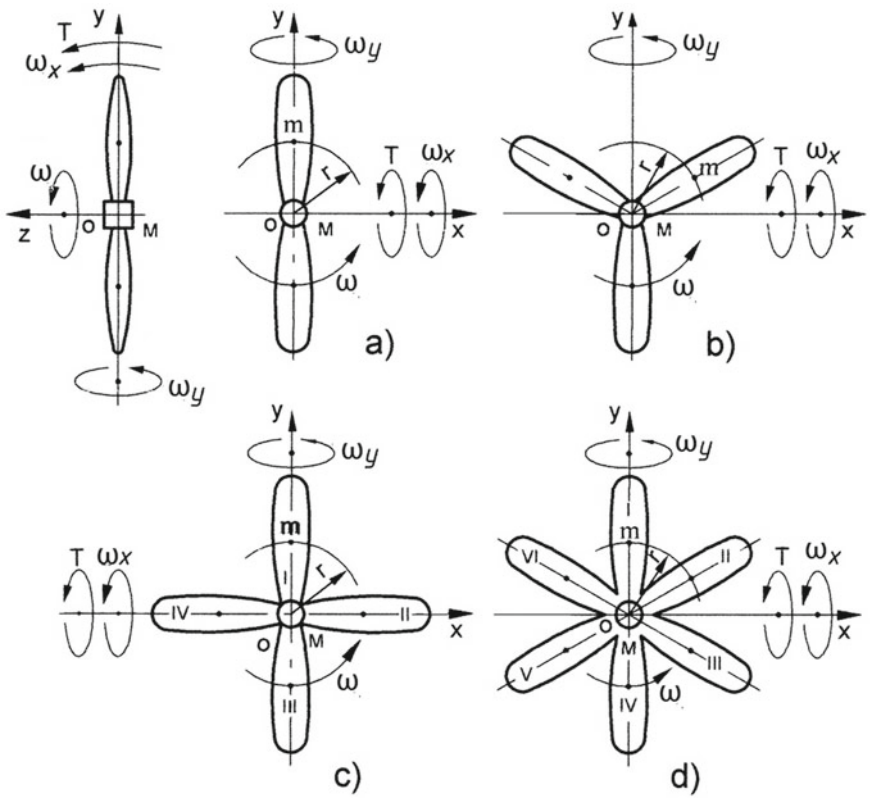

Fig. A.4 Schematic of the propeller design with two (**a**), three (**b**), four (**c**) and six (**d**) blades mounted on a hub

The equation for the axial component of the centrifugal force generated by the propeller blade's mass is presented by the following:

$$f_{\mathrm{ct}.z} = f_{\mathrm{ct}} \sin\alpha \sin\Delta\gamma = mr\omega^2 \sin\alpha \sin\Delta\gamma = mr\omega^2 \Delta\gamma \sin\alpha \tag{A.4.2}$$

where all parameters are as specified above at previous sections.

Substituting the defined parameters into Eq. (A.4.1) yields the following equation:

$$T_{\mathrm{ct}} = -mr^2\omega^2 \times \Delta\gamma \times \sin^2\alpha \tag{A.4.3}$$

Then replacing $\sin^2\alpha = (1/2)(1 - \cos 2\alpha)$that is the trigonometric identity and substituting into Eq. (A.4.3) the following equation emerges:

$$T_{\mathrm{ct}} = -mr^2\omega^2 \times \Delta\gamma \times \frac{1}{2}(1 - \cos 2\alpha) \tag{A.4.4}$$

The following steps of solutions are the same as presented in sections above

$$\frac{\mathrm{d}T_{\mathrm{ct}}}{\mathrm{d}t} = mr^2\omega^2 \frac{1}{2}(1 - \cos 2\alpha)\frac{\mathrm{d}\gamma}{\mathrm{d}t} \tag{A.4.5}$$

$t = \frac{\alpha}{\omega}$, $\mathrm{d}t = \frac{\mathrm{d}\alpha}{\omega}$,

$$\frac{\omega \mathrm{d}T_{\mathrm{ct}}}{\mathrm{d}\alpha} = mr^2\omega^2\omega_x \frac{1}{2}(1 - \cos 2\alpha) \tag{A.4.6}$$

$$\mathrm{d}T_{\mathrm{ct}} = mr^2\omega\omega_x \frac{1}{2}(1 - \cos 2\alpha)\alpha \mathrm{d}\alpha. \tag{A.4.7}$$

$$\int_0^{T_{\mathrm{ct}}} \mathrm{d}T_{\mathrm{ct}} = \int_0^{\pi} mr^2\omega\omega_x \frac{1}{2}(1 - \cos 2\alpha)\mathrm{d}\alpha \tag{A.4.8}$$

$$T_{\mathrm{ct}}\Big|_0^{T_{\mathrm{ct}}} = mr^2\omega\omega_x \frac{1}{2}\left(\alpha - \frac{\sin 2\alpha}{2}\right)\Big|_0^{\pi} \tag{A.4.9}$$

$$T_{\mathrm{ct}} = \frac{1}{2}\pi mr^2\omega\omega_x \tag{A.4.10}$$

The blades of the propeller are located at upper and lower sides relatively axis *ox*. The centrifugal forces act on the upper and lower blades, and then the total resistance torque T_{ct} for the propellers with several blades (Fig. A.4a–d) is obtained when the result of Eq. (A.4.10) is increased according to the number of propeller's blades. The value of the resistance torque generated by the rotating blade is changed by sinus law and expressed by the following equation:

$$T_{\mathrm{ct}} = \frac{1}{2} mr^2 \omega\omega_x \pi \sin\alpha = \frac{1}{2} \pi J \omega\omega_x \sin\alpha \tag{A.4.11}$$

where $J = mr^2$ is the conventional mass moment of inertia of the propeller's blade; other parameters are as specified above.

The change in the value of the total resistance torque T_{ct} for the propellers with several blades (Fig. A.4a–d) can be presented by the diagrams demonstrated in Fig. A.5. These diagrams show the change and fluctuation of the resistance torque T_{ct} generated by the centrifugal forces of the propeller with several blades. The equations for maximal and minimal values of the resistance torques for the propellers are represented in Table A.4. Analysis of Eq. (A.4.11) shows that the value of the resistance torque generated by the centrifugal forces of the rotating blades depends proportionally on the following components:

- the vertical, horizontal or angular location of the blades relative axis,
- the mass and the number of the blades,
- the radius of the location of the blade mass,
- the angular velocity of the propeller and
- the angular velocity of the precession.

A.4.2 Common Inertial Forces Acting on a Spinning Propeller

Inertial torque T_{in} is originally the result of the external torque's action and presents the precession torque which equation is as follows:

$$T_{\mathrm{in}} = f_{\mathrm{in}} x_{\mathrm{m}} = m a_z x_{\mathrm{m}} \tag{A.4.12}$$

where f_{in} is the inertial force of the rotating blade's mass; $x_{\mathrm{m}} = r\ \cos\alpha$; other components are represented in Sect. A.4.1.

The expression for a_{z} is presented by the following equation:

$$\begin{aligned} \alpha_z &= \frac{\mathrm{d}V_z}{\mathrm{d}t} = \frac{\mathrm{d}(V\cos\alpha\, r\ \cos\alpha\ \sin\Delta\gamma)}{\mathrm{d}t} \\ &= -Vr\Delta\gamma 2\cos\alpha\ \sin\alpha \frac{\mathrm{d}\alpha}{\mathrm{d}t} = r^2\omega^2\Delta\gamma 2\cos\alpha\ \sin\alpha \end{aligned} \tag{A.4.13}$$

where $a_{\mathrm{z}} = \mathrm{d}V_z/\mathrm{d}t$ is the acceleration of the blade's mass along with axis oz; $V_{\mathrm{z}} = V\cos\alpha\ r\cos\alpha\ \sin\Delta\gamma$ is the change in the tangential velocity of the blade's mass; $V = r\omega$; $\omega = \mathrm{d}\alpha/\mathrm{d}t$, $\sin\Delta\gamma = \Delta\gamma$; other parameters are as specified above.

Substituting the defined parameters into Eq. (A.4.12) yields the following equation:

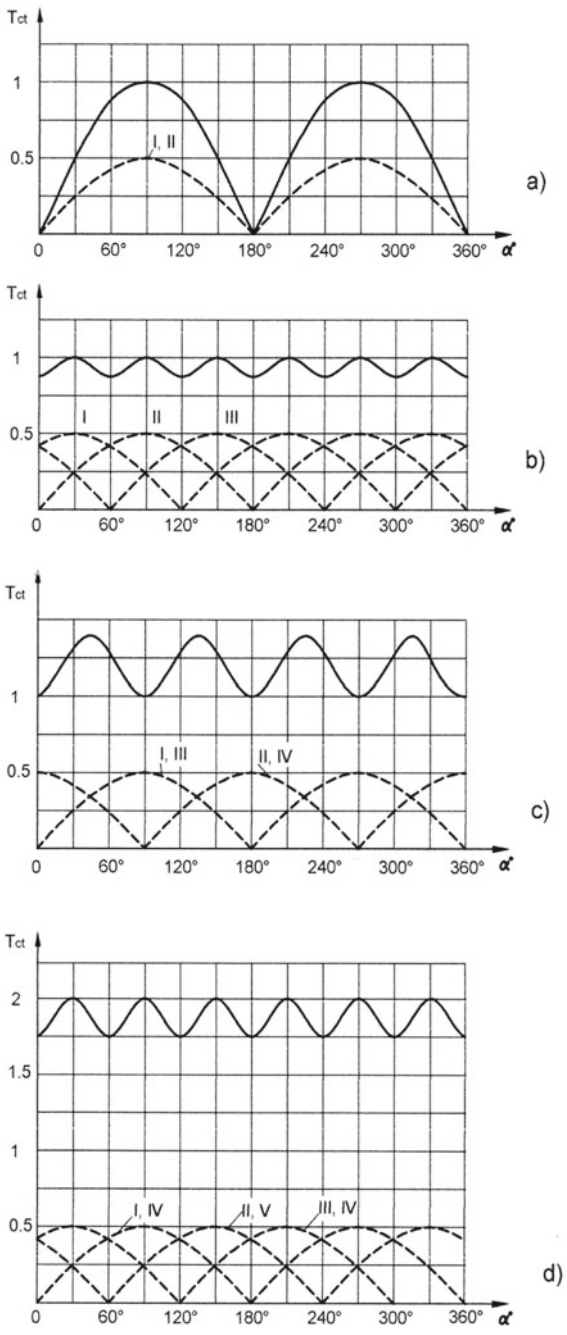

Fig. A.5 Change in the resistance torque generated by the propeller with two blades

Table A.4 Equations of resistance torques generated by the centrifugal forces of propeller's blades

Number blades, n	Equation, T_{ct}	Number of blades location		
		Vertical, n_v	Horizontal, n_h	Angular, n_i
Two	$T_{ct.max} = \pi J\omega\omega_x$	2	0	0
	$T_{ct.min} = 0$	0	2	0
Three	$T_{ct.max} = (n_v + n_a \sin 30°)\frac{1}{2}\pi J\omega\omega_x = \pi J\omega\omega_x$	1	0	2
	$T_{ct.min} = n_a \sin 60° \frac{1}{2}\pi J\omega\omega_x = 0.866\pi J\omega\omega_x$	0	1	2
Four	$T_{ct.max} = n_a \sin 45° \frac{1}{2}\pi J\omega\omega_x = 1.414\pi J\omega\omega_x$	0	0	4
	$T_{ct.min} = (n_v \sin 90°)\frac{1}{2}\pi J\omega\omega_x = J\omega\omega_x$	2	2	0
Six	$T_{ct.max} = (n_v + n_a \sin 30°)\frac{1}{2}\pi J\omega\omega_x = 2\pi J\omega\omega_x$	2	0	4
	$T_{ct.min} = n_a \sin 60° \frac{1}{2}\pi J\omega\omega_x = 1.732\pi J\omega\omega_x$	0	2	4

$$T_{in} = mr^2\omega^2\Delta\gamma 2\cos\alpha\sin\alpha \tag{A.4.14}$$

Equation (A.4.14) is solving as Eq. (A.4.4) with the same final expression.

$$\frac{dT_{in}}{dt} = mr^2\omega^2 2\cos\alpha\sin\alpha\frac{d\gamma}{dt} \tag{A.4.15}$$

$t = \frac{\alpha}{\omega}$, $dt = \frac{d\alpha}{\omega}$,

$$dT_{in} = mr^2\omega\omega_x 2\cos\alpha\sin\alpha\alpha\, d\alpha. \tag{A.4.16}$$

The expression$\cos\alpha\sin\alpha d\alpha = (\sin^2\alpha d\alpha)/2$ that replaced in the equation and following solution is the same as for Eq. (A.4.7).

$$\int_0^{T_{ct}} dT_{in} = \int_0^{\pi} mr^2\omega\omega_x\frac{2}{2}\sin^2\alpha d\alpha = mr^2\omega\omega_x\int_0^{\pi}\frac{1}{2}(1-\cos 2\alpha)d\alpha \tag{A.4.17}$$

$$T_{in}\Big|_0^{T_{in}} = mr^2\omega\omega_x\frac{1}{2}\left(\alpha - \frac{\sin 2\alpha}{2}\right)\Big|_0^{\pi} \tag{A.4.18}$$

$$T_{in} = mr^2\omega\omega_x\frac{1}{2}(\pi - 0) = \frac{1}{2}\pi mr^2\omega\omega_x = \frac{1}{2}\pi J\omega\omega_x \tag{A.4.19}$$

Table A.5 Equations of Coriolis torques generated by the mass of propeller's blades

Number blades, n	Equation, T_{cr}	Number of blades location		
		Vertical, n_v	Horizontal, n_h	Angular, n_i
Two	$T_{cr.max} = \frac{n}{2} mr^2 \omega\omega_x \cos 0° = J\omega\omega_x$	0	2	0
	$T_{cr.min} = 0$	2	0	0
Three	$T_{cr.max} = (n_v \cos 0° + n_a \cos 60°)\frac{1}{2} J\omega\omega_x = J\omega\omega_x$	1	0	2
	$T_{cr.min} = (n_v \cos 90° + n_a \cos 30°)\frac{1}{2} J\omega\omega_x = 0.866 J\omega\omega_x$	1	0	2
Four	$T_{cr.max} = n_a \cos 45° \frac{1}{2} J\omega\omega_x = 1.414 J\omega\omega_x$	0	0	4
	$T_{cr.min} = n_h \frac{1}{2} J\omega\omega_x \cos 0° = J\omega\omega_x$	2	2	0
Six	$T_{cr.max} = (n_h \cos 0° + n_a \cos 60°)\frac{1}{2} J\omega\omega_x = 2J\omega\omega_x$	0	2	4
	$T_{cr.min} = (n_v \cos 90° + n_a \cos 30°)\frac{1}{2} J\omega\omega_x = 1.732 J\omega\omega_x$	2	0	4

where $J = mr^2$ is the conventional mass moment of inertia of the propeller's blade; other parameters are as specified above.

The value of the precession torque generated by the rotating blade is changed by cosine law and expressed by the following equation:

$$T_{in} = \frac{1}{2}\pi J\omega\omega_x \cos\alpha \tag{A.4.20}$$

Equation (A.4.20) is similar to Eq. (A.4.11). The difference in the trigonometric factor in Eq. (A.4.11) is represented by sinα. Then, the precession torques for the propeller with the different number of blades are represented by equations of Table A.5 where the trigonometric factor sinα should be replaced by cosα.

A.4.3 Coriolis Forces Acting on a Spinning Propeller

The resistance torque T_{cr} generated by the Coriolis force f_{cr} of the blade's mass is expressed by the following equation:

$$T_{cr} = -f_{cr} y_m = -ma_z y_m \tag{A.4.21}$$

$y_m = r\sin\alpha$ is the distance to the blade's mass location along axis *oy;* the sign (−) means the action in the clockwise direction that is omitted for the following consideration; a_z is the Coriolis acceleration of the blade's mass along with axis *oz*; other components are presented in Eq. (A.4.2).

The expression for a_z is represented by the following equation:

$$\alpha_z = V\cos\alpha\omega_x = r\omega\omega_x\cos\alpha \tag{A.4.22}$$

where a_z is the acceleration of the blade's mass along with axis *oz*; $V_z = V\cos\alpha$ is the change in the axial velocity of the blade's mass; $V = r\omega$; ω_x is the angular velocity around axis *ox*; other parameters are as specified above.

Substituting Eq. (A.4.22) and defined parameters into Eq. (A.4.21) and transforming yield the following equation:

$$T_{cr} = -mr^2\omega\omega_x\cos\alpha\sin\alpha = -mr^2\omega\omega_x\Delta\gamma\cos\alpha\sin\alpha = -mr^2\omega\omega_x\frac{\sin 2\alpha}{2} \tag{A.4.23}$$

where $\sin 2\alpha = 2\cos\alpha\sin\alpha$is the trigonometric identity,

The following solutions are similar as presented Eq. (A.4.4), and comments are omitted

$$\frac{dT_{cr}}{dt} = -mr^2\omega\omega_x\frac{\cos 2\alpha}{4}\frac{d\alpha}{dt} \tag{A.4.24}$$

$t = \frac{\alpha}{\omega}$, $dt = \frac{d\alpha}{\omega}$, $\frac{d\alpha}{dt} = \omega$,

$$\frac{\omega dT_{cr}}{d\alpha} = -mr^2\omega^2\omega_x\frac{\cos 2\alpha}{4} \tag{A.4.25}$$

$$dT_{cr} = -mr^2\omega\omega_x\frac{\cos 2\alpha}{4}d\alpha. \tag{A.4.26}$$

$$\int_0^{T_{cr}} dT_{cr} = -\int_0^{\pi} mr^2\omega\omega_x\frac{\cos 2\alpha}{4}d\alpha \tag{A.4.27}$$

$$T_{cr}\Big|_0^{T_{cr}} = -\frac{1}{4}mr^2\omega\omega_x\frac{4\sin 2\alpha}{2}\Big|_0^{\pi/4}$$

where the solution of $\sin 2\alpha$ is solved for the limit of $\pi/4$ and result is increased proportionally giving rise to the following

$$T_{cr} = -\frac{1}{2}mr^2\omega\omega_x(1-0) = -\frac{1}{2}mr^2\omega\omega_x = -\frac{1}{2}J\omega\omega_x \tag{A.4.28}$$

where all parameters are as specified above.

The value of Coriolis torque generated by the rotating blade is changed by cosine law and expressed by the following equation:

$$T_{\mathrm{cr}} = -\frac{1}{2} J \omega \omega_x \cos\alpha \tag{A.4.29}$$

Equation (A.4.29) enables defining the maximal and minimal values of the Coriolis torques for the propellers with different numbers of blades. The diagrams of the change in the value of Coriolis torque T_{cr} generated by Coriolis forces of the propeller with different blades are similar to the diagrams for the centrifugal torque T_{ct} generated by the centrifugal forces (Fig. A.5). The differences are the diagrams for Coriolis torques shifted on 90° along the abscissa, and values are less on the factor π according to equations considered, respectively.

A.4.4 Attributes of the Inertial Torques Acting on a Spinning Propeller

The mathematical models for internal torques acting on the propeller's blade are presented in Table A.5.

The total value of the initial resistance torque T_{r} acting around axis *ox* is represented a sum of the resistance torques generated by the centrifugal and Coriolis forces of the blade's mass and propeller's hub.

$$\begin{aligned} T_{\mathrm{r}} &= T_{\mathrm{ct}} + T_{\mathrm{cr}} + T_{\mathrm{ct.h}} + T_{\mathrm{cr.h}} = n\frac{1}{2}\pi J \omega \omega_x \sin\alpha \\ &+ n\frac{1}{2} J \omega \omega_x \cos\alpha + J_{\mathrm{ct.h}} \omega \omega_x + J_{\mathrm{cr.h}} \omega \omega_x \\ &= \left[\frac{1}{2} n J (\pi \sin\alpha + \cos\alpha) + J_{\mathrm{ct.h}} + J_{\mathrm{cr.h}}\right] \omega \omega_x \end{aligned} \tag{A.4.30}$$

where $T_{\mathrm{ct.h}}$ and $T_{\mathrm{cr.h}}$ is the resistance torques of centrifugal and Coriolis forces, respectively, generated by the propeller's hub, $J_{\mathrm{ct.h}} = (2\pi^2/9) J_{\mathrm{h}}$ and $J_{\mathrm{cr.h}} = (8/9)$ J_{h} is their factored mass moment of inertia (Chap. 3); all other parameters are as specified above. Equation (A.4.30) is generic that enable the defining the maximal and minimal values of the resistance torques for the propellers with different numbers of blades.

The total and maximal value of the initial precession torque T_{p} acting around axis *oy* is represented as a sum of the precession torques generated by the inertial forces of the blade's masses and the change in the angular momentum of the propeller's hub, which expression is as follows.

$$T_{\mathrm{p}} = T_{\mathrm{in}} + T_{\mathrm{am}} + T_{\mathrm{in.h}} + T_{\mathrm{am.h}} = \frac{\pi n}{2} J \omega \omega_x \cos\alpha$$

$$+ nJ\omega\omega_x + \frac{2}{9}\pi^2 J_{in.h}\omega\omega_x + J_{am.h}\omega\omega_x$$
$$= \left[nJ\left(\frac{\pi}{2}\cos\alpha + 1\right) + \left(\frac{2}{9}\pi^2 + 1\right)J_h\right]\omega\omega_x \quad \text{(A.4.31)}$$

where $T_{\text{am}} = J\omega\omega_x$ is the torque of the angular momentum of one blade propeller; $T_{\text{in.h}} = \frac{2}{9}\pi^2 J_{\text{h}}\omega\omega_x$ is the torque generated by the centrifugal forces of the hub; $T_{\text{am.h}} = J_{\text{h}}\omega\omega_x$ is the torque generated by the change in the angular momentum of the hub; other parameters are as specified above.

Equation (A.4.31) is generic that enable defining the maximal and minimal values of the precession torques for the propellers based on equations of Table A.5 with the added value of the inertial torques generated by the spinning hub. The diagrams of the change in the value of the inertial torque T_{in} of the propeller with different blades are similar to the diagrams for the torque T_{ct} generated by the centrifugal forces (Fig. A.5). The differences are only the diagrams for inertial torques shifted on 90° along the abscissa.

A.4.5 Working Example

The propeller with two blades has a mass of $m = 6.0$ kg each, and a radius of $R = 0.5$ m about the hub axle. The length of propeller of $L = 0.8$ m and centre mass of the blade locates in the middle of its length. The mass moment of inertia of one blade is $J = mR^2 + mL^2/12$ (parallel-axis theorem). The hub mass is 10 kg and radius of 0.1 m, which the mass moment of inertia is $J_{\text{h}} = m_{\text{h}}R^2/2$. The propeller is spinning at 3000 rpm. An external torque acts on the propeller, which rotates with an angular velocity of precession 0.5 rpm. These data are used to determine the maximal value of the resistance and precession torques generated by the centrifugal, inertial and Coriolis forces, as well as the change in the angular momentum of the spinning propeller (Fig. A.4a). Solving this problem is based on Eqs. (A.4.31) and (A.4.30). Substituting the initial data into the aforementioned equations and transforming yield the following result:

$$T_{\text{p}} = \left[nJ\left(\frac{\pi}{2}\cos\alpha + 1\right) + \left(\frac{2}{9}\pi^2 + 1\right)J_{\text{h}}\right]\omega\omega_x$$
$$= \left[2 \times 5 \times \left(0.5^2 + \frac{0.8^2}{12}\right) \times \left(\frac{\pi}{2} + 1\right) + \left(\frac{2}{9}\pi^2 + 1\right) \times 10 \times \frac{0.1^2}{2}\right]$$
$$\times \frac{3000 \times 2\pi}{60} \times \frac{0.5 \times 2\pi}{60} = 130.899\,\text{Nm}$$

$$T_{\text{r}} = \left[\frac{1}{2}(\pi\sin\alpha + \cos\alpha)nJ + \left(\frac{2}{9}\pi^2 + 1\right)J_{\text{h}}\right]\omega\omega_x$$

$$= \left[\frac{1}{2} \times 3.297 \times 2 \times 5 \times \left(0.5^2 + \frac{0.8^2}{12}\right) + \frac{2}{9}\left(\pi^2 + 4\right) \times 10 \times \frac{0.1^2}{2}\right] \times \frac{3000 \times 2\pi}{60} \times \frac{0.5 \times 2\pi}{60} = 84.789\,\text{Nm}$$

where expression $\pi \sin\alpha + \cos\alpha = 0$ gives the maximal value defined by the first derivative $\pi \cos\alpha - \sin\alpha = 0$. Substituting the trigonometric identity $\cos\alpha = \sqrt{1 - \sin^2\alpha}$and solving yield the following $\alpha = 72.343^{\circ}$. Then $\pi \sin 72.343^{\circ} + \cos 72.343^{\circ} = 3.297$.$T_r$ and T_p are, respectively, the resistance and precession torques generated by the blade and hub masses of the spinning propeller.

The formulated mathematical models for the internal torques acting on propellers with different designs are distinguished and depend on the number of blades. The equations of the inertial torques acting on the propeller with n blades demonstrate that their values are fluctuated, variable and depends on the number of blades. Additionally, these torques proportionally depend on the mass moment of inertia of the propeller's blade and hub, and angular velocity of the spinning propeller as well as the angular velocity of its precession. Derived mathematical models enable for a description for all gyroscope properties and are useful for modelling of forces acting on an aircraft's, helicopter's and ship's propeller and other types of the rotating objects with embedded blades [15].

A.5 Inertial Forces Acting on a Spinning Gas Turbine

In aerospace and ship industries, the designs of gas turbines are more complex than aircraft gas turbines contain the narrow blades embedded radially and sequentially along the axis of the engine's shaft. The computing of the inertial forces acting on the blades of gas turbines is similar as for the multiple blade propellers. The difference in equations of the inertial torques acting on the blades of the turbine is in the numerous number of radial and serial blades located along the engine's stepped shaft. The sequentially located blades are mounted on different diameters of the shaft. Spinning gas turbines manifest the gyroscopic effects at the time of moving the aircraft in space or ship at sea. The blades with a shaft are considered as one spinning holistic object. For the simplicity of an analysis of the inertial forces acting on the complex design of a gas turbine is considered its one section. Such an analytical approach does not violet the scheme for computing inertial forces acting on a gas turbine. The same mathematical models give different values of the inertial forces acting on a gas turbine due to different geometry of its sections. A resulting value of inertial forces is presented their sum of forces acting on the whole construction of the gas turbine.

The action of inertial forces generated by the blade's and the shaft masses is considered for one section of a gas turbine (Fig. A.6). The blade's mass m is located on the defined distance r on the section, and the mass centre of the turbine shaft is

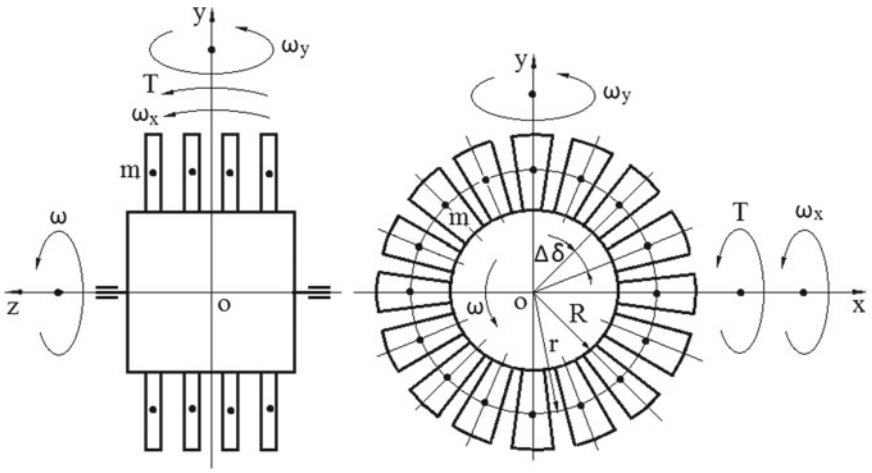

Fig. A.6 Schematic of the spinning gas turbine

m_s. The blade mass m are disposed on the circle of radius r and rotated around axis oz with a constant tangential velocity.

A.5.1 Centrifugal Forces Acting on Blades of a Spinning Gas Turbine

The rotation of the blade mass elements generates the plane of centrifugal forces, which disposes of perpendicular to the axis of the spinning shaft. If an external torque T is applied to the shaft, the plane of the rotating centrifugal forces inclines and resists to the action of the external torque. The change in the plane of the centrifugal force generates the resistance torque ΔT_{ct} produced by the centrifugal force $f_{\mathrm{ct}.z}$ of the blade mass (Fig. 3.2, Chap. 3) and is expressed as follows:

$$\Delta T_{\mathrm{ct}} = -f_{\mathrm{ct}.z} y_m = -m a_z y_{\mathrm{m}} \tag{A.5.1}$$

where y_{m} is the distance of the disposal of the mass element along axis oy,; other components are as specified at previous sections.

The change in the centrifugal force of the mass element is expressed by the following equation:

$$f_{ct.z} = f_{ct} \sin\alpha \sin\Delta\gamma = mr\omega^2 \sin\alpha \sin\Delta\gamma = \frac{Mr\omega^2}{n} \Delta\gamma \sin\alpha \tag{A.5.2}$$

where $f_{ct} = mr\omega^2 = \frac{Mr\omega^2}{n}\Delta n$is the centrifugal force of the blade m; $m = \frac{M\Delta nr}{nr} = \frac{M}{n}\Delta n$ in which M is the mass of the blades; n is the number of blades; Δn is the one blade; other components are as specified at previous sections.

Substituting the defined parameters into Eq. (A.5.1) yields the equation of the resistance torque generated by the centrifugal forces of the mass element.

$$\Delta T_{ct} = -\frac{Mr\omega^2}{n} \times \Delta n \times \Delta\gamma \times \sin\alpha \times y_m \tag{A.5.3}$$

where $y_m = r\sin\alpha$ is the distance of the mass of a blade location relative to axis ox (Fig. 6), and the other components are as specified above.

The location of the resultant force is the centroid (point A, Fig. 3.2, Chap. 3) which is calculated by the known integrated equation.

$$y_A = \frac{\int_{\alpha=0}^{\pi} f_{ct.z}\, y_m d\alpha}{\int_{\alpha=0}^{\pi} f_{ct.z} d\alpha} \tag{A.5.4}$$

Substituting Eq. (A.5.2) and other components into Eq. (A.5.4) and transforming yields the following expression.

$$\begin{aligned} y_A &= \frac{\int_{\alpha=0}^{\pi} f_{ct.z}\, y_m d\alpha}{\int_{\alpha=0}^{\pi} f_{ct.z} d\alpha} = \frac{\int_{\alpha=0}^{\pi} \frac{Mr\omega^2}{n} \times \Delta n \times \Delta\gamma \times r\sin\alpha \sin\alpha d\alpha}{\int_{\alpha=0}^{\pi} \frac{Mr\omega^2}{n} \times \Delta n \times \Delta\gamma \sin\alpha d\alpha} \\ &= \frac{\frac{Mr\omega^2}{n}\Delta n\Delta\gamma \int_{\alpha=0}^{\pi} r\sin^2\alpha d\alpha}{\frac{Mr\omega^2}{n}\Delta n\Delta\gamma \int_{\alpha=0}^{\pi} \sin\alpha d\alpha} = \frac{r\int_0^{\pi}(1-\cos 2\alpha)d\alpha}{2\int_0^{\pi}\sin\alpha d\alpha} \end{aligned} \tag{A.5.5}$$

where the expression $\frac{Mr\omega^2}{n}\Delta n\Delta\gamma$ is accepted as constant for Eq. (A.5.5); the expression $\sin^2\alpha = (1-\cos 2\alpha)/2$ is a trigonometric identity that replaced in the equation, and other parameters are as specified above.

Equation (A.5.3) is presented in a differential form. Substituting Eq. (A.5.5) and replacing $\sin\alpha = \int_0^{\pi/2}\cos\alpha d\alpha$ by the integral expression with defined limits before representing other components by the integral forms, the following equation emerges:

$$\begin{aligned} \int_0^{T_{ct}} dT_{ct} = -Mr\omega^2 \times \int_1^n \frac{1}{n} dn \times \int_0^{\gamma} d\gamma \\ \times \int_0^{\pi} \cos\alpha d\alpha \times \frac{r\int_0^{\pi}(1-\cos 2\alpha)d\alpha}{2\int_0^{\pi}\sin\alpha d\alpha} \end{aligned} \tag{A.5.6}$$

Solving integral Eq. (A.5.6) yields the following result

$$T_{ct}\Big|_0^{T_{ct}} = -Mr\omega^2 \times \left(\ln n\Big|_1^n\right) \times \left(\gamma\Big|_0^{\gamma}\right)$$

$$\times\, 2\left(\sin\alpha\Big|_0^{\pi/2}\right) \times \frac{R\left(\alpha - \frac{1}{2}\sin 2\alpha\right)\Big|_0^{\pi/2}}{-2\cos\alpha\Big|_0^{\pi}}$$

where the change of the limit of sinα leads to the increase twice its value, for sin2α remains the same due to the symmetrical location of the centroid.

$$T_{\mathrm{ct}} = -Mr\omega^2 \times (\lg n - 0) \times (\gamma - 0) \times 2(1 - 0) \times \frac{r\left(\frac{\pi}{2} - 0\right)}{-2(-1 - 1)} = -\frac{Mr^2\omega^2\pi \lg n}{4} \times \gamma \tag{A.5.7}$$

where all parameters are as specified above.

The rate of change in torque T_{ct} per time is expressed by the differential equation

$$\frac{\mathrm{d}T_{\mathrm{ct}}}{\mathrm{d}t} = -\frac{Mr^2\omega^2\pi \lg n}{4}\frac{\mathrm{d}\gamma}{\mathrm{d}t} \tag{A.5.8}$$

The following steps of solution are the same as presented in previous sections $t = \frac{\alpha}{\omega}$, $\mathrm{d}t = \frac{\mathrm{d}\alpha}{\omega}$, $\frac{\mathrm{d}\gamma}{\mathrm{d}t} = \omega_x$

$$\frac{\omega \mathrm{d}T_{\mathrm{ct}}}{\mathrm{d}\alpha} = -\frac{Mr^2\omega^2\pi \ln n}{4}\omega_x \tag{A.5.9}$$

$$\mathrm{d}T_{\mathrm{ct}} = -\frac{Mr^2 \lg n \times \omega\omega_x\pi}{4}\mathrm{d}\alpha \tag{A.5.10}$$

$$\int_0^{T_{\mathrm{ct}}} \mathrm{d}T_{\mathrm{ct}} = -\int_0^{\pi} \frac{Mr^2 \ln n \times \omega\omega_x\pi}{4}\mathrm{d}\alpha \tag{A.5.11}$$

$$T_{\mathrm{ct}}\Big|_0^{T_{\mathrm{ct}}} = -\frac{Mr^2 \ln n \times \omega\omega_x\pi}{4}\alpha\Big|_0^{\pi} \tag{A.5.12}$$

The change in centrifugal forces acts on the upper and lower sides of the blade's plane, then the total resistance torque T_{ct} of the blades for the gas turbine is obtained when the result of Eq. (A.5.12) is increased twice and on the number k of the blades located on along the turbine's shaft.

$$T_{\mathrm{ct}} = -\frac{2k\pi^2 Mr^2 \ln n\omega\omega_x}{4} = -\frac{\pi^2}{2}J\omega\omega_x \tag{A.5.13}$$

The mass moment of inertia for the blades located around the turbine's shaft is computed by the known method of classical mechanics. For simplicity of presentation at this chapter of the mass moment of inertia for the blades is accepted by the conditional expression $J = Mr^2\mathrm{klg}n$ where all parameters are as specified above. The change in the angular momentum is expressed by the following: $T_{\mathrm{am}} = J\omega\omega_x$.

A.5.2 Common Inertial Forces Acting on Blades of a Spinning Gas Turbine

The analytical approach for the modelling of the acting inertial forces generated by the mass elements of the blades of the gas turbine is the same as represented in previous sections. The precession torque T_{in} generated by the inertial forces of the blade's masses is expressed by the same equation as for the centrifugal forces:

$$T_{in} = \frac{\pi^2}{2} J \omega \omega_x \tag{A.5.14}$$

where all components are represented in Eq. (A.5.13).

A.5.3 Coriolis Forces Acting on Blades of a Spinning Gas Turbine

The resulting action of Coriolis force, generated by the mass elements of the rotating blade, is expressed as the resistance torque which is expressed by the following equation:

$$\Delta T_{\text{cr}} = f_{\text{cr}} y_{\text{m}} = m a_z y_{\text{m}} \tag{A.5.15}$$

where ΔT_{cr} is the torque generated by the Coriolis force f_{cr} of the rotating blade, $m = \frac{M}{n} \Delta n$, (Eq. (A.5.2)); $y_{\text{m}} = r \sin\alpha$ is the distance to the blade's mass location along axis *oy*, a_z is the Coriolis acceleration of the blade along with axis *oz*, and other components are represented in Eq. (A.5.1).

The expression for a_z is represented by the following equation:

$$\alpha_z = V \cos\alpha \omega_x = r \omega \omega_x \cos\alpha \tag{A.5.16}$$

where $V = r\omega \cos\alpha$ is the tangential velocity of the blade; ω_x is the angular velocity around axis *ox*, other parameters are as specified above.

Substituting defined parameters into an expression of f_{cr} and transforming yield the following:

$$f_{\text{cr}} = \frac{M}{n} \Delta n \omega \omega_x r \cos\alpha \tag{A.5.17}$$

Substituting these defined parameters into Eq. (A.5.15) and transforming yields the following equation:

$$\Delta T_{\text{cr}} = \frac{M}{n} \Delta n \omega \omega_x r \cos\alpha \times y_{\text{C}} \tag{A.5.18}$$

The Coriolis forces represent the distributed load applied along the length of the circle and the cone forming line where the cone's mass elements are located. The location of the resultant force is the centroid (point C, Fig. 3.4, Chap. 3) of the area under the Coriolis force's curve calculated by Eq. (3.4) of Chap. 3 but with its own symbols. The centroid is expressed by the following equation:

$$y_C = \frac{\int_{\alpha=0}^{\pi} f_{cr} y_m d\alpha}{\int_{\alpha=0}^{\pi} f_{cr} d\alpha} = \frac{\int_{\alpha=0}^{\pi} \frac{M}{n} \Delta n \omega \omega_x r \cos\alpha \times r \sin\alpha d\alpha}{\int_{\alpha=0}^{\pi} \frac{M}{n} \Delta n \omega \omega_x r \cos\alpha d\alpha} = \frac{\frac{M}{n} \Delta n \omega \omega_x r^2 \int_{\alpha=0}^{\pi} \sin\alpha \cos\alpha d\alpha}{\frac{M}{n} \Delta n \omega \omega_x r \int_{\alpha=0}^{\pi} \cos\alpha d\alpha} = \frac{r \int_0^{\pi} \sin\alpha \cos\alpha d\alpha}{\int_0^{\pi} \cos\alpha \alpha d\alpha} \tag{A.5.19}$$

where the expression $\frac{M}{n} \Delta n \omega \omega_x r$ is accepted as constant for Eq. (A.5.19), the expression $2 \sin\alpha \cos\alpha = \sin 2\alpha$ is a trigonometric identity that is replaced in the equation, and other parameters are as specified above.

Equation (A.5.19) is substituted into Eq. (A.5.18), and replacing $\cos\alpha = -\int_0^{\pi} \sin\alpha d\alpha$ by the integral expression with defined limits and presenting by the integral form that yield the following equation:

$$\int_0^{T_{cr}} dT_{cr} = M \omega \omega_x r \times \int_1^n \frac{dn}{n} \times \int_0^{\pi} -\sin\alpha d\alpha \times \frac{r \int_0^{\pi} \sin 2\alpha d\alpha}{2 \int_0^{\pi} \cos\alpha d\alpha} \tag{A.5.20}$$

The following solution is the same as presented in Sect. A.5.2 of Appendix A.

$$T_{\text{cr}} \Big|_0^{T_{\text{cr}}} = M \omega \omega_x r \times \left(\ln n \Big|_1^n\right) \times \left(-\cos\alpha \Big|_0^{\pi}\right) \times \frac{-r \cos 2\alpha \Big|_0^{\pi/2}}{8 \sin\alpha \Big|_0^{\pi/2}} \tag{A.5.21}$$

The limits for the integral solution of $\cos\alpha$ in increased twice and for $\sin 2\alpha$ remains the same due to the symmetrical location of the centroid, because the centroid locates symmetrically. Coriolis forces act on the upper and lower sides of the turbine's plane, and then, the total resistance torque T_{cr} is obtained when the result of Eq. (A.5.31) is increased twice and on the number k of the serial location of the blades along the shaft:

$$T_{\text{cr}} = k M r^2 \ln n \omega \omega_x = J \omega \omega_x \tag{A.5.22}$$

Table A.6 Equations of the internal torques acting on the blades of the gas turbine

Type of the torque generated by	Equation
Centrifugal forces	$T_{ct} = T_{in} = \frac{\pi^2}{2} J\omega\omega_x$
Inertial forces	
Coriolis forces	$T_{cr} = T_{am} = J\omega\omega_x$
Change in an angular momentum	
Resistance torque $T_r = T_{ct} + T_{cr}$	$T_r = T_p = \left(\frac{\pi^2}{2} + 1\right) J\omega\omega_x$

where $J = Mr^2 \text{klg}n$ is the accepted blades mass moment of inertia, and other parameters are as specified above.

A.5.4 Attributes of the Inertial Torques Acting on a Spinning Gas Turbine

The total initial precession torque T_p acting on the blades of the gas turbine has presented a sum of the precession torques generated by the inertial forces of the mass elements and the change in the angular momentum whose equation is as follows:

$$T_p = T_{in} + T_{am} = \left(\frac{\pi^2}{2} + 1\right) J\omega\omega_x \tag{A.5.23}$$

The total initial resistance torque T_r acting on the blades of the gas turbine has presented a sum of the resistance torques generated by the centrifugal and Coriolis forces of the cone's mass elements whose equation is as follows:

$$T_r = T_{ct} + T_{cr} = \left(\frac{\pi^2}{2} + 1\right) J\omega\omega_x \tag{A.5.24}$$

where all components are as specified above.

The mathematical models for internal torques acting on the blades of the spinning gas turbine are represented in Table A.6.

Analysis of the inertial torques acting the blades of the gas turbine demonstrates differences in the results compare with other spinning objects.

A.5.5 Working Example

The blades of the small gas turbine have a mass of 3.0 kg; the number of the radial blades is 12, the number of the serial blades is 4; the radius location of the blades is 0.1 m at about the spin axis and spinning at 3000 rpm. External torque acts on the gas

turbine, which rotates with an angular velocity of 0.05 rpm. It is determined by the value of the resistance and precession torques generated by the centrifugal, common inertial and Coriolis forces, as well as the change in the angular momentum of the blades of the gas turbine (Fig. A.6). Solving this problem is based on the equations in Table A.6. Substituting the initial data into the aforementioned equations and transforming yield the following result:

$$T_{\mathrm{p}} = T_{\mathrm{r}} = T_{\mathrm{ct}} + T_{\mathrm{cr}} = \left(\frac{\pi^2}{2} + 1\right) J\omega\omega_x = \left(\frac{\pi^2}{2} + 1\right) Mr^2 k \lg n\, \omega\omega_x$$
$$= \left(\frac{\pi^2}{2} + 1\right) \times 3.0 \times 0.1^2 \times 4 \times \ln 12$$
$$\times \frac{3000 \times 2\pi}{60} \times \frac{0.05 \times 2\pi}{60} = 2.9110258927\,\mathrm{Nm}$$

where T_{r} and T_{p} are, respectively, the initial resistance and precession torques generated by the blades of the spinning gas turbine.

References

1. Cordeiro, F.J.B.: The Gyroscope. Createspace, NV, US (2015)
2. Greenhill, G.: Report on Gyroscopic Theory. Relink Books, Fallbrook, CA, US (2015)
3. Scarborough, J.B.: The Gyroscope Theory and Applications. Nabu Press, London (2014)
4. Neil, B.: Gyroscope. The Charles Stark Draper Laboratory, Inc., Cambridge, Massachusetts. Publication year: 2014. http://dx.doi.org/10.1036/1097-8542.304100
5. Weinberg, H.: Gyro Mechanical Performance: The Most Important Parameter, Technical Article MS-2158, pp. 1–5. Analog Devices, Norwood, MA (2011)
6. Hibbeler, R.C., Yap K.B.: Mechanics for Engineers—Statics and Dynamics, 13th edn. Prentice Hall, Pearson, Singapore (2013)
7. Gregory, D.R.: Classical Mechanics. Cambridge University Press, New York (2006)
8. Taylor, J.R.: Classical Mechanics. University Science Books, California, USA (2005)
9. Aardema, M.D.: Analytical Dynamics. Theory and Application. Academic/Plenum Publishers, New York (2005)
10. Jewett, J., Serway, R.A.: Physics for Scientists and Engineers, 10 edn. Cengage Learning USA, Boston (2018)
11. Knight, R.D.: Physics for Scientists and Engineers: A Strategic Approach with Modern Physics, 4 edn. Pearson, London, UK (2016)
12. Polyanin, A.D., Manzhirov, A.V.: Mathematics for Engineers and Scientists. Chapman & Hall/CRC (2007)

13. Usubamatov, R.: Mathematical models for principles of gyroscope theory. In: Proceedings of American Institute of Physics, pp. 020133-1–020133-21 (2017) https://doi.org/10.1063/1.4972725
14. Usubamatov, R.: Inertial forces acting on gyroscope. J. Mech. Sci. Technol. **32**(1), 101–108 (2018)
15. Usubamatov, R.: Mathematical models for gyroscope properties. Math. Eng. Sci. Aerosp. **8**(3), 359–371 (2017)
16. Usubamatov, R.: Mathematical models for inertial forces acting on a spinning sphere. Int. J. Sci. Eng. Res. **8**(12) (2017)
17. Usubamatov, R., Zhumaev, T.: Inertial forces acting on a propeller of aircraft. Open Aerosp. Eng. J. **7** (2018). https://doi.org/10.2174/1874146001807010001
18. Usubamatov, R., Arzybaev, A.: Inertial Torques Acting on a Spinning Paraboloid. AIP Advances 10, 055124 (2020). https://doi.org/10.1063/1.5145389

Appendix B
Applications of Gyroscopic Effects in Engineering

The contemporary tendency of engineering processes is manifested in an increase of velocities of rotating objects. Naturally, the intensification of machine work will lead to proportional increases in the values of acting inertial forces and torques generated by the rotating masses of objects. Any kind of incorrectness in calculations of gyroscopic effects will create problems for manufacturers and practitioners that expressed by the machine failures or incorrect work. Such defects in engineering fall on engineers and researchers. To improve the quality of the machine work is necessary to use the correct theory of gyroscopic effects for rotating objects. The know textbooks of machine dynamics and handbooks contain the chapters of gyroscope theory [1–4] and typical examples with solutions of gyroscopic effects for different rotating objects as turbines, rotors, discs and other components of the mechanism [6–10]. The practice of applications the known mathematical models for gyroscopic defects does not validate them. Appendix B considers the application of the new mathematical models for inertial torques acting on the rotating objects. The solutions to complex problems presented in the known textbooks are revised in the light of a new analytical approach to gyroscopic effects. The new fundamental principles of gyroscope theory and applications for engineering problems are considered for the complex action of the inertial forces on the rotating objects [11–16].

B.1 Gyroscopic Torques Acting on an Airplane Propeller

The two blades propeller on an airplane has a mass of 15 kg and a radius of gyration 0.7 m about the axis of spin. The blades are mounted on the hub whose mass is 12 kg and diameter 0.2 m. The propeller is spinning at 350 rad/s in a counterclockwise direction. The airplane is travelling at 300 km/hr and enters a vertical curve having a radius of 80 m. Here is how to determine the maximal gyroscopic bending moment, which the propeller exerts on the bearings of the engine (Fig. B.1).

© The Editor(s) (if applicable) and The Author(s), under exclusive license to Springer Nature Singapore Pte Ltd. 2020

R. Usubamatov, *Theory of Gyroscopic Effects for Rotating Objects*,
https://doi.org/10.1007/978-981-15-6475-8

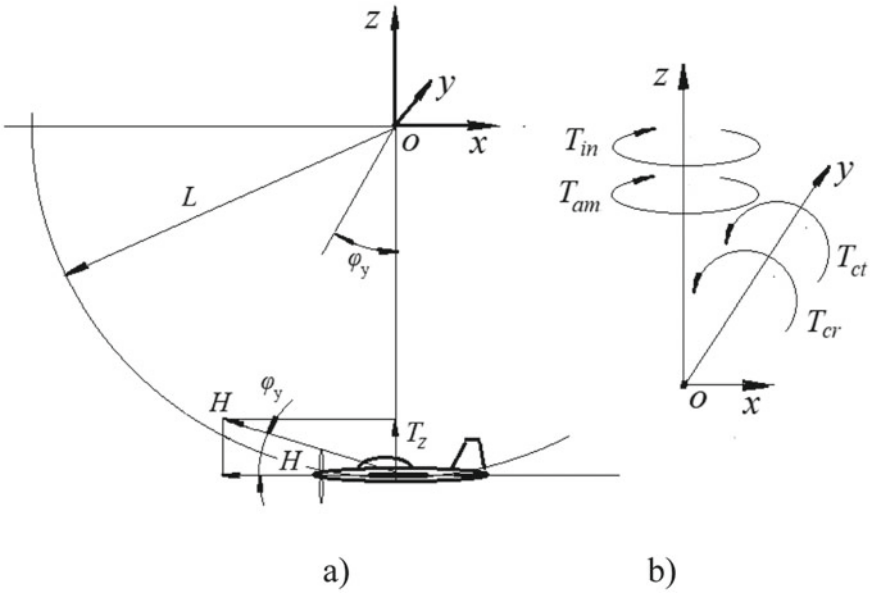

Fig. B.1 Schematic of calculating of the propeller's gyroscopic bending moment

Solution

The circular motion of the f airplane manifests gyroscopic effects as the action of the inertial torques generated by the propeller. At the starting time of the airplane flight by circular trajectory, the following inertial torques are acting on the propeller (Fig. B.1). The equations of inertial torques are represented in Tables A.1 and A.2 of Appendix A, whose components are as follows:

- the maximal resistance torques generated by the centrifugal $T_{\text{ct}} = \pi J \omega \omega_y$ and Coriolis $T_{\text{cr}} = J \omega \omega_y$ forces of the spinning propeller acting around axis *oy*.
- the maximal precession torques generated by the change in the angular momentum $T_{\text{am}} = J \omega \omega_y$ of the disc and the common inertial forces $T_{\text{in}} = \pi J \omega \omega_y$ acting around axis *oz*.

The pilot has blocked the side turn of the airplane around axis *oz* and the turnaround axis *ox*. The blocking of the turn of the airplane around axis *oz* deactivates the resistance inertial torques T_{ct} and T_{cr} acting on the propeller around axis *oy* (Chap. 8). The precession torques T_{in} and T_{am} act on the propeller.

The airplane flies along the curve, which creates the forced angular velocity of precession around axis *oy* that is as follows:

$$\omega_y = \frac{V}{L} = \frac{300000(\text{m})/3600(\text{s})}{80(\text{m})} = 1.04 \frac{\text{rad}}{\text{s}}. \tag{B.1.1}$$

The gyroscopic torques acting on the propeller are generated by the action of the common inertial forces and the change in the angular momentum around axis *oz* (Fig. A.6b, Appendix A). The flight of an aeroplane does not allow for acquiring the angular velocity around axes *oz* and *ox*. Hence, the torques generated by the centrifugal and Coriolis forces are deactivated around axis *oy* (Sect. A.5, Appendix A). The bending moment acts only around axis *oz*.

The equation of the mass moment of inertia of the propeller should be rearranged and represented by the equation of the propeller's gyration radius. The mass moment of the propeller's inertia is $J = Mr_g^2$, where M is mass and r_g is the radius of gyration. Then $J = M(r_g)^2/12$. The bending moments acting on the propeller are calculated by the equation of precession torque (Sect. A.4, Appendix A) and by property of deactivation of gyroscopic inertial torques. The flight trajectory of an airplane represents its rotation around one axis oy (Fig. B.1). In such condition, gyroscopic inertial torques of the propeller (T_{ct}, T_{in}, T_{cr}, Fig. B.1b) are deactivated, except the change in the angular momentum T_{am}. Then, the bending moment acting on the propeller is computed by the following equation:

$$\begin{aligned} T_p &= [J + J_h]\omega\omega_y \\ &= \left[15 \times 0.7^2/12 + \frac{12.0 \times 0.2^2}{2}\right] \times 350.0 \times 1.04 \\ &= 310.31\,\text{Nm} \end{aligned}$$

where T_p is the precession torque, J and J_h are mass moment of inertia of the two blades propeller and the hub, respectively; ω is the angular velocity of the propeller; ω_y is the forced angular velocity of precession of the propeller around axis *oy*.

Presented the example given above is typical for calculation the gyroscope effects acting on rotating shafts, discs, blades, etc., that can be demonstrated as the airplane jet turbines, rotors of the electric motors which are not stationary, ships gas turbines, etc. Except examples considered above, there are other numerous machines and mechanisms with rotating discs of high angular velocity that can be movable in space.

The terms that accepted in aviation and marine industries like the rolling, pitching and yawing of an object in space can cause the gyroscopic action of motors and turbines in three mutually perpendicular directions. Roiling is rotation about the longitudinal axis of the object, pitching is rotation about a transverse axis, and yawing is rotation about a vertical axis. The gyroscope effects that represented as motions of the rotating object under the action of the torques should be considered in each direction and plane. The results as motions or forces acting on bearings of mechanisms in space are defined according to the rules of classical mechanics.

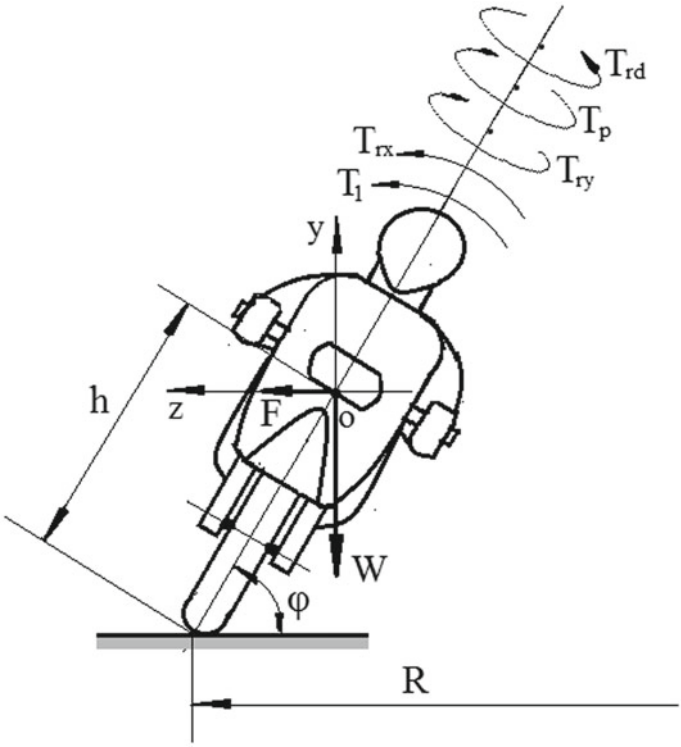

Fig. B.2 Motorcycle running by the circular track

B.2 Gyroscopic Torques Acting on a Motorcycle Rounding a Curve

A motorcycle with a rider weighs 2500.0 N and their combined centre of gravity is 600.0 mm above the road when a motorcycle is upright. The wheels are of 650 mm diameter and have the property of the disc. A moment of inertia of the wheel is 0.5 kg m^2. The moment of inertia of the rotating parts of the engine is 0.1 kg m^2. The axis of rotation of the engine crankshaft is parallel to that of the road wheels and the same sense. The gear ratio is 5 to 1. Determine the moment applied to the steering bar by the rider and the angle of heel necessary when the motorcycle is taking a turn over a track of 30.0 m radius at a speed of 60.0 km/h (Fig. B.2).

Solution

The presented data enable to calculate the torque generated by the centrifugal, Coriolis and common inertial forces and the change in angular momentum of the two wheels and an engine. The components of these equations are the mass moment of inertia, angular velocity and angular precession of the wheels (Table 3.1 of Chap. 3).

The angular velocity of the wheel is

$$\omega = \frac{V}{r} = \frac{60000\,\text{m}}{3600\,\text{s} \times 0.65/2\,\text{m}} = 51.282\,\text{rad/s} \tag{B.2.1}$$

where V is the linear velocity of the motorcycle, r is the radius of the wheel.

The angular precession of the motorcycle motion by the circular track is calculated by the following equation

$$\omega_\text{p} = \frac{V}{R} = \frac{60000\,\text{m}}{3600\,\text{s} \times 30.0\,\text{m}} = 0.5555\,\text{rad/s} \tag{B.2.2}$$

where R is the radius of the motorcycle track; all parameters are as specified above.

The rider applies the torque T_rd to the steering bar to overcome the resistance torques generated by the inertial forces and change in the angular momentum of the motorcycle's spinning parts. The resistance torques generated by the centrifugal T_ct and Coriolis T_cr forces of the rotating two wheels and an engine parts act at the direction of the driver's torque. The motorcyclist motions are conducted around axes ox and oy, and the torques of the inertial and centrifugal forces acting about these axes are compensated. The equation of the balance of acting torques is represented by the following equation:

$$T_\text{rd} = (2T_\text{amy.w} + T_\text{amy.en}) + (2T_\text{cry.w} + T_\text{cry.en}) + (2T_\text{cty.w} + T_\text{cty.en}) \tag{B.2.3}$$

where J_w and J_en are the angular momentum of the wheel and an engine, respectively, $\omega_\text{en} = 5\omega$ is the angular velocity of the engine, and all other parameters are as specified above.

Substituting appropriate equations of Table 3.1, Chap. 3 into Eq. (B.2.3) and transforming yield the following equation:

$$T_\text{rd} = \left(\frac{2}{9}\pi^2 + \frac{8}{9} + 1\right) \times \left(2J_\text{w}\omega\omega_\text{p} + J_\text{en}\omega_\text{en}\omega_\text{p}\right) \tag{B.2.4}$$

Substituting initial defined data into Eq. (B.2.4) and transforming yield the torque generated by the driver to control the motorcycle:

$$\begin{aligned} T_\text{rd} &= \left(\frac{2}{9}\pi^2 + \frac{8}{9} + 1\right) \times \left(2J_\text{w}\omega\omega_\text{p} + J_\text{en}\omega_\text{en}\omega_\text{p}\right) \\ &= \left(\frac{2}{9}\pi^2 + \frac{8}{9} + 1\right) \\ &\quad \times (2 \times 0.5 \times 51.282 \times 0.5555 + 0.1 \times 5 \times 51.282 \times 0.5555) \\ &= 174.449\,\text{Nm} \end{aligned} \tag{B.2.5}$$

The centrifugal moment T_1 tending to cause rollover of the motorcycle with the rider is defined about the contact point of the wheel with the road, and the result of calculation gives the following

$$T_1 = Fh\cos\phi = m\frac{V^2}{R}h = \frac{2500\,\text{N}}{9.8\,\text{m/s}^2} \times \frac{(60000/3600\,\text{m/s})^2}{30\,\text{m}} \times 0.6\,\text{m} \times \cos\phi = 85.0340\cos\phi\,\text{Nm} \tag{B.2.6}$$

where $F = MV^2/R$ is the centrifugal force, M is the mass of the motorcycle with the rider, V is the tangential velocity of the motorcycle, R is the radius of the motorcycle motion by the circular track, h is the height of the car's centre mass above the road.

The centrifugal T_1 and gyroscopic resistance torques T_{rx} act in the same direction. The torque created by the weight W of the motorcycle with the rider about the contact point of the wheel presents the resistance torque on the action of the centrifugal T_1 and gyroscopic T_{rx} torques. The angle of the inclination of the motorcycle is necessary for its balance that calculated by the following equation:

$$T_{\text{rx}} + T_1 = W \times h\sin\phi \tag{B.2.7}$$

Substituting expressions of the inertial torques defined above into Eq. (B.2.7) and solution yields the following result:

$$\phi = \arcsin\frac{\left(\frac{2}{9}\pi^2 + \frac{8}{9}\right) \times \left(2J_{\text{w}}\omega\omega_{\text{p}} + J_{\text{en}}\omega_{\text{en}}\omega_{\text{p}}\right) + T_1}{W \times h} = \arcsin\frac{\left(\frac{2}{9}\pi^2 + \frac{8}{9}\right) \times (2 \times 0.5 \times 51.282 \times 0.5555 + 0.1 \times 5 \times 51.282 \times 0.5555) + 85.0340}{2500 \times 0.6} = 8.3^\circ$$

where W is the weight of the motorcycle with the rider, h is the location of the centre of gravity above the road when the motorcycle is upright; other parameters are as specified above.

The gyroscopic effects of the rotating wheels and engine parts act on the motorcycle, which should have defined heel that depends on the radius of a circular track, the speed and weight of the motorcycle.

B.3 Gyroscopic Torques Acting on Crushing Mills

The principle of gyroscope effects has been applied in the crushing pendulum mills used for ore, seeds, etc, where the intense pressure is desired (Fig. B.3). The pendulum mill consists of a large steel pan in which two heavy flywheels of $M = 1000$ kg mass, with thick rims roll on the bottom of the pan without slipping. The internal and external radius of the flywheel about its axle is 0.3 m and 0.6 m, respectively. The total length of the axle is 1.2 m, and the angle φ of the pan cone is 30°. The

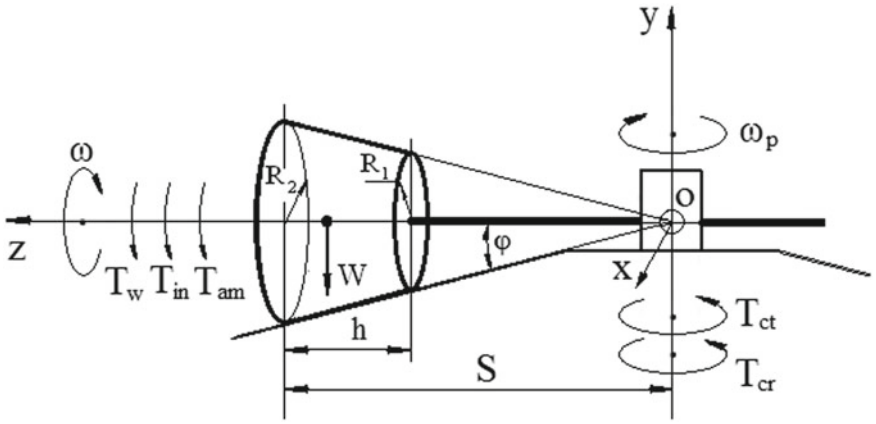

Fig. B.3 Crushing pendulum mill

flywheels revolve about a vertical shaft passing through the centre of the pan with the angular velocity of $\omega_p = \pi$ rad/s and with spinning about own axis of $n =$ 30.0 rpm. The pan and flywheels designed with conic surfaces that enable to avoid intensive friction processes of two surfaces due to different tangential velocities of the flywheel edges. The friction process is unavoidable for the horizontal design of the pan. The two flywheels are placed symmetrically about the shaft and rotated around horizontal axes. The axes of flywheels are attached to the vertical shaft using couplings that permit them to have enough vertical motion to roll over uneven lumps in the pan. Figure B.3 represents the general case of one flywheel where is considered the action of the gyroscopic effects. Define the power required for the work of the crushing pendulum mill.

Solution

The circular motion of the flywheels manifests gyroscopic effects as the action of the inertial torques generated by their rotating masses. At the starting condition, the following inertial torques are acting on the flywheels (Fig. B.3). The equations of inertial torques are represented in Table 3.1 of Chap. 3, whose components are as follows:

- the resistance torques generated by the centrifugal $T_{ct} = \frac{2\pi^2}{9} J\omega\omega_y$ and Coriolis $T_{cr} = \frac{8}{9} J\omega\omega_y$forces of the spinning disc acting around axis *oy*.
- the precession torques generated by the change in the angular momentum $T_{am} = J\omega\omega_y$of the disc and the common inertial forces $T_{in} = \frac{2\pi^2}{9} J\omega\omega_y$ acting around axis *ox*.

The turn of the flywheels around axis *ox* is blocked due to the construction of the pendulum mill. The blocking turn around axis *ox* deactivates the inertial torques T_{ct} and T_{cr} acting on the wheel around axis *oy* and inertial torque T_{in} around axis *ox*

(Chap. 8). The precession torques T_{am} acts on the rotating flywheels and hence on a conic pan.

If the vertical shaft is rotated with the constant speed, the gyroscopic effect of the flywheel on the bottom of the pan is given by the following equation:

$$T = WS_{\text{cg}} + T_{\text{p}} = Mg\left[S - h\left(1 - \frac{R_1}{R_2 + R_1}\right)\right]\cos\phi + J\omega\omega_{\text{p}}$$
$$= Mg\left[S - h\left(1 - \frac{R_1}{R_2 + R_1}\right)\right] + \left(\frac{20}{81}\pi^2 + 1\right)\frac{3}{10}\frac{M(R_2^5 - R_1^5)}{(R_2^3 - R_1^3)}\omega\omega_{\text{p}} \quad \text{(B.3.1)}$$

where T is the total moment of action the forces about the point o; $W = Mg$ is the weight of the flywheel; $S_{\text{cg}} = S - h\left(1 - \frac{R_1}{R_2+R_1}\right)$ is the length of axle (distanced from the point o to the centre of gravity) [Appendix A]; $T_{\text{p}} = J\omega\omega_{\text{p}}$is the precession torque generated by the rotating flywheel (Eq. 3.43); $J = \frac{3}{10}\frac{M(R_2^5-R_1^5)}{(R_2^3-R_1^3)}$ is the mass moment of inertia of the flywheel [1, 4, 6, 9]; ω is the angular velocity of the flywheel; ω_{p} is the angular velocity of the precession of the flywheel around the vertical axis O; other components are specified above and in Fig. B.5.

$$\omega_{\text{p}} = \pi \text{ rad/s} = 3.141 \text{ rad/s} \quad \text{(B.3.2)}$$

Since by hypothesis the flywheel does not slip on the plate of the pan, the angular velocity of the flywheel rotation is defined by its tangential velocity. The average tangential velocity of the rotation the flywheel about axis of the pane is as follows

$$V = 2\pi nS = 2\pi \times \frac{30}{60} \times 0.6 = 1.885 \text{ m/s} \quad \text{(B.3.3)}$$

The angular velocity of the flywheel is as follows

$$\omega = 2\pi n/60 = 2\pi \times 30/60 = 3.141 \text{ rad/s} \quad \text{(B.3.4)}$$

The mass moment of the flywheel inertia is (Sect. A.2, Appendix A)

$$J = \frac{3}{10}\frac{M(R_2^5 - R_1^5)}{(R_2^3 - R_1^3)} = \frac{3}{10} \times \frac{1000 * (0.6^5 - 0.3^5)}{(0.6^3 - 0.3^3)} = 119.571428571 \text{ kg m}^2 \quad \text{(B.3.5)}$$

The crushing torque is as follows

$$T = Mg\left[S - h\left(1 - \frac{R_1}{R_2 + R_1}\right)\right] + \frac{3}{10}\frac{M(R_2^5 - R_1^5)}{(R_2^3 - R_1^3)}\omega\omega_p$$
$$= 1000 \times 9.81 \times \left[1.2 - 0.6 \times \left(1 - \frac{0.3}{0.6 + 0.3}\right)\right]$$
$$+ 119.571428571 \times 3.141 \times 3.141 = 9027.677485281\,\text{Nm} \quad \text{(B.3.5)}$$

The total crushing force is

$$F = T/\left(S_{cg}\cos 30^\circ\right) = 9027.677485281/(0.8\cos 30^\circ) = 13030.330065\,\text{N} \quad \text{(B.3.6)}$$

The weight of the flywheel gives the following crushing force:

$$F_W = Mg/\cos\varphi = 1000 \times 9.81 \times \cos 30^\circ = 11327.612281500\,\text{N} \quad \text{(B.3.7)}$$

The gyroscope precession torque (Sect. A.2, Appendix A) of the flywheel gives the following crushing force:

$$\frac{3}{10}\frac{M(R_2^5 - R_1^5)}{(R_2^3 - R_1^3)}\omega\omega_p = F_p S_{cg}\cos 30^\circ \text{ or}$$
$$F_p = \frac{119.571428571 \times 3.141 \times 3.141}{0.8 \times \cos 30^\circ} = 6284.882859\,\text{N} \quad \text{(B.3.8)}$$

The force of the gyroscopic effect is $F_W/F_p = 1.802$ times less than the action of the flywheel weight. The power required for the crushing process by two flywheels is calculated by the following equation

$$P = 2FR_{cg}f\omega_p \quad \text{(B.3.9)}$$

where $R_{cg} = 0.4$ m is the radius of the flywheel at the point of the gravity centre (Fig. B.3).

Substituting defined parameters and initials data into this equation yield the following result:

$$P = 2FR_{cg}f\omega_p = 2 \times 13030.330065 \times 0.4 \times 0.2 \times 3.141$$
$$= 6548.522677\,\text{W} \approx 6.550\,\text{kW} \quad \text{(B.3.10)}$$

where $f = 0.2$ is the crashing coefficient, and other parameters are as specified above.

The crushing pendulum mill should be equipped with the motor of the power not less than 6.550 kW.

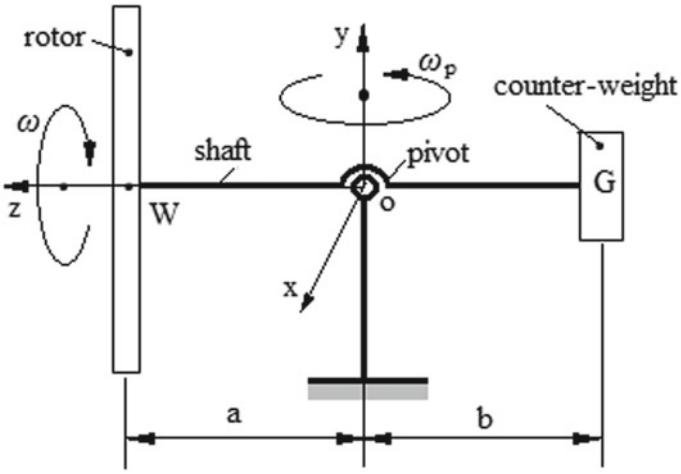

Fig. B.4 Gyroscopic device with counterweight

B.4 Gyroscopic Torques Acting on a Rotor with CounterWeight

The 3.0 kg rotor with the mass moment of inertia about a spin axis is 0.1×10^{-4} kg m^2 rotates with constant angular velocity $\omega = 50.0$ rad/s in the counterclockwise direction. The rotor locates on 300 mm from the spherical pivot. The disc-type counterweight has a mass 4.0 kg, and by adjusting its position b from the spherical pivot can change in the precession of the rotor about its supporting spherical pivot while the shaft remains horizontal (Fig. B.4). The mass moment of inertia around axis ox of the rotor is 4.0×10^{-4} kg m^2 and the counterweight is 5.0×10^{-4} kg m^2. Determine the position b that enables the rotor to have a constant precession $\omega_p = 0.5$ rad/s around the pivot. Neglect the weight of the shaft and friction forces in the pivot.

The origin of the coordinate system $\Sigma oxyz$ is located at the fixed-point o. In the conventional sense, the oz axis is chosen along the axis of precession and the axis of the spin. Since the precession is steady, the equation of the gyroscopic device motion around axis ox is presented by the following system (Chap. 5, Eq. 5.6).

$$J_x \frac{d\omega_x}{dt} = Mga - Gb - \left(\frac{2}{9}\pi^2 + \frac{8}{9}\right) J\omega\omega_x - J\omega\omega_y \tag{B.4.1}$$

$$\omega_y = (4\pi^2 + 17)\omega_x \tag{B.4.2}$$

where M is the rotor mass; G is the counterweight mass; a and b is the distance of the rotor and counterweight location from the pivot, respectively; J is the mass moment of inertia of the rotor, J_x is the mass moment of inertia of the gyroscopic

device around axis *ox; ω* is the angular velocity of the rotor; ω_x and ω_y is the angular velocity of the gyroscopic device around axes *ox,* and *oy,* respectively; and t is the time.

Substituting initial data and Eq. (B.4.2) into Eq. (B.4.1) and transforming yield the following:

$$\begin{aligned} 9.0 \times 10^{-4} \frac{\mathrm{d}\omega_x}{\mathrm{d}t} &= 3.0 \times 9.81 \times 0.3 - 4.0 \times 9.81 \\ &\times b - \left(\frac{2}{9}\pi^2 + \frac{8}{9}\right) \times 0.1 \times 10^{-4} \times 50.0 \times \omega_x \\ &- 0.1 \times 10^{-4} \times 50.0 \times (4\pi^2 + 17)\omega_x \end{aligned} \tag{B.4.3}$$

Simplification of Eq. (B.4.3) yields the following

$$0.030221 \frac{\mathrm{d}\omega_x}{\mathrm{d}t} = 296.471397 - 1317.650653b - \omega_x \tag{B.4.4}$$

Separating variables and transforming for the differential equation gives the following

$$\frac{\mathrm{d}\omega_x}{296.471397 - 1317.650653b - \omega_x} = 33.089195\,\mathrm{d}t \tag{B.4.5}$$

Equation (B.4.5) is represented by the integral forms at definite limits

$$\int_0^{\omega_x} \frac{\mathrm{d}\omega_x}{296.471397 - 1317.650653b - \omega_x} = -33.089195 \int_0^t \mathrm{d}t \tag{B.4.6}$$

The left integral of the equation is tabulated and represented the integral $\int \frac{\mathrm{d}x}{a-x} = -\ln x + C$. The right integral is simple, and integrals have the following solution:

$$\ln(296.471397 - 1317.650653b - \omega_x)\Big|_0^{\omega_x} = -33.089195t$$

giving rise to the following

$$1 - \frac{\omega_x}{296.471397 - 1317.650653b} = \mathrm{e}^{-33.089195t} \tag{B.4.7}$$

Solving Eq. (B.4.7) gives the equation of the precession angular velocity for the gyroscope around axis *ox* as the result of the action of the load torques

$$\omega_x = (296.471397 - 1317.650653b)(1 - \mathrm{e}^{-33.089195t}) \tag{B.4.8}$$

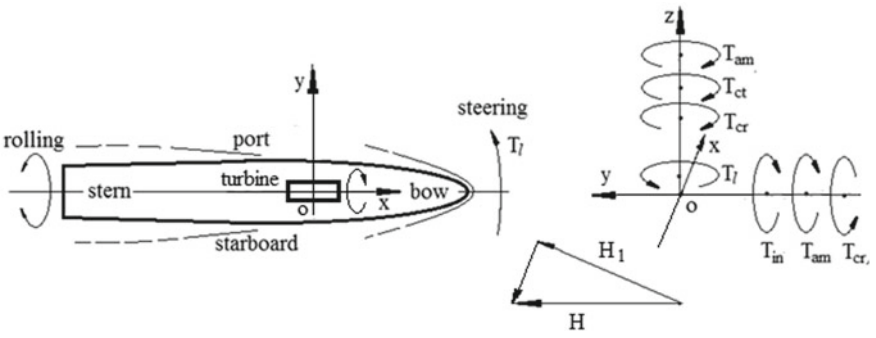

Fig. B.5 Torques acting on the ship

The expression $e^{-33.089195t}$ has a small magnitude and can be neglected. Hence, the angular velocity of the gyroscope precessions around axis ox is as follows:

$$\omega_x = 296.471397 - 1317.650653b \tag{B.4.9}$$

Substituting defined expression and initial data into Eq. (B.4.2) and transforming yield the following:

$0.5 = (4\pi^2 + 17)(296.471397 - 1317.650653b)$, which sowing yields the following result:

$$b = 0.225\,\text{m}$$

The location of the counterweight from the pivot should be 225 mm that supports constant precession around axis oy, which is $\omega_y = 0.5$ rad/s.

B.5 Gyroscopic Torques Acting on a Ship

The ship equipped with the turbine engine which rotating masses (spinning rotor) are horizontal and across the breadth of the ship (Fig. B.5). The direction of the angular velocity of the rotor in the clockwise direction when viewed from the tip of the ox axis. During the motion in the sea, the ship can get the steering to the left and right side around axis oz, pitching on the limited angle of motion about the transverse axis oy and rolling on the limited angle of motion about the longitudinal axis ox. The terms of the ship components, acting torques and motions are represented in Fig. B.5.

Gyroscope torques act during steering. When the ship turns left by the action of the torque T_l, the angular momentum of the spinning turbine changes from H to H_l. The spinning turbine produces the following torques:

– the resulting precession torque generated by the inertial forces T_{in}, the rate change in the angular momentum T_{am} and the resistance torque of Coriolis forces tend to raise the bow and lower the stern;
– the resulting resistance torque generated by the centrifugal T_{ct} and Coriolis forces T_{cr} and the change in the angular momentum T_{am} counteracts on the left turn (Fig. B.5).
– The huge mass of the ship is many times bigger than the mass of the turbine. This is the reason that the ship does not demonstrate the sensitive raise of the bow, i.e. no pitching around axis *oy*. This situation means all inertial torques generated by the rotating mass of the turbine are deactivated and the ship turns only under the action of the steering torque. The steering process of the ship's turn is manifested by the action of the inertial torques of the change in the angular momentum of the turbine.

The rolling of the ship does not relate to gyroscopic inertial torques. The axes of the rolling of the ship and the spinning turbine are parallel, and there is no precession of the spin axis and thus no gyroscopic effects.

Example. The turbine rotor of the ship has a mass of 3.0 tonnes, length of 3 m and rotates 2000 rpm in the clockwise direction (Fig. B.5). The radius of gyration of the turbine rotor is 0.4 m. The mass and size of the ship are many times bigger than the turbine. Determine the maximal force acting on the supports of the turbine when the ship turns left at the radius of 200 m with a speed of 30.0 km/h and the steering torque applied on the ship is 130 kNm.

Solution

The ship turns left under the action of the external torque. At the starting condition of the turn, the rotating turbine generates the resistance and precession inertial torques produced by the centrifugal, common inertial and Coriolis forces and the change in the angular momentum acting around axis *oz* and *oy*. The action of the resulting precession torque at the starting condition manifests the minor pitching of the ship that can be neglected. Then, it is accepted the absence of the pitching, and hence, deactivation of the gyroscopic inertial torques accepts the change in the angular momentum of the turbine. The latter acting around axis oy on the supports of the turbine. The components of the turbine weight act on the supports along the axis oz (Fig. B.5). The force acting on one support of the turbine due to the action of the change in the angular momentum is as follows:

$$F_y = \frac{T_y}{a} = \frac{J\omega\omega_z}{3.0} = \frac{240 \times 209.439510239 \times 0.041666666}{3.0} = 698.13058\,\text{N}$$

where a is the length of the turbine or distance between its supports, and other components are as specified above.

The force acting on one support of the turbine due to the action of is weight is as follows:

$$F_z = \frac{Mg}{a/2} = \frac{3000 \times 9.81}{3.0/2} = 19620\,\text{N}$$

where M is the mass of the turbine.

Then, the maximal force acting on one support of the turbine is as follows:

$$F = F_y + F_z = 698.13058 + 19620 = 20318.131\,\text{N}$$

B.6 Forces Acting on the Rolling Disc and Motion on the Flat Surface

The simple bicycle wheel or thin disc is unstable on the vertical plane, but a rolling motion demonstrates its stability and steerability when the disc tilts. This tilt results in a turn of the rolling disc to the direction of the tilt. This motion of the inclined thin disc manifests the gyroscopic effects as the action of the centrifugal, common inertial and Coriolis forces and the change in the angular momentum. The action of these forces enables the rolling disc to be brought back to a vertical position. The study of the action of the inertial forces and motion of a rolling thin disc on a flat surface assumes that the disc rolls with the constant angular velocity. A rolling disc is slightly tilted in its path on a flat surface (Fig. B.6). This tilt causes its variable travel on a curved path. The rolling disc produces the torque generated by its gyroscopic weight. In turn, this torque results in the following inertial torques (Table 3.1, Chap. 3):

- The resistance torques based on the action of the centrifugal $T_{\text{ct}x}$ and Coriolis forces $T_{\text{cr}x}$ acting around axis ox.
- The precession torques based on the action of the change in the angular momentum $T_{\text{am}x}$ of the rolling disc and the common inertial forces $T_{\text{in}x}$ acting around axis oy.
- The action of the precession torques $T_{\text{am}x}$ and $T_{\text{in}x}$ generates the resistance torques of Coriolis forces T_{cry} acting around axis oy.
- The combined torques acting around axis oy generate the precession torques based on the action of the change in the angular momentum $T_{\text{am}y}$ acting around axis ox and adding to the action of the resistance torques $T_{\text{ct}x}$ and $T_{\text{cr}x}$.
- The precession torques acting around axis oy turn the rolling disc to the direction of the tilting and the disc rolls in a curved path with the variable radius l.
- The curvilinear motion of the disc generates the centrifugal force in the disc centre mass which acts horizontally and creates the torque $T_{\text{ct.m}}$ about the contact point of the disc with the surface. This torque acts in the same direction as the combined resistance torques around axis ox that altogether bring the disc to a vertical position.
- The frictional force generated by the disc weight at the contact point with the surface produces the frictional torque $T_{\text{f.}y}$ that acts around axis oy in the clockwise direction.

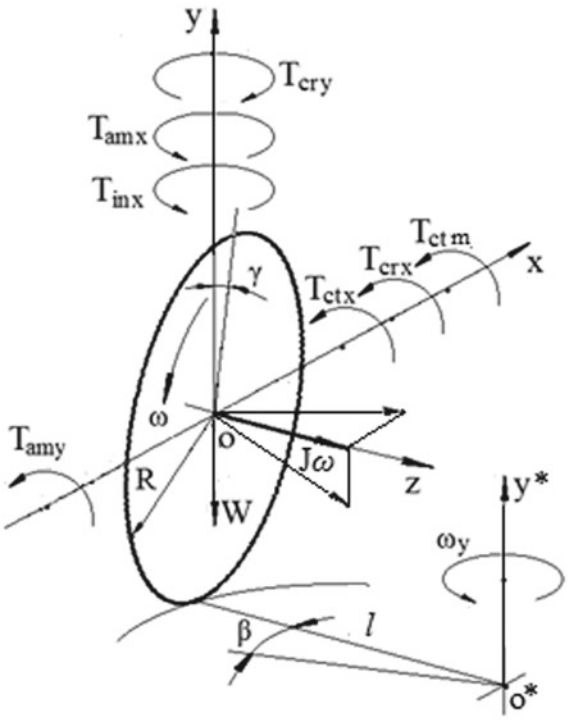

Fig. B.6 Torques acting on the free rolling disc on a flat surface

Figure B.6 demonstrates the action of the external and inertial torques on the rolling disc that moves on the flat surface. The mathematical models for the motions of the rolling disc are based on the action of torques mentioned above around axes *ox* and *oy* and represented by the following equations in Euler's form:

$$J_x \frac{\mathrm{d}\omega_x}{\mathrm{d}t} = T - T_{\mathrm{ct}.m} - T_{\mathrm{ct}.x} - T_{\mathrm{cr}.x} - T_{\mathrm{am}.y} \tag{B.6.1}$$

$$J_y \frac{\mathrm{d}\omega_y}{\mathrm{d}t} = T_{\mathrm{in}.x} \cos\gamma + T_{\mathrm{am}.x} \cos\gamma - T_{\mathrm{cr}.y} \cos\gamma \tag{B.6.2}$$

where $J_x = J_{y=} MR^2/4 + MR^2$ is the mass moment of the disc inertia around axis *ox* and *oy,* respectively, that calculated by the parallel axis theorem; ω_x and ω_y is the angular velocity of precession around axis *ox* and *oy,* respectively; $T = Mg\ R\ \sin\gamma$ is the torque generated by the disc weight W around axis *ox;* $T_{\mathrm{ct,my}}$ is the torque generated by the centrifugal forces of the centre mass of the rolling disc around axis *oy*. $T_{\mathrm{ct}.x}$ is the resistance torque generated by centrifugal forces of the disc mass elements around axes *ox*; $T_{\mathrm{in}.x}$ is the precession torque generated by inertial forces around axes *ox*; $T_{\mathrm{cr}.x}$ and $T_{\mathrm{cr}.y}$ is the resistance torque generated by Coriolis forces around axes *ox* and *oy,* respectively; $T_{\mathrm{am}.x}$ and $T_{\mathrm{am}.y}$ is the precession and resistance torque generated by the change in the angular momentum of the spinning rotor around

axes *ox* and *oy,* respectively; $T_{\text{cr,my}}$ is the torque generated by Coriolis force of the rotating gyroscope centre mass around axes *ox* and *oy.*

The torque acting around axis oy^* on the rolling disc generated by the centrifugal force of the centre mass and the weight of the disc is defined by the following equation:

$$T_{\text{ct}.m} = -F_{\text{ct}} R \cos\gamma + MgR \sin\gamma \tag{B.6.3}$$

where $F_{\text{ct}} = M\omega^2 l \cos^2\gamma$ is the centrifugal force of the disc centre mass rotating around axis oy^*, M is the disc mass; R is the radius of the disc; γ is the angle of the disc inclination; g is the gravity acceleration, l is the radius of the curved path.

The variable radius l of the disc rolling around axis oy^* is defined from the expressions $V = \omega R = \omega_y l \cos\gamma$, where V and ω is the linear and angular velocity of the disc, respectively, ω_y is the angular velocity of the disc around axis oy^*. Then $l = \omega R/\omega_y \cos\gamma$, and other components are as specified above. Substituting defined parameters into Eq. (B.6.3) and simplifying yield the following expression:

$$T_{\text{ct.m}} = MR\left(g \sin\gamma - \frac{\omega^3 R \cos^2\gamma}{\omega_y}\right) \tag{B.6.4}$$

The torque generated by Coriolis force of the centre mass of the rolling disc and the motion of the disc around axis *ox* and *oy* is not considered due to a small value. The action of the frictional torque T_{fy} generated by the weight of the rolling disc is considered due to a small value.

The resistance torque acting around axis *ox* in the clockwise direction is generated by the centrifugal and Coriolis forces of the disc mass elements and the change in the angular momentum. This torque is represented by the following equation (Table 3.1, Chap. 3):

$$T_{\text{r}.x} = \left(\frac{2\pi^2 + 8}{9}\right) J\omega\omega_x + J\omega\omega_y \tag{B.6.5}$$

The torques generated by the common inertial forces of the mass elements and the change in the angular momentum of the rolling disc and Coriolis forces are acting around axis *oy.* These torques are represented by the following equation (Table 3.1, Chap. 3):

$$T_{\text{p}.x} = \left(\frac{2\pi^2 + 9}{9}\right) J\omega\omega_x + \frac{8}{9} J\omega\omega_y \tag{B.6.7}$$

Substituting defined parameters (Eqs. B.6.3–B.6.7B.7) into Eqs. (B.6.1) and (B.6.2), transforming and adding the ratio of the angular velocities around axis *ox* and *oy* (Eq. (4.9), Chap. 4) yield the following system:

$$J_x \frac{\mathrm{d}\omega_x}{\mathrm{d}t} = MR\left\{ g\sin\gamma - \frac{\omega^3 R\cos^2\gamma}{\left[\frac{2\pi^2+8+(2\pi^2+9)\cos\gamma}{2\pi^2+9-(2\pi^2+8)\cos\gamma}\right]\omega_x}\right\} - \left[\frac{2\pi^2+8}{9} + \frac{2\pi^2+8+(2\pi^2+9)\cos\gamma}{2\pi^2+9-(2\pi^2+8)\cos\gamma}\right] J\omega\omega_x \tag{B.6.8}$$

$$J_y \frac{\mathrm{d}\omega_y}{\mathrm{d}t} = \left(\frac{2\pi^2+9}{9}\right)\omega_x + \frac{8}{9} J\omega\cos\gamma \tag{B.6.9}$$

where $J = MR^2/2$ is the mass moment of inertia of the disc; other parameters are as specified above.

Solving Eq. (B.6.8) enables for the computing the angular velocities of the rolling disc around axes ox and oy on the flat surface. Additionally, the numerical solution of the right side of Eq. (B.6.8) will show that inertial torques turn up the inclined rolling disc to the vertical position. Substituting the expression of J, transformation of the right side of Eq. (B.6.8) and separating the torques acting in opposite directions yield the following equation:

$$MRg\sin\gamma = \frac{MR^2\omega^3\cos^2\gamma}{\left[\frac{2\pi^2+8+(2\pi^2+9)\cos\gamma}{2\pi^2+9-(2\pi^2+8)\cos\gamma}\right]\omega_x} + \left[\frac{2\pi^2+8}{9} + \frac{2\pi^2+8+(2\pi^2+9)\cos\gamma}{2\pi^2+9-(2\pi^2+8)\cos\gamma}\right] J\omega\omega_x \tag{B.6.10}$$

The value of the inertial torques of the right side of Eq. (B.6.10) can be bigger than the left side, but it depends on the value of ω and γ. For the high value of the angular velocity ω, the right side of Eq. (B.6.10) is always bigger than its left side. This is the reason that free rolling disc on the flat surface does not fall to the side until its angular velocity reached the minimal value.

B.6.1 Working Example

The mathematical model for the motion of the rolling disc on the flat surface is considered for the example whose data is presented in Table B.1. The action of the external and internal torques on the disc is represented in Fig. B.6. The rolling disc initially possesses an inclined axle. It is necessary to find the values of the internal torques exerted on the rolling disc and its precessions.

Table B.1 Technical data of the thin disc

Parameter		Data
Angular velocity, ω		3.0 rad/s
Radius of the disc, R		0.3 m
Angle of tilt, γ		30.0°
Mass		0.5 kg
Radius of the turn of the disc, l		0.2 m
Mass moment of inertia, kg m^2	Around axis oz, $J = MR^2/2$	0.0225
	Around axes ox and oy of the centre mass, $J_i = MR^2/4$	0.01125
	Around axes ox and oy at the point of support, $J_x = J_y = MR^2/4 + MR^2$	0.05625

Substituting given data into Eq. (B.6.8) yields the following:

$$0.05625\frac{\mathrm{d}\omega_x}{\mathrm{d}t} = 0.5 \times 0.3 \times \left\{9.81\sin 30^\circ - \frac{3^3 \times 0.3 \times \cos^2 30^\circ}{\left[\frac{2\pi^2+8+(2\pi^2+9)\cos 30^\circ}{2\pi^2+9-(2\pi^2+8)\cos 30^\circ}\right]\omega_x}\right\} - \left[\frac{2\pi^2+8}{9} + \frac{2\pi^2+8+(2\pi^2+9)\cos 30^\circ}{2\pi^2+9-(2\pi^2+8)\cos 30^\circ}\right] \times 0.0225 \times 3.0\omega_x \quad \text{(B.6.11)}$$

Separating variables, transforming and representing in the integral form give the following:

$$\int_0^{\omega_x} \frac{\mathrm{d}\omega_x}{\omega_x^2 - 0.675359339\omega_x + 0.074961015} = -\frac{19.367467413}{\omega_x}\int_0^t \mathrm{d}t \quad \text{(B.6.12)}$$

The left integral is represented by the following form:

$$\int_0^{\omega_x} \frac{\mathrm{d}\omega_x}{(\omega_x - 0.53533225)(\omega_x - 0.1400270844)} = -\frac{13.390398749}{\omega_x}\int_0^t \mathrm{d}t \quad \text{(B.6.13)}$$

The left integral after transformation yields the following:

$$\frac{1}{0.395305169}\int_0^{\omega_x}\left(\frac{1}{\omega_x - 0.53533225} - \frac{1}{\omega_x - 0.1400270844}\right)\mathrm{d}\omega_x$$

$$= -\frac{13.390398749}{\omega_x}\int_0^t \mathrm{d}t \tag{B.6.14}$$

Solving the integral equations yields the following:

$$[\ln(\omega_x - 0.53533225) - \ln(\omega_x - 0.1400270844)]\Big|_0^{\omega_x} = -\frac{5.293293842}{\omega_x}t\Big|_0^t$$

giving rise to the following:

$$\ln\left[\frac{-0.1400270844(\omega_x - 0.53533225)}{-0.0.53533225(\omega_x - 0.1400270844)}\right] = -\frac{5.293293842}{\omega_x}t \tag{B.6.15}$$

Solution of Eq. (B.6.15) yields the following:

$$\omega_x - 0.53533225 = \frac{(\omega_x - 0.1400270844)}{0.261570425}\mathrm{e}^{-\frac{5.293293842}{\omega_x}t} \tag{B.6.16}$$

where the expression $\mathrm{e}^{-\frac{5.293293842}{\omega_x}t}$ has the small value of high order that can be neglected.

Then, the angular velocities of precessions for the rolling disc around axes ox and oy (Eq. 4.9, Chap. 4) are as follows:

$$\omega_x = 0.53533225\,\text{rad/s} \tag{B.6.17}$$

$$\omega_y = \left[\frac{2\pi^2 + 8 + (2\pi^2 + 9)\cos 30^\circ}{2\pi^2 + 9 - (2\pi^2 + 8)\cos 30^\circ}\right] \times 0.53533225 = 5.97358556\,\text{rad/s} \tag{B.6.18}$$

The angular velocity ω_x rotates the disc around axis ox in the clockwise direction that leads to its vertical location. The presented data of a tilted rolling disc allow considering the values of the acting torques. Substituting the obtained data into Eq. (B.6.11) and computing yield the following result:

$$0.5 \times 0.3 \times 9.81 \sin 30^\circ = \frac{3^3 \times 0.3 \times \cos^2 30^\circ}{\left[\frac{2\pi^2+8+(2\pi^2+9)\cos 30^\circ}{2\pi^2+9-(2\pi^2+8)\cos 30^\circ}\right] \times 0.53533225}$$
$$+\left[\frac{2\pi^2 + 8 + (2\pi^2 + 9)\cos 30^\circ}{2\pi^2 + 9 - (2\pi^2 + 8)\cos 30^\circ}\right] \times 0.0225 \times 3.0 \times 0.53533225$$
$$0.73575 < 1.420158042 \tag{B.6.19}$$

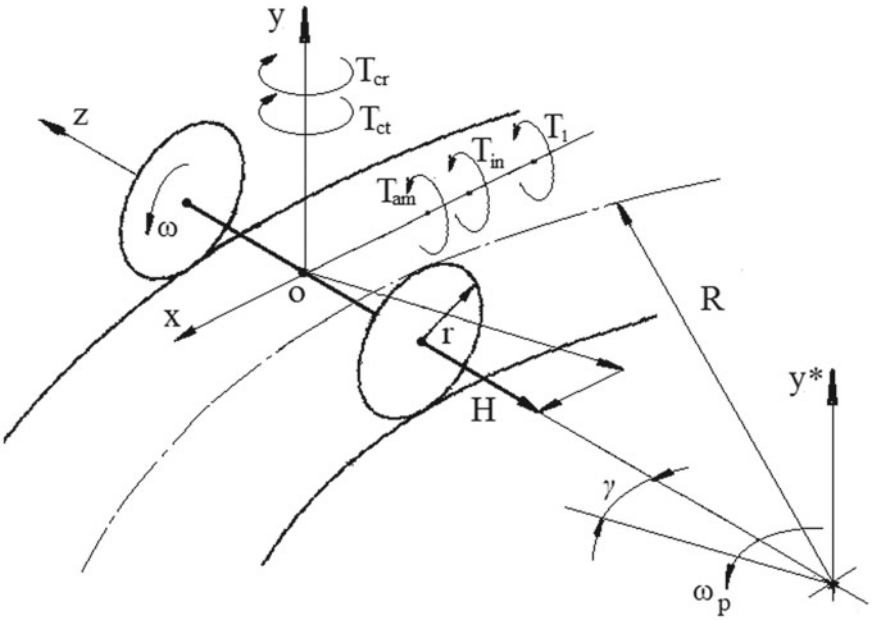

Fig. B.7 Car's wheels following a circular path

The right side of this expression is bigger than the left one; i.e., the inertial torques of the rolling disc turn up the disc until vertical position. The rolling disc of the vertical position does not manifest gyroscopic effects and demonstrates the rectilinear motion.

B.7 Gyroscopic Torques Acting on a Car Wheels Rounding a Curve

The car of the mass of 2500 kg with its centre of mass at 0.5 m in above the road and its four the disc-type wheels have 0.4 m radius and 50 kg weight each. For simplicity, two wheels are connected by a straight axle with a length of 2.0 m. The car is moving on a road with a velocity 40 km/hr by a circular path of radius 10 m with the centre of the axle as shown in Fig. B.7. Find the gyroscopic torques, exerted on the car.

Solution

The moving wheel manifests gyroscopic effects as the action of the inertial torques generated by its rotating mass. The equations of inertial torques are represented in Table 3.1 of Chap. 3, whose components are as follows:

- The resistance torques generated by the centrifugal $T_{\text{ct}} = \frac{2\pi^2}{9} J\omega\omega_y$ and Coriolis $T_{\text{cr}} = \frac{8}{9} J\omega\omega_y$forces of the spinning disc acting around axis *oy*.

- The precession torques generated by the change in the angular momentum $T_{\text{am}} = J\omega\omega_y$ of the disc and the common inertial forces $T_{\text{in}} = \frac{2\pi^2}{9} J\omega\omega_y$ acting around axis ox.

The turn of the car around axis ox is blocked due to its heavy weight but the precession torques T_{am} and T_{in} have tended to cause rollover of the car. The blocking turn around axis ox deactivates the resistance inertial torques T_{ct} and T_{cr} acting on the wheel around axis oy (Chap. 8). The precession torques T_{in} and T_{am} act on the rotating wheel and hence on a car and opposite to the action of the car weight.

The circular turn of the car generates the centrifugal forces of the centre mass tending to cause the rollover of the car. Taking the moment T about the contact point of the outer wheel, the result of calculation gives the following:

$$T_1 = Fh = m\frac{V^2}{R}h = 2500\,\text{kg} \times \frac{(40000/3600\,\text{m/s})^2}{10\,\text{m}} \times 0.5\,\text{m} = 15432.0987\,\text{Nm}$$

where $F = mV^2/R$ is the centrifugal force, m is the mass of the car, V is the tangential velocity of the car, R is the radius of the car motion by the circular path, h is the height of the car's centre mass above the road.

In order to make a quantitative comparison of the gyroscopic and centrifugal moments acting on the car, the torque generated by the precession torques T_{am} and T_{in} of the four wheels is calculated. The components of the equations of precession torques are the mass moment of inertia, angular velocity and angular precession of the wheels.

The wheel's moment of inertia is calculated by the following equation

$$J = mr^2/2 = 50\,\text{kg} \times (0.4\,\text{m})^2/2 = 4.0\,\text{kg}\,\text{m}^2$$

where r is the radius of the wheel; other parameters are as specified above.

The angular velocity of the wheel is

$$\omega = \frac{V}{r} = \frac{40000\,\text{m}}{3600s \times 0.4\,\text{m}} = 27.7777\,\text{rad/s}$$

where V is the linear velocity of the car.

The angular precession of the car motion by the circular path is calculated by the following equation

$$\omega_{\text{p}} = \frac{V}{R} = \frac{40000\,\text{m}}{3600s \times 10\,\text{m}} = 1.1111\,\text{rad/s}$$

where all parameters are as specified above.

The gyroscopic inertial torques acting on the car wheels around axis ox are directed to rollover but the weight of the car is blocking this action. In such condition, the inertial torques of the wheels are deactivated except the torque of the change in the angular momentum (Chap. 8). This torque is calculated by the following equation:

$$T_{\mathrm{p}} = 4T_{\mathrm{am}} = 4J\omega\omega_{\mathrm{p}} = 4 \times 4.0 \times 27.7777 \times 1.1111 = 493.827\,\mathrm{Nm}$$

The torque generated by the weight of the car about the contact point of the outer wheel presents the resistance torque on the action of the centrifugal T_1 of the centre mass of the car and precession T_{p} torques. The torque, which leads to rollover of the car, is calculated by the following equation:

$$T_{\mathrm{r}} = W \times b/2 - T_1 - T_{\mathrm{p}} = 2500 \times 9.81 \times 2/2 - 15432.0987 - 493.827 = 8599.0743\,\mathrm{Nm}$$

where $W = mg$ is the weight of the car, g is the gravity acceleration, b is the length of axle between two wheels, and other parameters are as specified above.

The total resistance torque is positive; the car does not roll over on the circular path. However, the torque of the centrifugal force generated by the centre mass of the car and gyroscopic torque of the wheels produce the following torque:

$$T = T_1 + T_{\mathrm{p}} = 15432.0987 + 493.827 = 15925.9257\,\mathrm{Nm}$$

that represented 36.062% from the resistance torque of the car's weight $T_{\mathrm{c}} = W \times b/2 = 24525.0$ Nm. Definitely, the gyroscopic effects of wheels' act on the car and at the critical velocity can lead to rolling over in a circular path that depends on both the radius of the turn and the speed of the car.

B.8 Gyroscopic Forces Acting on a Bearing of an Electric Motor for the Railway Carriage Rounding a Curve

The electric railway carriage rounding a curve and its electric motor is loaded by inertial torques that manifest gyroscopic effects. The curvilinear motion of the electric motor demonstrates the gyroscope effects of the spinning rotor, which presented by the action of centrifugal, common inertial and Coriolis forces and the change in the angular momentum. The action of these forces presents the additional load on the bearings of the electric motor. The study of the action of the inertial forces on the rotor is assumed that electric railway carriage rolls with a constant angular velocity. Find the reaction force acting on the bearings when the carriage rolls on the curvilinear track.

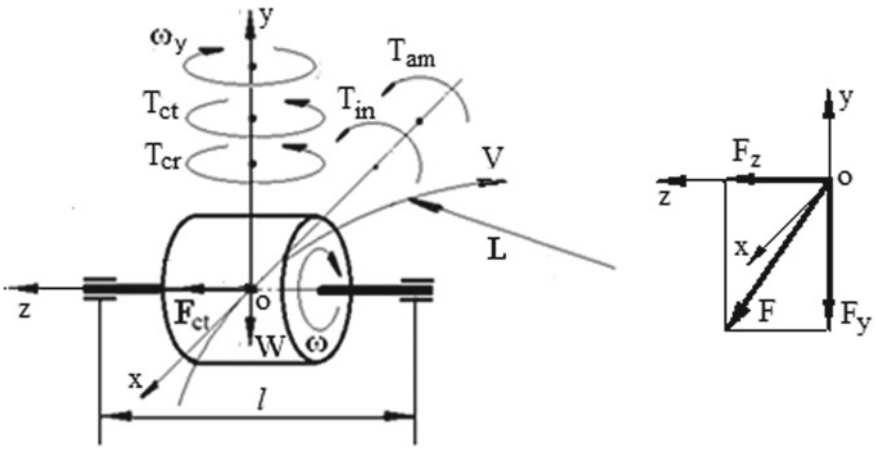

Fig. B.8 Torques and forces acting on the spinning rotor of the carriage

Solution

The curvilinear turn of the electric motor produces the several inertial torques generated by the spinning rotor's mass. The action of the inertial and external torques produces the reactive forces on the bearings of the electric rotor's supports. The inertial torques and external loads acting on the spinning rotor around axes *ox* and *oy,* respectively, are represented by the components in Fig. B.8. The equations of inertial torques generated by the rotating mass of the rotor are represented in Table 3.1 of Chap. 3, whose components are as follows:

- The resistance torques generated by the centrifugal $T_{\text{ct}} = \frac{2\pi^2}{9} J\omega\omega_y$ and Coriolis $T_{\text{cr}} = \frac{8}{9} J\omega\omega_y$ forces of the spinning rotor acting around axis *oy*.
- The precession torques generated by the change in the angular momentum $T_{\text{am}} = J\omega\omega_y$ of the rotor and the common inertial forces $T_{\text{in}} = \frac{2\pi^2}{9} J\omega\omega_y$ acting around axis *ox*.

The curvilinear turn of the electric motor on railway generates the centrifugal forces of the centre mass acting on bearings of the electric rotor. The weight of the electric rotor generates the reactive forces on its bearings.

The centrifugal force generated by the centre mass of the rotor at the time of the curvilinear motion of the carriage is defined by the following equation:

$$F_{\text{ct,mz}} = F_z = mV^2/L = m\omega_y^2 L \tag{B.8.1}$$

where $F_{\text{ct.mz}}$ is the centrifugal force generated by the of the centre mass of the rotor; m is the rotor mass; V is the tangential velocity of the carriage; L is the radius of the curvilinear rail track; ω_y is the angular velocity of the carriage on the rail track.

The rotor's weight produces the load forces on the rotor's bearing that is defined by the following equation:

$$F_{Wy} = W/2 = mg/2 \tag{B.8.2}$$

where F_{Wy} is the load force generated by the of the centre mass of the rotor acting on the radial-thrust bearing; W is the rotor's weight; g is the gravity acceleration; other parameters are as specified above.

The turn of the spinning rotor around axis ox is blocked due to heavy weight of the carriage that turns only around axis oy. The blocking turn around axis ox deactivates the inertial torques T_{ct} and T_{cr} around axis oy and the precession torques T_{in} (Chap. 8). The precession torque T_{am} of the change in the angular momentum acts on the spinning rotor and produces the loads on the bearings.

The total force acting on the bearing of the rotor along axis oy and oz is represented by the following equations with substituting of the expressions of the inertial torques and the component of the weight of the rotor:

$$F_y = \frac{T_{\text{am}}}{l} + F_w = \frac{J\omega\omega_y}{l} + \frac{mg}{2} = \frac{J\omega\omega_y}{l} + \frac{mg}{2} \tag{B.8.3}$$

$$F_z = m\omega_y^2 L \tag{B.8.4}$$

where F_y and F_z are the total forces acting on the bearing of the rotor along axes oy an oz, respectively; l is the distance between the bearings symmetrical located relatively of the centre mass of the rotor.

The combined load acting on the most loaded bearing of the rotor is defined by the following equation (Fig. B.8):

$$F = \sqrt{F_y^2 + F_z^2} = \sqrt{\left[\frac{J\omega\omega_y}{l} + \frac{mg}{2}\right]^2 + (m\omega_y^2 L)^2} \tag{B.8.5}$$

where all parameters are as specified above.

8.1 Working Example

An electric carriage is rolling on the curvilinear rail track of radius 300 m with a linear velocity of 90.0 km/h. The motor used for traction has a rotor of mass 600 kg and a radius of gyration 300 mm. The motor shaft is parallel to the axes of the carriage's running wheels. The rotor is supported in bearings 750 mm apart symmetrically and rotates of 160.0 rad/s (Fig. B.8). Determine the combined force generated by the inertial forces of the rotor and its weight acting on the most loaded bearing.

For solution is defined as the following:

(a) the angular velocity of precession:

$$\omega_{\text{p}} = V/L = (90000/3600)/300 = 0.083333\ \text{rad/s}$$

where V is the linear velocity of the carriage, L is the radius of the rail curve.

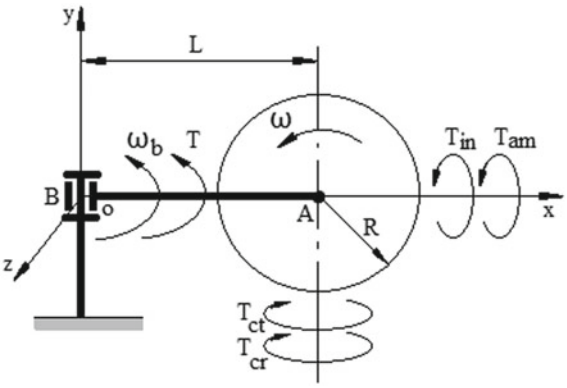

Fig. B.9 Torques acting on the shaft with the rotating bar and spinning disc

(b) the rotor's mass moment of inertia

$$J = mr^2 = 600 \times 0.3^2 = 54.0\,\text{kg m}^2$$

where m is the rotor's electric motor mass, r is the radius of gyration.

(c) the rotor's angular velocity

$$\omega = 160.0\,\text{rad/s}$$

(d) the combined force acting on the bearing is defined by the substituting defined above parameters into Eq. (B.8.5)

$$F = \sqrt{\left[\frac{54.0 \times 160 \times 0.083333}{0.75} + \frac{600 \times 9.81}{2}\right]^2 + (600 \times 0.083333^2 \times 300)^2}$$
$$= 4098.274\,\text{Nm}$$

Analysis of the obtained result demonstrates that inertial forces acting on the bearing is commensurable to the weight of the motor at the given conditions of the carriage motion.

B.9 Gyroscopic Torques Acting on a Spinning Disc with Fixed Support

The spinning disc of mass m and radius R in Fig. B.9 is located on the support A of the bar of the length L. The disc rotates with the constant angular velocity ω, which direction is in the counterclockwise when viewed from the tip of axis oz. The other end of the bar located on a hinge B of the vertical shaft. The external torque applied to the bar is T that rotates it with the constant angular velocity ω_b is in the

counterclockwise direction. The mass of the light bar and friction forces acting on the hinge B and the support A is negligible and omitted from consideration. The centre of the coordinate system $\Sigma oxyz$ attached to the hinge. Find the reaction force acting on the shaft when the bar with the disc rotates around axis oy.

Solution

The turn of the spinning disc around axis oy in the counterclockwise direction generates the following inertial torques:

(a) The precession torque generated by the common inertial forces of the spinning disc acting around axis ox in the clockwise direction:
$T_{\text{in}} = \frac{2\pi^2}{9} J\omega\omega_{\text{b}}$, where $J = mr^2$is the mass moment of the disc's inertia; ω is the angular velocity of the disc; ω_b is the angular velocity of the precession of the bar with the disc around axis oy.

(b) The precession torque generated by the change in the angular momentum about the centre of mass for the spinning disc is acting around axis ox in the clockwise direction:

$$T_{\text{am}} = J\omega\omega_b \tag{B.9.1}$$

(c) The resistance torque generated by centrifugal forces of the spinning disc acting around axis oy in the clockwise direction:

$$T_{\text{ct}} = \frac{2\pi^2}{9} J\omega\omega_{\text{b}} \tag{B.9.2}$$

(d) The resistance torque generated by the Coriolis forces of the spinning disc is acting around axis oy in the clockwise direction:

$$T_{\text{cr}} = \frac{8}{9} J\omega\omega_{\text{b}} \tag{B.9.3}$$

The turn of the spinning disc around axis ox is blocked because the support A locates on the bar that turns only around axis oy. The blocking turn around axis ox deactivates the inertial torques T_{ct} and T_{cr} around axis oy and the precession torques T_{in} (Chap. 8). The precession torque T_{am} of the change in the angular momentum acts on the spinning disc and produces the twisting torque acting on the bar. The twisting torque of the bar generates the bending moment that applied at the pivot B of the shaft.

References

1. Awrejcewicz, J., Koruba, Z.: Classical Mechanics. Applied Mechanics and Mechatronics. Springer, New York (2012)
2. Ardema, M.D.: Analytical Dynamics. Theory and Application. Academic/Plenum Publishers, New York (2005)

3. Deimel, R.F.: Mechanics of the Gyroscope. Dover Publications Inc., New York (2003)
4. Gregory, D.R.: Classical Mechanics. Cambridge University Press, New York (2006)
5. Goldstein H, Poole C.P., Safko J.L.: Classical Mechanics, 3rd edn. Addison-Wesle, Reading, MA (2002)
6. Hibbeler, R.C., Yap, K.B.: Engineering Mechanics—Statics and Dynamics, 13th edn. Prentice Hall, Pearson, Singapore (2013)
7. Scouts-Little, R.W., Inman, D.J., Balint, D.S.: Engineering Mechanics. Dynamics Computational Edition. Cengage Learning, Toronto, ON (2008)
8. Syngley, J., Uicker J.J.: Theory of Machines and Mechanisms, 3rd edn. McGraw-Hill Book Company, New York (2002)
9. Taylor, J.R.: Classical Mechanics. University Science Books, Mill Valley (2005)
10. Waldron, K.J., Kinzel, G.L.: Kinematics, Dynamics and Design of Machinery, 2nd edn. Wiley, Hoboken (2004)
11. Usubamatov, R.: A Mathematical Model for Motions of Gyroscope Suspended from Flexible Cord. Cogent Engineering (2016). https://doi.org/10.1080/23311916.2016.1245901
12. Usubamatov, R.: Analysis of inertial forces acting on gyroscope precession. Int. Rev. Aerosp. Eng. **4**(N2), 103–108 (2011)
13. Usubamatov, R.: Mathematical models for gyroscope properties. Math. Eng. Sci. Aerosp. **8**(3), 359–371 (2017)
14. Usubamatov, R.: Inertial forces acting on gyroscope. J. Mechan. Sci. Technol. **32**(1), 101–108 (2018)
15. Usubamatov, R.: Deactivation of gyroscopic inertial forces. AIP Adv. **8**, 115310 (2018). https://doi.org/10.1063/1.5047103
16. Usubamatov, R.: Analysis of motion for a rolling disc on the flat surface. Int. Rob. Autom. J. **4**(5), 329–332 (2018). doi: 10.15406/iratj.2018.04.00145
17. Usubamatov, R.: Gyroscopic torques acting on crushing mill. Adv. Robot. Mech. Eng. **1**(4), 70–72 (2019)